UNIVERSITY OF CALIFORNIA, SAN DIEGO

Development of Self-Delivering, Bioreversible, Phosphotriester RiboNucleic Neutral (siRNN) Prodrug RNAi Therapeutics

A dissertation submitted in partial satisfaction of the

requirements for the degree Doctor of Philosophy

in

Biomedical Sciences

by

Alexander Sinclair Hamil

Committee in charge:

Professor Steven F. Dowdy, Chair
Professor Jeffrey D. Esko
Professor Stephen B. Howell
Professor Yitzhak Tor
Professor Gene W. Yeo

2016

The Dissertation of Alexander Sinclair Hamil is approved, and it is acceptable in quality and form for publication on microfilm and electronically:

_____

_____

_____

_____

_____

Chair

University of California, San Diego

2016

TABLE OF CONTENTS

LIST OF FIGURES

Chapter 1

Chapter 2

Chapter 3

Chapter 4

Chapter 5

Chapter 6

Chapter 7

ACKNOWLEDGEMENTS

First, I would like to thank my thesis advisor, Steven F. Dowdy, who has been everything I could ask for in a mentor and more. Without your indomitable enthusiasm and optimism, this project would never have succeeded. I have more gratitude for all that you have done for me than I can put into words.

I would like to thank the members of the Dowdy lab, both past and present that I've worked with over the years. The Dowdy lab works as a team and this dissertation would not have been possible without the contributions of a number of people. Special thanks to Bryan Meade for his mentoring, friendship, and for building the mountain and to Khirud Gogoi for synthesizing the continual flow of phosphoramidites and other molecules that made this project a reality. I would also like to thank: Jonathan Hagopian for taking under his wing in the lab; Peter Lönn and Manuel Kaulich for the stimulating conversation and friendship, both in lab and out; Aaron Springer for always making lab interesting; Akiko Eguchi and Asaf Presente for spending hours and hours training me in the mouse room; Xian-Shu Cui for keeping the Dowdy lab running smoothly and taking care of all of us; and Apollo Kacsinta for many amusing lunches.

Thank you to Anne Phan, who has been with me through all the highs and lows of graduate school. Not everyone is fortunate enough to have a partner that they can discuss science with and I have been all the better for it. Without your love and support, I don't know where I would be.

Lastly, I would like to thank my family. I've been fortunate to have a close and loving family that has always supported me in everything that I have done. Thank you to my Mother and Father who instilled in me the importance of kindness and hard work. Any success I have I owe to you. Thank you to my Brother for so many great times and

conversations. Finally, thank you to the rest of my family, the Hamils and Frys, for all of your support and for helping me pull my head out of science every once in a while.

During my graduate training, I was supported by a Cancer Cell Biology Training Grant from the National Cancer Institute and a Blasker Science & Technology Grant from the San Diego Foundation.

Chapter 3, 4, and 5 have, in part, been published in *Nature Biotechnology* co-authored by the dissertation author. The citation for the published work is: Bryan R. Meade, Khirud Gogoi, Alexander S. Hamil, Caroline Palm-Apergi, Asaf Presente, Arjen van den Berg, Jonathan Hagopian, Aaron D Springer, Akiko Eguchi, Apollo D Kacsinta, Connor F Dowdy, Asaf Presente, Peter Lönn, Manuel Kaulich, Naohisa Yoshioka, Edwige Gros, Xian-Shu Cui, and Steven F. Dowdy. Efficient Delivery of RNAi Prodrugs Containing Reversible Charge-Neutralizing Phosphotriester Backbone Modifications. Nature Biotechnology 32, 1256-1261 (2014). The dissertation author was a principal investigator and co-author of this material.

Phosphoramidites utilized in Chapter 3, 4, and 5 were synthesized by Khirud Gogoi. Byran Meade synthesized some oligonucleotides, worked out TBDMSO-SATE oligonucleotide synthesis and deprotection conditions, and performed some cellular treatments. Analysis of cMyc knockdown was performed by Manuel Kaulich. Caroline Palm-Apergi performed Plk1 knockdown experiments. Aaron Springer synthesized some RNN oligonucleotides. Apollo Kacsinta performed siRNN albumin binding assays.

Chapter 6 is currently being prepared for submission for publication of the material. Jonathan Hagopian performed some cellular treatments, 5'-RACE analysis, and *in vivo* experiments. Arjen van den Berg performed Ago2 co-immunoprecipitation experiments. Bryan Meade synthesized oligonucleotides. Akiko Eguchi performed *in*

vivo experiments. Caroline Palm-Apergi performed Plk1 knockdown experiments. The dissertation author was the primary investigator and author of this material.

VITA

EDUCATION:

2010 - 2016 Doctor of Philosophy, Biomedical Sciences Program
Department of Cellular and Molecular Medicine
University of California, School of Medicine
Graduate Advisor: Professor Steven F. Dowdy, Ph.D.

2005 - 2009 Bachelor of Science, *magna cum laude*
Major: Genetics
School of Biological Sciences
University of California, Irvine, Irvine, CA

RESEARCH EXPERIENCE:

2010 - 2016 Ph.D. Graduate Student with Prof. Steven F. Dowdy,
Dept. of Cellular & Molecular Medicine, UCSD School of Medicine.
Thesis Project: Development of Self-Delivering, Bioreversible, Phosphotriester RiboNucleic Neutral (siRNN) Prodrug RNAi Therapeutics

2010 Research Specialist, Lab of Profs. David M. Gardiner and Susan V. Bryant,
Dept. Developmental & Cell Biology, University of California Irvine

2007 - 2009 Undergraduate Researcher with Prof. Hung Fan, University of California Irvine
Project: Oncogenicity of Jaagsiekte Sheep Retrovirus (JSRV).

Summer 2008 Undergraduate Researcher with Prof. Hubert Schorle, University of Bonn,Germany
Project: Generation of Transgenic Mice Expressing AP-2 γ Transcription Factor.

2007 Undergraduate Researcher with Prof. Rainer Brachmann, Dept. Medicine, UCI
Project: Genomic Screen of p53 Mutants Prevalent in Prostate Cancer.

RESEARCH SUPPORT:

2013 - 2014 Science & Technology Blasker Grant Award, San Diego Foundation

2011 - 2013 Trainee, NCI Cancer Cell Biology Training Grant (PI: M. Farquhar)

TEACHING EXPERIENCE:

2013 Teaching Assistant, *Molecular Biology*
Division of Biological Sciences
University of California, San Diego, La Jolla, CA

2012 - 2013 Course Co-Director, *Cancer Cell Biology Journal Club*
Department of Cellular and Molecular Medicine
University of California, San Diego, La Jolla, CA

SCIENTIFIC PRESENTATIONS:

Oct, 2014 Poster Presentation: "RNAi by Self-Delivering, Bioreversible, PhosphoTriester RiboNucleic Neutral (siRNN) RNAi Prodrugs" Oligonucleotide Therapeutics Society Annual Meeting, San Diego, CA

Sep, 2014 Oral Presentation: "The Road to Anticancer RNAi Therapeutics: siRNN Prodrugs" UCSD Biomedical Sciences Graduate Program Retreat. Palm Springs, CA

Mar, 2014 Oral Presentation: "The Road to Anticancer RNAi Therapeutics: siRNN Prodrugs" UCSD Cellular and Molecular Medicine Symposium, UCSD, La Jolla, CA

May, 2013 Oral Presentation: "Synthesis of Novel BioReversible RNAi Therapeutics to Treat Cancer" NCI Cancer Cell Biology Training Grant, UCSD, La Jolla, CA

Nov, 2012 Poster Presentation: "Novel BioReversible Prodrug RNAi Therapeutics to Treat Cancer" Cancer Biology Chair and Directors Retreat, UCSD, La Jolla, CA

May, 2012 Oral Presentation: "Induction of RNAi Responses by Bioreversible PhosphoTriester siRNNs" NCI Cancer Cell Biology Training Grant, UCSD, La Jolla, CA

PUBLICATIONS:

Alexander S. Hamil, Jonathan C. Hagopian, Bryan R. Meade, and Steven F. Dowdy. Induction of RNAi Responses by Left-Handed Hairpin RNAs. (*in preparation*) (2016).

Peter Lönn, Apollo Kacsinta, Xian-Shu Cui, **Alexander S. Hamil**, Manuel Kaulich, Khirud Gogoi, and Steven F. Dowdy. Enhancing Endosomal Escape for Intracellular Delivery of Macromolecular Biologic Therapeutics. *Scientific Reports* 6, 32301 (2016).

Alexander S. Hamil, Khirud Gogoi, and Steven F. Dowdy. Conjugation of Duplexed siRNN Oligonucleotides with DD-HyNic Peptides for Cellular Delivery of RNAi Triggers. *Bio-Protocol* 6, e1782 (2016).

Alexander S. Hamil and Steven F. Dowdy. Synthesis and Conjugation of Small Interfering Ribonucleic Neutral SiRNNs. *Methods in Molecular Biology* 1364, 1-9 (2016).

Bryan R. Meade, Khirud Gogoi, **Alexander S. Hamil**, Caroline Palm-Apergi, Arjen van den Berg, Jonathan Hagopian, Aaron D Springer, Akiko Eguchi, Apollo D Kacsinta, Connor F Dowdy, Asaf Presente, Peter Lönn, Manuel Kaulich, Naohisa Yoshioka, Edwige Gros, Xian-Shu Cui, and Steven F. Dowdy. Efficient Delivery of RNAi Prodrugs Containing Reversible Charge-Neutralizing Phosphotriester Backbone Modifications. *Nature Biotechnology* 32, 1256-1261 (2014).

Xuefeng Wu, Weizhou Zhang, Joan Font-Burgada, Trenis Palmer, **Alexander S. Hamil**, Subhra K. Biswas, Michael Poidinger, Nicholas Borcherding, Qing Xie, Lesley G. Ellies, Nikki K. Lytle, Li-Wha Wu, Raymond G. Fox, Jing Yang, Steven F. Dowdy, Tannishtha Rey, and Michael Karin. Ubiquitin-Conjugating Enzyme Ubc13 Controls Breast Cancer Metastasis Through a TAK1-p38 MAP Kinase Cascade. *Proceedings of the National Academy of Sciences U.S.A.* 111, 13870-13875 (2013).

Stacey Hull, Joohyun Lim, **Alexander S. Hamil**, Takayuki Nitta, and Hung Fan. Analysis of Jaagsiekte Sheep Retrovirus (JSRV) Envelope Protein Domains in Transformation. *Virus Genes* 45, 508-517 (2012).

ABSTRACT OF THE DISSERTATION

Development of Self-Delivering, Bioreversible, Phosphotriester RiboNucleic Neutral (siRNN) Prodrug RNAi Therapeutics

by

Alexander Sinclair Hamil

Doctor of Philosophy in Biomedical Sciences

University of California, San Diego, 2016

Professor Steven F. Dowdy, Chair

The discovery of RNA interference (RNAi) and the subsequent demonstration that synthetic short interfering RNA (siRNA) molecules could induce sequence-specific silencing of mRNA expression in human cells has opened the door to a new class of therapeutics. However, unlike small molecule drugs (<500 Da) that can diffuse passively across cell membranes, siRNAs are both too large (~14,000 Da) and too charged to

enter cells unassisted. Consequently, delivery of siRNA is the major problem for the development of RNAi therapeutics.

To address the problem of siRNA delivery, our laboratory developed short interfering ribonucleic neutrals (siRNNs) whose anionic phosphate backbone is synthetically neutralized by bioreversible phosphotriester groups. The first generation of siRNNs utilized *t*-butyl-s-acyl-2-thioethyl (*t*Bu-SATE) phosphotriester groups that proved too hydrophobic for biologic use. To improve siRNNs, we synthesized more hydrophilic hydroxyl-SATE (O-SATE) phosphotriester groups and used them to generate maximally neutral siRNNs for delivery by conjugated cationic peptide transduction domains (PTDs). Unfortunately, despite an overall cationic charge, PTD-siRNN conjugates were incapable of self-delivery *in vitro*. To solve this problem, we utilized conjugatable Aldehyde-SATE (A-SATE) phosphotriesters to make multivalent PTD-siRNN conjugates. Multivalent PTD-siRNN conjugates were capable of non-cytotoxic self-delivery and the induction of dose-dependent RNAi responses *in vitro*, a first for siRNNs. To study the function of siRNNs *in vivo*, we employed *N*-acetylgalactosamine (GalNAc), a hepatocyte-specific targeting domain. Single dose systemically administered GalNAc-siRNN conjugates induced extended dose-dependent RNAi responses in mice. This work constituted the first instance of *in vivo* target gene knockdown by siRNNs containing bioreversible neutralizing phosphotriester groups. Finally, we investigated small, double-stranded, left-handed hairpin (LHP) RNAs as alternative RNAi triggers for the application of RNN technology. Taken together, this work describes the development of readily adaptable, monomeric siRNA prodrugs (siRNNs) and opens a new avenue for RNAi therapeutics to treat human disease.

CHAPTER 1

INTRODUCTION

INTRODUCTION

ABSTRACT

The discovery of RNA interference (RNAi) introduced a novel mechanism of post-transcriptional gene regulation where the expression of target genes could be repressed in a sequence-specific manner. The subsequent demonstration that synthetic short interfering RNAs (siRNAs) could induce an RNAi response in human cells opened the door to a new class of therapeutics. The unprecedented combination of selectivity, potency, and adaptability makes siRNAs an attractive drug to treat a host of human diseases, including cancer, pandemic influenza, and genetic diseases. However for all its promise, siRNAs are a poor candidate pharmacologically, with the excessive negative charge and size of siRNA molecules rendering them unable to enter cells without assistance from a delivery agent. While a wide variety of siRNA delivery strategies have been developed, most rely on encapsulation of siRNAs into nanoparticles. To avoid the fundamental problems of the nanoparticle approach, our lab has sought a novel solution for siRNA delivery where the siRNA charge is synthetically neutralized to make neutral monomeric RNAi prodrugs termed short interfering ribonucleic Neutrals (siRNNs) thereby shrinking the contemporary siRNA “drug” from a 100 megaDa nanoparticle to ~17 kDa molecule.

THE RNAi PATHWAYS

The world changed in 1998 when Andrew Fire, Craig Mello, and colleagues discovered that gene expression could be suppressed by exogenous double-stranded RNA in *Caenorhabditis elegans* through a mechanism called RNA interference (RNAi) (Fire et al., 1998). This revolutionary discovery earned Fire and Mello the 2006 Nobel Prize in Physiology or Medicine. In the following years, it was found that the process of RNAi is evolutionarily conserved and the cellular machinery that composes the RNAi pathways was identified. At the core of RNAi is a ribonucleoprotein complex known as the RNA-induced silencing complex (RISC) which is composed, minimally, of an Argonaute family protein bound to a single-stranded 20-30 nucleotide (nt) RNA (Carthew and Sontheimer, 2009a; Ender and Meister, 2010). RISC silences expression of target genes in a sequence-specific manner with the specificity granted by base-pairing between the bound small RNA and its target mRNA. The potential of leveraging RNAi to treat human disease was first established when it was shown that chemically synthesized short interfering RNAs (siRNAs) could silence the expression of specific genes when delivered into cultured human cells (Elbashir et al., 2001a). To understand the difficulties that must be overcome to fulfill this potential, I will briefly review the RNAi pathways.

The process of RNAi can be divided into two primary pathways that overlap but utilize disparate effector molecules: microRNA (miRNA) and siRNA. The miRNA pathway begins in the nucleus wherein long non-coding RNAs known as primary microRNAs (pri-miRNAs) are transcribed by RNA polymerases (Ohrt et al., 2012). A nuclear pri-miRNA contains one or more double-stranded hairpins which are recognized and trimmed out of the pri-miRNA by the microprocessor complex (comprised of the RNAase III enzyme Drosha and the hairpin recognition subunit DGCR8) to form 65-70 nt

precursor miRNAs (pre-miRNA) (Lee et al., 2003). Pre-miRNAs are then exported out of the nucleus and into the cytoplasm by the transport facilitators Exportin-5 and RanGTP (Lund et al., 2004). Once in the cytoplasm, pre-miRNAs are further processed by a complex of the RNAse III enzyme Dicer and dsRNA-binding proteins (dsRBP) TAR RNA-binding protein (TRBP) and PACT into mature miRNAs (Bernstein et al., 2001; Chendrimada et al., 2005; Heyam et al., 2015). These mature miRNAs are 21-25 nt duplexes with 3' dinucleotide single-stranded RNA (ssRNA) overhangs, 5' phosphates, and interspersed with mismatches, generally in the middle of the miRNA. The mature miRNA is then loaded into an Argonaute protein by TRBP to form the pre-RISC. Humans have four Argonaute proteins (Ago1-4), but only Ago2 exhibits slicer activity, the ability to cleave bound target ssRNA (Meister et al., 2004; Ender and Meister, 2010). During loading, one of the two RNA strands that comprises the miRNA is chosen on the basis of weaker thermodynamic stability of its 5' end (Preall et al., 2006). This chosen strand, termed the Guide strand or miRNA, remains bound to the Argonaute protein while the complementary RNA strand, known as the Passenger strand or miRNA*, is either unwound and ejected (when bound to Ago1,3,4) or, in rare cases, cleaved (Ago2) and removed from RISC (Kim et al., 2009) . The activated RISC is now able to identify and repress the expression of target mRNAs in a sequence-specific manner through complementary base pairing with the RISC-bound guide strand.

The siRNA pathway is similar to that of miRNA, but takes place entirely in the cytoplasm. As a form of viral defense, Dicer can process exogenous long dsRNAs into 21-23 nt siRNAs with characteristic 5' phosphate and 3' hydroxyl groups as well as 3' dinucleotide overhangs (Bernstein et al., 2001). siRNAs are subsequently loaded into pre-RISC and used as effector molecules to mediate RNAi responses. The siRNA pathway can be activated artificially by synthesizing and duplexing two RNA

oligonucleotides to generate a synthetic siRNA (Elbashir et al., 2001a). Once delivered to the cytoplasm, a synthetic siRNA will be engaged by the RNAi machinery to silence expression of the target gene. The entry point of a synthetic siRNA into the pathway is dependent on the structure of the synthetic siRNA. siRNAs with the standard 19+2 structure (19 nt RNA duplex with 2 nt 3' ssRNA overhangs) can bypass potentially rate-limiting Dicer binding entirely and instead be recognized directly by TRBP and loaded into Argonaute (Murchison et al., 2005). Alternatively, 25-27 nt dsRNA RNAi triggers, termed Dicer-substrate siRNAs (DsiRNA), that have a a blunt end and a 3' dinucleotide overhang on the other end that is recognized and bound by Dicer's PAZ domain (Sakurai et al., 2011). Even though miRNAs cannot activate Ago2's slicing activity, miRNAs and siRNAs are loaded into all four Ago family members.

Although the miRNA and siRNA pathways are convergent, the effector molecules differ in key ways. For both pathways, RISC selects target mRNAs by base-pairing between the bound small guide RNA and its target mRNA predominantly through a 7 nucleotide Seed region composed of nucleobases 2-8 of the guide strand or miRNA (Birmingham et al., 2006; Anderson et al., 2008). miRNAs are characterized by base pair mismatches between their guide and passenger strands, that eventually translates into mismatches between the guide strand and target mRNAs (Carthew and Sontheimer, 2009b). These mismatches decrease the specificity of a given miRNA for a single target, but also adds flexibility to this RNAi pathway by allowing a single miRNA to bind imperfectly to and modulate the expression of multiple genes through translational repression of mRNA. This allows the >3,000 human miRNAs to regulate the expression of more than one third of human genes (Kim et al., 2009; Londin et al., 2015). Conversely, siRNAs have complete or near-complete complementarity to the target

mRNA, thereby imbuing siRNAs with exquisite target selectivity as well as the ability to activate Ago2's slicer activity (Lam et al., 2015).

BARRIERS TO RNA DELIVERY

Cellular life first developed on this planet by the chemical separation of macromolecules due to a lipid bilayer whereby internal components could perform chemical reactions that were unencumbered by the external environment (Neveu et al., 2013; Blain and Szostak, 2014). Over ~3.5 billion years of evolution, unicellular organisms and, eventually, multicellular organisms have developed increasingly sophisticated mechanisms to carefully maintain their internal consistency and defend against invading pathogenic genetic material. Exogenous nucleic acid is amongst the most dangerous invaders to all forms of cellular life, as it is capable of taking control of any cell that it enters. For this reason, cell membranes have evolved from the beginning to prevent RNA and DNA from entering. Not surprisingly, as organisms evolved, they added on additional layers of various barriers to protect against genetic invaders. Consequently, successful delivery of siRNA therapeutics requires breaching these numerous barriers.

siRNA degradation

The first delivery barrier that a siRNA therapeutic is encounters after administration to a human is ribonuclease activity (Tsui et al., 2002). Nucleic acids, particularly RNAs, are subject to rapid degradation by nucleases present in serum and the extracellular environment. More than 99% of ssRNA is degraded by ribonucleases within seconds of exposure to human blood (Tsui et al., 2002). Double-stranded RNA, such as siRNAs, is somewhat more degradation resistant, but unmodified siRNA is still degraded within minutes in human blood (Gao et al., 2009). This instability limits the

circulation time of unmodified siRNAs and prevents siRNAs from concentrating to therapeutic levels at targeted tissue sites. A number of ribonucleases, including enzymes in the RNAse A family and the 3' exonuclease ERI-1, have been found to mediate siRNA degradation in human serum (Kennedy et al., 2004; Haupenthal et al., 2006; Gabel and Ruvkun, 2008). The majority of siRNA delivery approaches utilize agents that encapsulate siRNA into nanoparticles that protect the RNA from ribonuclease degradation. In contrast, the recent development of siRNA conjugate delivery approaches involves the direct exposure of siRNAs to serum. Once siRNAs have reached the cytoplasm of a cell, the threat of degradation is considerably reduced as the intracellular environment is more hospitable for unmodified siRNA (Hoerter et al., 2011).

Extravasation, tissue distribution, and excretion

The primary modes of administration for systemic delivery of siRNA therapeutic candidates are currently intravenous or subcutaneous injection as oral delivery involves getting past additional barriers. Intravenous injection gives direct access to the blood stream for rapid systemic distribution, whereas subcutaneous injection allows for a more gradual distribution as the therapeutic slowly escapes from the subcutaneous space (McLennan et al., 2005). To reach target tissues, siRNA therapeutics must extravasate across blood vessel endothelial cells and penetrate into the interstitial space. The degree that extravasation presents a barrier to delivery is dependent on the target tissue. For a lipid insoluble molecule to passively diffuse out of the blood stream and into the interstitial space, pores must exist through both the blood vessel wall (usually in the form of fenestrations) and the basement membrane that exceed the diameter of the molecule or nanoparticle. An unmodified 19+2 nt siRNA with an A-form helix is less than 6 nm in length and 3 nm in width. Many tissues, including as skin, intestine, and lung,

contain continuous or fenestrated capillaries. These capillaries only allow for the free diffusion of molecules that are less than 12 nm in size, while larger molecules will be subject to poor extravasation (Sarin, 2010). Naked siRNAs can easily access these tissues, but nanoparticle siRNA delivery vehicles are generally in the 100 nm size range and are therefore, prevented from readily entering these tissues.

In contrast, tissues that contain blood vessels with larger pores, including liver and spleen, are considered to be more “leaky” and therefore more permeable to extravasation of large macromolecules. Hepatic sinusoidal capillaries have pore sizes up to 180 nm, making the liver extremely permissive to nanoparticle-mediated delivery (Sarin, 2010). The resulting accumulation of nanoparticles to therapeutic concentrations in the liver has made this organ a prime target for nanoparticle siRNA delivery in both preclinical animal models and clinical trials (Schroeder et al., 2010). However, the affinity of nanoparticles for these organs possess a problem when attempting to target other organs. Conversely, the comparatively small size and highly anionic character of naked siRNA molecules leads to rapid kidney filtration and excretion following systemic administration (van de Water et al., 2006; Merkel et al., 2009). Indeed, intravenous injection of radio-labeled naked charged siRNAs into mice results in >90% of the dose in the bladder in less than five minutes (Gao et al., 2009). Thus, it is necessary to utilize delivery vehicles for siRNA that favor delivery to target organs and avoid renal clearance.

Tumors are thought to constitute a privileged site for the delivery of nanoparticles. Due to the rapid and poorly controlled angiogenesis, the blood vessel architecture in tumors is less organized than that of normal tissue (Matsumura and Maeda, 1986; Maeda, 2012). Tumor vasculature is astoundingly leaky, as the vessels have been shown to allow the passage of macromolecules 200 -1200 nm in size (Hobbs

et al., 1998). This combination of features causes the accumulation of macromolecules, particularly nanoparticles, within tumor tissue, a property which is known as the enhanced permeability and retention (EPR) effect (Matsumura and Maeda, 1986; Maeda, 2012). However, the ability of nanoparticles to treat tumors may be overstated due to the rapid growth of subcutaneous human tumor xenografts in preclinical mouse models, which is not representative of the more slowly growing human tumors (Kamb, 2005; Mak et al., 2014). This is a significant problem and potential artifact for using nanoparticle delivery devices to treat preclinical models of cancer.

Endocytosis and endosomal escape

The primary and most physical barrier that must be overcome for siRNA delivery is traversing the cell membrane itself (**Figure 1.1**). The phospholipid bilayer that composes the cell membrane has evolved to prevent entry of macromolecules, particularly invading nucleic acids, into the cell. Being highly anionic, lipid insoluble, and relatively large at 14,000 Da, siRNA molecules are unable to cross the cell membrane by passive diffusion. In fact, the biophysical characteristics of siRNA are in profound violation of Lipinski's rule-of-five used to evaluate the drug-likeness of a chemical compound (Lipinski et al., 2001; Lipinski, 2004). In an effort to promote cellular uptake, much research has been conducted to chemically modify siRNA, conjugate to delivery molecules, or encapsulate it in nanoparticles (Jeong et al., 2009; Bramsen and Kjems, 2011; Roberts et al., 2016). These delivery strategies seek to improve the lipophilicity of siRNAs and reduce the negative charge. For nanoparticles, this is accomplished non-covalently with cationic polymers or lipids that encapsulate ~100 siRNAs per nanoparticle (Whitehead et al., 2009). Other approaches have sought to mask the negative charge of siRNA with RNA-binding proteins (Eguchi et al., 2009; Palm-Apergi et al., 2011).

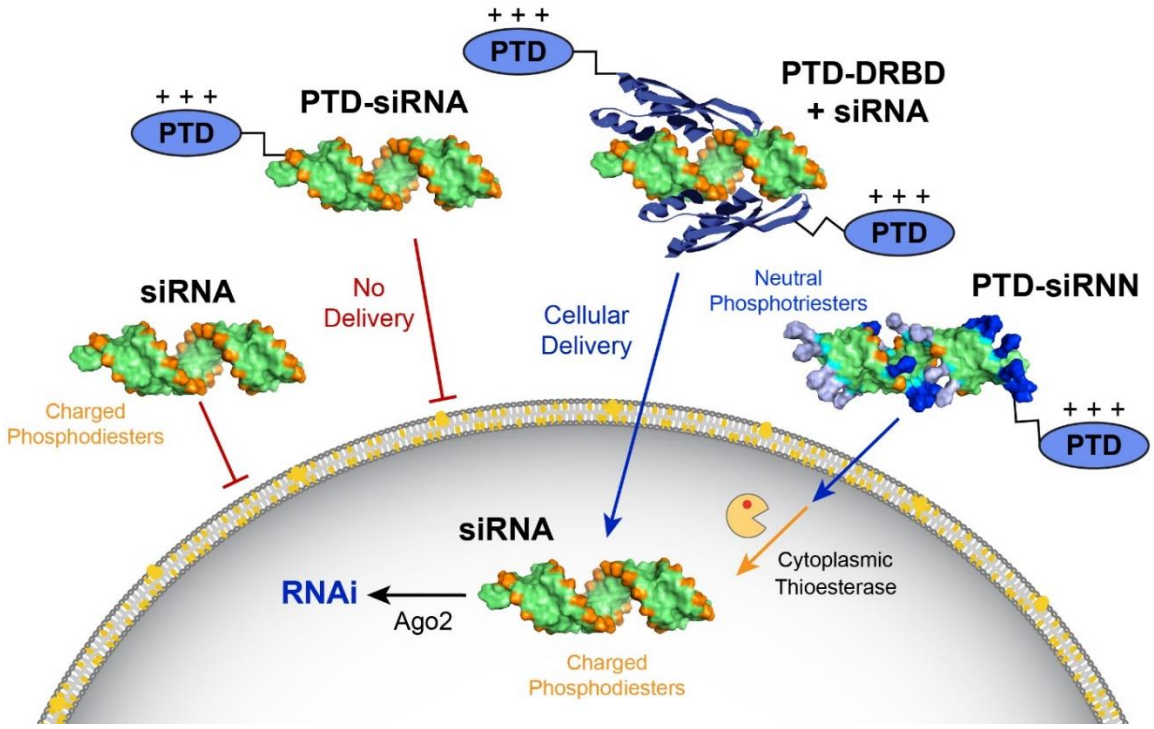

Figure 1.1. Overcoming the siRNA negative charge for PTD-mediated siRNA delivery. siRNA: The 14,000 Da size and negative charge of the phosphodiester backbone prevent native siRNA from traversing the cellular membrane unassisted. **PTD-siRNA:** Conjugation of a cationic peptide transduction domain (PTD) to a charged siRNA results in neutralization of the PTD and no cellular delivery. **PTD-DRBD + siRNA:** PTD-DRBD fusion proteins are able to complex and deliver siRNA across the cellular membrane. The double-stranded RNA binding domains (DRBDs) of the fusion protein mask the negative charge of the siRNA phosphodiester backbone and thereby allow cellular delivery of a single siRNA molecule by the fused PTD. **PTD-siRNN:** Short interfering ribonucleic neutrals (siRNNs) contain bioreversible phosphotriester groups that neutralize the negative charge of the phosphodiester backbone. This charge neutralization enables conjugated PTDs to deliver the monomeric, soluble siRNA prodrug across the cellular membrane. Upon cytosolic entry, ubiquitous cytoplasm-restricted thioesterases convert the neutral phosphotriester groups into charged phosphodiester groups, resulting in a charged siRNA capable of Ago2 loading and RNAi response induction.

In the end, all of the siRNA delivery approaches utilize some form of endocytosis to mediate cellular uptake of siRNA. While various forms of endocytosis have been identified, including clathrin-mediated, caveolin-dependent, phagocytosis, and macropinocytosis, the mechanism that siRNA is taken up into cells by is dependent on the delivery vehicle (Doherty and McMahon, 2009). For example, peptide transduction domains (PTDs, also known as cell penetrating peptides [CPPs]) and lipid nanoparticles have both been found to enter cells by macropinocytosis (Kaplan et al., 2005; Gilleron et al., 2013). Although endocytosed siRNA is technically inside a cell, it is still separated from the cytoplasm (where it must associate with RISC to induce an RNAi response) by the endosomal lipid bilayer membrane, which has a similar architecture to that of the cell membrane. Because of the inherent difficulty in trafficking siRNAs out of the endosomal compartment and into the cytoplasm, endosomal escape is the rate-limiting step for siRNA delivery into cells (Dominska and Dykxhoorn, 2010). It has been shown that when lipid nanoparticles are used to deliver siRNA into cultured mammalian cells under ideal conditions, 98-99% of the endocytosed material remains trapped in endosomes (Gilleron et al., 2013). In other words, only 1-2% of the lipid nanoparticles escape into the cytoplasm. Independent of the endocytotic mechanism, endocytosed material enters into a pathway of endosomal maturation wherein early endosomes undergo acidification, lowering the pH from 7 to 5, convert to late endosomes through fusion with other intracellular vesicles, and eventually are routed to the lysosome (Huotari and Helenius, 2011). To avoid siRNA degradation, it is desirable that siRNA escape into the cytoplasm prior to the final step of this pathway, as the lysosome contains nucleases which can degrade siRNA cargo (Dominska and Dykxhoorn, 2010). Enhancement of endosomal escape remains a critical challenge to siRNA delivery and must be improved upon to generate efficient siRNA therapeutics.

Innate immune response

The immune system constitutes a significant obstacle to siRNA delivery that must be overcome for the therapeutic application of siRNA. Most relevant to siRNA delivery is that dsRNA, often a signature of viral infection, is recognized by mammalian cells as a dangerous cargo that can trigger an innate immune response (Whitehead et al., 2011). As the body's front line defense against pathogens, the innate immune system has evolved a variety of receptors to recognize and respond to foreign substances and bodies. Recognition by the innate immune system can lead to the induction of high levels of inflammatory cytokines and interferons (Robbins et al., 2009). siRNAs can trigger the innate immune system in two primary ways: through Toll-like receptor (TLR)-mediated pathways and by TLR-independent pathways in the cytoplasm (Whitehead et al., 2011). TLRs are Pathogen-Associated Molecular Patterns (PAMPs) sensors that recognize the phospho-ribose backbone pattern of double stranded RNAs(Whitehead et al., 2011). Within the TLR family, TLR3, TLR7, and TLR8 are the primary mediators of recognizing synthetic, double stranded siRNAs (Heil et al., 2004; Karikó et al., 2004). TLR3 is primarily localized on the cell surface, whereas TLR7/8 are mainly localized to the endosomal compartment.

TLR-independent cytoplasmic detection of siRNA in human cells occurs through several molecular sensors including helicase Retinoic Acid Inducible gene 1 (RIG-1), dsRNA responsive Protein Kinase R (PKR), and Melanoma Differentiation-Associated gene 5 (Mda5) (Kang et al., 2002; Marques et al., 2006; Puthenveetil et al., 2006). Additionally, particular RNA sequences, such as GUCCUUCAA or certain GU-rich sequences, have been found to be more immunostimulatory than others (Heil et al., 2004; Hornung et al., 2005). It is important to avoid induction of an innate immune response as it can alter or reduce the efficacy of a siRNA therapeutic. An innate

immune response may even produce a false positive result. This was true in clinical trials of Bevasiranib, a naked unmodified (all 2'-OH) VEGF siRNA, that was administered to patients suffering from age-related macular degeneration (AMD). Bevasiranib suppressed angiogenesis, but did so by activating a TLR3 innate immune response instead of through RNAi gene silencing (Kleinman et al., 2008). Fortunately, chemical modifications can be applied to siRNA to prevent recognition by TLRs and thereby avoid induction of an innate immune response (**Figure 1.2**).

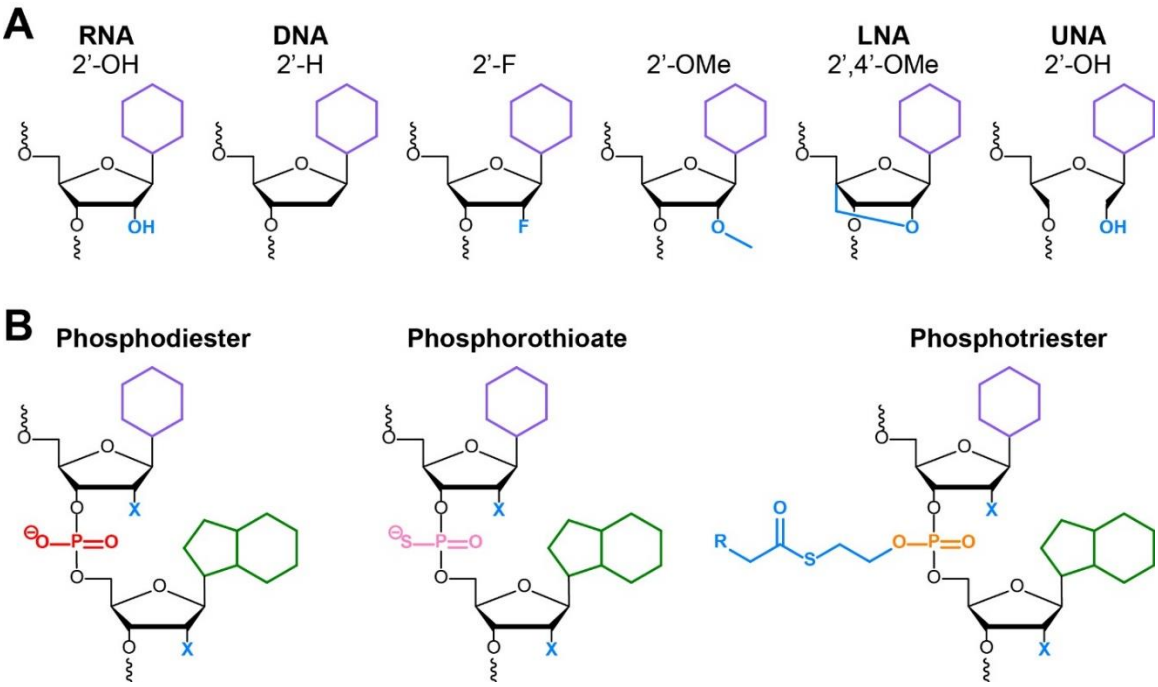

Figure 1.2. Chemical modification of siRNA. A) Modifications to the ribose 2'-position: native RNA 2'-Hydroxyl (OH); native DNA 2'-Deoxy (H); 2'-Fluoro (F); 2'-Hydroxymethyl (OMe); 2',4'-Bicyclic containing O-Methylene bridge or locked nucleic acid (LNA); deletion of the ribose C2-C3 bond or unlocked nucleic acid (UNA). **B)** Phosphate backbone modifications: native RNA, anionic charged phosphodiester (achiral phosphorus); charged phosphorothioate (chiral phosphorus); neutral phosphotriester (chiral phosphorus, becomes achiral after intracellular conversion to charged phosphodiester).

Off-target silencing

Off-target gene silencing is another significant issue faced by siRNA therapeutics. siRNAs are highly specific for their target mRNA, with the potential to discriminate a single base difference between sequences (Huang et al., 2009). However, full complementarity between a guide RNA and a target mRNA is not necessary to mediate gene silencing, as is the case with miRNAs, and this can result in unintended off-target gene knockdown (Vickers et al., 2009). The Seed region (nucleobases 2-8 of the guide strand) is the most important part of an siRNA for identifying target mRNAs and complementarity of only the seed region with an mRNA is sufficient to induce a moderate miRNA-like off-target regulation of gene expression (Jackson et al., 2003; Birmingham et al., 2006; Jackson and Linsley, 2010). Another source of potential off-target activity is unintended loading of the passenger strand into RISC, instead of the guide strand, that would cause off-target gene silencing of targets specified by the passenger strand. This can be mitigated by reducing the thermodynamic stability of the 5' end of the guide strand to enhance selection of the proper guide strand by Dicer and/or by chemical modification of the passenger strand to block RISC loading (Jackson et al., 2006; Preall et al., 2006; Chen et al., 2008). Unlike small molecule inhibitors that bind to any number of unknown targets, genes that are subject to siRNA off-target effects (OTEs) can be predicted from sequence data and measured by gene expression assays, qRT-PCR or RNAseq. Well-designed and validated siRNAs are selected based on their low to no off-target effects. In light of this, one simple solution to decrease off-target silencing is to use a pool of siRNAs that target different sequences in the same mRNA (Cullen, 2006). This approach minimizes the OTE contribution of each individual siRNA, while maximizing silencing of the target transcript that the pool of siRNAs have in common.

CHEMICAL MODIFICATION OF SYNTHETIC siRNAS

In the 15 years following Fire and Mello's ground-breaking work (Fire et al., 1998), siRNA-mediated gene silencing has become an indispensable tool for in vitro laboratory research; however, very few safe and effective siRNA delivery systems have reached the clinic for the treatment of human disease (Wittrup and Lieberman, 2015). The reason for this disparity between the success of siRNA delivery *in vitro* and *in vivo* is due to the nature of siRNA molecules themselves. In particular, as discussed above, siRNAs are highly susceptible to degradation by circulating ribonucleases, siRNAs can be immunostimulatory, siRNAs can induce knockdown genes other than the intended target, and siRNAs have poor pharmacokinectic profiles as discussed above (Jackson et al., 2003; Soutschek et al., 2004; Marques and Williams, 2005; Turner et al., 2007; Merkel et al., 2009). Fortunately, efficient and flexible synthetic chemistries have been developed that enable engineering siRNAs that overcome these difficulties through the incorporation of specific chemical modifications (Beaucage, 1992; Gao et al., 2009). Additionally, the modular synthesis of oligonucleotides allows for unparalleled control over the exact placement of chemical modifications on siRNAs.

However, the opportunities for chemical modification of siRNA are limited by the requirement that the biophysical characteristics of siRNAs must be strictly maintained to retain compatibility with the endogenous RNAi machinery (Behlke, 2008). Briefly, the RISC loading enzyme TRBP requires contact through its double-stranded RNA binding domains (DRBDs) with two minor grooves of A-form dsRNA by way of 2'-OHs and charged phosphodiester backbone (Yamashita et al., 2011; Vukovic et al., 2014). Argonaute-2 (Ago2), the catalytic core of slicing RISC, requires numerous interactions with the siRNA guide strand to activate RISC to cleave target mRNA, including the 5'-

phosphosphate binding to Ago2's MID pocket, 3'-OH binding to the Ago2 PAZ domain, and multiple contacts along the phosphodiester backbone of the guide strand (Schirle and MacRae, 2012; Schirle et al., 2016). These structural requirements allow for heavy modification at the 2' position, but render the siRNA phosphodiester backbone remains recalcitrant to chemical manipulation. However, a number of RNAi compatible chemical modifications have been identified for use on siRNA (**Figure 1.2**) (Behlke, 2008).

A remarkable variety of siRNA chemical modifications have been developed in the effort to improve siRNA performance, with these efforts benefitting from nearly two decades of research on antisense oligonucleotide (ASO) design and nucleotide modification (Kurreck, 2003). However, in contrast to ASOs, siRNA require more careful modification to not only maintain the ability of the two oligonucleotides to duplex, but also to remain compatible with the RNA-interacting proteins that comprise the core of RISC and TRBP loading enzymes. Therefore, to maintain potency, many of the chemical modifications used successfully in ASOs require alteration or very specific application to be integrated into the siRNA (Behlke, 2008). The majority of chemical modifications made to siRNAs can be classified into 3 categories: 1) modifications to or substitutions of the nucleotide ribose sugar, 2) modifications to the phosphodiester backbone, and 3) modifications to the nucleobase itself. However, the type of siRNA modification is secondary to the effect that the modification has on the properties and behavior of siRNAs, therefore this section will discuss siRNA modifications within the context of the barriers to in vivo siRNA delivery and which modifications may be useful for overcoming particular difficulties. An exhaustive review of all siRNA chemical modifications is beyond the scope of this introduction, but the subject has been well-reviewed in the literature (Behlke, 2008; Ge et al., 2010; Rettig and Behlke, 2012a; Juliano, 2016).

Modifications that enhance siRNA stability

Nucleic acids, particularly RNAs, are rapidly degraded in the extracellular environment by nucleases. Ribonuclease degradation of RNA proceeds by transesterification, in which the enzyme coordinates the ribose 2'-OH in a nucleophilic attack of the adjacent 3'-phosphate, hydrolyzing the RNA backbone and forming a 2',3'-cyclic phosphate in a two-step cleavage event (Usher, 1969). This mechanism suggests two obvious methods of increasing siRNA stability is serum: (1) replacement of the hydroxyl at the ribose 2'-position and (2) modification of the phosphodiester backbone. Modifications to the ribose 2'-position are perhaps the most extensively studied nucleic acid modification and it has been shown that a 2'-OH group is not required for siRNA-mediated RNAi, so long as the modification mimics the biophysical properties of a hydroxyl group (Chiu and Rana, 2003). A large variety of 2' modifications including 2'-deoxy (DNA), 2'-O-methyl (2'-OMe), 2'-fluoro (2'-F), and locked nucleic acids (LNA) have been applied to siRNA with varying results (**Figure 1.2A**).

2'-O-methyl (2'-OMe) (**Figure 1.2A**) is a naturally occurring RNA modification present in a variety of eukaryotic cellular RNAs (Kiss, 2002; Züst et al., 2011). 2'-OMe is the most commonly used and tested siRNA 2' modification and, as a natural modification, is nontoxic to human cells (Amarzguioui et al., 2003). Physically, the 2'-OMe protrudes further out into the siRNA minor groove and is more hydrophobic than endogenous hydrophilic 2'-OH. It also increases the melting temperature (T_m) of a siRNA duplex by reinforcing the preferred the 3'-endo "pucker" configuration of the ribose sugar in A-form dsRNA. The 2'-OMe modification confers significant nuclease resistance and an alternating pattern of 2'-OMe modifications increases siRNA stability to 24 hours in 10% human serum (Choung et al., 2006). Importantly, 2'-OMe modified siRNAs are well tolerated by the RNAi machinery, inducing an Ago2-dependent RNAi response with high potency. Indeed, the first successful *in vivo* gene knockdown was

achieved with 2'-OMe modified siRNA (Chiu and Rana, 2003; Soutschek et al., 2004; Choung et al., 2006; Kraynack and Baker, 2006). However, extensive or full 2'-OMe modification can reduce the potency of or completely eliminate the activity of an siRNA (Chiu and Rana, 2003).

2'-Fluoro (2'-F) is a well characterized and widely used non-natural siRNA modification (**Figure 1.2A**), that despite being a very hydrophobic modification, closely mimics the electronegativity and electron shell size of a 2'-OH. This similarity makes the 2'-F modification well tolerated and some fully 2'-F modified siRNAs can be as potent as unmodified siRNAs (Blidner et al., 2007). The 2'-F modification also strongly stabilizes siRNAs against RNase degradation (Layzer et al., 2004). Moreover, due to a further enhancement of reinforcing the 3'-endo confirmation, 2'-F also have an added benefit of increasing the melting temperature (T_m) by 1-2 degrees per insertion (Patra et al., 2012).

Bicyclic ribose ring structures, such as locked nucleic acids (LNAs), are a more radical modification where the 2'-O and the 4'-C of the ribose ring are connected by a methylene bridge (**Figure 1.2A**) (Braasch et al., 2003; Elmén et al., 2005). This methylene bridge "locks" the ribose ring into the preferred RNA 3'-endo confirmation that allows moderately LNA-modified siRNAs to induce RNAi responses with high potency while dramatically enhancing nuclease stability. However, extensive LNA modification of siRNAs decreases the siRNA knockdown efficiency, to a greater degree than 2'-OMe modifications. Due to this, the number of LNA substitutions should be kept to a minimum and excluded from the central region of siRNA. It should be noted that LNA and 2'-OMe modifications cannot be present on a siRNA passenger strand at the Ago2 cleavage site (opposite bases 10 and 11 of the guide strand) as these modifications prevent AGO2 cleavage of the passenger strand (Dallas et al., 2012). 2'-F

modifications, on the other hand, are well tolerated in the passenger strand cleavage site (Blidner et al., 2007).

Modification of the phosphodiester backbone of siRNA constitutes another well-studied means of increasing siRNA biostability by interfering with the mechanism of ribonuclease degradation (**Figure 1.2B**). The A-form structure of siRNAs is critical for maintaining potency and allowing interaction of proteins that comprise the RNAi machinery, particularly the RNA-binding protein TRBP. So phosphate backbone modifications that do not heavily impact the overall siRNA structure can be made. Phosphodiester backbone modifications have been used extensively in ASOs, but only a subset of these modifications are compatible with siRNA function (Kurreck, 2003; Aboul-Fadl, 2005). Amongst these, phosphorothioate (PS) modifications, where a single non-bridging oxygen of the phosphate backbone is replaced by a sulfur, are the most well-studied, due to the ease of PS synthesis and compatibility with siRNA function (**Figure 1.2B**). Although when used in moderation PS modifications can improve the stability of siRNA while maintaining high potency, extensive PS modification decreases silencing (Braasch et al., 2003; Chiu and Rana, 2003; Choung et al., 2006), likely due to impeding TRBP binding. Despite this, highly potent fully PS-modified siRNAs can be created by careful selection of the siRNA sequence (Lima et al., 2012). But this remains an exception and the vast majority of highly potent siRNAs have phosphodiester backbones, except for their ends.

Modifications that decrease siRNA immunogenicity

As discussed above, the innate immune system constitutes a significant obstacle to siRNA delivery that must be overcome for therapeutic siRNA application (Robbins et al., 2009). A number of strategies have been devised to reduce the immunogenicity of siRNAs through chemical modification. Endogenous mammalian rRNAs and tRNAs

avoid aberrant immune activation through post-transcriptional chemical modifications, including pseudouridine, N6-methyl-A and 2'-OMe. These and other chemical modifications can be synthesized into siRNAs to decrease immunogenicity in a similar manner (Chiu and Rana, 2003; Karikó et al., 2005). In fact, 2'-OMe modification of only 2 or 3 residues can prevent an immune response when placed on select rU and rG residues (Judge et al., 2006). Additionally, 2'-OMe modified siRNAs can act as competitive inhibitors of TLR7 and thereby protect siRNAs in cis or in trans, so that only one strand needs to be modified to prevent immune activation (Robbins et al., 2007).

2'-F and LNA modifications have also been found to be effective at preventing siRNA-triggered immune responses. Modification of only uridine residues with 2'-F abolished innate immune responses in peripheral blood mononuclear cells (PBMCs) and full 2'-F/OMe modified siRNAs delivered in vivo by SNALP liposome prevented induction of innate immune responses (Morrissey et al., 2005; Sioud, 2006). Fewer studies have looked at the effect of LNAs on immune induction. LNA modification at the 5' or 3' ends of siRNA abolishes immune responses in dendritic cells, but LNA incorporation in the guide strand strongly inhibits silencing activity (Hornung et al., 2005).

Reduction of off-target effects by chemical modification

Although siRNA targeting can be highly selective for discrimination of a single base with careful siRNA design, siRNAs can also induce knockdown of off-target mRNAs through Ago2-RISC-mediated silencing or through unintended participation in miRNA pathways (Huang et al., 2009; Vickers et al., 2009; Jackson and Linsley, 2010). Even with careful siRNA guide sequence selection, therapeutic applications of siRNA still require a reduction in siRNA OTEs, a function well-suited for siRNA chemical modifications.

As the seed region is the primary source of many OTEs, efforts have been made to limit seed region-related OTEs by using chemical modifications to destabilize the seed region while maintaining on-target efficiency. A screen of 10 siRNA chemical modifications to reduce OTEs identified unlocked nucleic acids (UNAs) as particularly effective at reducing OTEs when placed at position 7 in the seed region of the guide strand (Bramsen et al., 2010; Vaish et al., 2011). UNAs are an exotic base modification that lacks the C2-C3 bond of the ribose ring (**Figure 1.2A**) (Langkjaer et al., 2009). Incorporation of UNAs into siRNA destabilizes the duplex locally, with each UNA insertion decreasing the T_m by 5-8°C. This duplex destabilization severely limits the number of UNA modifications that can be made to siRNA strands and UNAs are not well tolerated in many positions of the guide strand (Kenski et al., 2010; Laursen et al., 2010). Consequently, they are rarely used, but when used it is in the Seed domain to mitigate OTEs.

2'-OMe and DNA modifications have also been found to reduce OTEs when inserted into the guide strand Seed region. Placement of a single 2'-OMe residue in the Seed region at the position 2 of the guide strand significantly decreased Seed region-associated OTEs (Jackson et al., 2006). However, a 2'-OMe at position 2 on the guide strand was also found to reduce potency in certain sequences, suggesting that this technique cannot be applied universally to all siRNA sequences. A study by Ui-Tei and colleagues demonstrated that replacement of the entire seed region with DNA residues reduced seed region-associated OTEs while still maintaining siRNA on-target potency (Ui-Tei et al., 2008). However, this appears to be a rare exception for siRNAs as DNA bases push the double-stranded structure to B-form, rather than A-form. Moreover, TRBP makes multiple strong contacts with the 2'-OH in opposing minor grooves and the insertion of DNA dramatically reduces TRBP binding and recognition.

siRNAs have two strands, but incorporation of only the guide strand into RISC is the goal. Unintended loading of the passenger strand into RISC can comprise a significant source of OTEs (Clark et al., 2008). Exacting study of RISC and associated siRNAs has revealed methods of siRNA design that facilitate preferential loading of the intended guide strand, but the bias established by these methods is in no way complete as some passenger strand will still be loaded into RISC (Ui-Tei et al., 2012). In light of this, a number of approaches have been devised to prevent passenger strand incorporation into RISC. It should be noted that preventing passenger strand loading into RISC will not only decrease OTEs, but will also increase the overall potency of an siRNA by preventing loss of siRNAs loading into RISC in the opposite orientation.

Chemical modification of the passenger strand can be used to prevent loading into RISC. While siRNAs are synthesized with 5'-OHs on both the passenger and guide strands, a 5'-PO_4 is necessary for Ago2 loading (Schirle and MacRae, 2012). However, synthetic siRNAs with 5'-OHs are rapidly converted intracellularly by the RNA kinase CLP1 into 5'-PO_4s that are compatible with Ago2 loading (Weitzer and Martinez, 2007). It is therefore possible to prevent passenger strand loading into RISC by blocking phosphorylation of the passenger strand 5'-terminus. 5'-O-methylation has been shown to decrease passenger strand-related OTEs by blocking phosphorylation of the passenger strand (Chen et al., 2008). Prevention of passenger loading and associated OTEs has also been accomplished by the incorporation of LNA and UNA residues at the 5' end of the passenger strand (Elmén et al., 2005; Vaish et al., 2011).

Chemical modification is necessary for the development of safe and efficacious siRNA therapeutics. Indeed, all contemporary siRNA drugs under clinical consideration are heavily chemically modified (Rettig and Behlke, 2012a; Sehgal et al., 2015; Juliano, 2016). While a great number of siRNA chemical modifications have been characterized,

most function only in certain sequence-specific contexts. For this reason LNA, UNA, and 2'-deoxy modifications are seldom utilized in therapeutic siRNAs. siRNAs currently under evaluation in clinical trials are partially or fully modified with 2'-F and 2'-OMe groups due to their close mimicry of a 2'OH and compatibility with the RNAi machinery. Additionally, backbone phosphorothioate modification is common in therapeutic candidates to enhance stability, but only at select positions on siRNA, such as the 3' and 5' ends, as phosphorothioates can inhibit critical interactions with RNAi proteins. While these chemical modifications address issues of increased siRNA stability, reduced innate immune activation, and reduction in OTEs, they do not allow for the self-delivery of siRNA and a delivery agent is still required.

siRNA DELIVERY STRATEGIES

Nanoparticle delivery of siRNA

As mentioned previously, siRNAs are pharmacokinetically unfavorable molecules and a variety of barriers make *in vivo* delivery of naked siRNA unfeasible (**Figure 1.1**). In light of these issues, a wide variety of siRNA delivery strategies have been developed. The majority of these strategies involve nanoparticle-based delivery systems where the siRNA is encapsulated by synthetic cationic lipids or polymers. Describing the full extent of published siRNA delivery approaches is beyond the scope of this introduction, but has been well reviewed in the literature (Whitehead et al., 2009; Alabi et al., 2012; Rettig and Behlke, 2012b; Wittrup and Lieberman, 2015; Zatsepin et al., 2016).

Nanoparticle delivery of siRNAs grew from efforts made in the years prior to the discovery of RNAi for non-viral mediated gene therapy and antisense oligonucleotide therapy (Meade and Dowdy, 2009). Once mammalian RNAi was shown to occur (Elbashir et al., 2001b), these platforms were rapidly adapted for siRNA delivery. A multitude of different compounds have been utilized for nanoparticle formulation,

including lipids, polymers, and inorganic materials (Zhou et al., 2013). In general, nanoparticle-based delivery systems are delivery agents that condense siRNAs into particles in the size range of hundreds of nanometers. The principal nanoparticle packaging strategy utilizes the electrostatic interaction between cationic polymers or lipids to compact ~100 siRNA molecules into large nanoparticles. The agents that comprise the packing formulation are varied to generate particles of the desired characteristics, but most approaches involve the addition of 4-5 components at exacting ratios, each with their own cytotoxicity profiles (Schroeder et al., 2010). In addition to cationic agents necessary for siRNA nanoparticle packaging, a variety of other delivery and targeting motifs such as antibodies, ligands, and peptide transduction domains (PTDs) can be introduced onto the surface of particles to add unique features (Zhou et al., 2013; Farkhani et al., 2014; Zatsepin et al., 2016), but also further increase the overall size.

Encapsulation of siRNAs in these non-covalent, self-assembling complexes addresses several of the problems associated with *in vivo* siRNA delivery. Encapsulation of siRNAs within nanoparticles prevents access of circulating ribonucleases to the siRNA, thereby greatly increasing the half-life of siRNA *in vivo* (Schroeder et al., 2010). In addition, the large size and hydrophobic nature of nanoparticles both prevents the renal filtration that systemically administered naked siRNA are normally subjected to and facilitates interactions with serum factors that prolong circulation time. This enhanced circulation time increases the probability of engaging target cells and delivering siRNA cargo across the cell membrane.

Although nanoparticle siRNA delivery strategies address several of the problems opposing siRNA delivery, the approach has inherent and inescapable flaws that preclude its widespread use. First and foremost is the size of the nanoparticles themselves. On a

human scale ‘nano’ means very small, but on the molecular scale, the nanoparticles utilized for siRNA delivery are on the order of 100,000,000 Da in size, which is 5,000-fold larger than the siRNA drug. The ~100 nm size of nanoparticles is well beyond the size of normal blood vessel fenestrations (Sarin, 2010), which complicates extravasation into many potential organs and generates inherently poor diffusion coefficients *in vivo*. Although too large to be subject to renal filtration, nanoparticle size and biophysical properties result in clearance by the hepatic reticuleoendothelial system (Akinc et al., 2009; Schroeder et al., 2010). While this facilitates delivery to liver hepatocytes, it severely limits extra-hepatic delivery of siRNA by nanoparticles to other tissues.

The process required to formulate nanoparticles of homogeneous size is difficult, requiring exacting ratios of multiple compounds and siRNAs, as well as precise timing and condensation conditions (Schroeder et al., 2010). Additionally, each of the non-natural polymers and lipids used in nanoparticle generation can induce cytotoxic and immune responses, necessitating transient immune suppression with steroids in the clinic. Because nanoparticles are essentially noncovalent aggregates, maintaining nanoparticle size can also be problematic due to shedding of components in solution. Indeed, "100 nm" nanoparticles actually range in size from 60 to 180 nm and merely have a mode at 100 nm.

To avoid the problems inherent in nanoparticle-based formulations, our lab sought to develop a siRNA delivery strategy that avoids encapsulation of siRNA into large particles. We hypothesized that a more favorable pharmacokinetic profile and higher potency could be achieved if synthetic siRNA molecules were delivered as a monomeric, soluble drug, thereby bypassing the barriers to *in vivo* delivery that are inescapable for nanoparticle-based delivery systems. For this purpose, we turned to a cellular delivery tool for macromolecules that our laboratory has extensive experience: a

diverse class of small cationic delivery peptides known as protein transduction domains (PTDs).

PTD-mediated delivery of siRNA

A promising approach to deliver macromolecules is by use of PTDs (Lönn and Dowdy, 2015). The first evidence that PTDs could deliver macromolecules inside of cells by a process termed transduction, came in 1988 from Frankel and Pabo, with the observation that full-length HIV-1 Trans-Activator of Transcription (TAT) protein could translocate into cells and modulate transcription of the HIV-1 promoter (Frankel and Pabo, 1988; Green and Loewenstein, 1988). Subsequent experimentation led to the determination of a minimal 9 amino acid, arginine rich TAT-PTD was responsible for transduction (Ezhevsky et al., 1997; Vives, 1997). Since the identification of TAT-PTD, more than 100 different PTD variants have been discovered and engineered from chimeric and synthetic peptides including Penetratin, Transportan, and many others (Derossi et al., 1994; Pooga et al., 2001; Lindgren and Langel, 2011; Marín et al., 2011; Koren and Torchilin, 2012). The most successful PTDs contain patches of 4-9 basic arginine residues (van den Berg and Dowdy, 2011).

PTDs have been employed to deliver a multitude of different macromolecular cargos including peptides and proteins, antisense nucleic acids, charge neutral peptide nucleic acids (PNAs) and morpholinos (PMOs), and even iron beads (Schwarze, 1999; Lewin et al., 2000; Gait, 2003; Wadia and Dowdy, 2005; van den Berg and Dowdy, 2011). This wide range of cargo, both in type and size emphasizes the versatility that PTDs offer for delivery into cells. The potential of PTD-mediated *in vivo* delivery was realized in the late 1990s when our lab generated a TAT-PTD recombinant fusion protein with β-galactosidase (βgal) and administered it to mice (Schwarze, 1999). Following intraperitoneal injection, the TAT-βgal was delivered into most tissues of the

treated mice, including the brain. Importantly, βgal without the TAT-PTD lacked bioavailability and was not taken up into any tissues.

The uptake mechanism of PTDs differs by the PTD used and the type of cell tested, but endocytosis appears to be the predominant mechanism of internalization (Wadia et al., 2004; Foerg et al., 2005). Macropinocytosis, a specialized form of fluid phase endocytosis, has been found to be the primary method of internalization for Arginine containing PTDs, TAT and octa-arginine (R8) (Nakase et al., 2004; Wadia et al., 2004). Following internalization by endocytosis, PTDs and cargo must translocate across the endocytic membrane to access the intracellular environment. While the biophysical mechanism of transduction across the lipid bilayer is still under debate, studies have found evidence for PTD-mediated disruption of the endocytic membrane, escape utilizing the inherent leakiness of some endosomes, and retrograde transport of PTD-containing endocytic bodies (Fischer et al., 2004; Rothbard et al., 2005; Kawamura et al., 2006). Additionally, PTDs do not merely bind to the cell surface and await constitutive endocytosis. Instead, PTDs induce cellular uptake upon binding to the cell surface by a mechanism that is independent of heparan sulfate proteoglycan binding (Gump et al., 2010). In summary, PTDs perform two critical delivery functions: 1) stimulation of their own uptake by endocytosis and 2) facilitating escape from endosomes.

Although PTDs have been employed to deliver a variety of macromolecular cargo *in vitro*, *in vivo*, and in >25 clinical trials, few studies have reported successful delivery of siRNAs into cells using PTDs (Wadia and Dowdy, 2005; Lönn and Dowdy, 2015). Two approaches have been developed for PTD-mediated siRNA delivery: 1) Noncovalent complexing of PTDs and siRNA into nanoparticles by electrostatic interaction between the two types of molecules, and 2) covalent attachment of PTDs to siRNAs through

disulfide bond formation. The first method, while relatively simple in a technical sense, suffers from many of the problems associated with other nanoparticle delivery systems. Mixing of cationic PTDs with anionic siRNAs results in aggregation into large nanoparticles (Nakase et al., 2013). The covalent attachment method is more ideal in that it has the potential to produce small, monomeric, and soluble PTD-siRNA molecules; however, it comes with its own share of problems (Glover et al., 2005). The dense cationic charge of some PTDs is crucial to their ability to transduce across the cell membrane (Gonçalves et al., 2005). When cationic PTDs and charged siRNA are covalently linked, the PTD is effectively neutralized and unable to mediate cellular internalization (Jiang et al., 2004). Moreover, just like non-covalent PTDs plus siRNAs, due to charge-charge interactions, PTD-siRNA conjugates form large aggregates. With this in mind, work was begun to find a method of neutralizing the siRNA's negative charge so that it could be delivered into cells in a monomeric form by a covalently conjugated PTD.

Due to the 40 negative charges on of phosphodiester backbone, conjugation of siRNAs to a cationic PTD (6-8 positive charges) leads to neutralization of the PTD, aggregation of the conjugate, and no cellular delivery (Moschos et al., 2007). To circumvent this problem, our lab developed a TAT PTD fusion protein with a dsRNA Binding Domain (DRBD) termed PTD-DRBD (Eguchi et al., 2009). This fusogenic peptide binds to and physically masks the siRNA's negative charges, thereby allowing for efficient, non-cytotoxic PTD-mediated delivery into an entire population of cells. With the siRNA's negative charge neutralized by the DRBD, the fused TAT-PTD was able to deliver the siRNA in the same manner as a neutral macromolecular peptide or protein cargo. PTD-DRBD successfully delivered siRNA *in vitro* and induce an RNAi response in a variety of tested cell types (**Figure 1.1**). Additionally, PTD-DRBD plus EGFR and

Akt2 siRNAs were able to induce an *in vivo* tumor-specific synthetic lethal RNAi response that resulted in a significant increase in survival when administered to intracerebral glioblastoma mouse models (Michiue et al., 2009).

While the PTD-DRBD siRNA delivery approach effectively demonstrated PTD-mediated delivery of siRNA to cells, there was an inherent flaw in the strategy: at high siRNA concentrations needed for systemic delivery, the PTD and DRBD domains are able to independently contact multiple siRNAs, leading to aggregation, precipitation, and reducing its therapeutic utility. Despite these problems, the TAT-DRBD siRNA delivery system taught us that masking the siRNA negative charge allows for PTDs to properly mediate efficient cell delivery (Eguchi et al., 2009). With these lessons in mind, our lab pursued a new, strictly synthetic approach to neutralize the siRNA's prohibitive negative charge by phosphotriester modifications.

SMALL INTERFERING RIBONUCLEIC NEUTRALS (siRNNS)

To test directly test the hypothesis of PTD-mediated charge neutral siRNA delivery and to examine the degree that the negatively charged siRNA phosphodiester backbone must be neutralized to facilitate PTD-mediated delivery, the lab performed experiments with surrogate siRNA oligonucleotides neutralized with irreversible methyltriester modifications (Meade, 2010). The RNAi machinery requires siRNAs with native charged phosphodiester backbones for the induction of RNAi responses (Behlke, 2008; Schirle and MacRae, 2012; Vukovic et al., 2014), therefore any modifications made to the siRNA phosphodiester backbone must be bioreversible. However, the neutralizing methyltriester modifications utilized for these experiments were non-bioreversible and, as such, methyltriester containing siRNAs were used as surrogates to study delivery, but were unable to induce RNAi responses. Methyltriester modifications

were chosen due to their compatibility with standard oligonucleotide synthesis, commercial availability and of course, being a neutral charge. A collection of cyanine dye (Cy3) labeled siRNAs containing various numbers of methyltriester groups were synthesized. The methyltriester Cy3-siRNAs were then conjugated to TAT-PTDs through a stable hydrazone linkage and used to treat cells. Treated cells were thoroughly washed and trypsinized to remove surface-bound material and then analyzed by flow cytometry to examine siRNA uptake. Under these conditions, only PTD-siRNA conjugates with sufficient charge neutralization accumulated in cells, predominantly in endosomes. Interestingly, treatment of cells with methyltriester-neutralized PTD-siRNA conjugates showed positive Cy3 cell association only when the conjugate and had a theoretical overall positive charge. Together, these key experiments demonstrated that ~70% phosphodiester neutralization was necessary for PTD-mediated delivery of neutralized siRNAs.

The strategy to neutralize active siRNA phosphodiester backbones required that the phosphotriesters were bioreversible, so that upon delivery into the cytoplasm, they would be enzymatically converted into native charged phosphodiester containing siRNAs that are compatible with the RNAi machinery. For this purpose we choose to use a *t*-butyl-S-acyl-2-thioethyl (*t*Bu-SATE) phosphotriester group that was originally developed for mononucleoside inhibitors of HIV (Lefebvre et al., 1995; Gröschel et al., 2002). The bioreversibility of the *t*Bu-SATE phosphotriester is made possible through processing by cytoplasm-restricted thioesterases (Zeidman et al., 2009). Cleavage by thioesterase initiates a rapid two step conversion of the neutral *t*Bu-SATE phosphotriester group into a native charged phosphodiester that is fully compatible with RNAi machinery (**Figure 1.3**). Although the *t*Bu-SATE group perfectly fit the requirements for siRNA phosphodiester charge neutralization, due to an abundance of synthetic issues that

required orthogonal solutions, it had never been successfully applied to siRNA or oligonucleotide synthesis. Through years of research and development, our lab developed orthogonal solutions to each synthesis problem and completed the first groundbreaking synthesis of *t*Bu-SATE siRNA prodrugs, that we termed short interfering ribonucleic neutrals (siRNNs).

Importantly, *t*Bu-SATE siRNNs were bioreversible and capable of inducing robust, dose-dependent RNAi responses upon transfection into cells (**Figure 1.1**). *t*Bu-SATE siRNNs were also stable for > 24 hours in human serum and did not induce innate immune responses, thereby effectively addressing two prominent issues for *in vivo* siRNA delivery. However extensive experimentation revealed fundamental problems with the use of *t*Bu-SATE siRNNs for PTD-mediated delivery. Steric congestion between *t*Bu-SATE phosphotriesters in the siRNA major groove limited phosphodiester neutralization to < 50%, insufficient for PTD-mediated delivery of *t*Bu-SATE siRNNs. Furthermore, the hydrophobicity of the *t*-butyl moiety made *t*Bu-SATE siRNNs insoluble in biologically compatible solutions and prevented efficient PTD conjugation.

In summary, our lab's work with PTD-DRBD demonstrated the potential for PTD-mediated delivery of siRNA if the anionic character of the siRNA can be masked. Work with surrogate methyltriester-neutralized PTD-siRNA conjugates supported the hypothesis that PTDs can deliver siRNA if the anionic phosphodiester backbone if sufficiently modified synthetically with neutralizing phosphotriester groups. Finally, experimentation with *t*Bu-SATE siRNNs showed that siRNAs could be synthesized with bioreversible neutralizing phosphotriester groups and that these groups could be converted intracellularly into charged phosphodiesters compatible with the RNAi machinery.

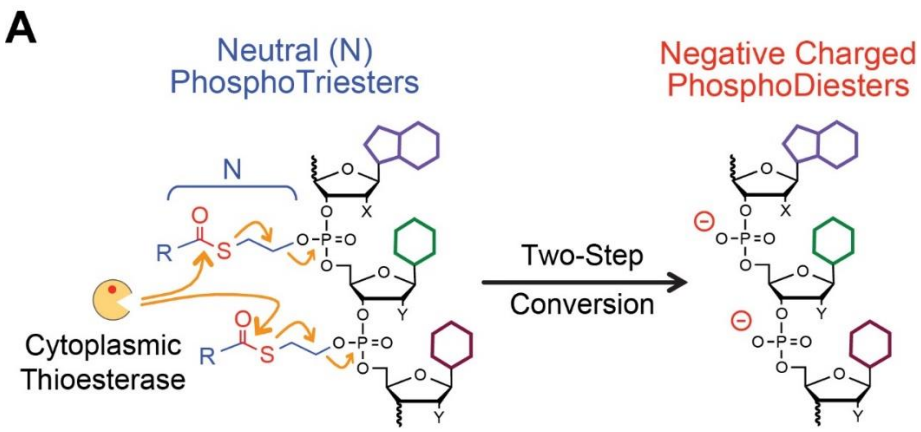

Figure 1.3. Bioreversal of neutralizing phosphotriesters. A) Phosphotriester cleavage by cytoplasmic thioesterase initiates a two-step conversion that resolves into a charged phosphodiester linkage which is fully compatible with the RNAi machinery.

CONCLUSIONS

The discovery that synthetic siRNAs could induce RNAi responses in human cells created the potential for development of an entirely new class of drugs for the treatment of human disease: RNAi therapeutics. Unfortunately, the 14,000 Da size and highly anionic character of siRNA prevent cellular delivery and limit the use of siRNA as a therapeutic. A varied toolbox of siRNA chemical modifications has been developed to enhance ribonuclease stability, prevent innate immune activation, and reduce off-target effects. Chemical modification is necessary for the use of siRNA *in vivo*, but modified siRNA still require the assistance of a delivery agent to enter cells. An enormous variety of nanoparticle-based siRNA delivery strategies have been published and while some have shown success in animal models, nanoparticles approaches suffer from inescapable limitations and with the exception of liver hepatocyte delivery, have grossly failed in clinical trials. To bypass the *in vivo* barriers faced by nanoparticle-based siRNA delivery, our laboratory sought an alternative approach where siRNA molecules are delivered as soluble, monomeric drugs by cationic PTDs. To enable cationic PTD-mediated delivery, the anionic phosphodiester backbone of siRNAs must first be neutralized. PTD-DRBD constituted the first attempt at this siRNA delivery approach and its ability to deliver siRNAs into cells demonstrated the feasibility of this approach. The development of siRNNs containing neutralizing bioreversible *t*Bu-SATE phosphotriester groups capable of inducing RNAi responses upon cellular delivery brought this approach closer to fruition. The next step must be the development of a bioreversible phosphotriester groups that can neutralize the charge of the siRNA phosphate backbone without suffering from the hydrophobic issues associated with the *t*Bu-SATE and, in doing so, allow greater phosphodiester neutralization and efficient conjugation to PTDs for cellular delivery. For this purpose we synthesized the O-SATE

phosphotriester that contains a terminal hydroxyl group (**Chapter 3**) and the Amino-SATE (N-SATE) that contains a primary amine (Meade, 2010).

REFERENCES

Aboul-Fadl, T. (2005). Antisense oligonucleotides: the state of the art. Curr. Med. Chem. *12*, 2193–2214.

Akinc, A., Goldberg, M., Qin, J., Dorkin, J.R., Gamba-Vitalo, C., Maier, M., Jayaprakash, K.N., Jayaraman, M., Rajeev, K.G., Manoharan, M., Koteliansky, V., Röhl, I., Leshchiner, E.S., Langer, R., and Anderson, D.G. (2009). Development of lipidoid-siRNA formulations for systemic delivery to the liver. Mol. Ther. *17*, 872–879.

Alabi, C., Vegas, A., and Anderson, D. (2012). Attacking the genome: emerging siRNA nanocarriers from concept to clinic. Curr. Opin. Pharmacol.

Amarzguioui, M., Holen, T., Babaie, E., and Prydz, H. (2003). Tolerance for mutations and chemical modifications in a siRNA. Nucleic Acids Res. *31*, 589–595.

Anderson, E.M., Birmingham, A., Baskerville, S., Reynolds, A., Maksimova, E., Leake, D., Fedorov, Y., Karpilow, J., and Khvorova, A. (2008). Experimental validation of the importance of seed complement frequency to siRNA specificity. RNA *14*, 853–861.

Beaucage, S. (1992). Advances in the Synthesis of Oligonucleotides by the Phosphoramidite Approach. Tetrahedron *48*, 2223–2311.

Behlke, M.A. (2008). Chemical modification of siRNAs for in vivo use. Oligonucleotides *18*, 305–319.

van den Berg, A., and Dowdy, S.F. (2011). Protein transduction domain delivery of therapeutic macromolecules. Curr. Opin. Biotechnol. 6–11.

Bernstein, E., Caudy, A.A., Hammond, S.M., and Hannon, G.J. (2001). Role for a bidentate ribonuclease in the initiation step of RNA interference. Nature *409*, 363–366.

Birmingham, A., Anderson, E.M., Reynolds, A., Ilsley-Tyree, D., Leake, D., Fedorov, Y., Baskerville, S., Maksimova, E., Robinson, K., Karpilow, J., Marshall, W.S., and Khvorova, A. (2006). 3’ UTR seed matches, but not overall identity, are associated with RNAi off-targets. Nat. Methods *3*, 199–204.

Blain, J.C., and Szostak, J.W. (2014). Progress toward synthetic cells. Annu. Rev. Biochem. *83*, 615–640.

Blidner, R.A., Hammer, R.P., Lopez, M.J., Robinson, S.O., and Monroe, W.T. (2007). Fully 2’-deoxy-2’-fluoro substituted nucleic acids induce RNA interference in mammalian cell culture. Chem. Biol. Drug Des. *70*, 113–122.

Braasch, D. a, Jensen, S., Liu, Y., Kaur, K., Arar, K., White, M. a, and Corey, D.R. (2003). RNA interference in mammalian cells by chemically-modified RNA. Biochemistry *42*, 7967–7975.

Bramsen, J.B., and Kjems, J. (2011). Chemical modification of small interfering RNA. Methods Mol. Biol. *721*, 77–103.

Bramsen, J.B., Pakula, M.M., Hansen, T.B., Bus, C., Langkjær, N., Odadzic, D., Smicius, R., Wengel, S.L., Chattopadhyaya, J., Engels, J.W., Herdewijn, P., Wengel, J., and Kjems, J. (2010). A screen of chemical modifications identifies position-specific modification by UNA to most potently reduce siRNA off-target effects. Nucleic Acids Res. *38*, 5761–5773.

Carthew, R.W., and Sontheimer, E.J. (2009a). Origins and Mechanisms of miRNAs and siRNAs. Cell *136*, 642–655.

Carthew, R.W., and Sontheimer, E.J. (2009b). Origins and Mechanisms of miRNAs and siRNAs. Cell *136*, 642–655.

Chen, P.Y., Weinmann, L., Gaidatzis, D., Pei, Y., Zavolan, M., Tuschl, T., and Meister, G. (2008). Strand-specific 5'-O-methylation of siRNA duplexes controls guide strand selection and targeting specificity. RNA *14*, 263–274.

Chendrimada, T.P., Gregory, R.I., Kumaraswamy, E., Norman, J., Cooch, N., Nishikura, K., and Shiekhattar, R. (2005). TRBP recruits the Dicer complex to Ago2 for microRNA processing and gene silencing. Nature *436*, 740–744.

Chiu, Y.-L., and Rana, T.M. (2003). siRNA function in RNAi: a chemical modification analysis. RNA *9*, 1034–1048.

Choung, S., Kim, Y.J., Kim, S., Park, H.-O., and Choi, Y.-C. (2006). Chemical modification of siRNAs to improve serum stability without loss of efficacy. Biochem. Biophys. Res. Commun. *342*, 919–927.

Clark, P.R., Pober, J.S., and Kluger, M.S. (2008). Knockdown of TNFR1 by the sense strand of an ICAM-1 siRNA: dissection of an off-target effect. Nucleic Acids Res. *36*, 1081–1097.

Cullen, B.R. (2006). Enhancing and confirming the specificity of RNAi experiments. Nat. Methods *3*, 677–681.

Dallas, A., Ilves, H., Ge, Q., Kumar, P., Shorenstein, J., Kazakov, S.A., Cuellar, T.L., McManus, M.T., Behlke, M.A., and Johnston, B.H. (2012). Right- and left-loop short shRNAs have distinct and unusual mechanisms of gene silencing. Nucleic Acids Res. *40*, 9255–9271.

Derossi, D., Joliot, A.H., Chassaing, G., and Prochiantz, A. (1994). The third helix of the Antennapedia homeodomain translocates through biological membranes. J. Biol. Chem. *269*, 10444–10450.

Doherty, G.J., and McMahon, H.T. (2009). Mechanisms of endocytosis. Annu. Rev. Biochem. *78*, 857–902.

Dominska, M., and Dykxhoorn, D.M. (2010). Breaking down the barriers: siRNA delivery

and endosome escape. J. Cell Sci. *123*, 1183–1189.

Eguchi, A., Meade, B.R., Chang, Y.-C., Fredrickson, C.T., Willert, K., Puri, N., and Dowdy, S.F. (2009). Efficient siRNA delivery into primary cells by a peptide transduction domain-dsRNA binding domain fusion protein. Nat. Biotechnol. *27*, 567–571.

Elbashir, S.M., Harborth, J., Lendeckel, W., Yalcin, A., Weber, K., and Tuschl, T. (2001a). Duplexes of 21-nucleotide RNAs mediate RNA interference in cultured mammalian cells. Nature *411*, 494–498.

Elbashir, S.M., Harborth, J., Lendeckel, W., Yalcin, A., Weber, K., and Tuschl, T. (2001b). Duplexes of 21-nucleotide RNAs mediate RNA interference in cultured mammalian cells. Nature *411*, 494–498.

Elmén, J., Thonberg, H., Ljungberg, K., Frieden, M., Westergaard, M., Xu, Y., Wahren, B., Liang, Z., Ørum, H., Koch, T., and Wahlestedt, C. (2005). Locked nucleic acid (LNA) mediated improvements in siRNA stability and functionality. Nucleic Acids Res. *33*, 439–447.

Ender, C., and Meister, G. (2010). Argonaute proteins at a glance. J. Cell Sci. *123*, 1819–1823.

Ezhevsky, S.A., Nagahara, H., Vocero-Akbani, A.M., Gius, D.R., Wei, M.C., and Dowdy, S.F. (1997). Hypo-phosphorylation of the retinoblastoma protein (pRb) by cyclin D:Cdk4/6 complexes results in active pRb. Proc. Natl. Acad. Sci. U. S. A. *94*, 10699–10704.

Farkhani, S.M., Valizadeh, A., Karami, H., Mohammadi, S., Sohrabi, N., and Badrzadeh, F. (2014). Cell penetrating peptides: efficient vectors for delivery of nanoparticles, nanocarriers, therapeutic and diagnostic molecules. Peptides *57*, 78–94.

Fire, A., Xu, S., Montgomery, M.K., Kostas, S.A., Driver, S.E., and Mello, C.C. (1998). Potent and specific genetic interference by double-stranded RNA in Caenorhabditis elegans. Nature *391*, 806–811.

Fischer, R., Köhler, K., Fotin-Mleczek, M., and Brock, R. (2004). A stepwise dissection of the intracellular fate of cationic cell-penetrating peptides. J. Biol. Chem. *279*, 12625–12635.

Foerg, C., Ziegler, U., Fernandez-Carneado, J., Giralt, E., Rennert, R., Beck-Sickinger, A.G., and Merkle, H.P. (2005). Decoding the entry of two novel cell-penetrating peptides in HeLa cells: lipid raft-mediated endocytosis and endosomal escape. Biochemistry *44*, 72–81.

Frankel, A.D., and Pabo, C.O. (1988). Cellular uptake of the tat protein from human immunodeficiency virus. Cell *55*, 1189–1193.

Gabel, H.W., and Ruvkun, G. (2008). The exonuclease ERI-1 has a conserved dual role in 5.8S rRNA processing and RNAi. Nat. Struct. Mol. Biol. *15*, 531–533.

Gait, M.J. (2003). Peptide-mediated cellular delivery of antisense oligonucleotides and their analogues. Cell. Mol. Life Sci. *60*, 844–853.

Gao, S., Dagnaes-Hansen, F., Nielsen, E.J.B., Wengel, J., Besenbacher, F., Howard, K.A., and Kjems, J. (2009). The effect of chemical modification and nanoparticle formulation on stability and biodistribution of siRNA in mice. Mol. Ther. *17*, 1225–1233.

Ge, Q., Dallas, A., Ilves, H., Shorenstein, J., Behlke, M.A., and Johnston, B.H. (2010). Effects of chemical modification on the potency, serum stability, and immunostimulatory properties of short shRNAs. RNA *16*, 118–130.

Gilleron, J., Querbes, W., Zeigerer, A., Borodovsky, A., Marsico, G., Schubert, U., Manygoats, K., Seifert, S., Andree, C., Stöter, M., Epstein-Barash, H., Zhang, L., Koteliansky, V., Fitzgerald, K., Fava, E., Bickle, M., Kalaidzidis, Y., Akinc, A., Maier, M., and Zerial, M. (2013). Image-based analysis of lipid nanoparticle-mediated siRNA delivery, intracellular trafficking and endosomal escape. Nat. Biotechnol. *31*, 638–646.

Glover, D.J., Lipps, H.J., and Jans, D.A. (2005). Towards safe, non-viral therapeutic gene expression in humans. Nat. Rev. Genet. *6*, 299–310.

Gonçalves, E., Kitas, E., and Seelig, J. (2005). Binding of oligoarginine to membrane lipids and heparan sulfate: structural and thermodynamic characterization of a cell-penetrating peptide. Biochemistry *44*, 2692–2702.

Green, M., and Loewenstein, P.M. (1988). Autonomous functional domains of chemically synthesized human immunodeficiency virus tat trans-activator protein. Cell *55*, 1179–1188.

Gröschel, B., Cinatl, J., Périgaud, C., Gosselin, G., Imbach, J.-L., and Doerr, H.W. (2002). S-acyl-2-thioethyl (SATE) pronucleotides are potent inhibitors of HIV-1 replication in T-lymphoid cells cross-resistant to deoxycytidine and thymidine analogs. Antiviral Res. *53*, 143–152.

Gump, J.M., June, R.K., and Dowdy, S.F. (2010). Revised role of glycosaminoglycans in TAT protein transduction domain-mediated cellular transduction. J. Biol. Chem. *285*, 1500–1507.

Haupenthal, J., Baehr, C., Kiermayer, S., Zeuzem, S., and Piiper, A. (2006). Inhibition of RNAse A family enzymes prevents degradation and loss of silencing activity of siRNAs in serum. Biochem. Pharmacol. *71*, 702–710.

Heil, F., Hemmi, H., Hochrein, H., Ampenberger, F., Kirschning, C., Akira, S., Lipford, G., Wagner, H., and Bauer, S. (2004). Species-specific recognition of single-stranded RNA via toll-like receptor 7 and 8. Science *303*, 1526–1529.

Heyam, A., Lagos, D., and Plevin, M. (2015). Dissecting the roles of TRBP and PACT in double-stranded RNA recognition and processing of noncoding RNAs. Wiley Interdiscip. Rev. RNA *6*, 271–289.

Hobbs, S.K., Monsky, W.L., Yuan, F., Roberts, W.G., Griffith, L., Torchilin, V.P., and Jain, R.K. (1998). Regulation of transport pathways in tumor vessels: role of tumor type and microenvironment. Proc. Natl. Acad. Sci. U. S. A. *95*, 4607–4612.

Hoerter, J.A.H., Krishnan, V., Lionberger, T.A., and Walter, N.G. (2011). siRNA-like double-stranded RNAs are specifically protected against degradation in human cell extract. PLoS One *6*, e20359.

Hornung, V., Guenthner-Biller, M., Bourquin, C., Ablasser, A., Schlee, M., Uematsu, S., Noronha, A., Manoharan, M., Akira, S., de Fougerolles, A., Endres, S., and Hartmann, G. (2005). Sequence-specific potent induction of IFN-alpha by short interfering RNA in plasmacytoid dendritic cells through TLR7. Nat. Med. *11*, 263–270.

Huang, H., Qiao, R., Zhao, D., Zhang, T., Li, Y., Yi, F., Lai, F., Hong, J., Ding, X., Yang, Z., Zhang, L., Du, Q., and Liang, Z. (2009). Profiling of mismatch discrimination in RNAi enabled rational design of allele-specific siRNAs. Nucleic Acids Res. *37*, 7560–7569.

Huotari, J., and Helenius, A. (2011). Endosome maturation. EMBO J. *30*, 3481–3500.

Jackson, A.L., and Linsley, P.S. (2010). Recognizing and avoiding siRNA off-target effects for target identification and therapeutic application. Nat. Rev. Drug Discov. *9*, 57–67.

Jackson, A.L., Bartz, S.R., Schelter, J., Kobayashi, S. V, Burchard, J., Mao, M., Li, B., Cavet, G., and Linsley, P.S. (2003). Expression profiling reveals off-target gene regulation by RNAi. Nat. Biotechnol. *21*, 635–637.

Jackson, A.L., Burchard, J., Leake, D., Reynolds, A., Schelter, J., Guo, J., Johnson, J.M., Lim, L., Karpilow, J., Nichols, K., Marshall, W., Khvorova, A., and Linsley, P.S. (2006). Position-specific chemical modification of siRNAs reduces “off-target” transcript silencing. RNA *12*, 1197–1205.

Jeong, J.H., Mok, H., Oh, Y.-K., and Park, T.G. (2009). siRNA conjugate delivery systems. Bioconjug. Chem. *20*, 5–14.

Jiang, T., Olson, E.S., Nguyen, Q.T., Roy, M., Jennings, P.A., and Tsien, R.Y. (2004). Tumor imaging by means of proteolytic activation of cell-penetrating peptides. Proc. Natl. Acad. Sci. U. S. A. *101*, 17867–17872.

Judge, A.D., Bola, G., Lee, A.C.H., and MacLachlan, I. (2006). Design of noninflammatory synthetic siRNA mediating potent gene silencing in vivo. Mol. Ther. *13*, 494–505.

Juliano, R.L. (2016). The delivery of therapeutic oligonucleotides. Nucleic Acids Res. *347*, 6518–6548.

Kamb, A. (2005). What’s wrong with our cancer models? Nat. Rev. Drug Discov. *4*, 161–165.

Kang, D., Gopalkrishnan, R. V, Wu, Q., Jankowsky, E., Pyle, A.M., and Fisher, P.B. (2002). mda-5: An interferon-inducible putative RNA helicase with double-stranded RNA-dependent ATPase activity and melanoma growth-suppressive properties. Proc. Natl. Acad. Sci. U. S. A. *99*, 637–642.

Kaplan, I.M., Wadia, J.S., and Dowdy, S.F. (2005). Cationic TAT peptide transduction domain enters cells by macropinocytosis. J. Control. Release *102*, 247–253.

Karikó, K., Bhuyan, P., Capodici, J., and Weissman, D. (2004). Small interfering RNAs mediate sequence-independent gene suppression and induce immune activation by signaling through toll-like receptor 3. J. Immunol. *172*, 6545–6549.

Karikó, K., Buckstein, M., Ni, H., and Weissman, D. (2005). Suppression of RNA recognition by Toll-like receptors: the impact of nucleoside modification and the evolutionary origin of RNA. Immunity *23*, 165–175.

Kawamura, K.S., Sung, M., Bolewska-Pedyczak, E., and Gariépy, J. (2006). Probing the impact of valency on the routing of arginine-rich peptides into eukaryotic cells. Biochemistry *45*, 1116–1127.

Kennedy, S., Wang, D., and Ruvkun, G. (2004). A conserved siRNA-degrading RNase negatively regulates RNA interference in C. elegans. Nature *427*, 645–649.

Kenski, D.M., Cooper, A.J., Li, J.J., Willingham, A.T., Haringsma, H.J., Young, T.A., Kuklin, N.A., Jones, J.J., Cancilla, M.T., McMasters, D.R., Mathur, M., Sachs, A.B., and Flanagan, W.M. (2010). Analysis of acyclic nucleoside modifications in siRNAs finds sensitivity at position 1 that is restored by 5'-terminal phosphorylation both in vitro and in vivo. Nucleic Acids Res. *38*, 660–671.

Kim, V.N., Han, J., and Siomi, M.C. (2009). Biogenesis of small RNAs in animals. Nat. Rev. Mol. Cell Biol. *10*, 126–139.

Kiss, T. (2002). Small nucleolar RNAs: an abundant group of noncoding RNAs with diverse cellular functions. Cell *109*, 145–148.

Kleinman, M.E., Yamada, K., Takeda, A., Chandrasekaran, V., Nozaki, M., Baffi, J.Z., Albuquerque, R.J.C., Yamasaki, S., Itaya, M., Pan, Y., Appukuttan, B., Gibbs, D., Yang, Z., Karikó, K., Ambati, B.K., Wilgus, T.A., DiPietro, L.A., Sakurai, E., Zhang, K., Smith, J.R., Taylor, E.W., and Ambati, J. (2008). Sequence- and target-independent angiogenesis suppression by siRNA via TLR3. Nature *452*, 591–597.

Koren, E., and Torchilin, V.P. (2012). Cell-penetrating peptides: breaking through to the other side. Trends Mol. Med. *18*, 385–393.

Kraynack, B.A., and Baker, B.F. (2006). Small interfering RNAs containing full 2'-O-methylribonucleotide-modified sense strands display Argonaute2/eIF2C2-dependent activity. RNA *12*, 163–176.

Kurreck, J. (2003). Antisense technologies. Improvement through novel chemical

modifications. Eur. J. Biochem. *270*, 1628–1644.

Lam, J.K.W., Chow, M.Y.T., Zhang, Y., and Leung, S.W.S. (2015). siRNA Versus miRNA as Therapeutics for Gene Silencing. Mol. Ther. Nucleic Acids *4*, e252.

Langkjaer, N., Pasternak, A., and Wengel, J. (2009). UNA (unlocked nucleic acid): a flexible RNA mimic that allows engineering of nucleic acid duplex stability. Bioorg. Med. Chem. *17*, 5420–5425.

Laursen, M.B., Pakula, M.M., Gao, S., Fluiter, K., Mook, O.R., Baas, F., Langklaer, N., Wengel, S.L., Wengel, J., Kjems, J., and Bramsen, J.B. (2010). Utilization of unlocked nucleic acid (UNA) to enhance siRNA performance in vitro and in vivo. Mol. Biosyst. *6*, 862–870.

Layzer, J.M., McCaffrey, A.P., Tanner, A.K., Huang, Z., Kay, M.A., and Sullenger, B.A. (2004). In vivo activity of nuclease-resistant siRNAs. RNA *10*, 766–771.

Lee, Y., Ahn, C., Han, J., Choi, H., Kim, J., Yim, J., Lee, J., Provost, P., Rådmark, O., Kim, S., and Kim, V.N. (2003). The nuclear RNase III Drosha initiates microRNA processing. Nature *425*, 415–419.

Lefebvre, I., Périgaud, C., Pompon, A., Aubertin, A.M., Girardet, J.L., Kirn, A., Gosselin, G., and Imbach, J.L. (1995). Mononucleoside phosphotriester derivatives with S-acyl-2-thioethyl bioreversible phosphate-protecting groups: intracellular delivery of 3'-azido-2',3'-dideoxythymidine 5'-monophosphate. J. Med. Chem. *38*, 3941–3950.

Lewin, M., Carlesso, N., Tung, C.H., Tang, X.W., Cory, D., Scadden, D.T., and Weissleder, R. (2000). Tat peptide-derivatized magnetic nanoparticles allow in vivo tracking and recovery of progenitor cells. Nat. Biotechnol. *18*, 410–414.

Lima, W.F., Prakash, T.P., Murray, H.M., Kinberger, G.A., Li, W., Chappell, A.E., Li, C.S., Murray, S.F., Gaus, H., Seth, P.P., Swayze, E.E., and Crooke, S.T. (2012). Single-stranded siRNAs activate RNAi in animals. Cell *150*, 883–894.

Lindgren, M., and Langel, Ü. (2011). Classes and Prediction of Cell-Penetrating Peptides. Peptides *683*.

Lipinski, C.A. (2004). Lead- and drug-like compounds: the rule-of-five revolution. Drug Discov. Today. Technol. *1*, 337–341.

Lipinski, C.A., Lombardo, F., Dominy, B.W., and Feeney, P.J. (2001). Experimental and computational approaches to estimate solubility and permeability in drug discovery and development settings. Adv. Drug Deliv. Rev. *46*, 3–26.

Londin, E., Loher, P., Telonis, A.G., Quann, K., Clark, P., Jing, Y., Hatzimichael, E., Kirino, Y., Honda, S., Lally, M., Ramratnam, B., Comstock, C.E.S., Knudsen, K.E., Gomella, L., Spaeth, G.L., Hark, L., Katz, L.J., Witkiewicz, A., Rostami, A., Jimenez, S.A., Hollingsworth, M.A., Yeh, J.J., Shaw, C.A., McKenzie, S.E., Bray, P., Nelson, P.T., Zupo, S., Van Roosbroeck, K., Keating, M.J., Calin, G.A., Yeo,

C., Jimbo, M., Cozzitorto, J., Brody, J.R., Delgrosso, K., Mattick, J.S., Fortina, P., and Rigoutsos, I. (2015). Analysis of 13 cell types reveals evidence for the expression of numerous novel primate- and tissue-specific microRNAs. Proc. Natl. Acad. Sci. U. S. A. *112*, E1106-15.

Lönn, P., and Dowdy, S.F. (2015). Cationic PTD/CPP-mediated macromolecular delivery: charging into the cell. Expert Opin. Drug Deliv. *12*, 1627–1636.

Lund, E., Güttinger, S., Calado, A., Dahlberg, J.E., and Kutay, U. (2004). Nuclear export of microRNA precursors. Science (80-.). *303*, 95–98.

Maeda, H. (2012). Macromolecular therapeutics in cancer treatment: the EPR effect and beyond. J. Control. Release *164*, 138–144.

Mak, I.W.Y., Evaniew, N., and Ghert, M. (2014). Lost in translation: Animal models and clinical trials in cancer treatment. Am. J. Transl. Res. *6*, 114–118.

Marín, S., Pujals, S., Giralt, E., and Merkoçi, A. (2011). Electrochemical investigation of cellular uptake of quantum dots decorated with a proline-rich cell penetrating peptide. Bioconjug. Chem. *22*, 180–185.

Marques, J.T., and Williams, B.R.G. (2005). Activation of the mammalian immune system by siRNAs. Nat. Biotechnol. *23*, 1399–1405.

Marques, J.T., Devosse, T., Wang, D., Zamanian-Daryoush, M., Serbinowski, P., Hartmann, R., Fujita, T., Behlke, M.A., and Williams, B.R.G. (2006). A structural basis for discriminating between self and nonself double-stranded RNAs in mammalian cells. Nat. Biotechnol. *24*, 559–565.

Matsumura, Y., and Maeda, H. (1986). A new concept for macromolecular therapeutics in cancer chemotherapy: mechanism of tumoritropic accumulation of proteins and the antitumor agent smancs. Cancer Res. *46*, 6387–6392.

McLennan, D.N., Porter, C.J.H., and Charman, S.A. (2005). Subcutaneous drug delivery and the role of the lymphatics. Drug Discov. Today Technol. *2*, 89–96.

Meade, B.R. (2010). Synthesis of bioreversible, phosphotriester-modified siRNA oligonucleotides. University of California, San Diego.

Meade, B.R., and Dowdy, S.F. (2009). The road to therapeutic RNA interference (RNAi): Tackling the 800 pound siRNA delivery gorilla. Discov. Med. *8*, 253–256.

Meister, G., Landthaler, M., Patkaniowska, A., Dorsett, Y., Teng, G., and Tuschl, T. (2004). Human Argonaute2 mediates RNA cleavage targeted by miRNAs and siRNAs. Mol. Cell *15*, 185–197.

Merkel, O.M., Librizzi, D., Pfestroff, A., Schurrat, T., Béhé, M., and Kissel, T. (2009). In vivo SPECT and real-time gamma camera imaging of biodistribution and pharmacokinetics of siRNA delivery using an optimized radiolabeling and purification procedure. Bioconjug. Chem. *20*, 174–182.

Michiue, H., Eguchi, A., Scadeng, M., and Dowdy, S.F. (2009). Induction of in vivo synthetic lethal RNAi responses to treat glioblastoma. Cancer Biol. Ther. *8*, 2306–2313.

Morrissey, D. V, Lockridge, J.A., Shaw, L., Blanchard, K., Jensen, K., Breen, W., Hartsough, K., Machemer, L., Radka, S., Jadhav, V., Vaish, N., Zinnen, S., Vargeese, C., Bowman, K., Shaffer, C.S., Jeffs, L.B., Judge, A., MacLachlan, I., and Polisky, B. (2005). Potent and persistent in vivo anti-HBV activity of chemically modified siRNAs. Nat. Biotechnol. *23*, 1002–1007.

Moschos, S.A., Jones, S.W., Perry, M.M., Williams, A.E., Erjefalt, J.S., Turner, J.J., Barnes, P.J., Sproat, B.S., Gait, M.J., and Lindsay, M.A. (2007). Lung delivery studies using siRNA conjugated to TAT(48-60) and penetratin reveal peptide induced reduction in gene expression and induction of innate immunity. Bioconjug. Chem. *18*, 1450–1459.

Murchison, E.P., Partridge, J.F., Tam, O.H., Cheloufi, S., and Hannon, G.J. (2005). Characterization of Dicer-deficient murine embryonic stem cells. Proc. Natl. Acad. Sci. U. S. A. *102*, 12135–12140.

Nakase, I., Niwa, M., Takeuchi, T., Sonomura, K., Kawabata, N., Koike, Y., Takehashi, M., Tanaka, S., Ueda, K., Simpson, J.C., Jones, A.T., Sugiura, Y., and Futaki, S. (2004). Cellular uptake of arginine-rich peptides: roles for macropinocytosis and actin rearrangement. Mol. Ther. *10*, 1011–1022.

Nakase, I., Tanaka, G., and Futaki, S. (2013). Cell-penetrating peptides (CPPs) as a vector for the delivery of siRNAs into cells. Mol. Biosyst. *9*, 855–861.

Neveu, M., Kim, H.-J., and Benner, S.A. (2013). The “strong” RNA world hypothesis: fifty years old. Astrobiology *13*, 391–403.

Ohrt, T., Muetze, J., Svoboda, P., and Schwille, P. (2012). Intracellular localization and routing of miRNA and RNAi pathway components. Curr. Top. Med. Chem. *12*, 79–88.

Palm-Apergi, C., Eguchi, A., and Dowdy, S.F. (2011). PTD-DRBD siRNA delivery. Methods Mol. Biol. *683*, 339–347.

Patra, A., Paolillo, M., Charisse, K., Manoharan, M., Rozners, E., and Egli, M. (2012). 2’-fluoro RNA shows increased watson-crick H-bonding strength and stacking relative to RNA: Evidence from NMR and thermodynamic Data. Angew. Chemie - Int. Ed. *51*, 11863–11866.

Pooga, M., Kut, C., Kihlmark, M., Hällbrink, M., Fernaeus, S., Raid, R., Land, T., Hallberg, E., Bartfai, T., and Langel, U. (2001). Cellular translocation of proteins by transportan. FASEB J. *15*, 1451–1453.

Preall, J.B., He, Z., Gorra, J.M., and Sontheimer, E.J. (2006). Short interfering RNA strand selection is independent of dsRNA processing polarity during RNAi in Drosophila. Curr. Biol. *16*, 530–535.

Puthenveetil, S., Whitby, L., Ren, J., Kelnar, K., Krebs, J.F., and Beal, P.A. (2006). Controlling activation of the RNA-dependent protein kinase by siRNAs using site-specific chemical modification. Nucleic Acids Res. *34*, 4900–4911.

Rettig, G.R., and Behlke, M.A. (2012a). Progress toward in vivo use of siRNAs-II. Mol. Ther. *20*, 483–512.

Rettig, G.R., and Behlke, M.A. (2012b). Progress toward in vivo use of siRNAs-II. Mol. Ther. *20*, 483–512.

Robbins, M., Judge, A., Liang, L., McClintock, K., Yaworski, E., and MacLachlan, I. (2007). 2'-O-methyl-modified RNAs act as TLR7 antagonists. Mol. Ther. *15*, 1663–1669.

Robbins, M., Judge, A., and MacLachlan, I. (2009). siRNA and innate immunity. Oligonucleotides *19*, 89–102.

Roberts, T.C., Ezzat, K., El Andaloussi, S., and Weinberg, M.S. (2016). Synthetic SiRNA Delivery: Progress and Prospects. Methods Mol. Biol. *1364*, 291–310.

Rothbard, J.B., Jessop, T.C., and Wender, P.A. (2005). Adaptive translocation: the role of hydrogen bonding and membrane potential in the uptake of guanidinium-rich transporters into cells. Adv. Drug Deliv. Rev. *57*, 495–504.

Sakurai, K., Amarzguioui, M., Kim, D.-H., Alluin, J., Heale, B., Song, M., Gatignol, A., Behlke, M.A., and Rossi, J.J. (2011). A role for human Dicer in pre-RISC loading of siRNAs. Nucleic Acids Res. *39*, 1510–1525.

Sarin, H. (2010). Physiologic upper limits of pore size of different blood capillary types and another perspective on the dual pore theory of microvascular permeability. J. Angiogenes. Res. *2*, 14.

Schirle, N.T., and MacRae, I.J. (2012). The crystal structure of human Argonaute2. Science *336*, 1037–1040.

Schirle, N.T., Kinberger, G.A., Murray, H.F., Lima, W.F., Prakash, T.P., and MacRae, I.J. (2016). Structural Analysis of Human Argonaute-2 Bound to a Modified siRNA Guide. J. Am. Chem. Soc. *138*, 8694–8697.

Schroeder, A., Levins, C.G., Cortez, C., Langer, R., and Anderson, D.G. (2010). Lipid-based nanotherapeutics for siRNA delivery. J. Intern. Med. *267*, 9–21.

Schwarze, S.R. (1999). In Vivo Protein Transduction: Delivery of a Biologically Active Protein into the Mouse. Science (80-.). *285*, 1569–1572.

Sehgal, A., Barros, S., Ivanciu, L., Cooley, B., Qin, J., Racie, T., Hettinger, J., Carioto, M., Jiang, Y., Brodsky, J., Prabhala, H., Zhang, X., Attarwala, H., Hutabarat, R., Foster, D., Milstein, S., Charisse, K., Kuchimanchi, S., Maier, M. a, Nechev, L., Kandasamy, P., Kel'in, A. V, Nair, J.K., Rajeev, K.G., Manoharan, M., Meyers, R., Sorensen, B., Simon, A.R., Dargaud, Y., Negrier, C., Camire, R.M., and

Akinc, A. (2015). An RNAi therapeutic targeting antithrombin to rebalance the coagulation system and promote hemostasis in hemophilia. Nat. Med. *21*, 492–497.

Sioud, M. (2006). Single-stranded small interfering RNA are more immunostimulatory than their double-stranded counterparts: a central role for 2'-hydroxyl uridines in immune responses. Eur. J. Immunol. *36*, 1222–1230.

Soutschek, J., Akinc, A., Bramlage, B., Charisse, K., Constien, R., Donoghue, M., Elbashir, S., Geick, A., Hadwiger, P., Harborth, J., John, M., Kesavan, V., Lavine, G., Pandey, R.K., Racie, T., Rajeev, K.G., Röhl, I., Toudjarska, I., Wang, G., Wuschko, S., Bumcrot, D., Koteliansky, V., Limmer, S., Manoharan, M., and Vornlocher, H.-P. (2004). Therapeutic silencing of an endogenous gene by systemic administration of modified siRNAs. Nature *432*, 173–178.

Tsui, N.B.Y., Ng, E.K.O., and Lo, Y.M.D. (2002). Stability of endogenous and added RNA in blood specimens, serum, and plasma. Clin. Chem. *48*, 1647–1653.

Turner, J.J., Jones, S.W., Moschos, S.A., Lindsay, M.A., and Gait, M.J. (2007). MALDI-TOF mass spectral analysis of siRNA degradation in serum confirms an RNAse A-like activity. Mol. Biosyst. *3*, 43–50.

Ui-Tei, K., Naito, Y., Zenno, S., Nishi, K., Yamato, K., Takahashi, F., Juni, A., and Saigo, K. (2008). Functional dissection of siRNA sequence by systematic DNA substitution: modified siRNA with a DNA seed arm is a powerful tool for mammalian gene silencing with significantly reduced off-target effect. Nucleic Acids Res. *36*, 2136–2151.

Ui-Tei, K., Nishi, K., Takahashi, T., and Nagasawa, T. (2012). Thermodynamic Control of Small RNA-Mediated Gene Silencing. Front. Genet. *3*, 101.

Usher, D.A. (1969). On the mechanism of ribonuclease action. Proc. Natl. Acad. Sci. U. S. A. *62*, 661–667.

Vaish, N., Chen, F., Seth, S., Fosnaugh, K., Liu, Y., Adami, R., Brown, T., Chen, Y., Harvie, P., Johns, R., Severson, G., Granger, B., Charmley, P., Houston, M., Templin, M. V, and Polisky, B. (2011). Improved specificity of gene silencing by siRNAs containing unlocked nucleobase analogs. Nucleic Acids Res. *39*, 1823–1832.

Vickers, T.A., Lima, W.F., Wu, H., Nichols, J.G., Linsley, P.S., and Crooke, S.T. (2009). Off-target and a portion of target-specific siRNA mediated mRNA degradation is Ago2 "Slicer" independent and can be mediated by Ago1. Nucleic Acids Res. *37*, 6927–6941.

Vives, E. (1997). A Truncated HIV-1 Tat Protein Basic Domain Rapidly Translocates through the Plasma Membrane and Accumulates in the Cell Nucleus. J. Biol. Chem. *272*, 16010–16017.

Vukovic, L., Koh, H.R., Myong, S., and Schulten, K. (2014). Substrate recognition and

specificity of double-stranded RNA binding proteins. Biochemistry *53*, 3457–3466.

Wadia, J.S., and Dowdy, S.F. (2005). Transmembrane delivery of protein and peptide drugs by TAT-mediated transduction in the treatment of cancer. Adv. Drug Deliv. Rev. *57*, 579–596.

Wadia, J.S., Stan, R. V, and Dowdy, S.F. (2004). Transducible TAT-HA fusogenic peptide enhances escape of TAT-fusion proteins after lipid raft macropinocytosis. Nat. Med. *10*, 310–315.

van de Water, F.M., Boerman, O.C., Wouterse, A.C., Peters, J.G.P., Russel, F.G.M., and Masereeuw, R. (2006). Intravenously administered short interfering RNA accumulates in the kidney and selectively suppresses gene function in renal proximal tubules. Drug Metab. Dispos. *34*, 1393–1397.

Weitzer, S., and Martinez, J. (2007). The human RNA kinase hClp1 is active on 3' transfer RNA exons and short interfering RNAs. Nature *447*, 222–226.

Whitehead, K.A., Langer, R., and Anderson, D.G. (2009). Knocking down barriers: advances in siRNA delivery. Nat. Rev. Drug Discov. *8*, 129–138.

Whitehead, K.A., Dahlman, J.E., Langer, R.S., and Anderson, D.G. (2011). Silencing or Stimulation? siRNA Delivery and the Immune System. Annu. Rev. Chem. Biomol. Eng. *2*, 77–96.

Wittrup, A., and Lieberman, J. (2015). Knocking down disease: a progress report on siRNA therapeutics. Nat. Rev. Genet. *16*, 543–552.

Yamashita, S., Nagata, T., Kawazoe, M., Takemoto, C., Kigawa, T., Güntert, P., Kobayashi, N., Terada, T., Shirouzu, M., Wakiyama, M., Muto, Y., and Yokoyama, S. (2011). Structures of the first and second double-stranded RNA-binding domains of human TAR RNA-binding protein. Protein Sci. *20*, 118–130.

Zatsepin, T.S., Kotelevtsev, Y. V, and Koteliansky, V. (2016). Lipid nanoparticles for targeted siRNA delivery - going from bench to bedside. Int. J. Nanomedicine *11*, 3077–3086.

Zeidman, R., Jackson, C.S., and Magee, A.I. (2009). Protein acyl thioesterases (Review). Mol. Membr. Biol. *26*, 32–41.

Zhou, J., Shum, K.-T., Burnett, J.C., and Rossi, J.J. (2013). Nanoparticle-Based Delivery of RNAi Therapeutics: Progress and Challenges. Pharmaceuticals (Basel). *6*, 85–107.

Züst, R., Cervantes-Barragan, L., Habjan, M., Maier, R., Neuman, B.W., Ziebuhr, J., Szretter, K.J., Baker, S.C., Barchet, W., Diamond, M.S., Siddell, S.G., Ludewig, B., and Thiel, V. (2011). Ribose 2'-O-methylation provides a molecular signature for the distinction of self and non-self mRNA dependent on the RNA sensor Mda5. Nat. Immunol. *12*, 137–143.

CHAPTER 2

MATERIALS AND METHODS

MATERIALS AND METHODS

Phosphoramidite Synthesis

All phosphoramidites with bioreversible phosphotriester groups were synthesized using the general synthetic protocol in Figure 2.1. Specific methods for synthesizing each of the phosphoramidites used in this work are described in Meade *et al.* (Meade et al., 2014). An example protocol for the synthesis of 5'-O-(4,4'-Dimethoxytrityl)-2'-F-uridine 3'-O-[(S-pivaloyl-2-thioethyl) N,N-diisopropylphosphoramidite] is as follows: A solution of bis-(*N,N*-disiopropylamino)-chlorophosphine (1 g, 0.4 mmol) in dry CH_2Cl_2 (5 ml) was added drop-wise to a magnetically stirred cooled solution (-78 ^{0}C) of 5'-*O*-(4,4'-Dimethoxytrityl)-2'-F-uridine (2 g, 0.364 mmol) and *N,N*-diisopropylethylamine (0.71 ml, 0.4 mmol) in dry CH_2Cl_2 (24 ml). The reaction mixture was allowed to warm to room temperature (25° C) while stirring was maintained (45 min). S-(2-hydroxyethyl) thiopivaloate (0.65 g, 0.4 mmol) in 5 ml dry CH_2Cl_2 was added portion wise and stirred for 10 min. Ethyl thiotetrazole (7.3 ml, 0.25 M solution in acetonitrile, 0.182 mmol) was then added to the reaction mixture and the mixture was stirred for 2-12 hr. CH_2Cl_2 (60 ml) was then added and the reaction mixture was washed with saturated aqueous sodium hydrogen carbonate (20 ml) and brine (2 x 20 ml). The mixture was then dried over anhydrous sodium sulfate. The solvent was evaporated *in vacuo* and the residue was subjected to flash silica gel column purification on a CombiFlash instrument (Teledyne Isco) using hexane-ethyl acetate (0.5% triethylammonium acetate) as the solvent (0-70 %). The fractions containing the products were pooled together and evaporated until dry. The resulting foamy residue was redissolved in benzene, frozen and lyophilized which afforded a colorless powder (2.6 g). The yield was 85% as a diastereomeric mixture.

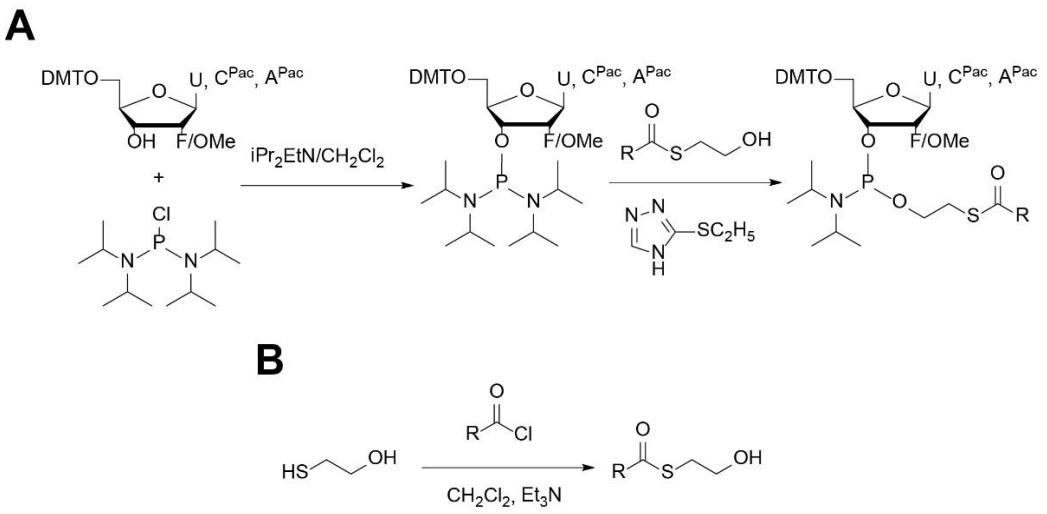

Figure 2.1. General scheme for RNN phosphoramidite synthesis. A) General synthetic routes for U, C, and A phosphoramidites containing SATE groups. **B)** General synthetic scheme of the SATE alcohol used in SATE phosphoramidite synthesis.

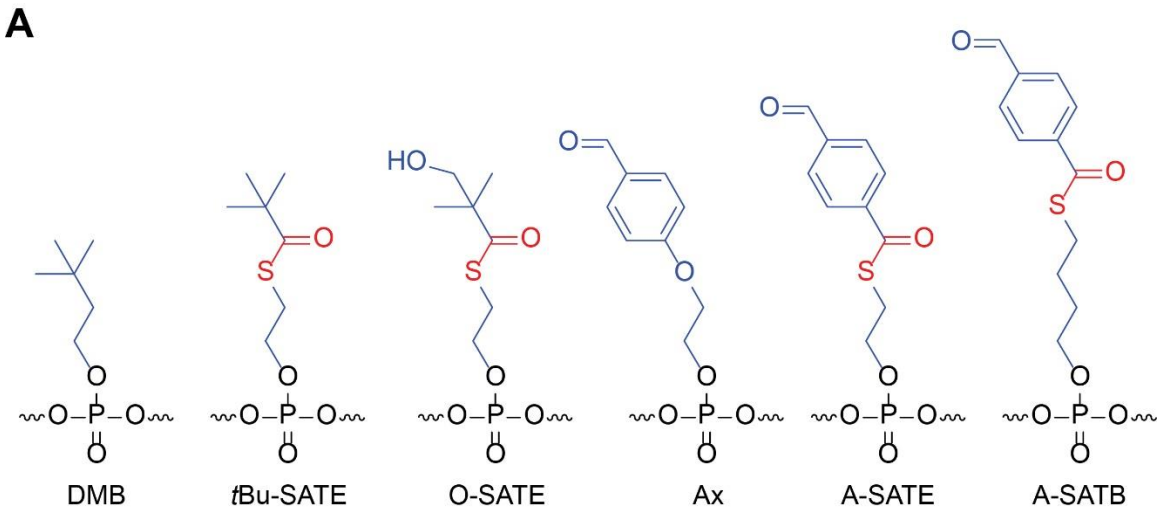

Figure 2.2. Phosphotriester group structures. A) Structures of the phosphotriester groups discussed in this dissertation. All structures are shown in the deprotected form utilized for biological studies. At the time of oligonucleotide synthesis O-SATE hydroxyl group is protected by a tert-butyldimethylsilyl (TBDMS) group and the benzaldehyde present on the Ax, A-SATE, and A-SATB is protected by an acetal. DMB and Ax are *irreversible* phosphotriester groups that do not contain a thioester bond. Nomenclature: DMB = 2,2-DiMethylButyl; A = Aldehyde; SATE = S-Acyl-ThioEthyl; SATB = S-Acyl-ThioButyl.

Oligonucleotide Synthesis

All oligonucleotides were synthesized on a BioAutomation Mermade-6 oligonucleotide synthesizer (BioAutomation, MerMade6). Oligonucleotide synthesis reagent usage was as follows: Activator = 0.25 M 5-Benzylthio-1H-tetrazole (BTT) in acetonitrile (Glen Research, 30-3170); Cap A = 5% Phenoxyacetic anhydride (w/v), 90% THF (v/v), 10% pyridine (Glen Research, 40-4210); Cap Mix B = 16% 1-Methylimidazole (v/v), 84% THF (Glen Research, 40-4220); Deblock = 3% Trichloroacetic (w/v) acid in DCM (VWR, EM-BI0830-0950); Oxidizing Reagent = 0.02 M Iodine in 70% THF(v/v), 20% pyridine, 10% water (VWR, EM-BI0420-4000); Sulfurizing Reagent = 0.05 M 3-((N,N-dimethylaminomethylidene)amino)-3H-1,2,4-dithiazole-5-thione (Sulfurizing Reagent II) in 40% pyridine (v/v), 60% acetonitrile (Glen Research, 40-4137-52); Anhydrous acetonitrile (VWR, AX0151-1). Commercially available dT-CE (Glen Research, 10-1030), 2'-OMe-5'-O-DMTr-PAC-A-CE (Glen Research, 10-3601), 2'-Fluoro-5'-O-DMTr-PAC-C-CE (R. I. Chemicals, P1500-01), 2'-OMe-5'-O-DMTr-iPr-PAC-G-CE (Glen Research, 10-3621), 2'-Fluoro-5'-O-DMTr-U-CE (R. I. Chemicals, F-1015), 2'-OMe-5'-O-DMTr-PAC-A-CE (Glen Research, 10-3601), 2'-Fluoro-5'-O-DMTr-PAC-C-CE (R. I. Chemicals, P1500-01), 2'-OMe-5'-O-DMTr-iPr-PAC-G-CE (Glen Research, 10-3621), and 2'-Fluoro-5'-O-DMTr-U-CE (R. I. Chemicals, F-1015) phosphoramidites were coupled at coupling times and concentrations recommended by the manufacturer. For modifications, IRDye 800 phosphoramidite (LI-COR Biosciences, 4000-33), 5' Thiol modifier phosphoramidite (Glen Research, 10-1936), 5'-Aldehyde modifier phosphoramidite (Glen Research, 10-1933), and Cy3 phosphoramidite (Glen Research, 10-5913) were coupled per manufacturer's recommendation. All SATE-containing phosphoramidites were coupled at 100 mM with two coupling cycles of 6 min each. dT-Q-CPG 500 (Glen Research, 21-2230) were used for CPGs. Manual detritylation was

accomplished by flowing 1 ml of deblock solution through the CPG column into 4 ml of 100 mM toluenesulfonic acid in anhydrous acetonitrile. Absorbance readings at 498 nm were measured to quantify DMT concentration and ensure full-length coupling.

Primary Oligonucleotide Deprotection

For all wildtype (2'-OH) oligonucleotide deprotection, CPG was incubated in 1 mL of AMA (Ammonium Hydroxide/40% Aqueous Methylamine (1:1)) (Sigma-Aldrich, 295531) for 1 hr at 65° C. For all SATE-containing oligonucleotides, CPG was incubated in 1 mL of 10% diisopropylamine (v/v) (Sigma-Aldrich, 386464) 90% methanol for a 4 hr at room temperature (RT). After deprotection, oligonucleotide solutions were placed in centrifugal evaporator for drying.

For 2'O-TBDMS deprotection, oligonucleotides were dissolved in 100 µl of anhydrous DMSO. To each oligonucleotide solution, 125 µL of 98% triethylamine trihydrofluoride (Sigma Aldrich, 344648) was added and reactions were left at room temperature for 4 hr. After 4 hr, oligonucleotides were precipitated by the addition of 35 µl of 3 M sodium acetate and 1 mL of 1-Butanol. Oligonucleotides were then incubated at -80° C for 2 hr. After incubation, the oligonucleotides were centrifuged at 16,000 g for 5 min, supernatant was aspirated, oligonucleotide pellets were dissolved in 1 mL of water, and desalted with NAP-10 columns (GE Healthcare, 83-468).

For TBDMSO-SATE deprotection, oligonucleotides were dissolved in 219 µl of anhydrous DMSO. To each oligonucleotides solution, 31 µL of 98% triethylamine trihydrofluoride was added and reactions were incubated at RT for 1 hr per TBDMSO-SATE on the oligo. After deprotection, oligonucleotides were precipitated by the addition of 35 µL of 3 M sodium acetate and 1 mL of 1-Butanol. The oligonucleotides were then incubated at -80° C for 2 hr. After incubation, the oligonucleotides were centrifuged at

16,000 g for 5 min, supernatant was aspirated, and the oligonucleotides pellets were dissolved in 250 µL of 50% ACN for purification by RP-HPLC.

Oligonucleotide Purification

All oligonucleotides were purified by RP-HPLC on an Agilent 1200 Series Analytical HPLC with an Agilent SB-C18 column (9.4 x 150 mm) (Agilent, 883975-202). Linear gradients were run from water in 50 mM triethylammonium acetate (TEAA) to 90% acetonitrile at a flow rate of 2 ml/min. Length and steepness of gradient varied with amount of SATE groups present on oligonucleotides. For DMT-On purifications, DMT-On oligonucleotide HPLC peaks were collected, analyzed for the presence of full-length SATE oligonucleotides by MALDI-TOF mass spectrometry, and selected fractions were lyophilized two times to remove TEAA.

Mass Spectrometry

Oligonucleotides were analyzed by MALDI-TOF mass spectrometry using a Voyager-DE PRO MALDI-TOF mass spectrometer (Applied Biosystems). 10 pmol of RNA/RNN was spotted with 1 µL of matrix from a 20 mg/mL solution of 2',4',6'-Trihydroxyacetophenone (Sigma-Aldrich, 91928) in 50% acetonitrile/20 mM ammonium citrate dibasic (Sigma-Aldrich, 09831).

Secondary Oligonucleotide Deprotection and Desalting

For oligonucleotides that did not contain A-SATE phosphotriesters, detritylation and, if present, removal of acetal protection from acetal-AX phosphotriesters was accomplished by the addition of 200 µl 80% glacial acetic acid and heating at 65° C for 1 hr. After deprotection, oligonucleotides were frozen and lyophilized until dry.

For oligonucleotides that contained acetal-A-SATE phosphotriesters, detritylation and removal of acetal protection was accomplished by the addition of 200 µl 80% formic acid and incubation at room temperature for 4 hr. After deprotection, oligonucleotides were frozen and lyophilized until dry.

Lyophilized oligonucleotides were dissolved in 20% acetonitrile and desalted with NAP-10 columns (GE Healthcare Life Sciences 17-0854-02). Desalted oligonucleotides were dried in a centrifugal evaporator. Once dry, completed oligonucleotides were dissolved in 50% acetonitrile and stored at -20° C.

Gel Electrophoresis

ssRNA oligonucleotides were analyzed by denaturing gel electrophoresis using 15% acrylamide/7 M Urea denaturing gels and stained with methylene blue for visualization. dsRNA oligonucleotides were hybridized by heating to 65° C for 2 min and allowing to cool to room temperature. dsRNA analysis was performed by nondenaturing gel electrophoresis using 15% acrylamide nondenaturing gels and ethidium bromide staining for visualization.

siRNA Transfection

H1299-dGFP expressing cells were generated by infection with a lentivirus expressing Vesicular Stomatitis Virus Glycoprotein (VSVG) fused to dGFP and isolated by FACS. H1299-dGFP cells were cultured in high glucose DMEM media (ThermoFisher Scientific, 11965118), supplemented with 5% FBS and penicillin-streptomycin at 37° C, 5% CO2. For transfection, cells were plated in 24-well plates at a density of $4x10^4$ cells / well. Prior to transfection, cells were washed twice with PBS. 100 µl samples of corresponding siRNA concentrations in Opti-MEM (ThermoFisher

Scientific, 31985070) were mixed with 100 µL transfection mixture (98 µL OptiMEM + 2 µL of Lipofectamine 2000 [ThermoFisher Scientific, 11668-019]) and incubated at room temperature for 30 min prior to treatments. Transfection solutions were left on cells for 8 hr before removal of transfection medium and replacement with growth medium (5% FBS DMEM). Cells were trypsinized and analyzed on a flow cytometer (BD Sciences, model: LSRII) for dGFP expression at various time points post-transfection.

Peptide Synthesis

All protected amino acids and coupling reagents were purchased from Nova Biochem or Bachem, BOC 6-hydrazino-nicotinic acid (Solulink, s-3003-500), and Fmoc-N-amido-dPEG6-acid (Quanta Biodesign, 10063). Delivery domain peptides: HyNic-GG-RKKRRQRRR (TAT); HyNic-GG-(TAT)-PEG18-(TAT)-PEG18-(TAT). Peptide synthesis was performed at 25 µM scale using Fmoc solid phase peptide synthesis on Symphony Quartet peptide synthesizer (Ranin) and rink-amide MBHA resin as solid support. All Hynic peptides were cleaved and deprotected using standard conditions (92.5% TFA, 2.5% acetone, 2.5% water, 2.5% TIS) for 2 hr. Crude peptides were precipitated with cold diethylether and purified were purified by RP-HPLC on an Agilent 1200 Series Preparative HPLC Prep-C18 with a Prep-C18 30 × 250 mm column (Agilent, 410910-302). Peptide purity was confirmed by mass spectrometry using α-CHCA matrix (Sigma-Aldrich, 70990) and an Applied Biosystems Voyager-DE PRO MADLI-TOF mass spectrometer.

siRNA Conjugation

For delivery domain (DD) peptide conjugations, duplexed siRNN oligonucleotides were conjugated with DD-HyNic peptides at a 1:5 (oligo:peptide) molar ratio in the

presence of 10 mM HEPES, 10 mM aniline, 50 mM NaCl, and 5.25 M acetic acid in 50% acetonitrile and 50% water for 1 hr at RT. After conjugation, samples were frozen, and lyophilized. Resulting conjugated siRNN pellets were dissolved in water and spun with Amicon Ultra-0.5 ml 30 kDa Spin Filters (Millipore, UFC503024) to remove unconjugated DD peptide. siRNN conjugates were analyzed by silver stained SDS-PAGE.

For Tris-GalNAc conjugation, single-stranded RNN oligonucleotides were conjugated with tris-GalNAc-Hynic at a 1:5 oligonucleotide to A-SATE phosphotriester group molar ratio in the presence of 100 mM aniline in 50% acetonitrile and 50% water for 1 hr at room temperature. After conjugation, samples were frozen and lyophilized. Lyophilized pellets were washed with ethanol to remove unconjugated tris-GalNAc-Hynic. GalNAc-siRNN conjugates were resuspended in water, frozen, lyophilized, resuspended in 50% acetonitrile, and duplexed with complementary ssRNN oligonucleotides. GalNAc-siRNN conjugates were analyzed by PAGE and methylene blue staining.

DD-siRNN Cellular Transduction

H1299-dGFP expressing cells were trypsinized, centrifuged at 200 x g, supernatant was aspirated, cell pellet was rinsed in Opti-MEM, centrifuged at 200 x g, supernatant was aspirated, and the resulting cell pellet was resuspended in Opti-MEM. $1x10^5$ cells suspended in Opti-MEM were plated in each well on a 24-well plate. DD-siRNN conjugates were diluted in an equal volume of Opti-MEM and added to cells. Transduction solutions were left on cells for 2 hr before removal of transfection medium and replacement with growth medium (5% FBS DMEM). Cells were trypsinized and analyzed by flow cytometry on a BD Biosciences LSRII for dGFP expression at various time points post-transduction.

Luciferase Assay

H1299 cells stably expressing firefly luciferase (pGL3; Promega) were maintained and transfected as described previously (Eguchi et al., 2009). 24 hr post-transfection or transduction, cells were split into 96-well plates in triplicate to reach 90% confluency at the day of luciferase measurement. For luciferase measurement, each well to be measured was trypsinized. After trypsinization, a sample of each well was collected for cell counting and the remaining cells were lysed with 100 µL of Promega Lysis Reagent (25 mM Tris-phosphate (pH 7.8), 2 mM DTT, 2 mM 1,2-diaminocyclohexane-N,N,N´,N´-tetraacetic acid, 10% glycerol, 1% Triton X-100). Lysates were then transferred to a white wall 96-well assay plate. Luciferase assay was performed with a Veritas Microplate Lumniometer (Turner BioSystems, 998-9100). Luminescence was measured with the injector set to 100 µL of Luciferase Assay Reagent (20 mM tricine, 1.07 mM magnesium carbonate, 2.67 mM $MgSO_4$, 0.1 mM EDTA, 33.3 mM DTT, 270 µM coenzyme A (Affymetrix, 13785), 470 µM D-luciferin (GoldBio, LUCK), 470 µM ATP) with a 2 second measurement delay and a 10 second signal integration. Luciferase signals were normalized for each sample by cell count.

Immunoblot analysis and cell cycle analysis

All immunoblots were performed as described(Wadia et al., 2004; Eguchi et al., 2009) and used the following primary antibodies: anti-Plk1 (Santa Cruz Biotechnology, 3F8), anti-cMyc-HA (Roche, 3F10). Goat anti-mouse IgG HRP (Santa Cruz Biotechnology, SC-2005) was used as a secondary antibody. Immunoblots were developed on a ChemiDoc (Bio-Rad, ChemiDOC MP) and quantified using Image Lab (Bio-Rad) sub-saturating linear signals. Cell cycle position for Plk1 knockdown was

determined by flow cytometry of cells stained with propidium iodide using a BD LSR-II flow cytometer.

Synthesis of Tris-GalNAc-HyNic

The synthesis of Tris-GalNAc-HyNic was performed based on the methods described by Sliedregt *et al*.(Sliedregt et al., 1999) and Rensen *et al* (Rensen et al., 2004).

Preclinical Animal Models

For *in vivo* GalNAc-siRNN studies, purified GalNAc-siRNN and GalNAc-siRNA conjugates were administered subcutaneously or intravenously into randomly chosen 6- to 8-week-old female C57B/6 mice (Jackson Laboratory) in doses of 10, 17.5 or 25 mg/kg diluted in water for a total volume injection of 10 μL/g mouse. All animals in a given treatment protocol were analyzed at the same time point; therefore, no blinding was performed. Livers were isolated for mRNA extraction. For statistical analyses, data are expressed as mean ± standard deviation, as indicated, and compared by Student's t-test. Statistical significance was assigned at $P < 0.05$. All animals were maintained, treated, and euthanized in accordance with the UCSD Institutional Animal Care and Use Committee.

For subcutaneous delivery studies, transgenic ROSA26 loxP-Stop-loxP luciferase mice (Safran et al., 2003) (Jackson Labs, 005125) were injected subcutaneously with 100 μL of 0.5 mg/mL TAT-Cre (Wadia et al., 2004) to turn on luciferase gene by removal of a loxP-STOP-loxP DNA transcriptional terminator genetic element. After 2 weeks, d-Luciferin (150 mg/kg) was administrated intraperitoneally and luciferase expression was monitored by live-animal imaging (PerkinElmer, IVIS

Spectrum). After luciferin injection animals were anesthetized with isoflurane, placed in the IVIS imaging chamber, and kept under isoflurane anesthesia during imaging. Bioluminescent images were acquired for 10-20 min after luciferin injection. Following imaging, mice were returned to their cages for recovery. For knockdown studies, mice were injected subcutaneously with 100 µl of DD-siRNN (750 pmol) or PBS (mock) control. Luciferase expression was monitored as described by IVIS Spectrum imaging. Living Image software (PerkinElmer) was used to analyze bioluminescence data based on average radiance (p/s/cm^2/sr) in the regions of interest.

For intravenous DD-siRNN delivery studies, transgenic ROSA26 loxP-STOP-LoxP luciferase mice were inoculated intravenously with 1 x 10^{10} pfu Adenovirus-Cre (University of Iowa, gene transfer vector core). Cre recombination occurred specifically in the liver, where removal of the transcriptional terminator genetic element established functional luciferase gene expression. D-luciferin (150 mg/kg) was administrated intraperitoneally and luciferase expression levels were quantified by live-animal analysis using an IVIS Spectrum (PerkinElmer). Luciferase expression levels were stable within one month. For knockdown studies, mice were injected intravenously with 100 µl of DD-siRNN (12.5 nmol) or PBS (mock) control.

For *in vivo* LHP delivery studies, transgenic ROSA26 loxP-STOP-LoxP luciferase expressing luciferase in the liver as a result of intravenous mice Adenovirus-Cre treatment were used. Knockdown experiments were conducted using Invivofectamine 2.0 (Life Technologies) following the recommended protocol for complex formation with 2'-F/OMe Luc3-LHP2, Luc3-LHP7, GFP1-LHP2, and Luc3-siRNA. For knockdown experiments, 6 mg/kg doses of complexed oligonucleotides were administered intravenously. Luciferase expression was monitored as described by IVIS Spectrum imaging.

Real-time qRT-PCR

For liver RNA isolation, 50 mg of liver from mice was homogenized with a 21G needle in TRIzol (ThermoFisher, 15596018). 1 µg of RNA was used to synthesize cDNA with iScript cDNA Synthesis Kit (Bio-Rad, 170-8891) and qRT-PCR was performed on 10 ng of cDNA with SYBR Green PCR Master Mix (Applied Biosystems, 4309155) on Applied Biosystems 7300 Real-Time PCR System. ApoB primers: forward, 5′-ACAGGAGCTTACTCCAACGC; reverse, 5′-AGCTCATACCTTGTGTCCCC. B2M primers: forward, 5′-ACCGTCTACTGGGATCGAGA; reverse, 5′-TGCTATTTCTTTCTGCGTGCAT.

Serum Albumin Binding Assay

10 µL reactions were set up containing 0.5 nmol of siRNA or siRNN and BSA (Millipore, 126625) at a concentration of 0, 0.5, 1, 1.5, or 2 mg/mL. Reactions were incubated at RT for 15 min. After incubation, samples were diluted with loading buffer and analyzed by gel electrophoresis using 10% acrylamide native gels and stained with ethidium bromide for visualization.

5’ RACE

For 5′ RACE, 200 × 10^3 cells were reverse transfected with 100 nM siRNA or siRNN using Lipofectamine 2000. Cells were harvested in TRIzol 48 hr post-transfection. The aqueous phase was mixed with equal volume of 70% ethanol, loaded on an RNeasy column (Qiagen, 74104), and RNA was prepared according to the manufacturer's instruction. 3 µg of RNA was ligated to 0.25 µg of GeneRacer RNA oligonucleotide (ThermoFisher, L150201). Ligated RNA was reverse transcribed with

SuperScript III and Oligo dT primer. cDNA was amplified with the GeneRacer 5′ primer and a gene-specific primer (5′ TGGGCAGCGTGCCATCATCC for GFP, ATCATCCCCCTCGGGTGTAATCAGAA for GL3) using a step down PCR protocol. Second round amplification was performed using the GeneRacer 5′ nested primer and a gene-specific nested primer (5′-ATCATCCTGCTCCTCCACCTCCGG for GFP, TCAGTGAGCCCATATCCTTGCCTGAT for GL3) at 60° C. PCR products were analyzed on a 1.2% Agarose TBE gel and bands of predicted size were excised, purified on S.N.A.P. columns, cloned into TOPO-PCR4 vector, and sequenced.

Preparation and transfection of ^{32}P-labeled siRNA

400 pmol of guide strand was 5′ labeled with 2.5 units of T4 polynucleotide kinase (NEB, M0201S) and 200 μCiγ−^{32}P-ATP (6000 Ci/mmol) in a 50 μl volume for 20 min. Reaction was inactivated for 20 min at 65° C and free γ-^{32}P-ATP was removed from the reaction mixture using Amicon Ultra 3K centrifugal filter (Millipore, UFC500324). 400 pmol of wild-type passenger strand was added and annealed by heating reaction mixture to 65° C and cooling to RT. 400 pmol of labeled siRNA was diluted to a volume of 250 μL in Opti-MEM and mixed with 250 μL Opti-MEM containing 10 μL Lipofectamine 2000. After a 20 min incubation the mixture was added to 2.4×10^6 H1299-dGFP cells in 8 mL DMEM containing 5% FBS and seeded in a 10 cm tissue culture dish. Cells were transfected for 12 hr and washed with PBS before replacement with fresh growth medium (DMEM with 5% FBS).

Serum Stability

50 pmol of siRNA and siRNN GFP guide strands were incubated in 50% human complement active serum (Innovative Research, IPLA-CSER0S) at 37° C. At indicated

time points an aliquot was taken and diluted 10-fold in 7M urea loading buffer. Samples were heated to 95° C for 1 min, snap cooled on dry ice and stored at −80° C until analyzed by denaturing gel electrophoresis using 15% acrylamide/7 M urea denaturing gels and stained with methylene blue for visualization.

REFERENCES

Eguchi, A., Meade, B.R., Chang, Y.-C., Fredrickson, C.T., Willert, K., Puri, N., and Dowdy, S.F. (2009). Efficient siRNA delivery into primary cells by a peptide transduction domain-dsRNA binding domain fusion protein. Nat. Biotechnol. *27*, 567–571.

Meade, B.R., Gogoi, K., Hamil, A.S., Palm-Apergi, C., van den Berg, A., Hagopian, J.C., Springer, A.D., Eguchi, A., Kacsinta, A.D., Dowdy, C.F., Presente, A., Lönn, P., Kaulich, M., Yoshioka, N., Gros, E., Cui, X.-S., and Dowdy, S.F. (2014). Efficient delivery of RNAi prodrugs containing reversible charge-neutralizing phosphotriester backbone modifications. Nat. Biotechnol. *32*, 1256–1261.

Rensen, P.C.N., van Leeuwen, S.H., Sliedregt, L.A.J.M., van Berkel, T.J.C., and Biessen, E.A.L. (2004). Design and synthesis of novel N-acetylgalactosamine-terminated glycolipids for targeting of lipoproteins to the hepatic asialoglycoprotein receptor. J. Med. Chem. *47*, 5798–5808.

Safran, M., Kim, W.Y., Kung, A.L., Horner, J.W., DePinho, R.A., and Kaelin, W.G. (2003). Mouse reporter strain for noninvasive bioluminescent imaging of cells that have undergone Cre-mediated recombination. Mol. Imaging *2*, 297–302.

Sliedregt, L.A., Rensen, P.C., Rump, E.T., van Santbrink, P.J., Bijsterbosch, M.K., Valentijn, A.R., van der Marel, G.A., van Boom, J.H., van Berkel, T.J., and Biessen, E.A. (1999). Design and synthesis of novel amphiphilic dendritic galactosides for selective targeting of liposomes to the hepatic asialoglycoprotein receptor. J. Med. Chem. *42*, 609–618.

Wadia, J.S., Stan, R. V, and Dowdy, S.F. (2004). Transducible TAT-HA fusogenic peptide enhances escape of TAT-fusion proteins after lipid raft macropinocytosis. Nat. Med. *10*, 310–315.

CHAPTER 3

INCREASING siRNN NEUTRALITY FOR CELLULAR DELIVERY

INCREASING siRNN NEUTRALITY FOR CELLULAR DELIVERY

ABSTRACT

Peptide transduction domains (PTDs) are a class of small peptides with a proven ability to deliver a variety of macromolecular cargo across the cellular membrane. PTDs are potentially ideal for delivery of monomeric siRNA drugs, but PTD function is dependent on their dense cationic charge which is neutralized by the strong anionic charge of siRNA cargo. To solve this problem, our lab has developed small interfering ribonucleic neutrals (siRNNs) containing bioreversible phosphotriester groups that directly neutralize the negative charge of the siRNA backbone. The ground-breaking first generation of siRNNs utilized *t*-butyl-S-acyl-2-thioethyl (tBu-SATE) phosphotriester groups that were effective at charge neutralization, but the number of *t*Bu-SATE insertions on an siRNN was limited by the accumulated hydrophobicity of the terminal tert-butyl group. Here I describe siRNNs featuring a novel O-SATE neutralizing phosphotriester to test the hypothesis that PTD-siRNN prodrugs can be made and are capable of self-delivery. Through molecular modeling, I limited phosphotriester steric interference across the siRNA major grove to generate siRNNs with enhanced neutrality to enable PTD-mediated siRNN delivery.

INTRODUCTION

Peptide transduction domains (PTDs), also known as cell-penetrating peptides (CPPs), may be ideal for delivering single molecules of siRNA across the cellular membrane. PTDs have been utilized to deliver various cargo ranging from peptides and proteins to charge neutral, peptide nucleic acids (PNAs) both *in vitro* and *in vivo* (Schwarze, 1999; Gait, 2003; Kaplan et al., 2005; van den Berg and Dowdy, 2011). The uptake mechanism is dependent on the type of PTD used, but endocytosis appears to be the predominant mechanism of PTD-mediated internalization (Rothbard et al., 2004; Kawamura et al., 2006). Macropinocytosis, a specialized form of fluid phase endocytosis, has been found to be the primary method of internalization for cationic arginine rich PTDs, such as TAT PTD and octa-arginine (R8) (Nakase et al., 2004; Wadia et al., 2004). Following internalization by endocytosis, PTDs and their cargo transduce across the endocytic lipid bilayer membrane to access the cytoplasm through a poorly understood mechanism (Lönn and Dowdy, 2015).

PTDs have demonstrated the ability to deliver variety of macromolecular cargo *in vitro*, *in vivo* in preclinical animal models of human disease, and in >25 clinical trials, but very few studies have reported delivery of siRNA into cells using PTDs (Wadia and Dowdy, 2005; Lönn and Dowdy, 2015). The reason for this lies in the opposing characteristics of PTDs and siRNA: the dense cationic charge of PTDs is crucial to their ability to transduce across the cell membrane, while siRNAs have a strong anionic charge (Glover et al., 2005; Gonçalves et al., 2005). Upon covalent linkage, the anionic charge effectively neutralizes the cationic PTD, rendering it unable to mediate cellular internalization and generating large aggregates (**Figure 1.1**) (Jiang et al., 2004). With these problems in mind, our lab attempted to devise a method of synthetically

neutralizing the siRNA negative charge to enable cellular delivery of monomeric siRNA by PTDs.

To circumvent this problem, our lab developed a TAT PTD fusion protein with a dsRNA Binding Domain (DRBD) termed PTD-DRBD (Eguchi and Dowdy, 2009; Eguchi et al., 2009; Michiue et al., 2009). The DRBDs of this fusogenic protein bind to and physically mask the negatively charged siRNA backbone, thereby allowing for efficient, non-cytotoxic delivery by the fused TAT PTD into an entire population of cells. PTD-DRBD successfully delivered siRNA to cells and induced RNAi responses in a variety of tested cells (Eguchi et al., 2009) and was found to be functional *in vivo* when administered to intracerebral glioblastoma mouse models (Michiue et al., 2009).

The PTD-DRBD siRNA delivery approach effectively demonstrated PTD-mediated delivery of siRNA to cells, but could not be used for systemic delivery as at high siRNA concentrations the PTD and DRBD domains are able to independently contact multiple siRNAs, leading to aggregation and precipitation. Despite these problems, the TAT-DRBD siRNA delivery system demonstrated that masking the siRNA negative charge facilitates efficient PTD-mediated cellular delivery. With these lessons in mind, our lab sought to produce siRNAs neutralized by bioreversible phosphotriester modifications.

To develop bioreversible phosphotriester-containing siRNAs, our lab first focused on a *t*-butyl-S-Acyl-2-ThioEthyl (*t*Bu-SATE) phosphotriester group (**Figure 2.2**). The *t*Bu-SATE phosphotriester was originally developed as part of a prodrug mononucleoside (small molecule) inhibitor of HIV Reverse Transcriptase (Lefebvre et al., 1995). The bioreversibility of the SATE phosphotriester is made possible through processing by cytoplasm-restricted thioesterases (Zeidman et al., 2009). The thioester bond of a SATE phosphotriester is cleaved by cytoplasmic thioesterases, thereby

initiating a rapid two-step decomposition process that converts SATE phosphotriesters into wild-type, charged phosphodiesters capable of inducing an RNAi response (**Figure 1.3**). Although synthesis of a *t*Bu-SATE containing mononucleosides was demonstrated in 1995 (Lefebvre et al., 1995), no group had reported the successful synthesis of SATE-containing RNA oligonucleotides. This was due to the seemingly insurmountable number of synthetic problems that required orthogonal solutions to create such oligonucleotides. Through years of research and development, our lab determined orthogonal solutions to all of these problems was able to synthesize the first *t*Bu-SATE siRNA prodrugs that we termed short interfering ribonucleic neutrals (siRNNs). Over the course of creating *t*Bu-SATE siRNNs our lab identified several critical properties of the SATE phosphotriesters:

1. A 2'-OH group on the ribose ring is not tolerated as it participates in a nucleophilic attack on the phosphotriester, leading to strand cleavage. It is therefore necessary to substitute 2'-F and 2'-OMe modification in place of the 2'-OH (**Figure 1.2**). These 2' modifications are well-tolerated by cells and do not interfere with the induction of RNAi responses (Rublack et al., 2011).
2. SATE phosphotriester groups render siRNNs resistant to RNAses and esterases, giving siRNNs a >24 hour half-life in serum (**Figure 3.1D**). Additionally, the phosphotriester groups mask the dsRNA, thereby avoiding stimulation of the innate immune system (data not shown).
3. SATE phosphotriesters are selectively converted into charged phosphodiester backbones by thioesterases (**Figure 1.3**) only in the cytoplasm and are effectively loaded into Ago2 to induce robust and target-specific RNAi responses.

The generation of *t*Bu-SATE siRNNs capable of bioreversal and efficient RNAi induction upon delivery to cells by transfection was a groundbreaking achievement.

However, after extensive experimentation, fundamental problems were identified with the use of *t*Bu-SATE siRNNs for the PTD-mediated siRNN delivery strategy. Due to steric interference between *t*Bu-SATE phosphotriesters across the dsRNA major groove, less than 50% of the negatively charged phosphodiesters could be neutralized with *t*Bu-SATE groups and retain a double-stranded structure. This degree of siRNA charge neutralization was below the level (~70%) determined to be necessary for cationic PTD-mediated delivery (see Chapter 1). Additionally, the remaining charged phosphodiesters are susceptible to intermolecular electrostatic interactions with the cationic PTDs of other conjugates, which results in aggregation at therapeutic conjugate concentrations. The second fundamental problem posed by *t*Bu-SATE siRNN is the hydrophobic nature of the *t*-butyl moiety. This hydrophobicity makes *t*Bu-SATE siRNNs highly insoluble at physiologically relevant salt concentrations for cellular treatment (**Figure 3.1C**) and prevents effective PTD conjugation.

For these reasons, we sought to develop a bioreversible phosphotriester group able to neutralize the charge of the siRNA phosphate backbone without suffering from the hydrophobic issues associated with the *t*Bu-SATE. Furthermore, I delved into the problem of phosphotriester steric hindrance across the major groove to develop siRNNs with greater numbers of phosphotriesters and greater charge neutralization. These studies were pursued to enable PTD-mediated cellular delivery of siRNNs.

RESULTS & DISCUSSION

Synthesis and Biophysical Properties of O-SATE Phosphotriesters

To avoid the hydrophobicity problems that plagued *t*Bu-SATE siRNNs, O-SATE phosphotriesters were designed with a terminal hydroxyl group to improve hydrophilicity of the group. O-SATE-modified phosphoramidites were synthesized by the same

synthetic route used to produce *t*Bu-SATE phosphoramidites (**Figure 2.1**), but with TBDMS-O-SATE substituted for the S-(2-hydroxyethyl) thiopivaloate (**Figure 3.1A**). Unlike *t*Bu-SATEs, O-SATEs possess a terminal hydroxyl group that must be protected during oligonucleotide synthesis to prevent undesired side reactions leading to branching during synthesis. The t-butyldimethylsilyl (TBDMS) group was chosen for O-SATE terminal hydroxyl protection. TBDMS is commonly utilized as a 2'-OH protecting group during RNA oligonucleotide synthesis as it is stable under standard conditions for oligonucleotide synthesis and can be readily removed by treatment with fluoride ion to yield a 2'-OH (Ogilvie et al., 1977; Scaringe et al., 1990). Indeed, we found that TBDMS protecting groups could be efficiently removed from O-SATE phosphotriesters at room temperature by a solution of triethylamine trihydrofluoride (TEA · 3HF) in DMSO with no ill-effects on the rest of the oligonucleotide (**Figure 3.1B**). Specifically, we were concerned with the phosphotriester group being cleaved off of the oligonucleotide during deprotection.

A primary issue that opposed the synthesis of *t*Bu-SATE containing oligonucleotides was the use of a strong base for primary oligonucleotide deprotection. Following solid-phase synthesis of RNA or DNA oligonucleotides by the phosphoramidite method, a primary deprotection step is required that consists of base treatment to cleave the oligonucleotide from the solid support, remove 2-cyanoethyl phosphodiester protecting groups, and remove exocyclic amino protecting groups from the heterocyclic bases (Beaucage, 2008). Standard deprotection protocols use of ammonium hydroxide (NH_4OH) for primary oligonucleotide deprotection. However, we found that NH_4OH treatment was incompatible with *t*Bu-SATE containing oligonucleotides as it resulted in thioester decomposition and subsequent loss of *t*Bu-SATE insertions (Meade et al., 2014). To prevent base-mediated phosphotriester cleavage, *t*Bu-SATE modified

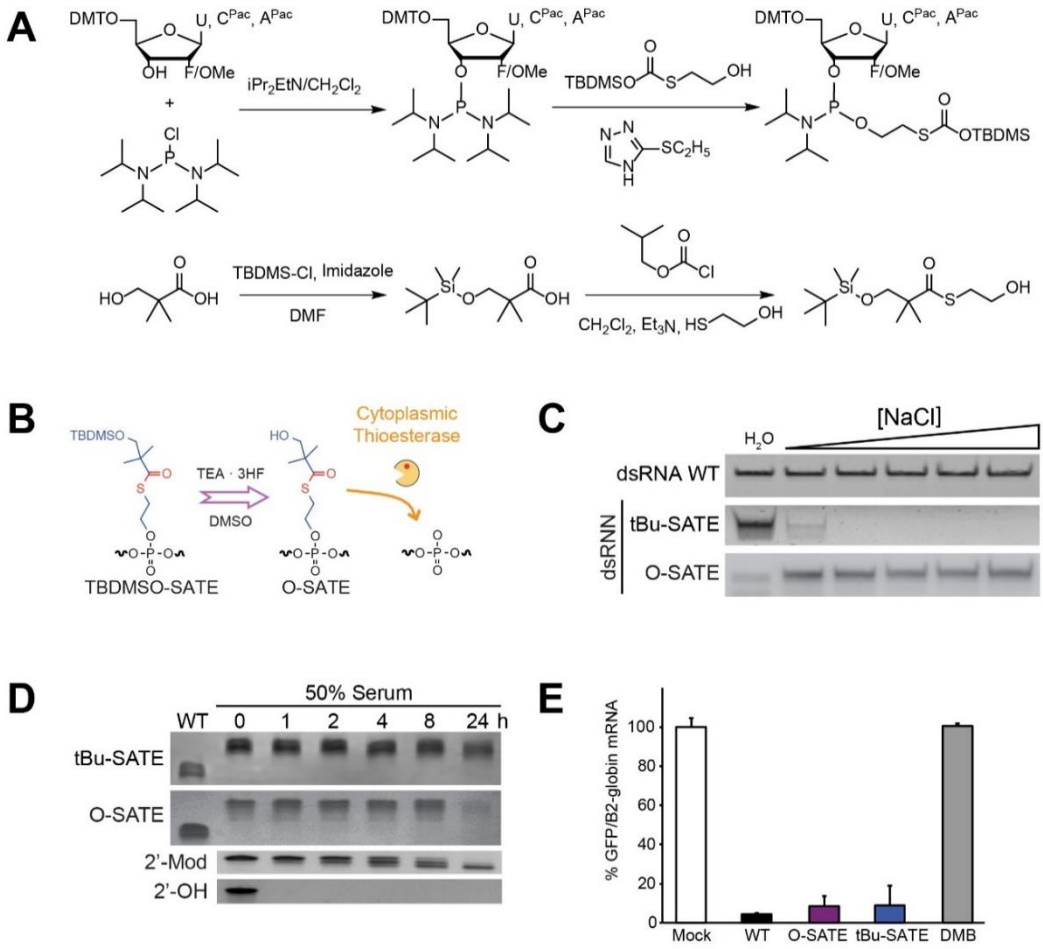

Figure 3.1. Synthesis and biophysical properties of O-SATE phosphotriesters. A) Synthetic routes for O-SATE U, C, and A phosphoramidites and O-SATE alcohol used in phosphoramidite synthesis. **B**) O-SATE phosphotriester modifications retain TBDMS protecting group after oligonucleotide synthesis and cleavage from solid support. TBDMS protection is removed with a solution of triethylamine trihydrofluoride and DMSO prior to HPLC purification of RNN oligonucleotides. Once delivered to cells, O-SATE phosphotriester groups are cleaved off by cytoplasmic thioesterases, resulting in a charged phosphodiester. **C**) Comparative salt sensitivity analysis of wild-type phosphodiester siRNA and siRNNs containing 18x tBu-SATE or O-SATE phosphotriesters. Wild-type siRNAs and O-SATE siRNNs remains soluble at high salt concentrations, but tBu-SATE siRNNs suffer from hydrophobic collapse. [NaCl] = 100, 200, 300, 400, 500 mM. **D**) Serum stability analysis of ssRNA containing wild-type phosphodiesters and 2'-OH or 2'-F/OMe (2'-Mod) vs ssRNNs containing 9x tBu-SATE or O-SATE phosphotriesters. **E)** qRT-PCR analysis of cells transfected with indicated siRNAs and siRNNs targeting GFP. Mean values normalized to β2 microglobulin and reported as percent of mock control.

oligonucleotides are synthesized with phosphoramidites containing phenoxyacetyl (Pac) protecting groups on adenine and cytosine bases and isopropyl-phenoxyacetyl (iPr-Pac) on guanine. This allowed for primary deprotection with an extremely mild basic solution of diisopropylamine (DIA) in methanol (see Chapter 2) that was highly compatible with *t*Bu-SATE groups. O-SATE phosphotriester groups were found to similarly decompose after exposure to NH_4OH, but were stable under the extremely mild basic primary deprotection conditions developed for *t*Bu-SATE containing oligonucleotides, thereby allowing continued use of this deprotection protocol for the synthesis of O-SATE containing oligonucleotides (data not shown).

As previously noted, SATE phosphotriesters are susceptible to nucleophilic attack by the ribose 2'-OH, which leads to strand cleavage. Therefore, stable insertion of a SATE phosphotriester requires modification of the ribose 2'-position. For this reason, all RNN oligonucleotides we have synthesized and discuss here, unless otherwise noted, are fully modified with 2'-F pyrimidines and 2'-OMe purines (**Figure 1.2**). Fully modified 2'-F/OMe siRNAs can be as effective or more effective at inducing RNAi responses as are standard 2'-OH siRNAs (Allerson et al., 2005). Additionally, full 2'-modification is increasingly common among therapeutic siRNAs as it greatly enhances siRNA nuclease stability and prevents induction of innate immune responses (see Chapter 1).

The principal difficulty with utilizing *t*Bu-SATE siRNNs is the significant hydrophobicity of the *t*-butyl moiety. At physiologically compatible NaCl concentrations this hydrophobicity renders siRNNs containing 18x *t*Bu-SATE groups (P(S9)/G(S9), where 'P' represents the siRNA passenger strand, 'G' represents the guide strand, 'P/G' represents the double-stranded siRNA, numbers in parentheses represent the phosphotriester modification present on each strand, and 'S' represents # of *t*Bu-SATE

insertions), the maximum number of insertions tolerated by double-stranded RNA, insoluble (**Figure 3.1C**). Substitution of 18x hydrophilic hydroxyl O-SATE phosphotriesters (P(O9)/G(O9), where O = # of O-SATE insertions) rescued solubility, putting O-SATE siRNNs on par with siRNA containing a wildtype phosphodiester backbone that remains soluble in >500 mM NaCl.

Maintaining stability in blood is essential for the development of successful RNAi therapeutics (see Chapter 1). To test the stability of O-SATE RNNs to serum ribonucleases, we incubated RNA and RNN oligonucleotides in 50% human serum at 37° C and examined oligonucleotide stability at various time points by urea denaturing gel electrophoresis. As expected, RNAs containing natural 2'-OH groups were highly liable to degradation by serum ribonucleases, being fully degraded in <1 hr when incubated in human serum (**Figure 3.1D**). Fully 2'-modified RNA (2'-F/OMe) was found to possess a greatly enhanced nuclease stability. RNN oligonucleotides containing 9x *t*Bu-SATE phosphotriesters have a half-life exceeding 24 hours in 50% human serum and O-SATE RNNs displayed similarly enhanced stability (**Figure 3.1D**).

Bioreversibility is key to the function of siRNNs and this property must be maintained by the O-SATE phosphotriester for the group to be therapeutically useful. By virtue of the thioester bond, SATE phosphotriesters are processed only by cytoplasm-restricted thioesterases to produce a wild type, charged phosphodiester that is compatible with the RNAi machinery (**Figure 1.3**). To assay for intracellular conversion and biological function of O-SATE phosphotriester siRNNs, we synthesized a set of GFP-targeted siRNAs and siRNNs: siRNA containing no phosphotriesters (P-wt/G-wt), 18x bioreversible *t*Bu-SATE phosphotriesters (P(S9)/G(S9)), 18x O-SATE phosphotriesters (P(O9)/G(O9)), and 18x *irreversible* 2,2-dimethylbutyl (DMB) phosphotriesters (P(D9)/G(D9)). The siRNA and siRNNs targeting GFP were

transfected into human H1299 lung adenocarcinoma cells containing an integrated and constitutively expressed destabilized GFP reporter gene. 48 hr later the transfected cells were analyzed by qRT-PCR for GFP expression. Due to the surface contacts between the siRNA guide strand and Ago2, chemical modifications to the guide strand, with the exception of some 2'-modification, are poorly tolerated and result in loss of RNAi activity (Bumcrot et al., 2006). For this reason, siRNNs were only able to induce an RNAi response if the phosphotriesters were converted intracellularly into charged phoshodiesters. In agreement with previously published studies (Manoharan, 2004; Allerson et al., 2005), the fully modified 2'-F/OMe GFP siRNA (P-wt/G-wt) induced a strong RNAi response (**Figure 3.1E**). The *t*Bu-SATE containing P(S9)/G(S9) knocked down GFP expression similarly to the P-wt/G-wt. As expected, the negative control irreversible P(D9)/G(D9) did not induce an RNAi response as the DMB phosphotriester lacks a cleavable thioester bond and cannot be converted into a phosphodiester backbone required by the RNAi machinery. Impressively, O-SATE phosphotriester siRNNs were removed by cytoplasmic thioesterases and the P(O9)/G(O9) induced an RNAi response on par with that of the equivalent *t*Bu-SATE containing siRNN.

With this we have demonstrated synthesis of O-SATE phosphotriesters are hydrophilic enough for O-SATE siRNNs to remain soluble in physiologically relevant salt concentrations at high phosphotriester numbers, are resistant to serum ribonucleases, and bioreversible, thereby allowing siRNNs containing O-SATE phosphotriesters to induce RNAi responses.

The Phosphate Interference Model

We hypothesized that if sufficient charge neutralization of the siRNA phosphodiester backbone could be achieved with bioreversible phosphotriesters, then cationic PTDs could facilitate delivery of siRNA. However, phosphotriester insertion has

been limited to 9x per strand. Placement of more than 9 phosphotriesters on each strand led to a sharp decrease in the ability of strands to base-pair into a double-stranded species as is required for induction of an RNAi response (**Figure 3.2A**). The cause for this double-stranded stability limit was not fully understood, but was suspected to involve steric hindrance across the dsRNA major groove. To address this problem and generate more siRNNs sufficiently neutral to enable PTD-mediated delivery, I developed the Phosphate Interference Model (**Figure 3.2B**).

To demonstrate the effect of phosphotriester insertions on the ability complementary oligonucleotides to become double-stranded, we synthesized a series of passenger strands with increasing numbers of *t*Bu-SATE phosphotriesters. Single-stranded passenger strand oligonucleotides that contained 0-16x phosphotriesters were mixed with a Cy3-labeled guide strand RNN oligonucleotide containing 9x *t*Bu-SATEs (**Figure 3.2A**). The oligonucleotides were hybridized at 90° C, cooled, subjected to native gel electrophoresis, and analyzed for efficiency of double-stranded RNN oligonucleotide (dsRNN) formation by visualization of the guide strand Cy3 signal. Passenger strands with 0-9x *t*Bu-SATEs readily hybridized to form dsRNN species with the 9x *t*Bu-SATE guide strand (**Figure 3.2A**). However, insertion of one additional phosphotriester (P(S10)/G(S9)-Cy3) resulted in an abrupt decrease in the formation of dsRNN species. Hybridization of the 9x *t*Bu-SATE guide strand to passenger strands containing 12-16x *t*Bu-SATEs resulted in no dsRNN formation. Similar results were obtained when attempting to hybridize a guide strand containing 9x O-SATEs with passenger strands containing > 9x O-SATE phosphotriesters (data not shown). These observations demonstrated that SATE phosphotriester modified oligonucleotides readily formed double stranded siRNNs, but that there was an upper limit to the total number of phosphotriester insertions that can be tolerated.

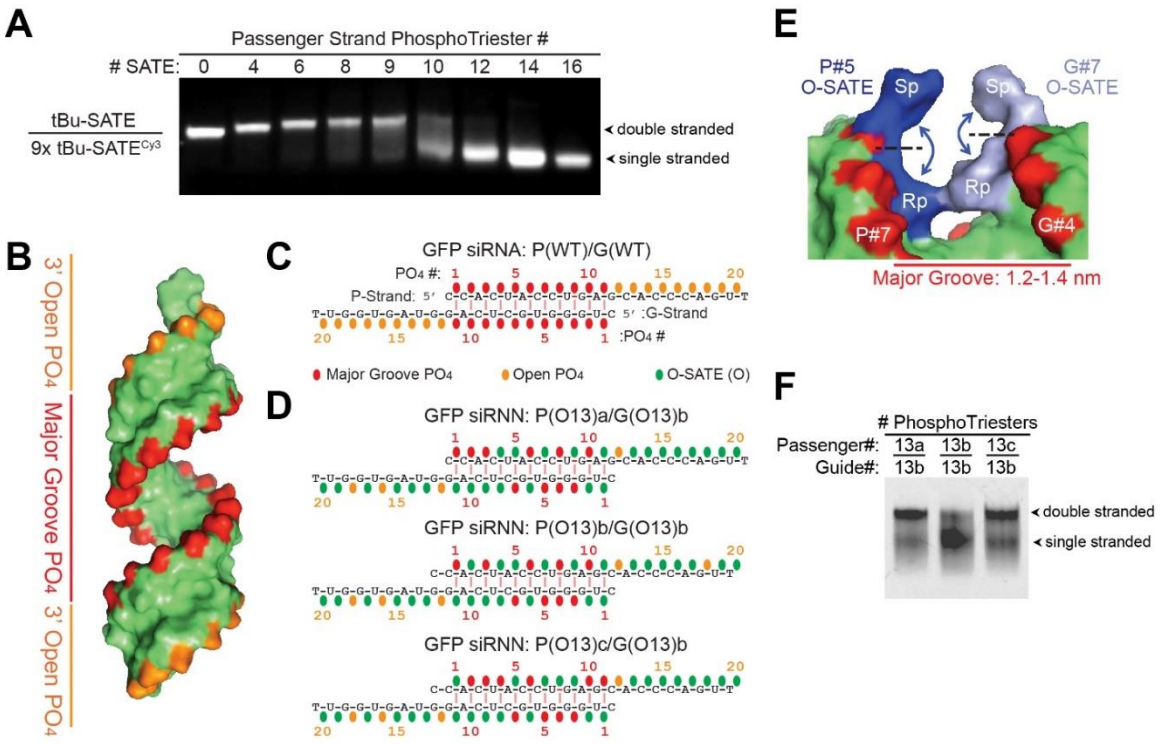

Figure 3.2. The Phosphate Interference Model. A) Placement of more than 9 phosphotriesters on each strand results in a sharp decrease in the affinity of the strands for duplexing, thereby limiting maximum neutralization to 45% of total phosphates. **B)** Structure of fully 2'-F/2'-OMe modified siRNA with 11 nt conflict zone, wherein phosphotristers may interfere across the major groove of the siRNA helix (colored red). Open phosphates on the 3'-ends of the strands are colored orange. **C)** Diagram of phosphotriester positions predicted to interfere across the siRNA helix major groove. **D)** Diagram of model applied to dGFP siRNNs tested for duplexing affinity. Numbers of phosphotriesters on each strand are represented as Passenger/Guide. "a" and "b" are strand identifiers for the pattern of phosphotriester placement on the oligonucleotide. Increasing numbers of phosphotriester modification conflicts in close proximity correlate with ability of the strands to base-pair. **E)** Model of Sp/Rp O-SATE phosphotriester diastereomers at passenger strand P#5 phosphate opposite guide strand G#7 phosphate. Note potential Rp/Rp phosphotriester steric congestion. **F)** Duplex test of oligonucleotides containing 13 O-SATE phosphotriesters. "a," "b," and "c" are identifiers for the pattern of phosphotriester placement on the oligonucleotide. 13a/13b duplexes well while 13b/13b cannot form a stable duplex. Minimizing steric conflict across the major groove raises the maximum number of phosphotriesters tolerated for strand duplexing.

This limit of 9 phosphotriesters on each strand allows for neutralization of only 45% of the negatively charged phosphodiesters present on a 21-mer siRNN. However, experiments where the siRNA charge is neutralized with irreversible methyltriesters (that inhibit RNAi) suggested that ~70% neutrality is necessary for TAT PTD-mediated delivery of siRNA (see Chapter 1).

I hypothesized that the phosphotriester duplex stability limit may be due to steric interference between phosphotriesters across the major groove of the dsRNA helix (**Figure 3.2E**) and that through molecular modeling, siRNNs could be designed with increased phosphotriester insertion and sufficient charge neutralization to allow PTD-mediated delivery. For modeling, I utilized a published NMR solution-state structure of a fully 2'-F/OMe modified 21mer siRNA (Podbevsek et al., 2010). A-form siRNAs contain a central 1.2-1.4 nm major groove core that encompasses phosphates #1-11 on each strand (**Figure 3.2B,C**). Analysis of the 2'-modified siRNA structure revealed that phosphates exist in opposition to each other across this groove. Passenger strand phosphate #1 (P#1) opposes guide strand phosphate G#11 across the major groove (**Figure 3.2C**). In this same manner, P#2 opposes G#10, and so on. In contrast, phosphates #12-20 on the 3' ends of each strand are not opposed to other phosphates and therefore have a greater solution accessibility. We termed these positions 3' open phosphates. We note that these 3' open phosphates are present on all dsRNA and dsDNA ends but had not been previously compared to phosphates present in the major groove. In the A-form RNA helix required by the RNAi machinery this phosphate opposition is of little consequence as the width of the major groove is sufficient to prevent steric interaction of opposing phosphates. However, this opposition becomes highly relevant when major groove phosphates are modified with phosphotriesters of sufficient size to interfere sterically with one another (**Figure 3.2E**).

Our pilot experiments utilized irreversible methyltriesters to neutralize the phosphodiester backbone charge (see Chapter 1). In these experiments up to 15 methyl phosphotriesters could be inserted on each strand without decreasing the ability of the strands to form double-stranded species. I hypothesize that this was possible because the small size of the methyl phosphotriesters prevented steric interaction across the dsRNA major groove. In contrast, bioreversible SATE phosphotriesters are sufficiently large to make inter-phosphate interaction problematic. The stereochemistry of phosphotriesters also adds another layer of complexity. During oligonucleotide synthesis, oxidation of the chiral phosphorous randomly generates either an Sp (outward) or an Rp (inward) diastereomer of the phosphotriester group (**Figure 3.2E**). While no steric conflicts are expected for Sp or Rp phosphotriester diastereomers amongst the 3' open phosphates (#12-#20), my modeling predicted that major groove phosphates would be more sensitive to the orientation of paired phosphotriesters. Phosphates in the major groove were predicted to have area sufficient for two paired Sp phosphotriesters or Sp/Rp paired phosphotriesters. However, two Rp paired phosphotriesters were predicted to potentially suffer from steric congestion.

In order to test this model (**Figure 3.2C**), I synthesized a collection of passenger and guide RNN oligonucleotides with increasing numbers of O-SATE phosphotriesters, designed to minimize potential phosphotriester steric conflicts along the major groove. By testing hybridization efficiency of these oligonucleotides, I found that 26x O-SATE phosphotriesters (~65% of total phosphates) could be placed at selected locations along the passenger and guide strands while maintaining a double-stranded siRNN helix of 19 base pairs (**Figure 3.2D,F**). Importantly, these highly neutral siRNNs retained the ability to induce robust RNAi responses (**Figure 3.3F**).

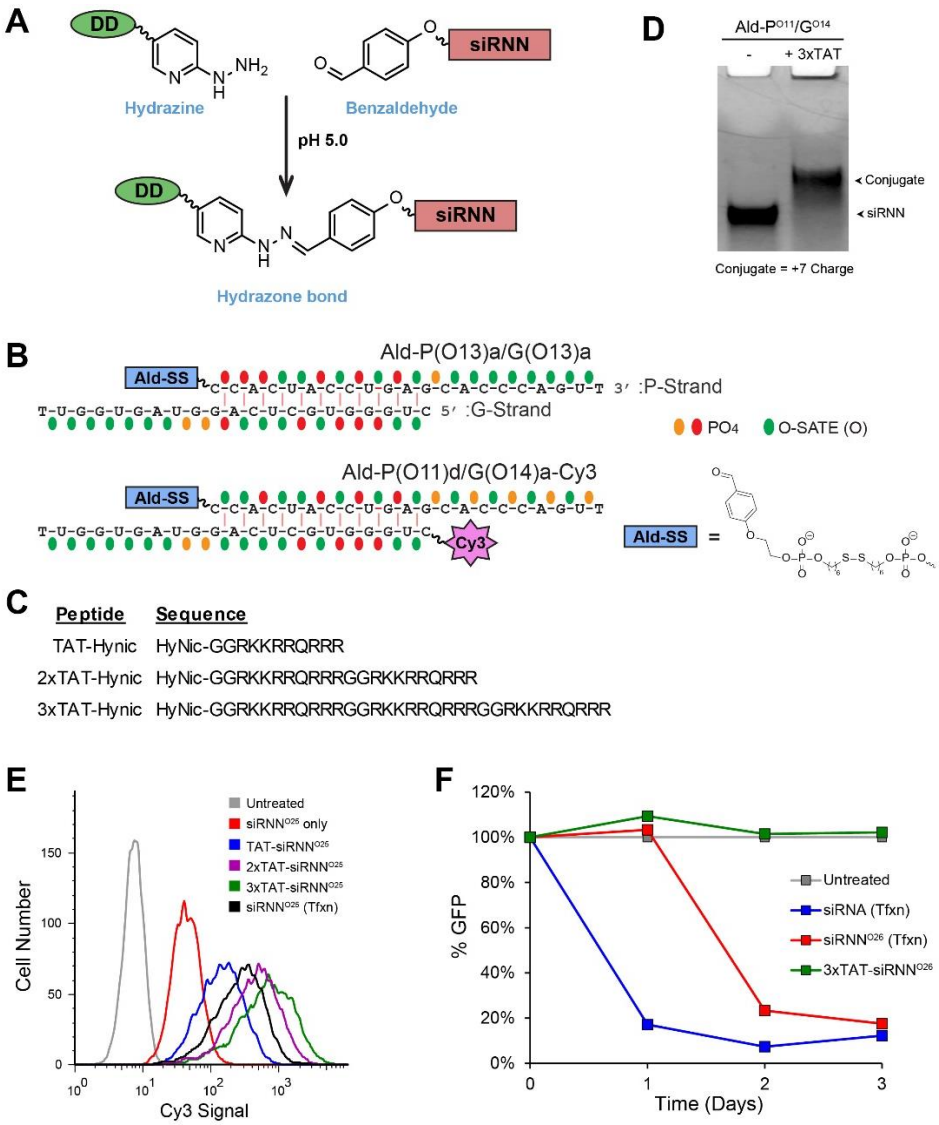

Figure 3.3. TAT PTD Conjugation and delivery of highly neutral siRNNs. A) The Hynic conjugation reaction between a hydrazine-modified delivery domain (DD) and a benzaldehyde functionalized siRNN results in the formation of a stable bis-aryl hydrazone linkage. The reaction occurs readily at pH 5.0 in aqueous buffers. **B)** Sequences and of on GFP-targeted siRNNs used in this study. "a" and "d" are identifiers for the pattern of phosphotriester placement on the oligonucleotide. Orange ovals represent 3' open phosphates, red ovals represent major groove phosphates that oppose phosphates on the opposing strand, and green ovals represent O-SATE phosphotriester groups. **C)** TAT-PTD peptides used in this study. **D)** SDS-PAGE gel analysis of Ald-P(O11)d/G(O14)a oligo only or conjugated to 3xTAT-Hynic peptide. Visualized by silver stain. **E)** Flow cytometry analysis of H1299 cells treated with Cy3-labled TAT-siRNN^{O25} conjugate. Cells were treated with 250 nM TAT-siRNN^{O25} conjugate for 6 hours, followed by trypsinization and washes with trypsin and PBS. 100 nM siRNN^{O25} was transfected with cationic lipids (Tfxn) as a control. siRNN^{O25} = Ald-P(O11)d/G(O14)a-Cy3. **F)** Flow cytometry analysis of 100 nM siRNN^{O26} transfected with cationic lipid (Tfxn) compared to 1 uM 3xTAT-siRNN^{O26}. Cells were treated for 8 hours before GFP RNAi analysis 1, 2, and 3 days post-treatment. 2'-modified siRNA (no phosphotriesters) was transfected as a positive control. siRNNO^{26} = Ald-P(O13)a/G(O13)a.

The effectiveness of the phosphate interference model is well illustrated when comparing the hybridization affinities of three different pairs of passenger and guide strands, each with 13x O-SATE phosphotriesters. I synthesized three different passenger strands that each contained 13x O-SATE groups, but in different locations: P(O13)a, P(O13)b, and P(O13)c (**Figure 3.2D**). Each of these passenger strands was mixed with the same G(O13)b guide strand at equimolar ratios and analyzed for dsRNN formation by native gel electrophoresis and visualized by silver stain (**Figure 3.2F)**. To avoid false dsRNN interpretation, silver staining was used due to decreased ethidium bromide intercalation of double-stranded siRNN oligonucleotides with high numbers O-SATE phosphotriesters (data not shown). I found that G(O13)b hybridized well to P(O13)c with only one predicted conflict (P#1 to G#11) or two predicted major groove phosphotriester conflicts (P#4 to G#8 and P#11 to G#1) with P(O13)b. However, G(O13)b hybridized poorly when I introduced three predicted conflicts (P#2 to G#10, P#4 to G#8, and P#11 to G#1) (**Figure 3.2D,F**). These experiments supported the predictions of the phosphate interference model as siRNNs with fewer conflicts amongst paired major groove phosphotriesters were more efficient in forming double-stranded species.

By employing the Phosphate Interference Model, I was able to generate double-stranded siRNNs with a maximal number of 26x O-SATE phosphotriester groups or ~65% of total phosphates neutralized. Importantly, these siRNNs remained highly functional as RNAi triggers. By using my model, I was able to increase the total number of phosphotriesters and increase phosphate neutralization by 20%, bringing the siRNNs within the range of neutrality (~70%) predicted to be necessary for TAT PTD-mediated delivery (see Chapter 1). We currently employ this model when designing every new

RNN oligonucleotide to choose the phosphotriester pattern that maximizes siRNN duplex stability.

TAT-PTD Conjugation and Delivery of Highly Neutral siRNNs

Through application of my Phosphate Interference Model, I was able to produce siRNNs with ~65% of the total phosphates neutralized. Previous experiments with methyltriester siRNAs suggested that this should be sufficient neutralization of the negative phosphodiester backbone to facilitate TAT PTD-mediated delivery (see Chapter 1). With these highly neutral siRNNs in hand, the next step was conjugation with TAT PTDs and then to assay the resulting TAT PTD-siRNN conjugates for cellular delivery and induction of RNAi responses.

For generation of PTD-siRNN conjugates, we chose to utilize Hynic conjugation chemistry due to the simplicity of the reaction conditions and high tolerability of the reactant groups for our deprotection conditions (**Figure 3.3A**). Briefly, peptides are produced by solid-phase synthesis and functionalized during synthesis with an N-terminal Hydrazinonicotinamide (Hynic) group (**Figure 3.3A,C**). RNN oligonucleotides were synthesized with chemically reactive benzaldehyde (Ald) functionalities for reaction with Hynic-PTDs (**Figure 3.3A,B**). Ald-RNN oligonucleotides and Hynic-PTDs readily form stable bis-arylhydrazone bonds in aqueous buffers at pH 5.0 using aniline as a catalyst (**Figure 3.3A,D**) (Dirksen et al., 2006; Dirksen and Dawson, 2008). As the 5'-end of the guide strand must remain unobstructed for phosphorylation by Clp1 upon cytoplasmic delivery (Weitzer and Martinez, 2007) and binding to the Ago2 MID domain (Schirle and MacRae, 2012), benzaldehydes were placed on the 5'-terminus of passenger strands during solid-phase synthesis (**Figure 3.3B**). To ensure disassociation of the PTD from the siRNN, a disulfide linkage was placed between the

benzaldehyde and the oligonucleotide causing the release of the PTD upon exposure to the reducing environment of the cytoplasm (Meade and Dowdy, 2007).

To examine the ability of highly neutral siRNNs to be delivered by cationic TAT PTDs we synthesized a series of TAT PTDs that ranged in cationic charge: +8 (TAT-Hynic), +16 (2xTAT-Hynic), and +24 (3xTAT-Hynic) (**Figure 3.3C**). These PTDs were reacted with a highly neutral aldehyde-modified and cynine dye-labeled GFP siRNN (Ald-P(O11)d/G(O14)a-Cy3) to form PTD-siRNN conjugates joined by a stable hydrazone bond (**Figure 3.3A,B**). With 25x O-SATE phosphotriesters, the Ald-P(O11)d/G(O14)a-Cy3 has 17 charged phosphodiesters remaining (including the two groups bordering the 5'-disulfide). To assay the extent of cellular delivery and determine if sufficient neutrality had been achieved, H1299 cells were treated with 250 nM siRNN-Cy3 or PTD-siRNN-Cy3 conjugates for 6 hr. As a positive control, cells were also transfected with 100 nM siRNN-Cy3, a concentration sufficient to induce maximal GFP target gene knockdown. After 6 hr, cells were trypsinized and then washed with trypsin and PBS to remove conjugate or oligo that had bound to the cellular membrane, but had not been internalized.

Due to its overall negative charge (-9), TAT-siRNN-Cy3 conjugate demonstrated poor cell association (**Figure 3.3E**). 2xTAT-siRNN-Cy3 and 3xTAT-siRNN-Cy3 both displayed enhanced Cy3 uptake that increased in intensity relative to overall charge. Importantly, the Cy3 uptake was greater than that of the siRNN-Cy3 transfected at a concentration sufficient to induce a strong RNAi response (**Figure 3.3E**), indicating that these PTD-siRNN conjugates may be capable of self-delivery to induce RNAi responses. The high association of the 2xTAT-siRNN conjugate was surprising as it had an overall neutral charge, which suggested sufficient charge neutralization was achieved to allow some TAT PTD-mediated cellular uptake. The 3xTAT-siRNN conjugate possessed an

overall positive charge of +7, which was reflected in its high Cy3 uptake, making it a promising candidate for cellular delivery.

I next tested the ability of highly neutral TAT PTD-siRNN conjugates to self-deliver *in vitro* and induce target-specific GFP RNAi responses. I treated human H1299 lung adenocarcinoma cells containing an integrated and constitutively expressed destabilized GFP (~2 hour half-life) with siRNNs and then measured target GFP gene expression by flow cytometry (**Figure 3.3F**). This *in vitro* model is ideal for analyzing siRNA delivery and RNAi responses as it allows for a rapid quantification of GFP target gene silencing on a single cell basis in the entire population of live cells. Cells were treated with 1 uM 3xTAT-P(O13)a/G(O13)a conjugate or transfected with 100 nM GFP wt siRNA or Ald-P(O13)a/G(O13)a siRNN. Treated cells were collected and GFP signal was analyzed by flow cytometer at various time points to determine GFP RNAi responses. GFP-targeted wt siRNA and the highly neutral Ald-P(O13)a/G(O13)a siRNN both induced strong RNAi responses 48 hr after transfection. Interestingly, the Ald-P(O13)a/G(O13)a siRNN RNAi response lagged behind the transfected wt siRNA, possibly due to the extra time necessary to remove the high number of phosphotriesters from the siRNN. Unfortunately, despite having an overall cationic charge and treatment with 10x the amount of transfected siRNN, the 3xTAT-P(O13)a/G(O13)a conjugate failed to induce an RNAi response. Treatment with a lower conjugate concentration, 2xTAT conjugate, and differently configured but similarly neutral 3xTAT-P(O11)d/G(O15)a also failed to induce RNAi responses (data not shown).

CONCLUSIONS

siRNA holds significant promise as a therapeutic, but the biophysical properties of siRNAs make them a poor pharmacological candidate. Our approach to deliver siRNA involves synthetic neutralization of the negatively charged phosphodiester backbone with bioreversible phosphotriester groups to allow for delivery by cationic PTDs. Previously, bioreversible *t*Bu-SATE phosphotriesters were developed that could stably neutralize the siRNA phosphodiester backbone. However, the *t*-butyl moiety proved to be excessively hydrophobic as siRNNs containing *t*Bu-SATE groups were insoluble in biologically compatible buffers (**Figure 3.1C**). Additionally, the number of *t*Bu-SATEs that could be placed on an siRNN while maintaining a double-stranded molecule was limited to 18x groups, providing insufficient charge neutralization to enable cationic PTD-mediated siRNN delivery.

Here I described novel O-SATE phosphotriester siRNNs that do not suffer from the hydrophobic problems of *t*Bu-SATE siRNNs, but maintain the same bioreversibility, stability to nucleases, and ability to induce robust RNAi responses (**Figure 3.1**). Through analysis of a fully 2'-F/OMe modified siRNA structure, I developed the Phosphate Interference Model that pairs phosphates predicted to be sterically opposed to each other across the siRNA major groove (**Figure 3.2**). By utilizing this model, I was able to produce highly neutral siRNNs containing 26x O-SATE phosphotriesters, the maximum number of phosphotriester groups tolerable for RNA double-stranding. These highly neutral siRNNs were ~20% more neutral than any we had previously synthesized, thereby bringing the total siRNN neutrality to ~65% and into the range of what was predicted to allow delivery by cationic PTDs (see Chapter 1). We also investigated insertion of locked nucleic acids (LNAs) to stabilize the siRNN duplex to allow for further phosphotriester placement (see Chapter 1) (Elmén et al., 2005). I found that while

insertion of LNAs does stabilize the siRNN duplex, placement of more than 2x LNAs inhibits induction of an RNAi response (data not shown), possibly by preventing ejection of cleaved passenger strand from Ago2 or by prevention of TRBP to recognize and load it into Ago2.

We next utilized Hynic conjugation chemistry to attach cationic TAT PTDs to the 5' end of highly neutral O-SATE siRNNs. I found that in cells treated with Cy3-labled TAT PTD-siRNNs, the Cy3 uptake correlated with the overall charge of the molecule and the more positively charged conjugates displayed Cy3 uptake in excess of transfected siRNA. However, TAT PTD-siRNN conjugates with overall cationic charge failed to induce RNAi responses upon cell treatment. Additional treatment with chloroquine to facilitate endosomal escape did not result in target gene knockdown as is the case with TAT-DRBD-siRNA treatments at otherwise sub-effective concentrations (data not shown).

While unsuccessful in generating PTD-siRNNs capable of self-delivery and RNAi induction, this study served to demonstrate the extent that siRNAs may be modified with bioreversible phosphotriesters, how the biophysical properties of siRNAs may be molecularly shaped through the insertion of different types of phosphotriesters, and how molecular modeling can be utilized to generate more neutral siRNNs.

ACKNOWLEDGEMENTS

The research described in Chapter 3 has, in part, been published in *Nature Biotechnology* co-authored by the dissertation author (Meade et al., 2014). Phosphoramidites utilized in Chapter 3 were synthesized by Khirud Gogoi. Byran Meade synthesized some oligonucleotides, worked out TBDMSO-SATE oligonucleotide synthesis and deprotection conditions, and performed some cellular treatments. The dissertation author was a principal investigator and co-author of this material.

REFERENCES

Allerson, C.R., Sioufi, N., Jarres, R., Prakash, T.P., Naik, N., Berdeja, A., Wanders, L., Griffey, R.H., Swayze, E.E., and Bhat, B. (2005). Fully 2'-modified oligonucleotide duplexes with improved in vitro potency and stability compared to unmodified small interfering RNA. J. Med. Chem. *48*, 901–904.

Beaucage, S.L. (2008). Solid-phase synthesis of siRNA oligonucleotides. Curr. Opin. Drug Discov. Devel. *11*, 203–216.

van den Berg, A., and Dowdy, S.F. (2011). Protein transduction domain delivery of therapeutic macromolecules. Curr. Opin. Biotechnol. 6–11.

Bumcrot, D., Manoharan, M., Koteliansky, V., and Sah, D.W.Y. (2006). RNAi therapeutics: a potential new class of pharmaceutical drugs. Nat. Chem. Biol. *2*, 711–719.

Dirksen, A., and Dawson, P.E. (2008). Rapid oxime and hydrazone ligations with aromatic aldehydes for biomolecular labeling. Bioconjug. Chem. *19*, 2543–2548.

Dirksen, A., Dirksen, S., Hackeng, T.M., and Dawson, P.E. (2006). Nucleophilic catalysis of hydrazone formation and transimination: implications for dynamic covalent chemistry. J. Am. Chem. Soc. *128*, 15602–15603.

Eguchi, A., and Dowdy, S.F. (2009). siRNA delivery using peptide transduction domains. Trends Pharmacol. Sci. *30*, 341–345.

Eguchi, A., Meade, B.R., Chang, Y.-C., Fredrickson, C.T., Willert, K., Puri, N., and Dowdy, S.F. (2009). Efficient siRNA delivery into primary cells by a peptide transduction domain-dsRNA binding domain fusion protein. Nat. Biotechnol. *27*, 567–571.

Elmén, J., Thonberg, H., Ljungberg, K., Frieden, M., Westergaard, M., Xu, Y., Wahren, B., Liang, Z., Ørum, H., Koch, T., and Wahlestedt, C. (2005). Locked nucleic acid (LNA) mediated improvements in siRNA stability and functionality. Nucleic Acids Res. *33*, 439–447.

Gait, M.J. (2003). Peptide-mediated cellular delivery of antisense oligonucleotides and their analogues. Cell. Mol. Life Sci. *60*, 844–853.

Glover, D.J., Lipps, H.J., and Jans, D.A. (2005). Towards safe, non-viral therapeutic gene expression in humans. Nat. Rev. Genet. *6*, 299–310.

Gonçalves, E., Kitas, E., and Seelig, J. (2005). Binding of oligoarginine to membrane lipids and heparan sulfate: structural and thermodynamic characterization of a cell-penetrating peptide. Biochemistry *44*, 2692–2702.

Jiang, T., Olson, E.S., Nguyen, Q.T., Roy, M., Jennings, P.A., and Tsien, R.Y. (2004). Tumor imaging by means of proteolytic activation of cell-penetrating peptides. Proc. Natl. Acad. Sci. U. S. A. *101*, 17867–17872.

Kaplan, I.M., Wadia, J.S., and Dowdy, S.F. (2005). Cationic TAT peptide transduction domain enters cells by macropinocytosis. J. Control. Release *102*, 247–253.

Kawamura, K.S., Sung, M., Bolewska-Pedyczak, E., and Gariépy, J. (2006). Probing the impact of valency on the routing of arginine-rich peptides into eukaryotic cells. Biochemistry *45*, 1116–1127.

Lefebvre, I., Périgaud, C., Pompon, A., Aubertin, A.M., Girardet, J.L., Kirn, A., Gosselin, G., and Imbach, J.L. (1995). Mononucleoside phosphotriester derivatives with S-acyl-2-thioethyl bioreversible phosphate-protecting groups: intracellular delivery of 3'-azido-2',3'-dideoxythymidine 5'-monophosphate. J. Med. Chem. *38*, 3941–3950.

Lönn, P., and Dowdy, S.F. (2015). Cationic PTD/CPP-mediated macromolecular delivery: charging into the cell. Expert Opin. Drug Deliv. *12*, 1627–1636.

Manoharan, M. (2004). RNA interference and chemically modified small interfering RNAs. Curr. Opin. Chem. Biol. *8*, 570–579.

Meade, B.R., and Dowdy, S.F. (2007). Exogenous siRNA delivery using peptide transduction domains/cell penetrating peptides. Adv. Drug Deliv. Rev. *59*, 134–140.

Meade, B.R., Gogoi, K., Hamil, A.S., Palm-Apergi, C., van den Berg, A., Hagopian, J.C., Springer, A.D., Eguchi, A., Kacsinta, A.D., Dowdy, C.F., Presente, A., Lönn, P., Kaulich, M., Yoshioka, N., Gros, E., Cui, X.-S., and Dowdy, S.F. (2014). Efficient delivery of RNAi prodrugs containing reversible charge-neutralizing phosphotriester backbone modifications. Nat. Biotechnol. *32*, 1256–1261.

Michiue, H., Eguchi, A., Scadeng, M., and Dowdy, S.F. (2009). Induction of in vivo synthetic lethal RNAi responses to treat glioblastoma. Cancer Biol. Ther. *8*, 2306–2313.

Nakase, I., Niwa, M., Takeuchi, T., Sonomura, K., Kawabata, N., Koike, Y., Takehashi, M., Tanaka, S., Ueda, K., Simpson, J.C., Jones, A.T., Sugiura, Y., and Futaki, S. (2004). Cellular uptake of arginine-rich peptides: roles for macropinocytosis and actin rearrangement. Mol. Ther. *10*, 1011–1022.

Ogilvie, K.K., Theriault, N., and Sadana, K.L. (1977). Synthesis of oligoribonucleotides. J. Am. Chem. Soc. *99*, 7741–7743.

Podbevsek, P., Allerson, C.R., Bhat, B., and Plavec, J. (2010). Solution-state structure of a fully alternately 2'-F/2'-OMe modified 42-nt dimeric siRNA construct. Nucleic Acids Res. *38*, 7298–7307.

Rothbard, J.B., Jessop, T.C., Lewis, R.S., Murray, B.A., and Wender, P.A. (2004). Role of membrane potential and hydrogen bonding in the mechanism of translocation of guanidinium-rich peptides into cells. J. Am. Chem. Soc. *126*, 9506–9507.

Rublack, N., Nguyen, H., Appel, B., Springstubbe, D., Strohbach, D., and Müller, S.

(2011). Synthesis of specifically modified oligonucleotides for application in structural and functional analysis of RNA. J. Nucleic Acids *2011*, 805253.

Scaringe, S.A., Francklyn, C., and Usman, N. (1990). Chemical synthesis of biologically active oligoribonucleotides using beta-cyanoethyl protected ribonucleoside phosphoramidites. Nucleic Acids Res. *18*, 5433–5441.

Schirle, N.T., and MacRae, I.J. (2012). The crystal structure of human Argonaute2. Science *336*, 1037–1040.

Schwarze, S.R. (1999). In Vivo Protein Transduction: Delivery of a Biologically Active Protein into the Mouse. Science (80-.). *285*, 1569–1572.

Wadia, J.S., and Dowdy, S.F. (2005). Transmembrane delivery of protein and peptide drugs by TAT-mediated transduction in the treatment of cancer. Adv. Drug Deliv. Rev. *57*, 579–596.

Wadia, J.S., Stan, R. V, and Dowdy, S.F. (2004). Transducible TAT-HA fusogenic peptide enhances escape of TAT-fusion proteins after lipid raft macropinocytosis. Nat. Med. *10*, 310–315.

Weitzer, S., and Martinez, J. (2007). The human RNA kinase hClp1 is active on 3’ transfer RNA exons and short interfering RNAs. Nature *447*, 222–226.

Zeidman, R., Jackson, C.S., and Magee, A.I. (2009). Protein acyl thioesterases (Review). Mol. Membr. Biol. *26*, 32–41.

CHAPTER 4

DEVELOPMENT OF SELF-DELIVERING PTD-siRNNS

DEVELOPMENT OF SELF-DELIVERING PTD-siRNNS

ABSTRACT

In contrast to small molecule drugs (<500 Da) that can diffuse passively across cell membranes, short interfering RNAs (siRNAs) are both too large (~14 kDa) and too charged (~40 charged phosphates) to enter cells on their own. Therefore, siRNAs require assistance from a delivery agent to enter cells. The ability of peptide transduction domains (PTDs), such as TAT PTD, to effectively mediate cellular delivery of macromolecular cargo makes them attractive candidates for siRNA delivery. However, PTD function is dependent on their dense cationic charge, which is neutralized upon interaction with strongly anionic siRNAs. To enable siRNA delivery, we have developed short interfering ribonucleic neutrals (siRNNs) where bioreversible phosphotriester groups neutralize the problematic negative charge of siRNA's phosphate backbone. Initial work focused on synthesis of siRNNs with *t*Bu-SATE phosphotriesters, but these groups proved too hydrophobic for use. To address this problem, we developed more hydrophilic, polar O-SATE groups that are compatible with biological solutions. Although O-SATE phosphotriesters could be applied to siRNNs in high enough numbers to provide sufficient charge neutralization to allow for PTD mediated siRNN delivery, these highly modified siRNNs remained incapable of cellular delivery. Here I describe the development of functionalized A-SATE phosphotriesters to solve the delivery problem. A-SATE groups both neutralize the charge of the phosphate backbone and serve as conjugation sites, thereby allowing site-selective multivalent conjugation. Importantly, A-SATE phosphotriesters are bioreversible even when conjugated to a PTD. This work comprises the first report of self-delivering PTD-siRNN conjugates that induce dose-dependent RNAi responses *in vitro*.

INTRODUCTION

siRNA-induced RNAi responses hold significant promise as a new class of therapeutics. siRNAs have high potency (EC_{50} ~10^{-12} M), exquisite target selectivity for any expressed mRNA, and the ability to adapt its sequence to pursue new genetic targets (Wittrup and Lieberman, 2015; Juliano, 2016). However, the high negative charge and size of siRNA molecules renders them unable to enter cells without assistance from a delivery agent. Most current methods of siRNA delivery rely on encapsulating siRNA molecules in very large nanoparticles or cationic liposomes. Unfortunately, these approaches suffer from a number of problems, including poor cellular delivery, cytotoxicity, and poor pharmacokinetics (Meade and Dowdy, 2009). Consequently, siRNA delivery remains *The Problem* to solve in developing RNAi therapeutics.

Peptide Transduction Domains (PTDs), also known as cell-penetrating peptides (CPPs), may be ideal for delivering single molecules of siRNA across the cellular membrane. PTDs have been utilized to deliver a wide range of cargos including peptides and proteins, both in vitro and in vivo, across the cell membrane (Schwarze, 1999; Lönn and Dowdy, 2015). Unfortunately, the cationic charge of PTDs is crucial to mediate delivery and conjugation to anionic siRNA neutralizes the PTD charge, resulting in aggregation and no cellular delivery (Jiang et al., 2004). To circumvent this problem, our lab previously developed a TAT PTD fusion protein with a dsRNA Binding Domain (DRBD) termed PTD-DRBD (Eguchi et al., 2009; Michiue et al., 2009). This fusogenic protein binds and physically masks the siRNA's negative charges, thereby allowing for efficient, non-cytotoxic PTD-mediated into an entire population of cells. The PTD-DRBD siRNA delivery approach effectively demonstrated PTD-mediated delivery of siRNA to cells upon masking of the siRNA negative charge. However, the PTD-DRBD approach

had inherent flaws prevented systemic administration and that limited its utility as a therapeutic (see Chapter 1).

To enable PTD-mediated delivery of siRNA, our lab developed short interfering ribonucleic neutrals (siRNNs). siRNNs feature bioreversible s-acyl-2-thioethyl (SATE) phosphotriester groups that neutralize the negative charge of the siRNA backbone (Meade et al., 2014). The bioreversibility of the SATE phosphotriester is made possible through processing by cytoplasm-restricted thioesterases (**Figure 1.3**) (Zeidman et al., 2009) that convert the neutral phosphotriester into a charged native phosphodiester compatible with the RNAi machinery. The first generation of siRNNs utilized *t*Bu-SATE phosphotriesters (Gröschel et al., 2002), made possible by the groundbreaking synthesis of RNA oligonucleotides containing *t*Bu-SATE groups (Meade et al., 2014). Although capable of bioreversal and induction of RNAi responses when transfected into cells with cationic lipids, the hydrophobicity of the *t*Bu-SATE group led to extreme insolubility of *t*Bu-SATE siRNNs in aqueous conditions.

To improve upon *t*Bu-SATE siRNNs, we synthesized the O-SATE phosphotriester that was more polar by addition of a terminal hydroxyl group (see Chapter 3). O-SATE phosphotriesters did not suffer from the hydrophobicity problems that plagued *t*Bu-SATE siRNNs, remaining soluble in physiologically compatible solutions. However, even with O-SATE groups we were limited to synthesizing siRNNs with 9x phosphotriesters on each strand. Insertion of additional phosphotriester groups resulted in a profound decrease in the affinity of the RNN oligonucleotides to from a double-stranded species. Through molecular modeling I was able to design and synthesize oligonucleotides with 20% more phosphotriester insertions to make highly neutral siRNNs. The neutrality of these siRNNs was in the range determined to be necessary for PTD mediated delivery (see Chapter 1). Yet, highly neutral TAT PTD-

siRNN conjugates were incapable of self-delivery despite having an overall cationic charge and did not induce RNAi responses in treated cells.

The reason for this delivery failure was not fully understood, but it may have been due to the linkage between the PTD and siRNN or due to the PTD itself being neutralized by the remaining negatively charged phosphodiesters on the siRNN. The 5'-end of the passenger contained a benzaldehyde with an adjacent 3' disulfide linkage to allow for cytoplasmic reductive separation (**Figure 3.3**). Upon reaction with a PTD functionalized with a hydrazine moiety, a stable hydrazone linkage was formed between PTD and siRNN. This approach, while orthogonal with siRNN synthesis, is potentially susceptible to premature disulfide linkage reduction in endosomes prior to escape to the cytoplasm (Yang et al., 2006; Hastings and Cresswell, 2011), thereby preventing PTD-mediated escape to the cytoplasm. Alternatively, despite the PTD-siRNN conjugates having an overall cationic charge, the PTD may have been affected by the remaining anionic phosphodiesters in a limited manner that prevented PTD mediated delivery but did not result in intermolecular interactions and aggregation.

To address these issues we developed Aldehyde-SATE (A-SATE) phosphotriesters that contain a chemically reactive benzaldehyde functional group. A-SATEs are multifunctional in that they both neutralize the phosphate negative charge, but are also conjugatable. Incorporation of A-SATE groups at select sites during synthesis into siRNNs facilitates site-specific multivalent conjugation of hydrazine functionalized molecules, such as PTDs Additionally, PTD-conjugated A-SATEs retain the proven ability of SATE phosphotriesters to be removed only upon entry into the cytoplasm, thereby avoiding usage of a potentially problematic disulfide linkage.

RESULTS & DISCUSSION

Synthesis and Deprotection of acetal-A-SATE RNN oligonucleotides

To be incorporated into siRNNs, A-SATE phosphotriesters were required to be compatible with standard oligonucleotide synthesis and remain stable under the ultramild base deprotection conditions utilized by *t*Bu-SATE and O-SATE RNN containing oligonucleotides (see Chapter 2). Because A-SATEs were designed to be conjugatable, they incorporated a chemically reactive benzaldehyde group that must be protected during oligonucleotide synthesis. The deprotection conditions for protected A-SATEs could not compromise phosphotriester integrity or degrade the oligonucleotide and also need to couple with a similar efficiency as *t*Bu-SATE and O-SATE phosphoramidites.

A-SATE-modified phosphoramidites were synthesized by the same method used to produce *t*Bu-SATE phosphoramidites (**Figure 2.1**), but with acetal-A-SATE (ac-A-SATE) substituted for the S-(2-hydroxyethyl) thiopivaloate (**Figure 4.1A**). Ac-A-SATE phosphoramidites were found to be compatible with the RNA oligonucleotide synthesis conditions used for oligonucleotides containing *t*Bu-SATE and O-SATE groups. However, during ultramild base primary deprotection A-SATE phosphotriesters were slightly less stable than *t*Bu-SATE phosphotriesters. As a result, some A-SATE decomposition was evident in the crude oligonucleotide following primary base deprotection (**Figure 4.1D**, lower left panel). In order to minimize this decomposition, acetic acid was added to the primary deprotection A-SATE oligonucleotide solution to neutralize the diisopropylamine (DIA) prior to drying by centrifugal evaporation.

Our standard protocol for the purification of crude RNN oligonucleotides utilized dimethoxytrityl-on (DMT) reversed-phase high-performance liquid chromatography (RP-HPLC). The presence of a 5'-DMT group is useful during oligonucleotide purification to separate the full length product from truncation products as only the full length product

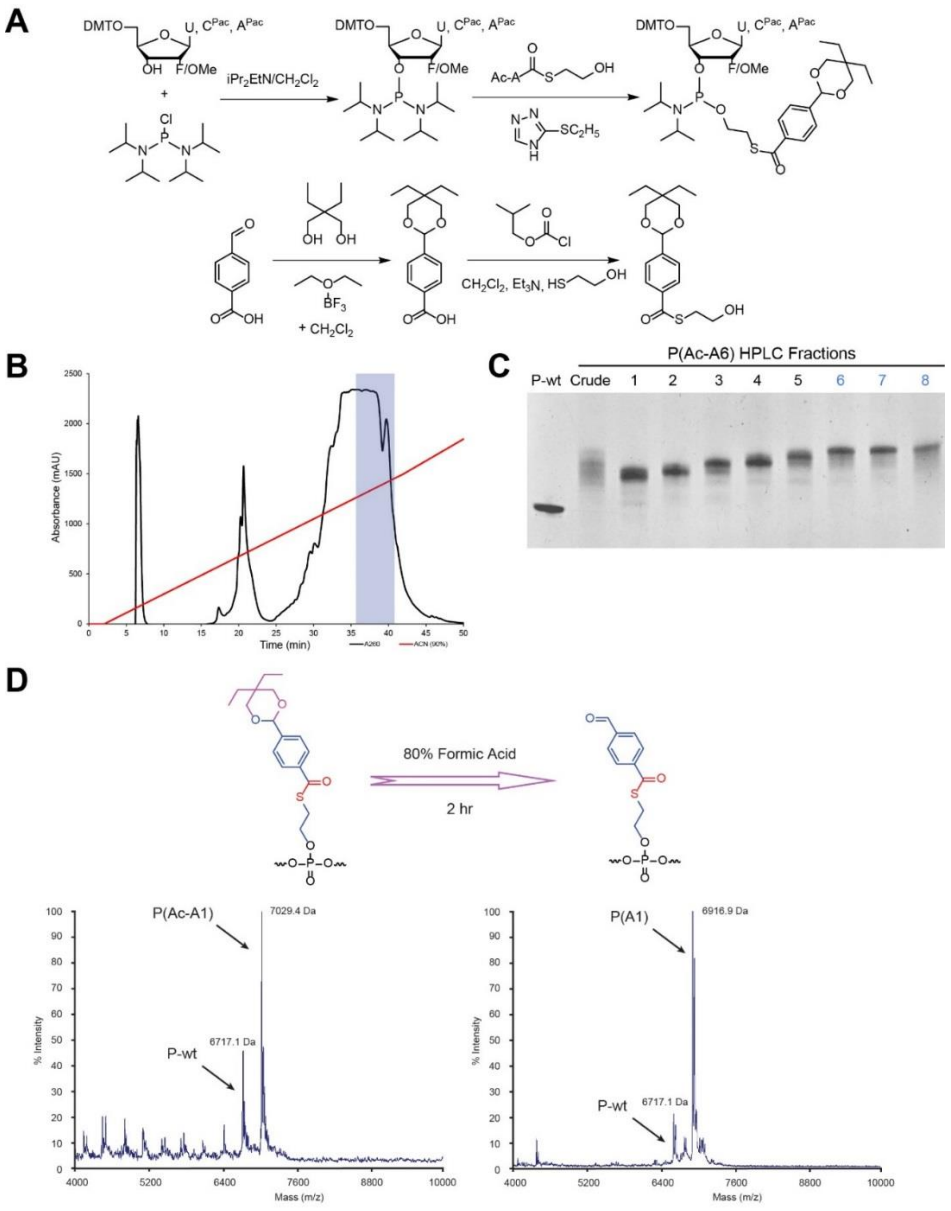

Figure 4.1. Synthesis and deprotection of A-SATE RNN oligonucleotides. A) Synthetic routes for U, C, and A phosphoramidites containing A-SATE groups and acetal-A-SATE alcohol used in phosphoramidite synthesis. **B)** RP-HPLC chromatogram of DMT-off purification of RNN oligonucleotide containing 6x acetal-protected A-SATE phosphotriesters. Buffer A = 50 mM triethylammonium acetate in water; Buffer B = 90% acetonitrile. Red line represents buffer B gradient: 0% buffer B for 0 – 2 min, 0 to 60% buffer B from 2 – 42 min. Blue box encompasses fractions collected for analysis. **C)** Crude P(Ac-A6) oligonucleotide and collected HPLC fractions. Fraction numbers colored blue indicate fractions retained and pooled for final product. 15% acrylamide urea denaturing gel, stained with methylene blue. P-wt is a reference oligonucleotide of the same sequence as the P(Ac-A6) oligonucleotide, but contains no phosphotriesters. **D)** MALDI-TOF mass spectrometry analysis of formic acid deprotection of RNN oligonucleotide containing 1x acetal-protected A-SATE. Spectra on left panel depicts oligonucleotide prior to treatment with 80% formic acid and right panel depicts spectra after 2 hr of treatment. Note removal of acetal protection without significant loss of the A-SATE phosphotriester.

contains a hydrophobic DMT group. However, we determined that a DMT-off purification protocol is more effective for ac-A-SATE RNN as the hydrophobicity of the acetal-protected A-SATE decreases the utility of DMT-on purification and can cause truncation products containing ac-A-SATE to co-elute with the full length product (**Figure 4.1B**). Furthermore, the addition of acetic acid after primary deprotection results in the loss of the 5'-DMT group from some of the full length product. Using these methods, we were able to readily purify RNN oligonucleotides containing a number of ac-A-SATE insertions (**Figure 4.1B,C**).

The key component of A-SATE phosphotriesters is incorporation of a benzaldehyde for reaction with hydrazine functionalized PTDs. However, this benzaldehyde is also reactive during oligonucleotide synthesis and the A-SATE benzaldehyde must therefore be protected to prevent undesired side reactions from occurring during synthesis. We have found branching can occur at a benzaldehyde during oligonucleotide synthesis if the group is not protected (data not shown). In addition, unprotected aldehydes are generally unstable in oligonucleotide deprotection conditions. We chose to protect the A-SATE benzaldehyde with a cyclic acetal (**Figure 4.1A,D**) that is stable during both oligonucleotide synthesis and during primary oligonucleotide deprotection, and can allow 'acetal-on' RP-HPLC purification (similar to DMT-on) of ac-A-SATE oligonucleotides. Acetal protection can be readily removed by treatment with 80% acetic acid (Podyminogin et al., 2001), which is compatible with RNN phosphotriester chemistry. This same cyclic acetal was used to protect the 5'-benzaldehyde group previously attached to the siRNN passenger strand 5'-end for PTD conjugation (**Figure 3.3**).

In contrast to the 5'-benzaldehyde group (Podyminogin et al., 2001), we found that acetic acid treatment at 65° C of an RNN oligonucleotide did not remove the acetal

protection from incorporated A-SATE phosphotriesters (data not shown). This difference in reactivity may due to the presence a thioester bond proximal to the protected benzaldehyde in an A-SATE phosphotriester group (**Figure 4.1A**). Instead, we found that treatment of an oligonucleotide containing ac-A-SATE groups with 80% formic acid for 2 hr at room temperature was sufficient to remove the majority of the acetal protecting groups (**Figure 4.1D**). Importantly, this deprotection method results in removal of acetal protection without significant loss of the A-SATE phosphotriester, strand scission, or nucleobase depurination.

Biological function of A-SATE siRNNs

Bioreversibility is a necessary characteristic for incorporation of A-SATE phosphotriesters into functionally active siRNNs (**Figure 4.2A**). The *t*Bu-SATE and O-SATE phosphotriesters are subject to processing by cytoplasmic thioesterases that converts them into native negatively charged phosphodiesters compatible with loading into RISC and induction of RNAi responses (**Figure 1.3**). However, the potential effect of the A-SATE's benzaldehyde group on the stability of the thioester bond or its suitability as a thioesterase substrate was unknown.

To test the bioreversibility of the A-SATE phosphotriester group, we synthesized a series of GFP RNN guide strands containing 6x phosphotriesters and duplexed them with wildtype (2'-F/OMe modified) passenger strands. Interaction with the guide strand phosphodiester backbone is necessary for Ago2 to mediate an RNAi response (Schirle and MacRae, 2012). Consequently, phosphotriester groups must be removed from the guide strand to induce an RNAi response. We transfected these tester siRNNs into H1299 cells constitutively expressing destabilized GFP (H1299-dGFP) and measured GFP expression by flow cytometry to determine RNAi induction (**Figure 4.2B**). As expected, positive control wt/wt siRNA induced robust dose-dependent RNAi responses.

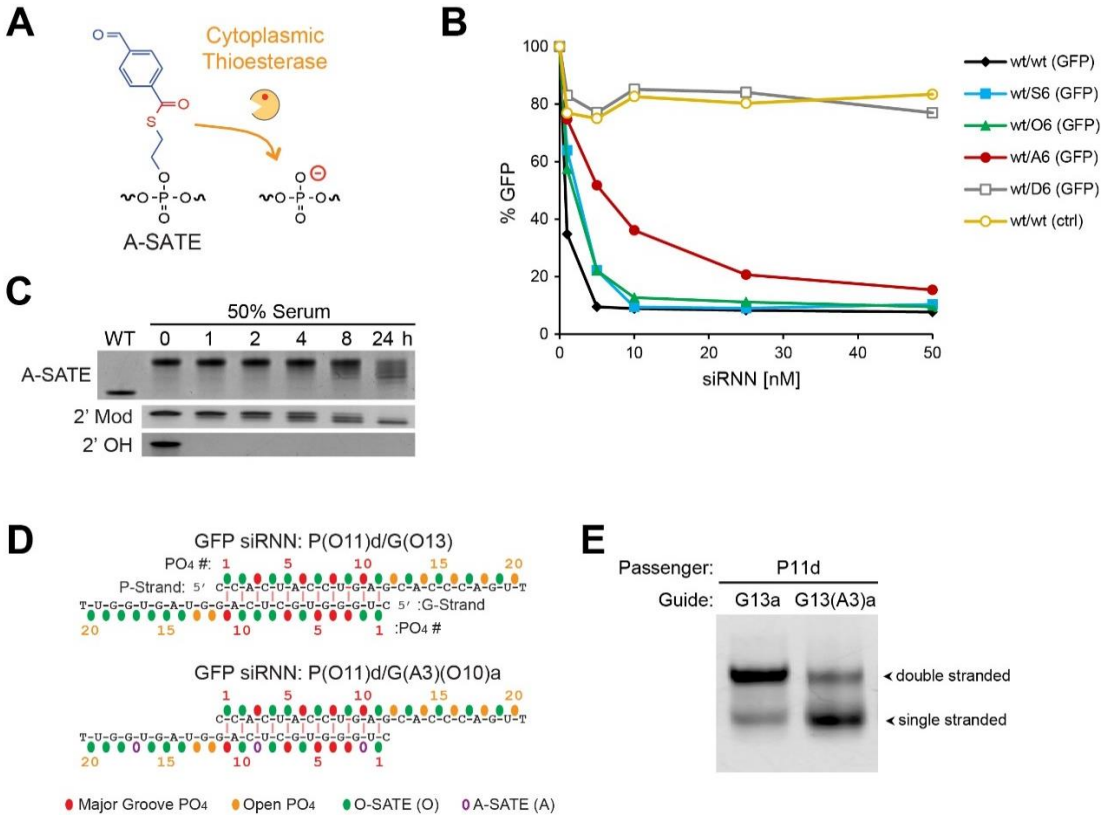

Figure 4.2. Biophysical properties and function of A-SATE siRNNs. A) Cytoplasmic thioesterase processing of A-SATE phosphotriester group induces rapid decomposition process resulting in an RNAi-compatible wildtype charged phosphodiester. **B)** Flow cytometry analysis of H1299-dGFP cells transfected with a dose curve of either 2'-F/OMe modified siRNA (wt) or siRNNs with guide strands containing 6x phosphotriesters targeting GFP or off-target control sequence (ctrl). S= *t*Bu-SATE, O = O-SATE, A = A-SATE, D = *irreversible* DMB. **C)** Serum stability analysis of ssRNA containing wild-type phosphodiesters and 2'-OH or 2'-F/OMe (2'-Mod) vs ssRNN containing 6x A-SATE phosphotriesters. **D)** Diagram of siRNNs used in panel E in phosphate interference model format. Red lines indicate pairs of phosphates that may interfere sterically across the siRNN major groove. **E)** Double-stranding test of RNN oligonucleotides containing O-SATE and A-SATE phosphotriesters. Strand identifiers: P11d = P(O11)d, G13a = G(O13)a, G13(A3)a = G(A3)(O10)a.

*t*Bu-SATE and O-SATE containing wt/S6 and wt/O6 siRNNs, respectively, tracked closely with wt/wt siRNA induced RNAi responses (**Figure 4.2B**). As anticipated, Non-Targeting Control (NTC) siRNA treatment failed to induce a GFP knockdown (**Figure 4.2B**). Additionally, the irreversible DMB phosphotriester GFP-targeted wt/D6 siRNN (**Figure 2.2**) failed to induce an RNAi response, verifying the assay (**Figure 4.2B**). Importantly, the A-SATE containing wt/A6 siRNN induced dose dependent RNAi responses, thereby confirming bioreversibility of the A-SATE phosphotriester. However, the dose curve of the wt/A6 siRNN lagged behind wt/S6 and wt/O6 siRNNs, suggesting that the A-SATE may be more difficult for intracellular thioesterases to remove. These results imply that while the A-SATE is bioreversible, we should avoid incorporation of a prohibitively high number of groups and avoid placement at sensitive locations such as on the guide strand in areas where Ago2 must contract the phosphodiester backbone.

Stability in blood is essential for the success of RNAi therapeutics. I therefore examined the stability of single-stranded RNN (ssRNN) oligonucleotides containing 6x A-SATE phosphotriesters to serum ribonucleases by incubation in 50% human serum at 37° C (**Figure 4.2C**). At various time points the oligonucleotides were analyzed by denaturing gel electrophoresis. A-SATE containing oligonucleotides were found to be far more stable in serum than natural 2'-OH RNA, although slightly less so than similar RNNs incorporating *t*Bu-SATE or O-SATE phosphotriesters (**Figure 3.1D**).

After characterizing A-SATE phosphotriesters, we sought to incorporate them into highly neutral siRNNs for site selective conjugation to TAT-PTD delivery peptides. Molecular modeling and hybridization testing had allowed me to design and synthesize highly neutral siRNNs by selective placement of the maximum number of O-SATE phosphotriesters tolerated for the formation of double-stranded species (**Chapter 3**). To test whether A-SATEs would disrupt hybridization of highly neutral RNN strands, we

synthesized highly neutral guide strands containing either only O-SATEs or a combination of O-SATEs and A-SATEs (**Figure 4.2D**). Native gel analysis of the affinity of these guide strands to form double-stranded species with a highly neutral passenger strand revealed that insertion of A-SATEs reduces hybridization affinity (**Figure 4.2E**). The phosphate interference model predicted only two potential phosphotriester conflicts across the siRNN major groove for these strands, which based on prior data (**Figure 3,2**), should be tolerated for strand duplexing. However, the larger size of the A-SATE phosphotriesters appears to have a greater destabilizing effect on double-stranded RNNs in contrast to the smaller and better tolerated O-SATEs (**Figure 3.2**). This data suggested that A-SATE placement must be carefully chosen and limits the number of overall phosphotriesters, and consequently degree of charge neutralization, that can be present on siRNNs. However, each inserted A-SATE potentially comes with a large amount of cationic charge addition by way of the PTD that will be conjugated to it and this may offset any charge deficits incurred by the duplex limiting presence of an A-SATE group.

Conjugation of TAT PTD delivery domain peptides to A-SATE siRNNs

Having demonstrated that A-SATE phosphotriester siRNNs could be synthesized, were bioreversible, and capable of inducing an RNAi response, the next step was to perform a PTD conjugation (**Figure 4.3A**). The terminal benzaldehyde of the A-SATE was designed to react with hydrazine functionalized peptides to form a stable hydrazone linkage between the siRNN and peptide. To examine reactivity of the A-SATE group, we reacted oligonucleotides containing either a 5'-benzaldehyde (Ald-P-wt) or an A-SATE phosphotriester (P(A1)) with increasing amounts of TAT-Hynic peptide (**Figure 4.3B**). We found that A-SATEs have a similar level of conjugation reactivity

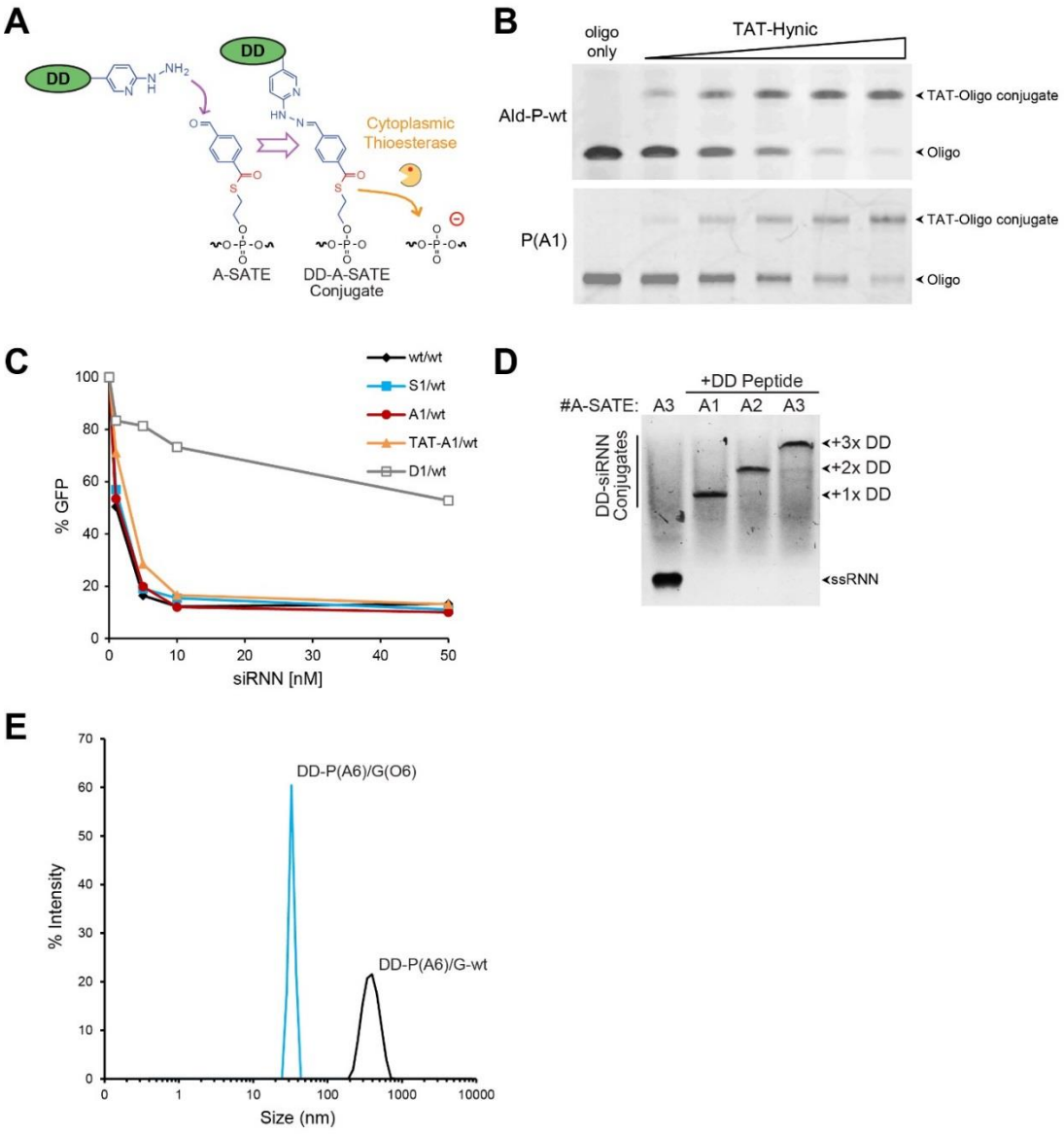

Figure 4.3. Conjugation of delivery domain peptides to A-SATE siRNNs. A) Conjugation of hydrazine functionalized delivery domain (DD) to A-SATE phosphotriester by Hynic reaction results in the formation of a stable bis-aryl hydrazone linkage. Cytoplasmic thioesterase processes DD-A-SATE conjugated phosphotriester resulting in an RNAi-compatible wildtype charged phosphodiester. **B)** Denaturing gel analysis of aldehyde functionalized oligonucleotides reacted with increasing amounts of TAT-Hynic peptide. From left to right, molar ratio of oligonucleotide to TAT-Hynic is 1 : 0, 0.2, 0.4, 0.6, 0.8, 1. TAT-Hynic peptide sequence: Hynic-GGRKKRRQRRR. **C)** Flow cytometry analysis of H1299-dGFP cells transfected with a dose curve of either 2'-F/OMe modified siRNA (wt) or siRNNs with containing 1x phosphotriester at the passenger strand cleavage site (P#9). All siRNAs and siRNNs target GFP. S= *t*Bu-SATE, A = A-SATE, TAT-A = TAT-Hynic peptide conjugated to A-SATE, D = *irreversible* DMB. **D)** Conjugation of 3x-TAT PEG spacer peptide (DD) to RNN oligonucleotides containing one (A1), two (A2), or three (A3) A-SATE phosphotriesters. DD peptide sequence = Hynic-GG-(TAT)-PEG18-(TAT)-PEG18-(TAT) where TAT is RKKRRQRRR. **E)** Dynamic light scattering particle size analysis of DD-siRNN conjugates at 1 uM in PBS.

when compared to the 5'-benzaldehyde that we previously used for PTD conjugation to siRNNs (**Figure 3.3**).

Although A-SATEs are bioreversible (**Figure 4.2B**), we had not yet determined whether PTD-conjugated A-SATEs could be intracellularly converted to charged phosphodiesters to release the conjugated peptide. This release is particularly important for large conjugated molecules that may prevent incorporation of the siRNA into RISC and subsequent induction of an RNAi response. To assay PTD-A-SATE bioreversibility, we synthesized a series of passenger strands containing a phosphotriester group at the Ago2 cleavage position and duplexed them with wildtype guide strands (**Figure 4.3C**). Cleavage of the passenger strand is critical to the maturation and function of RISC (Matranga et al., 2005) and requires a phosphodiester. Retention of a phosphotriester at this position prevents induction of an RNAi response.

We transfected these GFP-targeted siRNAs into H1299-dGFP cells and found that siRNAs containing either a *t*Bu-SATE (S1/wt) or A-SATE (A1/wt) at the passenger strand cleavage position induced dose-dependent RNAi responses on par with wild type siRNA (**Figure 4.3C**). Importantly, the siRNA containing a conjugated TAT PTD-A-SATE at the cleavage site (TAT-A1/wt) also induced robust RNAi responses comparable to the other siRNNs. Further experimentation revealed that regardless of length of the conjugated peptide, the entire peptide-A-SATE phosphotriester group is removed by intracellular thioesterase cleavage of the thioester bond (data not shown). In contrast, the negative control for this experiment, an irreversible DMB phosphotriester at the cleavage position (D1/wt), only induced a partial, poor GFP RNAi response at higher treatment concentrations. This may have been due to the ability of Ago1,3,4 to remove the passenger strand by a helicase, independent of removing the phosphotriester group.

The rationale for the synthesis of A-SATE phosphotriesters was to allow site-specific multivalent conjugation of TAT delivery domain (DD) peptides to a siRNN. I found that TAT DD-siRNN multiconjugates could be generated through insertion of multiple A-SATE phosphotriesters into the same RNN and reaction with DD-hynic peptides (**Figure 4.3D**).

The primary problem with conjugation of unmodified siRNA to PTDs is that the anionic siRNA neutralizes the cationic charge of the PTD, which is necessary for PTD-mediated delivery, causing aggregation and poor cellular delivery (Jiang et al., 2004). We performed dynamic light scattering particle size analysis of DD-siRNN conjugates to examine aggregation at high conjugate concentrations (1 uM) in physiologically compatible phosphate-buffered saline (**Figure 4.3E**). We found that DD-siRNNs containing neutralizing O-SATE phosphotriesters on the guide strand (DD-P(A6)/G(O6)) do not form aggregates under these conditions. Conversely, DD-siRNNs containing no phosphotriesters on the guide strand (DD-P(A6)/G-wt) form large particles, suggesting that presence of phosphotriesters is paramount to preventing aggregation. These DD-P(A6)/G(O6) and DD-P(A6)/G-wt siRNNs also contain neutralizing A-SATE phosphotriesters on the passenger strand that prevent greater aggregation from occurring.

***In vitro* delivery and biological activity of siRNNs**

Based on effect of A-SATE steric restrictions on RNN oligonucleotide hybridization (**Figure 4.2E**) and the lack of aggregation observed with DD-siRNNs containing fewer than the maximum number of phosphotriesters (**Figure 4.3E**), we synthesized a chimeric passenger strand, P(A4)(D1), containing 4x A-SATEs and an irreversible DMB on the 5'-end. The DMB group was placed on the 5'-end of the passenger strand to prevent passenger strand loading. This passenger strand was then

duplexed to an RNN guide strand containing 6x *t*Bu-SATE phosphotriesters (G(S6)) and conjugated to delivery domain peptides (DD-siRNN^{A4}). To test for self-delivery, we then treated H1299-dGFP cells with DD-siRNN^{A4} conjugates (no cationic lipid transfection or other delivery vehicle) and analyzed the cells for GFP knockdown by flow cytometry 48 hr after cell treatment. GFP DD-siRNN^{A4} conjugates self-delivered into cells to induce a dose-dependent GFP knockdown in the entire population, whereas non-targeting control DD-siRNN^{A4} conjugates failed to knock down GFP (**Figure 4.4A,B**). Additionally, this dose-dependent knockdown was induced in a non-cytotoxic fashion (**Figure 4.4C**). This constituted the first demonstration of siRNNs capable of self-delivery and induction of RNAi responses.

I had shown multivalent DD-RNN conjugates could be produced through insert of multiple A-SATE phosphotriesters (**Figure 4.3D**), but the effect of delivery domain (DD) valency and A-SATE location on DD-siRNN self-delivery was unexplored. To ascertain the requirements for the number and location of A-SATE phosphotriesters, we synthesized a series of RNN oligonucleotides containing passenger and guide strand A-SATEs. Regardless of position, delivery domain conjugation to 2x A-SATE phosphotriester siRNNs (DD-siRNN^{A2}) induced an intermediate GFP RNAi response compared with DD-siRNNs containing 3x (DD-siRNN^{A3}) or 4x (DD-siRNN^{A4}) DD-conjugated A-SATE phosphotriester groups (**Figure 4.4D**). These experiments suggested that while the number of conjugated delivery domains is important to DD-siRNN function, the location of the A-SATEs on the siRNN where the delivery domains are conjugated only has a limited impact. Additional experimentation where the DD valency was increased through insertion of up to 12x A-SATE phosphotriesters resulted in cytotoxicity without a concomitant increase in potency, effectively narrowing the DD-siRNN therapeutic window (data not shown).

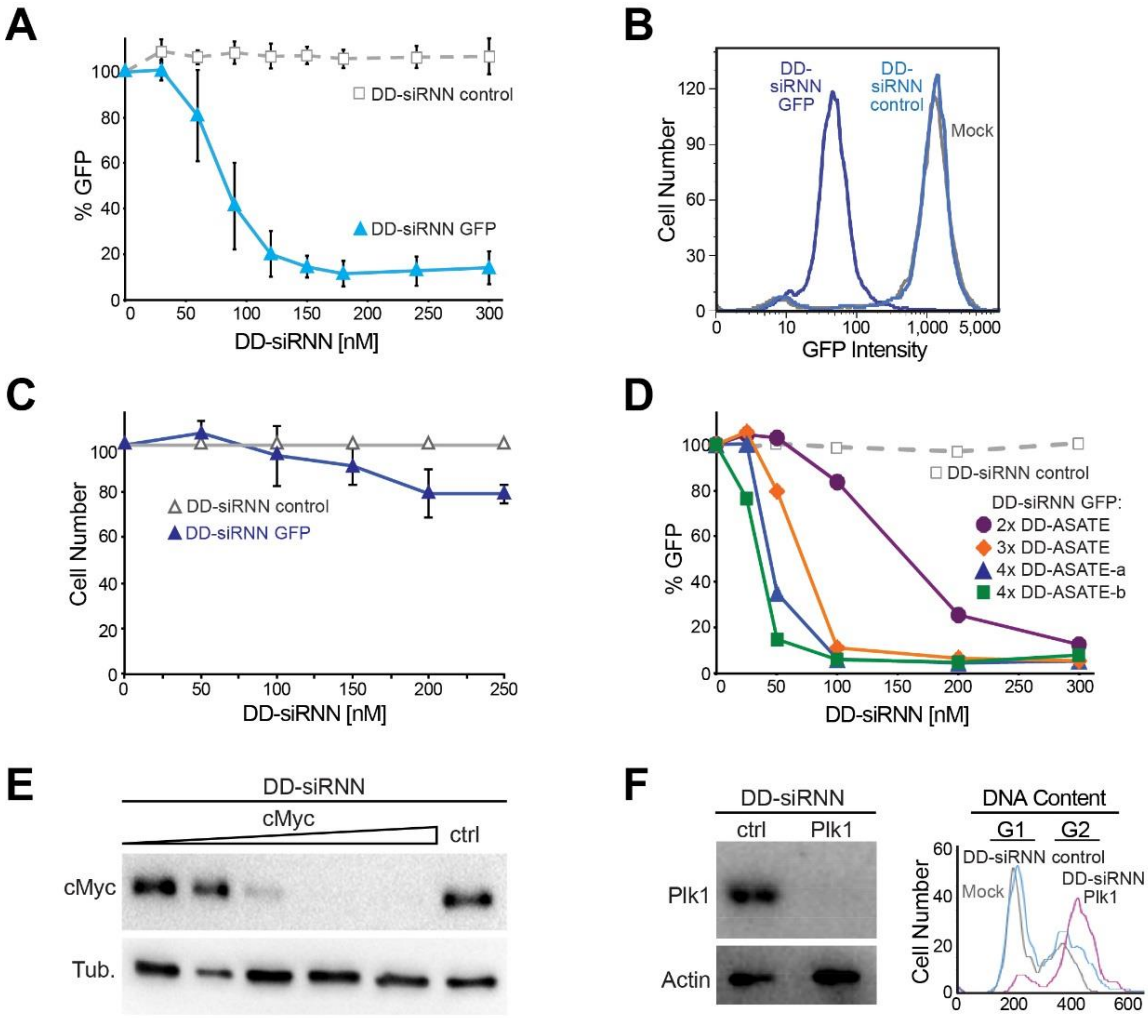

Figure 4.4. ***In vitro*** **delivery and biological activity of siRNNs. A)** Dose-dependent GFP RNAi responses in H1299-dGFP cells treated with self-delivering GFP DD-siRNN^{A4} conjugates vs. non-targeting control DD-siRNN^{A4} conjugates analyzed for GFP RNAi responses by flow cytometry 48 hr after treatment. siRNN^{A4} = P(A4)(D1)/G(S6). Error bar indicates standard deviation (s.d.). **B)** GFP RNAi histogram analysis of H1299-dGFP cells treated with GFP-target DD-siRNN^{A4} or control DD-siRNN^{A4} conjugates analyzed at 48 hr time point. Note entire population of cells undergoing GFP RNAi response. **C)** Cytotoxicity of DD-siRNN^{A4} treatments depicted in panel A. **D)** Dose-dependent GFP RNAi response comparison in H1299-dGFP cells treated with self-delivering GFP siRNNs conjugated to two delivery domains (DD-siRNN^{A2}), three delivery domains (DD-siRNN^{A3}) or two location variations of four delivery domains (DD-siRNN^{A4}-a,b) versus non-targeting control DD-siRNN^{A4} by flow cytometry at 48 hr time point. DD-siRNN^{A2} = P(A1)(S3)(D1)/G(A1)(S5), DD-siRNN^{A3} = P(A1)(S3)(D1)/G(A2)(S4), DD-siRNN^{A4}-a = P(A4)(D1)/G(S6), DD-siRNN^{A4}-b = P(A1)(S3)(D1)/G(A3)(S3). **E)** Dose-dependent cMyc immunoblot analysis of RNAi response (1, 5, 25, 50, 100 nM) in MDA-MB-231-cMyc-HA breast cancer cells by self-delivering cMyc DD-siRNN^{A4} vs. non-targeting control DD-siRNN^{A4} (ctrl) conjugate (100 nM) at 48 h. **F)** Immunoblot and flow cytometry analysis of U2OS osteosarcoma cell treatment with self-delivering Plk1 DD-siRNN^{A4} vs. non-targeting control DD-siRNN^{A4} (ctrl) conjugate. Plk1 DD-siRNN^{A4} conjugate induced Plk1 RNAi response and induced G2 phase cell cycle arrest, whereas control DD-siRNN^{A4} conjugate did not.

As the induction of an RNAi response is dependent on the siRNA target sequence and siRNAs all have similar biophysical properties independent of sequence, successful siRNA delivery and specific knockdown of one target implies that any expressed mRNA may be silenced by the same means by only changing the siRNA target sequence. After successful *in vitro* knockdown of GFP (**Figure 4.4A**) and luciferase reporter genes (data not shown) by DD-siRNNs, we next targeted c-Myc in MDA-MB-231 breast cancer cells and examined c-Myc knockdown by immunoblot (**Figure 4.4E**). Self-delivered c-Myc DD-siRNNs efficiently induced a dose-dependent c-Myc RNAi response, whereas non-targeting control DD-siRNN conjugates did not.

To examine the biological effect of endogenous gene knockdown, we targeted Plk1 in the U2OS human osteosarcoma tumor cell line. Plk1 is a Ser/Thr protein kinase required for proper M-phase progression that is overexpressed in various human cancers and, as such, is the target of a number of anti-cancer therapeutic agents (Murugan et al., 2011; Gutteridge et al., 2016). Due to its central role in cell-cycle progression, inhibition or knockdown of Plk1 results in mitotic arrest (Liu and Erikson, 2003). After treatment with Plk1 or control DD-siRNNs, treated cells were analyzed for target silencing and biological response by immunoblot and flow cytometry. Self-delivered Plk1 DD-siRNN conjugates induced strong Plk1 RNAi responses and appropriate G2 phase cell cycle arrest whereas the non-targeting control DD-siRNN did not (**Figure 4.4F**).

In vivo delivery and biodistribution of siRNNs

To measure the efficiency of DD-siRNN conjugate delivery *in vivo*, I targeted luciferase as a reporter gene and utilized a Rosa26-loxP-STOP-loxP-luciferase transgenic mouse strain (Safran et al., 2003). The mice used in this study contain the GL3 variant of the firefly luciferase gene inserted into the Rosa26 locus. Under normal

conditions, expression of luciferase is prevented by a STOP fragment flanked by loxP sites inserted between the luciferase gene and Rosa26 promoter (**Figure 4.5A**). Cre recombinase exposure induces removal of the STOP fragment and results in constitutive and permanent luciferase gene expression that can be detected by noninvasive live animal bioluminescent imaging (**Figure 4.5B,D**). Expression of luciferase only in target areas or organs can be induced in this mouse strain by selective application of TAT-Cre fusion protein (Wadia et al., 2004; Eguchi et al., 2009). In this system, TAT PTD delivers Cre recombinase cargo into cells at the site of TAT-Cre injection where it induces luciferase expression.

To examine the ability of DD-siRNNs to deliver and knockdown luciferase gene expression, I generated a subcutaneous luciferase back spot mouse model. To generate this model, I injected TAT-Cre subcutaneously in discrete spots on the back of the mouse, thereby activating luciferase expression in localized collections of cells susceptible to TAT-mediated delivery that could be readily analyzed by noninvasive live animal imaging when a mouse is in the prone position (**Figure 4.5B**). After stabilization of luciferase expression (3-7 days), I subcutaneously injected DD-siRNNs into the TAT-Cre treated areas. Treatment of multiple spots on the same animal allowed for in-animal controls, thereby limiting variability through normalization of each treatment to a mock treatment applied to the same animal at a separate spot. Single subcutaneous injection of 750 pmol or 3x 750 pmol injections (once per day for 3 days, q.d.) of luciferase-targeted DD-siRNN conjugate in PBS failed to induce RNAi responses in this model (**Figure 4.5C**). Likewise, single subcutaneous injection of 1.5 nmol Luc DD-siRNN, conjugates with higher DD valency, and alternative delivery domains also failed to induce an RNAi response (data not shown).

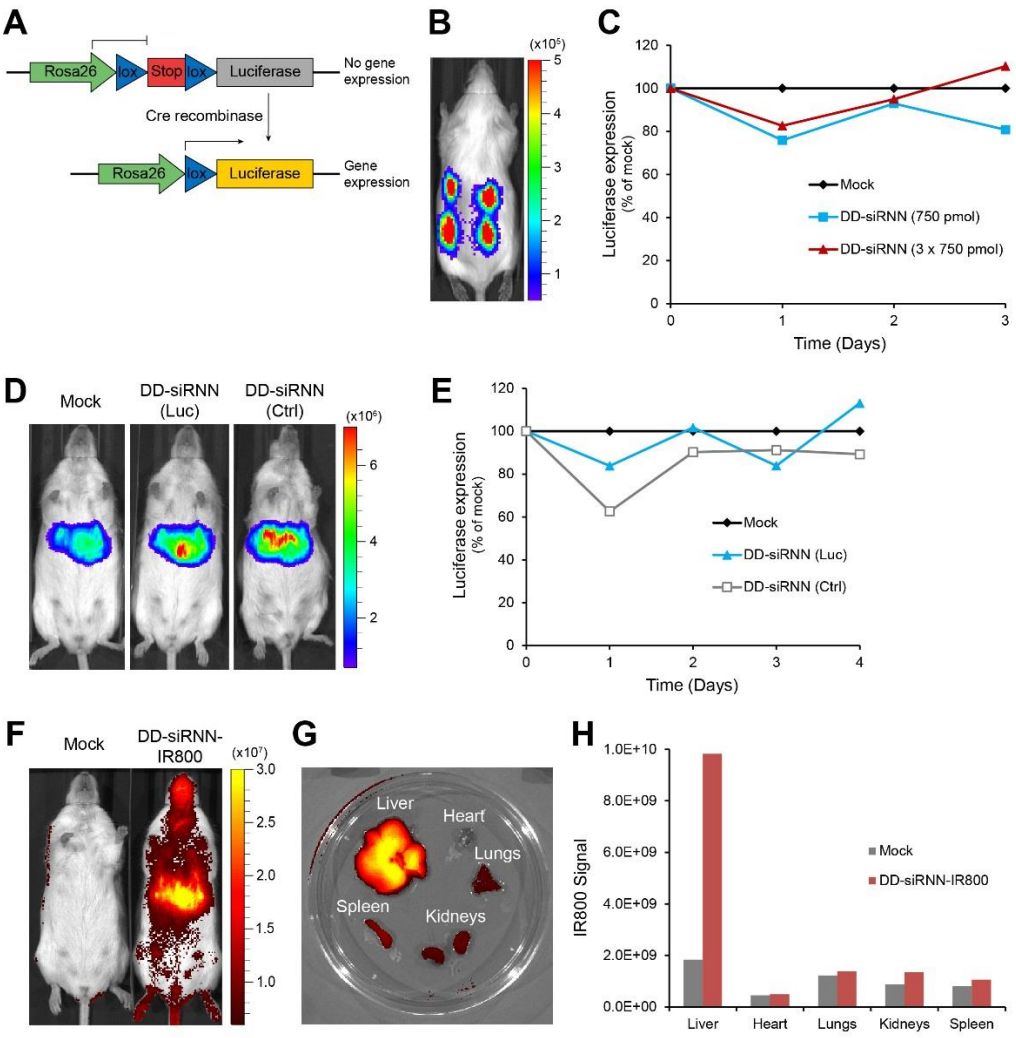

Figure 4.5. ***In vivo*** **delivery and biodistribution of siRNNs. A)** Diagram of Cre reporter in genetically engineered Rosa26-loxP-STOP-loxP-luciferase (LSL-luc) mice used in this study. Mice contain the firefly luciferase gene inserted into the Rosa26 locus. Expression of the inserted luciferase gene is normally blocked by a STOP fragment flanked by loxP sites placed between the luciferase gene and the Rosa26 promoter. Exposure to Cre recombinase results in removal of the STOP fragment and expression of luciferase detectable by live animal bioluminescent imaging. **B)** Subcutaneous luciferase back spot mouse model. LSL-luc mice were injected subcutaneously with TAT-Cre to generate localized subcutaneous expression of luciferase. Scale is in photons/s/cm^2/sr. **C)** Luciferase expression analysis of mouse subcutaneous luciferase back spots injected subcutaneously with luciferase-targeted DD-siRNN^{A4} conjugate once or three times (1 injection per day for 3 days, q.d.). Luciferase expression was normalized to mock treatment each day. **D)** Liver luciferase mouse model. LSL-luc mice were injected intravenously with adeno-Cre to induce stable expression of luciferase in the liver. Scale is in photons/s/cm^2/sr. **E)** Liver luciferase expression in live mice injected once intravenously with 12.5 nmol of Luc DD-siRNN^{A4} vs. non-targeting control DD-siRNN^{A4} (ctrl) conjugate. Luciferase expression was normalized to mock treatment each day. **F)** IRDye 800 signal imaged in live mice 1 hr after intravenous administration with DD-siRNN^{A4}-IR800 conjugate. siRNN^{A4}-IR800 = IR800-P(A4)(D1)/G(S6). Scale is in (photons/s/cm^2/sr) / (μ W/cm^2). **G)** Biodistribution of DD-siRNN^{A4}-IR800 conjugate 1 hr after intravenous administration. **H)** Quantification of IRDye 800 signal from organs depicted in panel G. Note conjugate IRDye 800 signal is highly concentrated in the liver.

To test TAT DD-siRNN *in vivo* delivery by systemic administration, I utilized a liver luciferase mouse model. To generate this mouse model, I intravenously administered adenovirus expressing Cre recombinase (adeno-Cre) to Rosa26-loxP-STOP-loxP-luciferase mice. As hepatocytes are efficiently transduced by intravenous administration of adenoviral vectors to mice (Connelly, 1999), this method resulted in strong recombination and expression of luciferase in the mouse liver (**Figure 4.5D**). After establishing stable liver luciferase expression, I treated mice with 12.5 nmols of Luc DD-siRNN or off-target control siRNN by intravenous injection, but no induction of an RNAi response (**Figure 4.5E**). Treatments with lower DD valency or alternative delivery domains also failed to induce measurable RNAi responses (data not shown).

To examine biodistribution of DD-siRNNs following systemic administration, we synthesized A-SATE containing RNN passenger oligonucleotides labeled with IRDye 800 (IR800), an near-infrared fluorescent dye that can be readily tracked and quantified by live animal imaging. Due to high tissue penetration of excitation light and low background autofluorescence in the near-infrared region (Sevick-Muraca et al., 2002; van Oosten et al., 2013), IR800 dyes can be readily monitored by our IVIS Spectrum imager. Using an IR800-labeled RNN passenger strand, I generated DD-siRNN-IR800 conjugates and injected them intravenously in mice. By live animal fluorescent imaging, I observed concentration of the IR800 signal from the injected conjugate in the liver within 1 hr of injection (**Figure 4.5F**). Subsequent mouse dissection and organ analysis revealed strong liver uptake of DD-siRNN-IR800 conjugate and some uptake by the lungs, kidneys, and spleen (**Figure 4.5G,H**).

CONCLUSIONS

Although siRNA holds significant therapeutic promise, its large size and strong anionic charge prevent cellular delivery. To solve the siRNA delivery problem, we developed bioreversible phosphotriester groups that neutralize the prohibitive phosphodiester backbone charge in order to facilitate delivery by cationic PTDs. Here I have presented the first instance of self-delivering TAT PTD-siRNNs conjugates capable of cellular delivery and induction of an RNAi response. This was made possible by the development of the A-SATE phosphotriester.

I have described a novel A-SATE phosphotriester that plays dual roles of both neutralizing a phosphodiester and also serving as a site of conjugation by way of a benzaldehyde moiety (**Figure 4.3B**). We demonstrated A-SATE phosphotriester RNN oligonucleotide synthesis and deprotection conditions and that A-SATE groups are stable under the ultramild base deprotection conditions necessary for *t*Bu-SATE and O-SATE RNN oligonucleotides (**Figure 4.1**). A-SATE siRNNs display enhanced serum stability and are bioreversible upon cytosolic delivery (**Figure 4.2**). The benzealdehyde terminus of A-SATE phosphotriesters is reactive and capable of forming stable hydrazone bonds with hydrazine functionalized delivery domain peptides (**Figure 4.3**). A-SATE conjugation allows for site-specific multivalent conjugation of TAT DD peptides to a siRNN. Importantly, DD-conjugated A-SATE phosphotriesters remain substrates for intracellular thioesterases independent of the length of the conjugated DD, thereby allowing for shedding of conjugated DD peptides upon cytosolic entry.

This work represents the first synthesis of DD-siRNNs capable of cellular self-delivery and induction of RNAi responses. DD-siRNNs function in a non-cytotoxic manner to induce dose dependent RNAi responses on an entire cell population against both reporter genes and endogenous genes with an observable biological effect of gene

knockdown *in vitro* (**Figure 4.4**). Despite this, DD-siRNNs failed to induce RNAi responses *in vivo* (**Figure 4.5**).

While subcutaneously injected TAT-Cre was able to deliver Cre recombinase and induce luciferase expression, TAT DD-siRNNs proved unsuccessful when administered to the same area (**Figure 4.5C**). In biodistribution studies with subcutaneously injected DD-siRNN-IR800 conjugates, the IR800 signal remained at the site of injection for days after administration (data not shown). It may be that multivalent TAT DD-siRNN conjugates are ill suited to delivery in the subcutaneous space.

Analysis of systemically administered DD-siRNN biodistribution suggests high liver uptake, as is expected for the cationic charge of DD-siRNN conjugates (**Figure 4.5F,G**). However, no induction of an RNAi response occurred upon liver uptake, suggesting a failure of delivery or stability of the siRNN in blood (**Figure 4.5H**).

This *in vivo* research was only conducted using TAT-PTD based delivery domains. Although TAT PTD has been demonstrated to deliver a variety of macromolecular cargos *in vivo* and siRNNs *in vitro*, it may not be ideal for *in vivo* delivery of siRNNs (Lönn and Dowdy, 2015). Fortunately, the modular nature of siRNNs and functionality of A-SATE conjugation allows for reconfiguration and conjugation to any molecule functionalized with a hydrazine moiety. Alternative delivery domains or other molecules to enhance delivery can and were also conjugated. Further work will include a more focused *in vivo* proof-of-concept siRNN delivery approach utilizing a delivery domain that targets a specific receptor highly expressed in a target tissue.

ACKNOWLEDGEMENTS

The research described in Chapter 4 has, in part, been published in Nature Biotechnology co-authored by the dissertation author (Meade et al., 2014). Phosphoramidites utilized in in Chapter 4 were synthesized by Khirud Gogoi. Byran Meade synthesized some oligonucleotides and performed some cellular treatments. Analysis of cMyc knockdown was performed by Manuel Kaulich. Caroline Palm-Apergi performed Plk1 knockdown experiments.

REFERENCES

Connelly, S. (1999). Adenoviral vectors for liver-directed gene therapy. Curr. Opin. Mol. Ther. *1*, 565–572.

Eguchi, A., Meade, B.R., Chang, Y.-C., Fredrickson, C.T., Willert, K., Puri, N., and Dowdy, S.F. (2009). Efficient siRNA delivery into primary cells by a peptide transduction domain-dsRNA binding domain fusion protein. Nat. Biotechnol. *27*, 567–571.

Gröschel, B., Cinatl, J., Périgaud, C., Gosselin, G., Imbach, J.-L., and Doerr, H.W. (2002). S-acyl-2-thioethyl (SATE) pronucleotides are potent inhibitors of HIV-1 replication in T-lymphoid cells cross-resistant to deoxycytidine and thymidine analogs. Antiviral Res. *53*, 143–152.

Gutteridge, R.E.A., Ndiaye, M.A., Liu, X., and Ahmad, N. (2016). Plk1 Inhibitors in Cancer Therapy: From Laboratory to Clinics. Mol. Cancer Ther. *15*, 1427–1435.

Hastings, K.T., and Cresswell, P. (2011). Disulfide reduction in the endocytic pathway: immunological functions of gamma-interferon-inducible lysosomal thiol reductase. Antioxid. Redox Signal. *15*, 657–668.

Jiang, T., Olson, E.S., Nguyen, Q.T., Roy, M., Jennings, P.A., and Tsien, R.Y. (2004). Tumor imaging by means of proteolytic activation of cell-penetrating peptides. Proc. Natl. Acad. Sci. U. S. A. *101*, 17867–17872.

Juliano, R.L. (2016). The delivery of therapeutic oligonucleotides. Nucleic Acids Res. *347*, 6518–6548.

Liu, X., and Erikson, R.L. (2003). Polo-like kinase (Plk)1 depletion induces apoptosis in cancer cells. Proc. Natl. Acad. Sci. U. S. A. *100*, 5789–5794.

Lönn, P., and Dowdy, S.F. (2015). Cationic PTD/CPP-mediated macromolecular delivery: charging into the cell. Expert Opin. Drug Deliv. *12*, 1627–1636.

Matranga, C., Tomari, Y., Shin, C., Bartel, D.P., and Zamore, P.D. (2005). Passenger-strand cleavage facilitates assembly of siRNA into Ago2-containing RNAi enzyme complexes. Cell *123*, 607–620.

Meade, B.R., and Dowdy, S.F. (2009). The road to therapeutic RNA interference (RNAi): Tackling the 800 pound siRNA delivery gorilla. Discov. Med. *8*, 253–256.

Meade, B.R., Gogoi, K., Hamil, A.S., Palm-Apergi, C., van den Berg, A., Hagopian, J.C., Springer, A.D., Eguchi, A., Kacsinta, A.D., Dowdy, C.F., Presente, A., Lönn, P., Kaulich, M., Yoshioka, N., Gros, E., Cui, X.-S., and Dowdy, S.F. (2014). Efficient delivery of RNAi prodrugs containing reversible charge-neutralizing phosphotriester backbone modifications. Nat. Biotechnol. *32*, 1256–1261.

Michiue, H., Eguchi, A., Scadeng, M., and Dowdy, S.F. (2009). Induction of in vivo synthetic lethal RNAi responses to treat glioblastoma. Cancer Biol. Ther. *8*,

2306–2313.

Murugan, R.N., Park, J.-E., Kim, E.-H., Shin, S.Y., Cheong, C., Lee, K.S., and Bang, J.K. (2011). Plk1-targeted small molecule inhibitors: molecular basis for their potency and specificity. Mol. Cells *32*, 209–220.

van Oosten, M., Schäfer, T., Gazendam, J.A.C., Ohlsen, K., Tsompanidou, E., de Goffau, M.C., Harmsen, H.J.M., Crane, L.M.A., Lim, E., Francis, K.P., Cheung, L., Olive, M., Ntziachristos, V., van Dijl, J.M., and van Dam, G.M. (2013). Real-time in vivo imaging of invasive- and biomaterial-associated bacterial infections using fluorescently labelled vancomycin. Nat. Commun. *4*, 2584.

Podyminogin, M.A., Lukhtanov, E.A., and Reed, M.W. (2001). Attachment of benzaldehyde-modified oligodeoxynucleotide probes to semicarbazide-coated glass. Nucleic Acids Res. *29*, 5090–5098.

Safran, M., Kim, W.Y., Kung, A.L., Horner, J.W., DePinho, R.A., and Kaelin, W.G. (2003). Mouse reporter strain for noninvasive bioluminescent imaging of cells that have undergone Cre-mediated recombination. Mol. Imaging *2*, 297–302.

Schirle, N.T., and MacRae, I.J. (2012). The crystal structure of human Argonaute2. Science *336*, 1037–1040.

Schwarze, S.R. (1999). In Vivo Protein Transduction: Delivery of a Biologically Active Protein into the Mouse. Science (80-.). *285*, 1569–1572.

Sevick-Muraca, E.M., Houston, J.P., and Gurfinkel, M. (2002). Fluorescence-enhanced, near infrared diagnostic imaging with contrast agents. Curr. Opin. Chem. Biol. *6*, 642–650.

Wadia, J.S., Stan, R. V, and Dowdy, S.F. (2004). Transducible TAT-HA fusogenic peptide enhances escape of TAT-fusion proteins after lipid raft macropinocytosis. Nat. Med. *10*, 310–315.

Wittrup, A., and Lieberman, J. (2015). Knocking down disease: a progress report on siRNA therapeutics. Nat. Rev. Genet. *16*, 543–552.

Yang, J., Chen, H., Vlahov, I.R., Cheng, J.-X., and Low, P.S. (2006). Evaluation of disulfide reduction during receptor-mediated endocytosis by using FRET imaging. Proc. Natl. Acad. Sci. U. S. A. *103*, 13872–13877.

Zeidman, R., Jackson, C.S., and Magee, A.I. (2009). Protein acyl thioesterases (Review). Mol. Membr. Biol. *26*, 32–41.

CHAPTER 5

IN VIVO DELIVERY OF siRNNS

IN VIVO DELIVERY OF siRNNS

ABSTRACT

Although small interfering RNA (siRNA) technology has great potential to treat human disease, the relatively large size and strong anionic character of siRNA molecules limits their utility as a drug. We addressed this issue by synthesis of short interfering ribonucleic neutrals (siRNNs) whose phosphate backbone contained bioreversible neutralizing phosphotriester groups, allowing for delivery into cells. Upon cellular entry siRNNs are converted by cytoplasmic thioesterases into native, charged phosphodiester backbone siRNAs capable of inducing robust RNA interference (RNAi) responses. Unlike siRNAs, siRNNs avidly bind serum albumin to positively influence pharmacokinetic properties. To test the *in vivo* ability of siRNNs to induce RNAi responses, I conjugated siRNNs to *N*-acetylgalactosamine (GalNAc), a hepatocyte-specific targeting domain, through chemically reactive A-SATE phosphotriester groups. I found that single dose systemically administered GalNAc-siRNN conjugates induced extended dose-dependent RNAi responses in mice. This work constitutes the first instance of *in vivo* target gene knockdown by siRNNs containing bioreversible neutralizing phosphotriester groups.

INTRODUCTION

The discovery that synthetic siRNA could induce RNAi responses in human cells (Elbashir et al., 2001) began a race to develop safe and effective siRNA delivery strategies for the treatment of human disease (de Fougerolles et al., 2007). siRNA has attributes that could make for an excellent therapeutic, including the ability to mediate highly selective gene-specific suppression and an EC_{50} in the picomolar (10^{-12}) range (Bumcrot et al., 2006). Additionally, siRNAs can be synthesized in a scalable and sequence independent manner, allowing for the rapid production of siRNAs directed against any target mRNA (Beaucage, 1992). The small molecules (<500 Da) that constitute the majority of drugs can diffuse passively across cellular membranes (Lipinski et al., 2001). In contrast, siRNAs are both too large (~14 kDa) and too charged (~40 anionic phosphodiesters) to traverse the cellular membrane unassisted (Meade and Dowdy, 2009; Rettig and Behlke, 2012). These attributes also make siRNAs pharmacokinetically unfavorable, as naked siRNAs are removed from the bloodstream by the kidneys within minutes of systemic administration (Merkel et al., 2009). Consequently, siRNA delivery is *the Problem* to overcome for the development of RNAi therapeutics.

The difficulties associated with *in vivo* siRNA delivery have spawned the development of a plethora of delivery strategies (Rettig and Behlke, 2012; Wittrup and Lieberman, 2015). The majority of siRNA delivery systems revolve around electrostatic encapsulation of many siRNA molecules into nanoparticles by cationic lipids and polymers to both assist siRNAs in crossing the cellular membrane and to persist in circulation for longer (Whitehead et al., 2009). Recent advancements in siRNA delivery have begun to move away from large lipid and synthetic nanoparticle (~10^8 Da) approaches that are >1,000x larger than the siRNA drug to more definable molecular

conjugates (Kanasty et al., 2013; Wittrup and Lieberman, 2015; Juliano, 2016). However, due to the strict structural requirements for siRNA to be utilized by the RNAi machinery, the negatively charged phosphodiester backbone of siRNA has proven difficult to manipulate (Carthew and Sontheimer, 2009; Joshua-Tor and Hannon, 2011; Schirle et al., 2016).

To address this problem, we have developed small interfering ribonucleic neutrals (siRNNs) containing neutralizing bioreversible phosphotriester groups that are intracellularly converted into native charged phosphodiesters by ubiquitously expressed cytoplasmic thioesterases (Périgaud et al., 1993; Meade et al., 2014). This conversion results in wildtype siRNA that can be utilized by RISC to induce RNAi responses. To test the *in vivo* ability of siRNNs to induce RNAi responses, we sought a targeting domain with a receptor whose expression is limited to the target tissue, is highly expressed, and rapidly turned over. For this purpose, we utilized *N*-acetylgalactosamine (GalNAc) as a targeting group.

In humans, exogenous glycoproteins (Grewal, 2010), aging secreted proteins (Yang et al., 2015), and other species that lack a terminal sialic acid are cleared from the blood by the hepatic asialoglycoprotein receptor (ASGPR), also known as the Ashwell-Morell receptor. ASGPR, a C-type lectin membrane protein, recognizes terminal galactose or GalNAc residues that do not contain a sialic acid, internalizes the bound species by clathrin-mediated endocytosis, and traffics it to the lysosome for degradation (Lee et al., 1983; Spiess, 1990; Park et al., 2005; Esko et al., 2009). Importantly, the ASGPR is highly abundant on hepatocytes (>10^6/cell) and is recycled at a rapid rate of every 10-15 min (Cummings and McEver, 2009). This blood clearance system has been exploited to specifically target therapeutic molecules to the liver. In the late 1990s, Erik Biessen's group developed a tri-antennary GalNAc (*tris*-GalNAc) targeting domain that

bound avidly to and was taken up by the ASGPR receptor (Sliedregt et al., 1999). In recent years, the *tris*-GalNAc targeting domain has been re-discovered and utilized to deliver next-generation chemically stabilized siRNAs (Nair et al., 2014; Matsuda et al., 2015; Rajeev et al., 2015; Sehgal et al., 2015; Butler et al., 2016) and antisense oligonucleotides (ASOs) (Yu et al.; Prakash et al., 2014, 2015, 2016a, 2016b; Kinberger et al., 2016), as well as dynamic polyconjugate siRNA delivery vehicles (Rozema et al., 2007, 2015; Wong et al., 2012; Wooddell et al., 2013). GalNAc-siRNA conjugate delivery has proven so successful that Alnylam Pharmaceuticals currently has seven GalNAc-siRNA clinical trials in progress for liver diseases (Wittrup and Lieberman, 2015; Juliano, 2016).

For these reasons, we chose use the *tris*-GalNAc targeting domain to test the ability of siRNNs to induce RNAi responses *in vivo*.

RESULTS & DISCUSSION

Analysis of siRNN-conjugated *tris*-GalNAc targeting domain structure-activity relationships

To examine the *in vivo* activity of siRNNs, we synthesized a series of hepatocyte-specific *tris*-*N*-acetylgalactosamine (GalNAc) targeting domains (Sliedregt et al., 1999). To test their *in vivo* function, GalNAc targeting domains were synthesized with a hydrazine moiety for reaction with siRNNs containing conjugatable phosphotriesters to make GalNAc-siRNN conjugates joined by a stable hydrazone bond (**Figure 5.1A**). The ASGPR functions as a trimer and therefore the GalNAc targeting domain contains three GalNAc ligands for efficient receptor engagement (**Figure 5.1A,B**) (Sliedregt et al., 1999; Westerlind et al., 2004; Esko et al., 2009). Additionally, an optimal relative geometry of the GalNAc ligands must be maintained for efficient binding to the hepatic

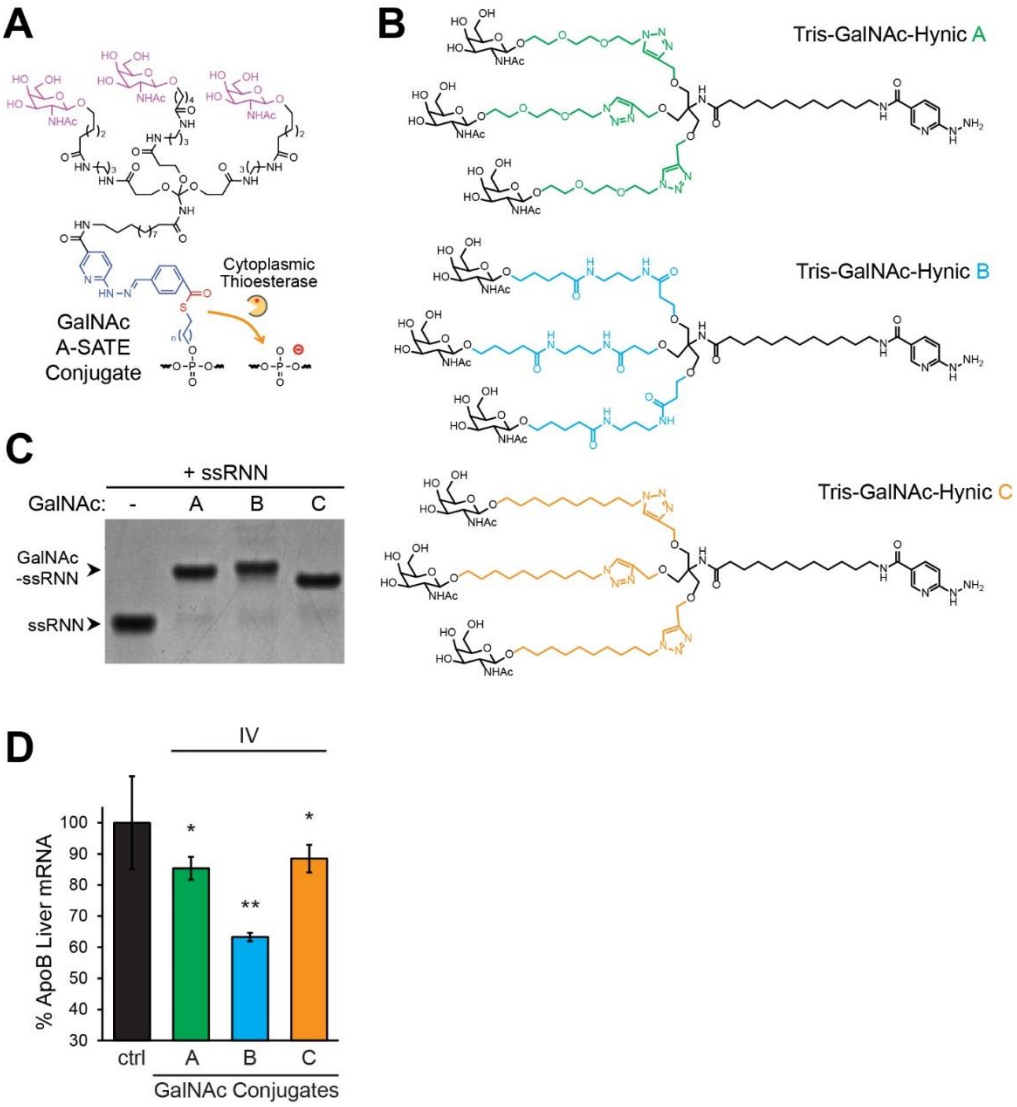

Figure 5.1. GalNAc targeting domain structure-activity relationship. A) Structure of GalNAc targeting domain conjugated to an A-SATE phosphotriester group. Cytoplasmic thioesterases process the conjugated GalNAc-A-SATE group resulting in an RNAi-compatible wildtype charged phosphodiester. **B)** Structures of *tris*-GalNAc-Hynic targeting domain variants. The targeting domain variants each contain the same three GalNAc targeting groups, conjugatable hydrazine moiety, and alkyl linker but differ in the GalNAc spacers. **C)** Conjugation of GalNAc targeting domains A, B, and C to an RNN oligonucleotide containing one conjugatable phosphotriester. **D)** Single-dose intravenous (IV) administration into C57BL/6 mice of GalNAc-siRNN conjugates targeting ApoB comparing GalNAc targeting domains variants A, B, and C. ApoB mRNA expression measured 72 hr after treatment by qRT-PCR (25 mg/kg; n = 3, each group). Values normalized to β2-microglobulin from water-treated control (ctrl) group (n = 5). Error bar indicates standard deviation (s.d.). *P < 0.05, **P < 0.01; one-tailed Student's t-test.

ASGPR. Mindful of these restrictions, the GalNAc targeting domain variants that we synthesized each contain the same three GalNAc ligands, conjugatable hydrazine moiety, and alkyl linker but differ in the GalNAc spacers utilized (**Figure 5.1B**). As GalNAc spacer length determines the GalNAc trimer geometry, modification concerned spacer composition, rather than spacer length. GalNAc targeting domain variant A contains ethoxy spacers, variant B contains amide spacers, and variant C contains alkyl spacers. While the spacers in targeting domains A and B are hydrophilic, C contains hydrophobic spacers synthesized with the intent of enhancing endosomal escape (Lönn et al., 2016). However, the hydrophobic spacers in GalNAc targeting domain variant C limited the solubility of GalNAc-siRNN conjugates in aqueous solutions.

I conjugated the GalNAc targeting domain variants A-C to ssRNN oligonucleotides containing a conjugatable phosphotriester on the 5'-end of the passenger strand (P#1). As seen with previous hydrazine containing molecules, the *tris*-GalNAc-Hynic targeting domains conjugated readily to siRNNs, reaching quantitative conjugation rapidly at a 1:5 molar ratio of siRNN to *tris*-GalNAc-Hynic. GalNAc-ssRNN conjugates were then purified to remove unreacted *tris*-GalNAc-Hynic and duplexed with complementary guide strands to make GalNAc-siRNN conjugates.

To compare the relative activities of the GalNAc targeting domain spacer variants, I treated C57BL/6 mice (n=3) with single intravenous doses of GalNAc-siRNN conjugates (25 mg/kg) targeting Apolipoprotein B (ApoB) as an endogenous *in vivo* hepatic target. 72 hr after treatment I sacrificed the animals, extracted liver mRNA, and analyzed ApoB mRNA expression by qRT-PCR normalized to β2-microglobulin (B2M) as a reference gene. I found that while all three GalNAc targeting domain variant siRNN conjugates induced statistically significant RNAi responses, variant B was the most efficient (**Figure 5.1D**). I therefore utilized GalNAc targeting domain variant B for siRNN

conjugation and animal treatments for the remainder of this study. Importantly, with these experiments, I demonstrated *in vivo* delivery of siRNNs and induction of RNAi responses for the first time.

Comparative analysis of siRNNs for GalNAc-mediated delivery

TRBP and Ago2 require close interaction with native phosphodiesters of the siRNA backbone for the successful induction of an RNAi response (Ohrt et al., 2012; Schirle and MacRae, 2012). In order to minimize potential disruption of the interactions between the RNAi machinery and siRNNs, particularly the crucial binding of Ago2 to the 5'-end of the guide strand, I synthesized siRNNs containing reactive phosphotriesters for *tris*-GalNAc conjugation on the 5'-end of the passenger strand. To examine the requirement of GalNAc removal for the efficient induction of *in vivo* RNAi responses by siRNNs, I tested three different conjugatable phosphotriester groups (**Figure 5.2A**). A-SATE and A-SATB phosphotriester groups contain a thioester bond and are intracellularly converted by cytoplasmic thioesterases into native charged phosphodiesters, releasing any domain conjugated through them (**Figure 4.3**). A-SATBs are similar to A-SATEs, but contain a butyl linker between the phosphate and thioester bond that makes the A-SATB group more stable and, consequently, more slowly converted by thioesterases (Meade et al., 2014). Due to this slower conversion rate, multiple insertions of SATB phosphotriester groups into an siRNN or insertion at critical positions, such as the passenger strand cleavage position (**Figure 4.3C**) (Matranga et al., 2005), can inhibit induction of RNAi responses. However, insertion of a single group at the 5'-end of the passenger strand is well-tolerated as is the irreversible DMB phosphotriester group (**Figure 4.4**). Ax is an irreversible phosphotriester group

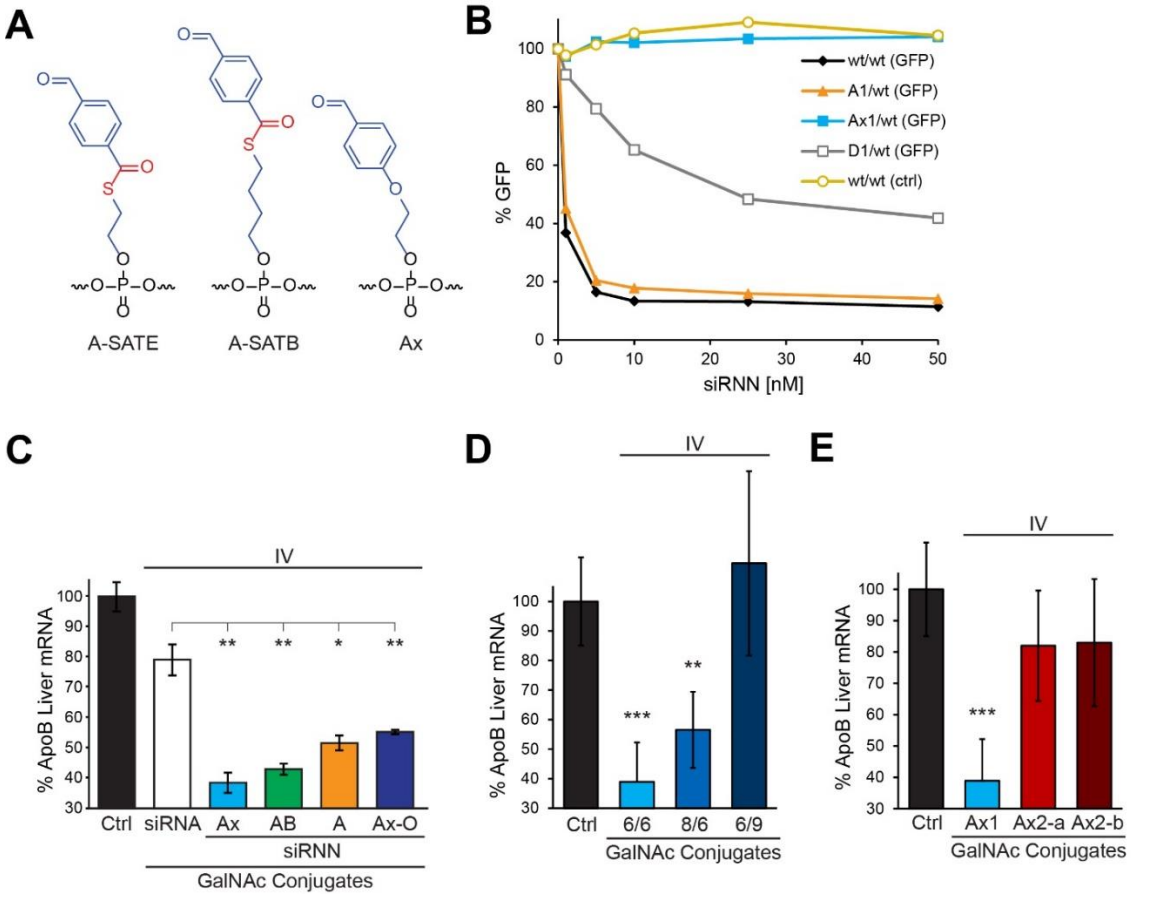

Figure 5.2. Comparative analysis of siRNNs for GalNAc-mediated delivery. A) Structures of the conjugatable phosphotriesters used in this study. A-SATE and A-SATB phosphotriester groups contain a thioester bond and are intracellularly converted by cytoplasmic thioesterases into native charged phosphodiesters. Ax is an irreversible phosphotriester group. **B)** Flow cytometry analysis of H1299-dGFP cells transfected with a dose curve of either 2'-F/OMe modified siRNA (wt) or siRNNs with containing 1x phosphotriester at the passenger strand cleavage site (P#9). All siRNAs and siRNNs target GFP. A = A-SATE, Ax = irreversible Ax, D = irreversible DMB. **C)** Single-dose intravenous (IV) administration into C57BL/6 mice of charged GalNAc-siRNA conjugates targeting ApoB compared with GalNAc conjugated neutral siRNNs via A-SATE (A), A-SATB (AB) or Ax-BOE (Ax) phosphotriester groups and containing tBu-SATE and O-SATE (O) phosphotriester groups. ApoB mRNA expression measured 72 hr after treatment by qRT-PCR (25 mg/kg; n = 3, each group). Values normalized to β2-microglobulin from water-treated control (ctrl) group (n = 5). **D)** Single intravenous dose of ApoB-targeted GalNAc-Ax-siRNN conjugates. Comparison of siRNNs containing increased numbers of phosphotriester groups (# of groups on passenger strand / # on guide strand). **E)** Single intravenous dose of ApoB-targeted GalNAc-Ax-siRNN conjugates. Comparison of siRNN containing 1x Ax group conjugated to one GalNAc targeting domain and siRNNs containing 2x Ax groups each conjugated to one GalNAc targeting domain. siRNN Ax2-a contains 2x Ax groups on its passenger strand and siRNN Ax2-b contains 1x Ax group on each of its strands. Error bar indicates s.d. *P < 0.05, **P < 0.01, ***P < 0.001; one-tailed Student's t-test.

acting as a functionally reactive analog of the A-SATE group, but lacking the prerequisite thioester bond for intracellular conversion to a phosphodiester (**Figure 5.2A**).

To assay Ax phosphotriester stability, I synthesized a series of passenger strands containing a phosphotriester group at the Ago2 cleavage position and duplexed them with wild type guide strands (**Figure 5.2B**). Cleavage of the passenger strand is crucial to the maturation and function of RISC (Matranga et al., 2005) and requires a phosphodiester. I transfected these GFP-targeted siRNAs into H1299 cells constitutively expressing a destabilized GFP reporter gene (dGFP). As expected, wildtype siRNA (wt/wt) and siRNAs containing an A-SATE (A1/wt) at the passenger strand cleavage position induced dose dependent RNAi responses following bioreversal of the A-SATE group. As seen previously, an irreversible DMB phosphotriester at the cleavage position (D1/wt) was only able to induce knockdown of GFP at higher treatment concentrations, potentially due to inefficient cleavage of a phosphate adjacent to the DMB-blocked cleavage site by Ago2. Not surprisingly, the siRNA containing an irreversible Ax phosphotriester group at the cleavage site failed to induce an RNAi response, even at high treatment concentrations. The contrast with the irreversible DMB may be the result of the larger Ax inhibiting Ago2 cleavage of neighboring phosphodiesters or the inability of helicases to remove an Ax containing passenger strand from Ago1,3,4. As expected, the non-targeting control (NTC) siRNA also failed to induce a GFP RNAi response.

To test the effect of GalNAc removal on *in vivo* induction of RNAi responses by siRNNs, I synthesized a set of conjugatable siRNNs and control siRNA designed for *in vivo* delivery (**Figure 5.2C**). For GalNAc conjugation, a conjugatable phosphotriester (A-SATE, A-SATB, or Ax) was placed at the 5'-end of the passenger strand. For enhanced nuclease stabilization of siRNNs, an irreversible DMB phosphotriester was placed at the 3'-end of each strand and phosphorothioate backbone modifications (**Figure 1.2**) were

included at the 5’ and 3’ ends of both strands for increased stability. Based on experiments conducted previously (see Chapter 4), *t*Bu-SATE groups have been inserted to make a total of 6x phosphotriester groups on each strand or 12 total for the siRNN. In addition to the P(A/AB/Ax1)(S5)(D1)/G(S5)(D1) siRNN just described, I also made a P(Ax1)(S5)(D1)/G(O5)(D1) siRNN with O-SATE groups substituted for *t*Bu-SATE groups on the guide strand. The control siRNA contained a 5’ Ax on the passenger strand for GalNAc conjugation and nuclease stabilizing 5’ and 3’ terminal phosphorothioates. All siRNNs and siRNAs were fully 2’-F/OMe modified and targeted liver specific ApoB.

ApoB siRNNs and control siRNA were conjugated to *tris*-GalNAc-Hynic (B) and a single intravenous 25 mg/kg dose was administered to mice. Treated mice were examined for ApoB mRNA expression 72 hr after dosing by qRT-PCR (**Figure 5.2C**). Each of the four ApoB GalNAc-siRNNs variants induced strong ApoB RNAi responses at 72 h, whereas GalNAc-siRNA induced a poor RNAi response. GalNAc-siRNNs induced significant ApoB RNAi responses compared with GalNAc-siRNA treated animals ($P < 0.05$ to <0.01). Surprisingly, the efficiency of RNAi response induction was inversely correlated with the reversibility of the phosphotriester that the GalNAc targeting domain was conjugated through. siRNNs containing an Ax phosphotriester induced the strongest RNAi response, followed by more stable A-SATB siRNNs, and then A-SATE siRNNs. Similar to 5’-DMB used previously in DD-siRNN delivery (**Figure 4.4**), the induction of RNAi responses by GalNAc-Ax siRNN suggests that GalNAc does not need to be cleaved off prior to siRNN loading into RISC (**Figure 5.2C**). Perhaps even more so than the smaller DMB group, the presence of the GalNAc-Ax conjugated group at the 5’-end of the passenger strand likely prevents passenger strand loading into active site of Ago2. Relative to the A-SATE, the irreversibility of the 5’ Ax also serves to further

stabilize the siRNN from degradation by exonucleases. GalNAc-Ax siRNN with guide strand O-SATEs performed slightly more poorly than did the same GalNAc-Ax-siRNN with *t*Bu-SATEs on the guide strand (**Figure 5.2C**).

Charged siRNAs do not bind serum albumin (**Figure 5.3B**) and are rapidly cleared by the kidneys (half-life <5 min) (Gao et al., 2009), thereby preventing effective intravenous administration. In contrast, we found that charge neutralized siRNNs avidly bound serum albumin. This albumin binding is dependent on neutralization of the anionic phosphodiesters by phosphotriester groups and decreases with the removal of phosphotriester groups or the smaller addition of charge that results from substitution of *t*Bu-SATE groups with O-SATE groups.

As neutralization of phosphodiester charge increases affinity for serum albumin and improves systemic delivery, I investigated the effect of increasing the overall phosphotriester content and neutrality of GalNAc-siRNNs on delivery and induction of RNAi responses *in vivo*. I synthesized siRNNs with additional *t*Bu-SATE modifications on the passenger strand (8/6 = P(Ax1)(S6)(D1)/G(S5)(D1)) or guide strand (6/9 = P(Ax1)(S4)(D1)/G(S8)(D1)), conjugated them to *tris*-GalNAc-Hynic (B), and administered them intravenously to mice (**Figure 5.2D**). I found that additional insertions of *t*Bu-SATE groups has an inhibitory effect on GalNAc-siRNN *in vivo* delivery. Although 6/9 GalNAc-siRNNs were soluble in aqueous solutions, siRNNs containing 9x *t*Bu-SATE phosphotriester groups on each strand suffered from extreme insolubility (see Chapter 3). The added hydrophobicity of the inserted *t*Bu-SATE groups in the 6/9 GalNAc-siRNN may have negatively affected biodistribution Additionally, further modification of the guide strand (6/9) resulted in a greater inhibition of RNAi induction than did *t*Bu-SATE insertions on the passenger strand (8/6), potentially because the guide strand is more

sensitive to modification due to close phosphodiester interactions with Ago2 (Schirle and MacRae, 2012).

Although *tris*-GalNAc is an efficient ligand for binding to the hepatic ASGPR, enhanced uptake efficiency of multivalent *tris*-GalNAc has been reported (Westerlind et al., 2004). Potentially, increasing the number of presented *tris*-GalNAc domains may enhance the probability of successful ASGPR binding. Additionally, my own work with TAT DD-siRNNs suggested that increased TAT PTD valency enhanced delivery (**Figure 4.4D**). For these reasons, I investigated *in vivo* delivery by multivalent GalNAc-siRNNs (**Figure 5.2E**). We synthesized siRNNs containing either one Ax phosphotriester group on the 5' end of the passenger strand (Ax1 = P(Ax1)(S4)(D1)/G(S5)(D1)), two Ax phosphotriester groups on the 5' end of the passenger strand (Ax2-a = P(Ax2)(S3)(D1)/G(S5)(D1)), or one Ax group on the 5' terminal end of the passenger strand and one Ax group on the 3' end of the guide strand (Ax2-b = P(Ax1)(S4)(D1)/G(Ax1)(S5)). I conjugated these siRNNs to *tris*-GalNAc-Hynic targeting domain (B) and administered a single intravenous dose of each to mice. Interestingly, the multivalent GalNAc-siRNNs induced poor RNAi responses when ApoB mRNA levels were examined 72 hr after treatment. This inhibition of systemic delivery may be the result of the additional *tris*-GalNAc groups altering biodistribution of the GalNAc-siRNNs and/or disrupting serum albumin binding (**Figure 5.2E**).

Following these results, I characterized the biological activity of the nuclease-stabilized lead candidate, *tris*-GalNAc-P(Ax1)(S4)(D1)/G(S5)(D1).

In vivo delivery of GalNAc-siRNN conjugates

GalNAc-siRNA conjugates have been reported to function well upon subcutaneous injection (Nair et al., 2014; Matsuda et al., 2015; Rajeev et al., 2015; Sehgal et al., 2015; Butler et al., 2016; Prakash et al., 2016a). Charged siRNAs are

rapidly cleared from the blood by renal filtration (half-life < 5 min) (Gao et al., 2009). Subcutaneous administration allows for slow release of GalNAc-siRNA conjugates so as not to overload the ASGPR binding capacity of the liver and lose unbound conjugate to kidney filtration (McLennan et al., 2005; Wittrup and Lieberman, 2015; Juliano, 2016). To compare GalNAc-siRNN and GalNAc-siRNA conjugate delivery, I administered each conjugate subcutaneously into C57BL/6 mice (**Figure 5.3A**). In vivo, due to biophysical attributes of the target ApoB mRNA, including Ago2 accessibility and mRNA synthesis rates combined with the siRNA sequence used, a single subcutaneous 25 mg/kg dose into mice of both charged ApoB GalNAc-siRNA and neutral ApoB GalNAc-siRNN was required to induce significant ApoB RNAi responses at 72 h, although GalNAc-siRNN induced a stronger RNAi response. Charged siRNAs do not bind to serum albumin and are therefore subject to rapid removal from the blood by kidney filtration, thereby preventing efficient delivery by intravenous administration (**Figure 5.3B**). We hypothesized that due to charge neutralization, siRNNs would not be subject to the same degree of renal clearance and could thus be more effective by intravenous administration. Indeed, we found that charge neutralized siRNNs readily bind to serum albumin (**Figure 5.3B**), allowing for induction of strong ApoB RNAi responses following a single intravenous dose of a variety of siRNNs (**Figure 5.2C**). Additionally, the biophysical properties of siRNNs can be shaped by the type and number of phosphotriesters as substitution of more polar O-SATE groups for hydrophobic *t*Bu-SATE groups results in less avid serum albumin binding (data not shown) and less efficient induction of RNAi responses following systemic administration (**Figure 5.2C**)

To examine GalNAc-siRNN conjugates for dose dependent activity, I administered single intravenous doses of 10, 17.5, and 25 mg/kg to mice and measured ApoB mRNA expression 72 hr after treatment (**Figure 5.3C**). GalNAc-siRNNs induced a

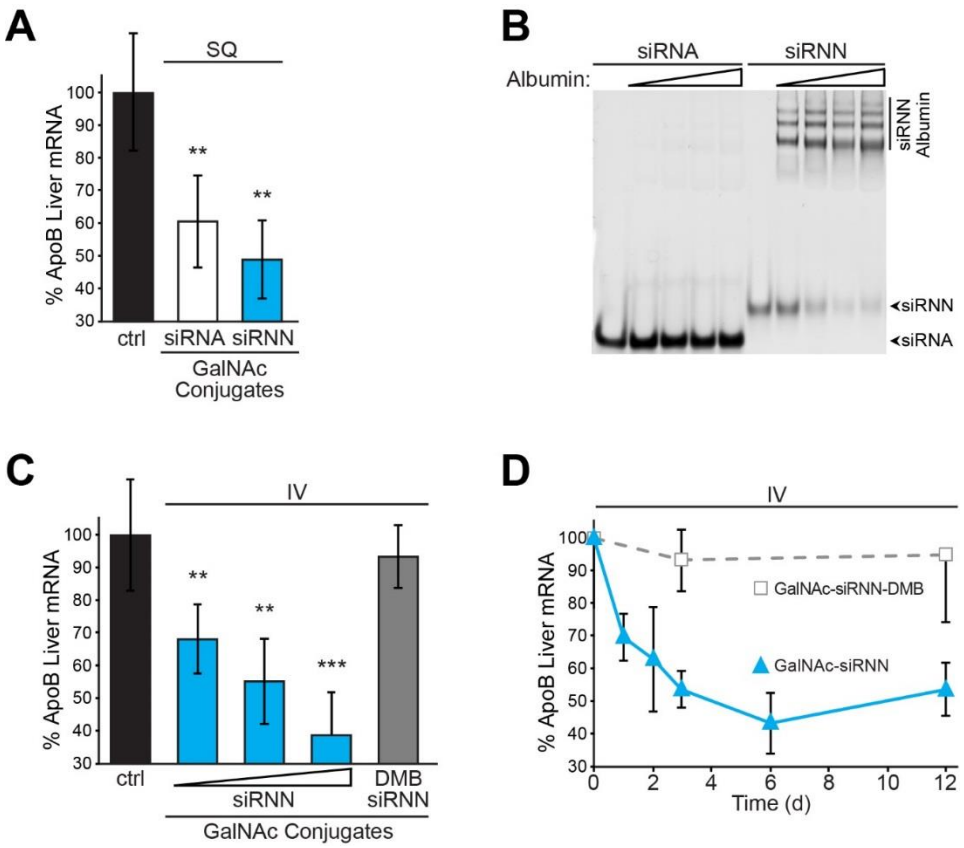

Figure 5.3. Analysis of *in vivo* GalNAc-siRNN conjugate delivery. A) Single-dose subcutaneous (SQ) administration into C57BL/6 mice of charged GalNAc-siRNA and neutral GalNAc-siRNNs targeting ApoB. ApoB mRNA expression measured 72 hr after treatment by qRT-PCR (25 mg/kg; n = 3, each group). Values normalized to β2-microglobulin from water-treated control (ctrl) group (n = 5). Error bar indicates s.d. **P < 0.01; one-tailed Student's t-test. **B)** Charged siRNA and neutral siRNNs were assayed for albumin binding by incubation with 0, 0.5, 1.0, 1.5 or 2.0 mg/ml serum albumin, then separated by gel electrophoresis mobility shift and ethidium bromide staining. Note that due to charge neutralization, siRNNs do not stain as efficiently as charged siRNAs. **C)** Single intravenous dose curve of GalNAc- Ax-siRNN ApoB (10, 17.5, 25 mg/kg; n = 3 each group) compared with irreversible control GalNAc-Ax-siRNN-DMB ApoB (6 irreversible DMBs on guide strand; 25 mg/kg; n = 3). ApoB mRNA expression measured 72 hr after treatment by qRT-PCR. Values normalized to β2-microglobulin from water-treated control (ctrl) group (n = 5). Error bar indicates s.d. **P < 0.01, ***P < 0.001; one-tailed Student's t-test. **D)** Single intravenous dose kinetic comparison of ApoB-targeted GalNAc-siRNN vs. irreversible control GalNAc-siRNN-DMB targeting ApoB. ApoB mRNA expression measured 72 hr after treatment by qRT-PCR (25 mg/kg; n = 3, each time point). Values normalized to β2-microglobulin from water treated control group (n = 5). Error bar indicates s.d.

significant dose-dependent ApoB RNAi response (median effective dose, ED_{50} ~10 mg/kg) compared with control GalNAc-siRNN-DMBs ($P < 0.01$ to <0.001) that contained six irreversible DMB phosphotriester groups on the guide strand and were incapable of inducing an RNAi response (**Figure 4.2B**).

Lastly, I conducted kinetic analysis of *in vivo* GalNAc-siRNN delivery through single intravenous dosing of mice with ApoB-targeted GalNAc-siRNNs and control GalNAc-siRNN-DMBs (**Figure 5.3D**). GalNAc-siRNN treated mice showed partial ApoB RNAi responses at the 24 and 48 hr time points. Maximum RNAi responses were reached between 3 and 6 days after treatment and was maintained for > 12 days. Control irreversible DMB GalNAc-siRNNs failed to induce an RNAi response over the course of the experiment.

CONCLUSIONS

The siRNN project was initiated with the goal of reversibly neutralizing the siRNA phosphodiester charge to facilitate *in vivo* delivery and induction of RNAi responses. Here I report the accomplishment of that goal. These observations demonstrate for the first time the ability to synthesize and self-deliver phosphotriester siRNN conjugates that are intracellularly converted into charged phosphodiester siRNAs that induce robust RNAi responses *in vivo*.

To examine the ability of siRNNs to induce RNAi responses *in vivo* we utilized a hepatocyte-specific *tris*-*N*-acetylgalactosamine (GalNAc) targeting domain with high affinity for the hepatic ASGPR (Sliedregt et al., 1999), of which hepatocytes express millions of copies on their cell surface and recycle at an astonishingly rapid rate of every 10-15 min (Cummings and McEver, 2009). The *tris*-GalNAc targeting domain has proven to be an astoundingly efficient and safe liver delivery and is currently under examination in clinical trials (Wittrup and Lieberman, 2015).

We utilized the *tris*-GalNAc targeting domain to make GalNAc-siRNN conjugates to test *in vivo* siRNN function (**Figure 5.1A**). I found that while nuclease-stabilized GalNAc-siRNN and GalNAc-siRNA conjugates induced similar moderate RNAi responses upon subcutaneous administration (**Figure 5.3A**), GalNAc-siRNNs were far more functional than their siRNA equivalent following intravenous administration (**Figure 5.3C,D**). Charged siRNAs are prohibited from efficient intravenous administration by rapid renal clearance. In contrast, the biophysical attributes of siRNNs facilitate avid binding to serum albumin and enable systemic delivery by intravenous injection (**Figure 5.3B**).

To optimize *in vivo* siRNN delivery, we synthesized and tested a series of *tris*-GalNAc targeting domains featuring different GalNAc spacers and found that use of an

amide spacer made the most efficient *tris*-GalNAc targeting domain (**Figure 5.1**). I also examined several conjugatable phosphotriesters and found that an irreversible Ax phosphotriester on the 5' terminus of the passenger strand resulted in the strongest RNAi response induction when used for *tris*-GalNAc-Hynic conjugation to siRNNs (**Figure 5.2C**). Through comparative analysis of phosphotriester content and degree of charge neutralization, I found that insertion of an abundance of hydrophobic *t*Bu-SATE phosphotriester groups or substitution with more polar O-SATE groups reduced induction of RNAi responses by GalNAc-siRNN conjugates *in vivo* (**Figure 5.2C,D**).

Following reports that use of multiple *tris*-GalNAc targeting domains could enhance uptake, I synthesized multivalent *tris*-GalNAc-siRNN conjugates and administered them intravenously into mice. However, I found that increased *tris*-GalNAc delivery domain valency inhibited siRNN delivery (**Figure 5.2E**). The failure of multivalent *tris*-GalNAc targeting domains to enhance siRNN delivery may have been due to the decreased ratio of GalNAc to siRNN resulting in lower overall siRNN internalization by hepatic ASGPRs upon systemic administration. Finally, I conducted dose-response and kinetic analyses of intravenously administered GalNAc-siRNN conjugates (**Figure 5.3C,D**). I found that GalNAc-siRNNs induced dose-dependent RNAi responses (ED_{50} ~10 mg/kg) with endogenous ApoB mRNA expression nadir reached between 3 and 6 days after administration and RNAi response maintained > 12 days.

Overall, I conclude that GalNAc-siRNN conjugates have multiple positive attributes, including ease of synthesis, serum stability, and a 5,000-fold smaller size than nanoparticle approaches that dramatically increases its diffusion coefficient. Additionally, the modular nature of siRNN phosphotriester chemistry allows for precise modification of the molecule's biophysical properties to facilitate *in vivo* delivery. My

establishment of GalNAc-siRNN *in vivo* delivery gives us a tester system to examine the function of new phosphotriesters, conjugation schemes, delivery domains, and endosomal escape domains *in vivo*. Additionally, usage of the GalNAc *in vivo* tester system facilitates the development of siRNNs with enhanced persistence in the blood to enable delivery to cancer cells and other tissues that are less accessible than the liver. I believe siRNNs represent a technology that has the potential to open new avenues for RNAi therapeutics.

Utilization of the amazingly efficient *tris*-GalNAc delivery domain has facilitated efficient siRNA delivery to the liver and GalNAc conjugate RNAi therapeutics will begin to enter the market for the treatment of liver diseases with a genetic component. The next great challenge will be extra-hepatic delivery of RNAi triggers. No other cell surface receptor is known to possess the optimal combination of high expression, rapid turnover, and tissue specificity as does the hepatic ASGPR. Further efforts must center on targeted delivery of RNAi triggers to other tissues and enhancement of cellular delivery. I believe that the versatility of the siRNN approach to siRNA delivery makes it uniquely suited to meeting this challenge.

ACKNOWLEDGEMENTS

The research described in Chapter 5 has, in part, been published in Nature Biotechnology co-authored by the dissertation author (Meade et al., 2014). Phosphoramidites utilized in in Chapter 5 were synthesized by Khirud Gogoi. Aaron Springer synthesized some RNN oligonucleotides. Apollo Kacsinta performed siRNN albumin binding assays.

REFERENCES

Beaucage, S. (1992). Advances in the Synthesis of Oligonucleotides by the Phosphoramidite Approach. Tetrahedron *48*, 2223–2311.

Bumcrot, D., Manoharan, M., Koteliansky, V., and Sah, D.W.Y. (2006). RNAi therapeutics: a potential new class of pharmaceutical drugs. Nat. Chem. Biol. *2*, 711–719.

Butler, J.S., Chan, A., Costelha, S., Fishman, S., Willoughby, J.L.S., Borland, T.D., Milstein, S., Foster, D.J., Gonçalves, P., Chen, Q., Qin, J., Bettencourt, B.R., Sah, D.W., Alvarez, R., Rajeev, K.G., Manoharan, M., Fitzgerald, K., Meyers, R.E., Nochur, S. V., Saraiva, M.J., and Zimmermann, T.S. (2016). Preclinical evaluation of RNAi as a treatment for transthyretin-mediated amyloidosis. Amyloid *6129*, 109–118.

Carthew, R.W., and Sontheimer, E.J. (2009). Origins and Mechanisms of miRNAs and siRNAs. Cell *136*, 642–655.

Cummings, R.D., and McEver, R.P. (2009). C-type Lectins. In Essentials of Glycobiology, A. Varki, R.D. Cummings, J.D. Esko, H.H. Freeze, P. Stanley, C.R. Bertozzi, G.W. Hart, and M.E. Etzler, eds. (New York: Cold Spring Harbor Laboratory Press), p.

Elbashir, S.M., Harborth, J., Lendeckel, W., Yalcin, A., Weber, K., and Tuschl, T. (2001). Duplexes of 21-nucleotide RNAs mediate RNA interference in cultured mammalian cells. Nature *411*, 494–498.

Esko, J.D., Kimata, K., and Lindahl, U. (2009). Proteoglycans and Sulfated Glycosaminoglycans. In Essentials of Glycobiology, (Cold Spring Harbor Laboratory Press), p. 784.

de Fougerolles, A., Vornlocher, H.-P., Maraganore, J., and Lieberman, J. (2007). Interfering with disease: a progress report on siRNA-based therapeutics. Nat. Rev. Drug Discov. *6*, 443–453.

Gao, S., Dagnaes-Hansen, F., Nielsen, E.J.B., Wengel, J., Besenbacher, F., Howard, K.A., and Kjems, J. (2009). The effect of chemical modification and nanoparticle formulation on stability and biodistribution of siRNA in mice. Mol. Ther. *17*, 1225–1233.

Grewal, P.K. (2010). The Ashwell-Morell receptor. Methods Enzymol. *479*, 223–241.

Joshua-Tor, L., and Hannon, G.J. (2011). Ancestral roles of small RNAs: an Ago-centric perspective. Cold Spring Harb. Perspect. Biol. *3*, a003772.

Juliano, R.L. (2016). The delivery of therapeutic oligonucleotides. Nucleic Acids Res. *347*, 6518–6548.

Kanasty, R., Dorkin, J.R., Vegas, A., and Anderson, D. (2013). Delivery materials for

siRNA therapeutics. Nat. Mater. *12*, 967–977.

Kinberger, G.A., Prakash, T.P., Yu, J., Vasquez, G., Low, A., Chappell, A., Schmidt, K., Murray, H.M., Gaus, H., Swayze, E.E., and Seth, P.P. (2016). Conjugation of mono and di-GalNAc sugars enhances the potency of antisense oligonucleotides via ASGR mediated delivery to hepatocytes. Bioorg. Med. Chem. Lett.

Lee, Y.C., Townsend, R.R., Hardy, M.R., Lönngren, J., Arnarp, J., Haraldsson, M., and Lönn, H. (1983). Binding of synthetic oligosaccharides to the hepatic Gal/GalNAc lectin. Dependence on fine structural features. J. Biol. Chem. *258*, 199–202.

Lipinski, C.A., Lombardo, F., Dominy, B.W., and Feeney, P.J. (2001). Experimental and computational approaches to estimate solubility and permeability in drug discovery and development settings. Adv. Drug Deliv. Rev. *46*, 3–26.

Lönn, P., Kacsinta, A.D., Cui, X.-S., Hamil, A.S., Kaulich, M., Gogoi, K., and Dowdy, S.F. (2016). Enhancing Endosomal Escape for Intracellular Delivery of Macromolecular Biologic Therapeutics. Sci. Rep. *6*, 32301.

Matranga, C., Tomari, Y., Shin, C., Bartel, D.P., and Zamore, P.D. (2005). Passenger-strand cleavage facilitates assembly of siRNA into Ago2-containing RNAi enzyme complexes. Cell *123*, 607–620.

Matsuda, S., Keiser, K., Nair, J.K., Charisse, K., Manoharan, R.M., Kretschmer, P., Peng, C.G., Kel'in, A. V., Kandasamy, P., Willoughby, J.L.S., Liebow, A., Querbes, W., Yucius, K., Nguyen, T., Milstein, S., Maier, M.A., Rajeev, K.G., and Manoharan, M. (2015). siRNA Conjugates Carrying Sequentially Assembled Trivalent N-Acetylgalactosamine Linked Through Nucleosides Elicit Robust Gene Silencing In Vivo in Hepatocytes. ACS Chem. Biol. *10*, 1181–1187.

McLennan, D.N., Porter, C.J.H., and Charman, S.A. (2005). Subcutaneous drug delivery and the role of the lymphatics. Drug Discov. Today Technol. *2*, 89–96.

Meade, B.R., and Dowdy, S.F. (2009). The road to therapeutic RNA interference (RNAi): Tackling the 800 pound siRNA delivery gorilla. Discov. Med. *8*, 253–256.

Meade, B.R., Gogoi, K., Hamil, A.S., Palm-Apergi, C., van den Berg, A., Hagopian, J.C., Springer, A.D., Eguchi, A., Kacsinta, A.D., Dowdy, C.F., Presente, A., Lönn, P., Kaulich, M., Yoshioka, N., Gros, E., Cui, X.-S., and Dowdy, S.F. (2014). Efficient delivery of RNAi prodrugs containing reversible charge-neutralizing phosphotriester backbone modifications. Nat. Biotechnol. *32*, 1256–1261.

Merkel, O.M., Librizzi, D., Pfestroff, A., Schurrat, T., Béhé, M., and Kissel, T. (2009). In vivo SPECT and real-time gamma camera imaging of biodistribution and pharmacokinetics of siRNA delivery using an optimized radiolabeling and purification procedure. Bioconjug. Chem. *20*, 174–182.

Nair, J.K., Willoughby, J.L.S., Chan, A., Charisse, K., Alam, M.R., Wang, Q., Hoekstra, M., Kandasamy, P., Kel'in, A. V, Milstein, S., Taneja, N., O'Shea, J., Shaikh, S., Zhang, L., van der Sluis, R.J., Jung, M.E., Akinc, A., Hutabarat, R., Kuchimanchi,

S., Fitzgerald, K., Zimmermann, T., van Berkel, T.J.C., Maier, M.A., Rajeev, K.G., and Manoharan, M. (2014). Multivalent N-acetylgalactosamine-conjugated siRNA localizes in hepatocytes and elicits robust RNAi-mediated gene silencing. J. Am. Chem. Soc. *136*, 16958–16961.

Ohrt, T., Muetze, J., Svoboda, P., and Schwille, P. (2012). Intracellular localization and routing of miRNA and RNAi pathway components. Curr. Top. Med. Chem. *12*, 79–88.

Park, E.I., Mi, Y., Unverzagt, C., Gabius, H.-J., and Baenziger, J.U. (2005). The asialoglycoprotein receptor clears glycoconjugates terminating with sialic acid alpha 2,6GalNAc. Proc. Natl. Acad. Sci. U. S. A. *102*, 17125–17129.

Périgaud, C., Gosselin, G., Lefebvre, I., Girardet, J.-L., Benzaria, S., Barber, I., and Imbach, J.-L. (1993). Rational design for cytosolic delivery of nucleoside monphosphates : “SATE” and “DTE” as enzyme-labile transient phosphate protecting groups. Bioorg. Med. Chem. Lett. *3*, 2521–2526.

Prakash, T.P., Graham, M.J., Yu, J., Carty, R., Low, A., Chappell, A., Schmidt, K., Zhao, C., Aghajan, M., Murray, H.F., Riney, S., Booten, S.L., Murray, S.F., Gaus, H., Crosby, J., Lima, W.F., Guo, S., Monia, B.P., Swayze, E.E., and Seth, P.P. (2014). Targeted delivery of antisense oligonucleotides to hepatocytes using triantennary N-acetyl galactosamine improves potency 10-fold in mice. Nucleic Acids Res. *42*, 8796–8807.

Prakash, T.P., Brad Wan, W., Low, A., Yu, J., Chappell, A.E., Gaus, H., Kinberger, G.A., Østergaard, M.E., Migawa, M.T., Swayze, E.E., and Seth, P.P. (2015). Solid-phase synthesis of 5’-triantennary N-acetylgalactosamine conjugated antisense oligonucleotides using phosphoramidite chemistry. Bioorg. Med. Chem. Lett. *25*, 4127–4130.

Prakash, T.P., Kinberger, G.A., Murray, H.M., Chappell, A., Riney, S., Graham, M.J., Lima, W.F., Swayze, E.E., and Seth, P.P. (2016a). Synergistic effect of phosphorothioate, 5???-vinylphosphonate and GalNAc modifications for enhancing activity of synthetic siRNA. Bioorganic Med. Chem. Lett. *26*, 2817–2820.

Prakash, T.P., Yu, J., Migawa, M.T., Kinberger, G.A., Wan, W.B., Østergaard, M.E., Carty, R.L., Vasquez, G., Low, A., Chappell, A., Schmidt, K., Aghajan, M., Crosby, J., Murray, H.M., Booten, S.L., Hsiao, J., Soriano, A., Machemer, T., Cauntay, P., Burel, S.A., Murray, S.F., Gaus, H.J., Graham, M.J., Swayze, E.E., and Seth, P.P. (2016b). Comprehensive Structure Activity Relationship of Triantennary N-Acetylgalactosamine Conjugated Antisense Oligonucleotides for Targeted Delivery to Hepatocytes. J. Med. Chem.

Rajeev, K.G., Nair, J.K., Jayaraman, M., Charisse, K., Taneja, N., O’Shea, J., Willoughby, J.L.S., Yucius, K., Nguyen, T., Shulga-Morskaya, S., Milstein, S., Liebow, A., Querbes, W., Borodovsky, A., Fitzgerald, K., Maier, M.A., and Manoharan, M. (2015). Hepatocyte-Specific Delivery of siRNAs Conjugated to Novel Non-nucleosidic Trivalent N-Acetylgalactosamine Elicits Robust Gene

Silencing in Vivo. ChemBioChem *16*, 903–908.

Rettig, G.R., and Behlke, M.A. (2012). Progress toward in vivo use of siRNAs-II. Mol. Ther. *20*, 483–512.

Rozema, D.B., Lewis, D.L., Wakefield, D.H., Wong, S.C., Klein, J.J., Roesch, P.L., Bertin, S.L., Reppen, T.W., Chu, Q., Blokhin, A. V, Hagstrom, J.E., and Wolff, J.A. (2007). Dynamic PolyConjugates for targeted in vivo delivery of siRNA to hepatocytes. Proc. Natl. Acad. Sci. U. S. A. *104*, 12982–12987.

Rozema, D.B., Blokhin, A., Wakefield, D.H., Benson, J., Carlson, J., Klein, J.J., Almeida, L., Perillo-Nicholas, A., Hamilton, H.L., Chu, Q., Hegge, J.O., Wong, S.C., Trubetskoy, V., Hagen, C., Kitas, E., Wolff, J.A., and Lewis, D.L. (2015). Protease-triggered siRNA delivery vehicles. J. Control. Release.

Schirle, N.T., and MacRae, I.J. (2012). The crystal structure of human Argonaute2. Science *336*, 1037–1040.

Schirle, N.T., Kinberger, G.A., Murray, H.F., Lima, W.F., Prakash, T.P., and MacRae, I.J. (2016). Structural Analysis of Human Argonaute-2 Bound to a Modified siRNA Guide. J. Am. Chem. Soc. *138*, 8694–8697.

Sehgal, A., Barros, S., Ivanciu, L., Cooley, B., Qin, J., Racie, T., Hettinger, J., Carioto, M., Jiang, Y., Brodsky, J., Prabhala, H., Zhang, X., Attarwala, H., Hutabarat, R., Foster, D., Milstein, S., Charisse, K., Kuchimanchi, S., Maier, M. a, Nechev, L., Kandasamy, P., Kel'in, A. V, Nair, J.K., Rajeev, K.G., Manoharan, M., Meyers, R., Sorensen, B., Simon, A.R., Dargaud, Y., Negrier, C., Camire, R.M., and Akinc, A. (2015). An RNAi therapeutic targeting antithrombin to rebalance the coagulation system and promote hemostasis in hemophilia. Nat. Med. *21*, 492–497.

Sliedregt, L.A., Rensen, P.C., Rump, E.T., van Santbrink, P.J., Bijsterbosch, M.K., Valentijn, A.R., van der Marel, G.A., van Boom, J.H., van Berkel, T.J., and Biessen, E.A. (1999). Design and synthesis of novel amphiphilic dendritic galactosides for selective targeting of liposomes to the hepatic asialoglycoprotein receptor. J. Med. Chem. *42*, 609–618.

Spiess, M. (1990). The asialoglycoprotein receptor: a model for endocytic transport receptors. Biochemistry *29*, 10009–10018.

Westerlind, U., Westman, J., Törnquist, E., Smith, C.I.E., Oscarson, S., Lahmann, M., and Norberg, T. (2004). Ligands of the asialoglycoprotein receptor for targeted gene delivery, part 1: Synthesis of and binding studies with biotinylated cluster glycosides containing N-acetylgalactosamine. Glycoconj. J. *21*, 227–241.

Whitehead, K.A., Langer, R., and Anderson, D.G. (2009). Knocking down barriers: advances in siRNA delivery. Nat. Rev. Drug Discov. *8*, 129–138.

Wittrup, A., and Lieberman, J. (2015). Knocking down disease: a progress report on siRNA therapeutics. Nat. Rev. Genet. *16*, 543–552.

Wong, S.C., Klein, J.J., Hamilton, H.L., Chu, Q., Frey, C.L., Trubetskoy, V.S., Hegge, J., Wakefield, D., Rozema, D.B., and Lewis, D.L. (2012). Co-injection of a targeted, reversibly masked endosomolytic polymer dramatically improves the efficacy of cholesterol-conjugated small interfering RNAs in vivo. Nucleic Acid Ther. *22*, 380–390.

Wooddell, C.I., Rozema, D.B., Hossbach, M., John, M., Hamilton, H.L., Chu, Q., Hegge, J.O., Klein, J.J., Wakefield, D.H., Oropeza, C.E., Deckert, J., Roehl, I., Jahn-Hofmann, K., Hadwiger, P., Vornlocher, H.-P., McLachlan, A., and Lewis, D.L. (2013). Hepatocyte-targeted RNAi therapeutics for the treatment of chronic hepatitis B virus infection. Mol. Ther. *21*, 973–985.

Yang, W.H., Aziz, P. V, Heithoff, D.M., Mahan, M.J., Smith, J.W., and Marth, J.D. (2015). An intrinsic mechanism of secreted protein aging and turnover. Proc. Natl. Acad. Sci. U. S. A. *112*, 13657–13662.

Yu, R.Z., Graham, M.J., Post, N., Riney, S., Zanardi, T., Hall, S., Burkey, J., Shemesh, C.S., Prakash, T.P., Seth, P.P., Swayze, E.E., Geary, R.S., Wang, Y., and Henry, S. Disposition and Pharmacology of a GalNAc3-conjugated ASO Targeting Human Lipoprotein (a) in Mice. Mol. Ther. Nucleic Acids *5*, e317.

CHAPTER 6

INDUCTION OF RNAI RESPONSES BY LEFT-HANDED HAIRPIN RNAS

INDUCTION OF RNAI RESPONSES BY LEFT-HANDED HAIRPIN RNAS

ABSTRACT

Small double-stranded, left-handed hairpin (LHP) RNAs containing a 5'-guide-loop-passenger-3' structure induce RNAi responses by a poorly understood mechanism. To explore LHPs, we synthesized fully 2'-modified LHP RNAs targeting multiple genes and found all to induce robust RNAi responses. Deletion of the loop and nucleotides at the 5'-end of the equivalent passenger sequence resulted in a smaller LHP that induced still strong RNAi responses. Surprisingly, progressive deletion of up to 10 nucleotides from the 3'-end of the guide sequence resulted in a 32mer LHP capable of inducing robust RNAi responses. However, further guide sequence deletion inhibited LHP activity, thereby defining the minimal length guide targeting length to 13 nucleotides. To dissect LHP processing, we examined LHP species that co-immunoprecipitated with Argonaute 2 (Ago2), the catalytic core of RISC, and found that the Ago2-associated processed LHP species was of a length that correlated with Ago2 cleavage of the passenger sequence. Placement of a blocking 2'-OMe blocking modification at the LHP predicted Ago2 cleavage site resulted in an intact LHP loaded into Ago2 and no RNAi response. Taken together, these data argue that in the absence of a substantial loop, this novel class of small LHP RNAs enters the RNAi pathway by a Dicer-independent mechanism that involves Ago2 cleavage and results in an extended guide strand. Additionally, we demonstrated that fully 2'-modified minimal-length LHPs are functional *in vivo*. This work establishes LHPs as efficient alternative RNAi triggers that can be produced from a single synthesis and are functional as fully 2'-modified species as necessary for potential use as an RNAi therapeutic.

INTRODUCTION

The discovery of RNA interference (RNAi) in *Caenorhabditis elegans* (Fire et al., 1998) revealed a novel post-transcriptional mechanism of gene regulation mediated by double-stranded RNA. The combined activity of Drosha and Dicer ribonucleases cleave and process long double-stranded RNA hairpin loops into 21-23 nucleotide double stranded micro-RNAs (miRNAs) with 3' dinucleotide overhangs that are loaded by TRBP into Argonaute proteins, the catalytic subunit of RNA-Induced Silencing Complex (RISC), to induce RNAi responses (Ender and Meister, 2010). The sense strand or "passenger" strand is removed and the anti-sense or "guide" strand remains loaded in RISC to scan mRNA transcript for target sequences. The ability of exogenously administered synthetic short interfering RNAs (siRNA) 21-23 nucleotides in length with two nucleotide 3' overhangs to engage the RNAi machinery downstream of Dicer opened the door for performing selective gene silencing (Elbashir et al., 2001). Given the specificity, potency, and ability to target the undruggable genome, siRNA induced RNAi responses have great potential for treating human disease, particularly cancer with its myriad of genetic mutations (Hahn and Weinberg, 2002; Wittrup and Lieberman, 2015). Moreover, due to the ability to induce synthetic lethal RNAi responses and to evolve the siRNA "drug" as fast as the patient's tumor genetics evolve, RNAi therapeutics stand alone in their potential for development of personalized cancer treatment (Meade and Dowdy, 2009; Michiue et al., 2009; Kacsinta and Dowdy, 2016).

Beyond siRNA, multiple groups have demonstrated efficacy with alternative RNAi inducing molecular structures, including long double-stranded RNA (Kim et al., 2005) and short-hairpin RNAs (shRNAs) that contain large intervening loops based on miRNA stem-loop characteristics and employ DNA based viral vectors driven by RNA polymerase II or III promoters (Harborth et al., 2003; Siolas et al., 2005; Vlassov et al.,

2007; Rao et al., 2009). Several studies investigating the potency of synthetic shRNAs have found combined influences contributed by the stem, loop, and 3'-end structure (McManus et al., 2002; Harborth et al., 2003; Siolas et al., 2005; Vlassov et al., 2007). Interestingly, the orientation of the passenger and guide sequences within the hairpin molecule has a profound impact on the RNAi-trigger's activity profile. Right-handed hairpin loop (RHP) RNAs, containing a 5'-passenger-loop-guide-3' structure, generally induce stronger RNAi responses with the presence of a double-stranded stem length exceeding 19 base pairs, a large loop, and a 3' 2 nucleotide overhang as this structure facilitates crucial Dicer processing (McManus et al., 2002; Harborth et al., 2003; Siolas et al., 2005; Li et al., 2007; Vlassov et al., 2007; Dallas et al., 2012; Liu et al., 2013). In contrast, left-handed hairpin loop (LHP) RNAs, with 5'-guide-loop-passenger-3' structure, have been found to maintain RNAi potency independent of loop size and 3' structure (McManus et al., 2002; Harborth et al., 2003; Ge et al., 2010a, 2010b; Dallas et al., 2012). The difference in structural tolerance between RHPs and LHPs reflects alternative mechanisms of entry into the RNAi pathway. LHPs contain an exposed 5' guide sequence end that can bind readily to the Ago2 PAZ domain, whereas RHPs do not and therefore, require specific ribonuclease processing of the loop to obtain a free 5' guide sequence end for the induction of an RNAi response. Thus, the structural properties of functional small LHPs places them in a distinct class of RNAi-inducing molecules from RHPs.

Few studies have investigated the LHP class of RNAi triggers and none had examined fully 2'-modified LHPs, so to investigate the mechanistic processing of LHP-induced RNAi responses, we synthesized a series of LHPs targeting GFP, Luciferase, and Plk1 with deleted guide and passenger sequence nucleotides proximal to a shortened intervening loop. We find that LHPs can be reduced in length from 51mers to

minimal-length 32mers and still induce robust, specific RNAi responses. However, LHPs require greater than 13 nucleotides of complimentary targeting sequence on the guide strand for induction of RNAi responses. Additionally, we demonstrate that minimal-length LHPs also efficiently function in *in vivo*. Lastly, we find that LHPs are processed in a Dicer-independent manner that requires Ago2 cleavage of the accompanying passenger sequence, resulting in an extended 3'-end of the loaded guide strand that is well tolerated by Ago2. Together, these observations define the LHP structural requirements and determine the mechanism of LHP RNA processing.

RESULTS & DISCUSSION

Synthetic fully 2'-modified LHP RNAs are potent RNAi triggers

At the time of this study, few groups had examined the LHP class of RNAi inducing molecules (McManus et al., 2002; Harborth et al., 2003; Ge et al., 2010a, 2010b). Consequently, little was understood about the mechanism of LHP RNA processing. To understand LHP structural requirements for efficient induction of RNAi responses, we first synthesized LHPs targeting GFP (GFP1) that contained a fully complementary 19 base pair (bp) stem with a 3' dinucleotide overhang, a loop of variable size, and the guide sequence positioned on the 5'-end of the molecule. A 51mer LHP1 was synthesized that contained an endonuclease-liable eleven nucleotide loop and a 42mer LHP2 containing an endonuclease resistant short utlrastable CUUG tetraloop (Woese et al., 1990; Ge et al., 2010a) (**Figure 6.1A**). Additionally, canonical 19mer siRNAs with 3' dinucleotide overhangs with the same GFP-targeting sequence or a control luciferase-targeted sequence were synthesized.

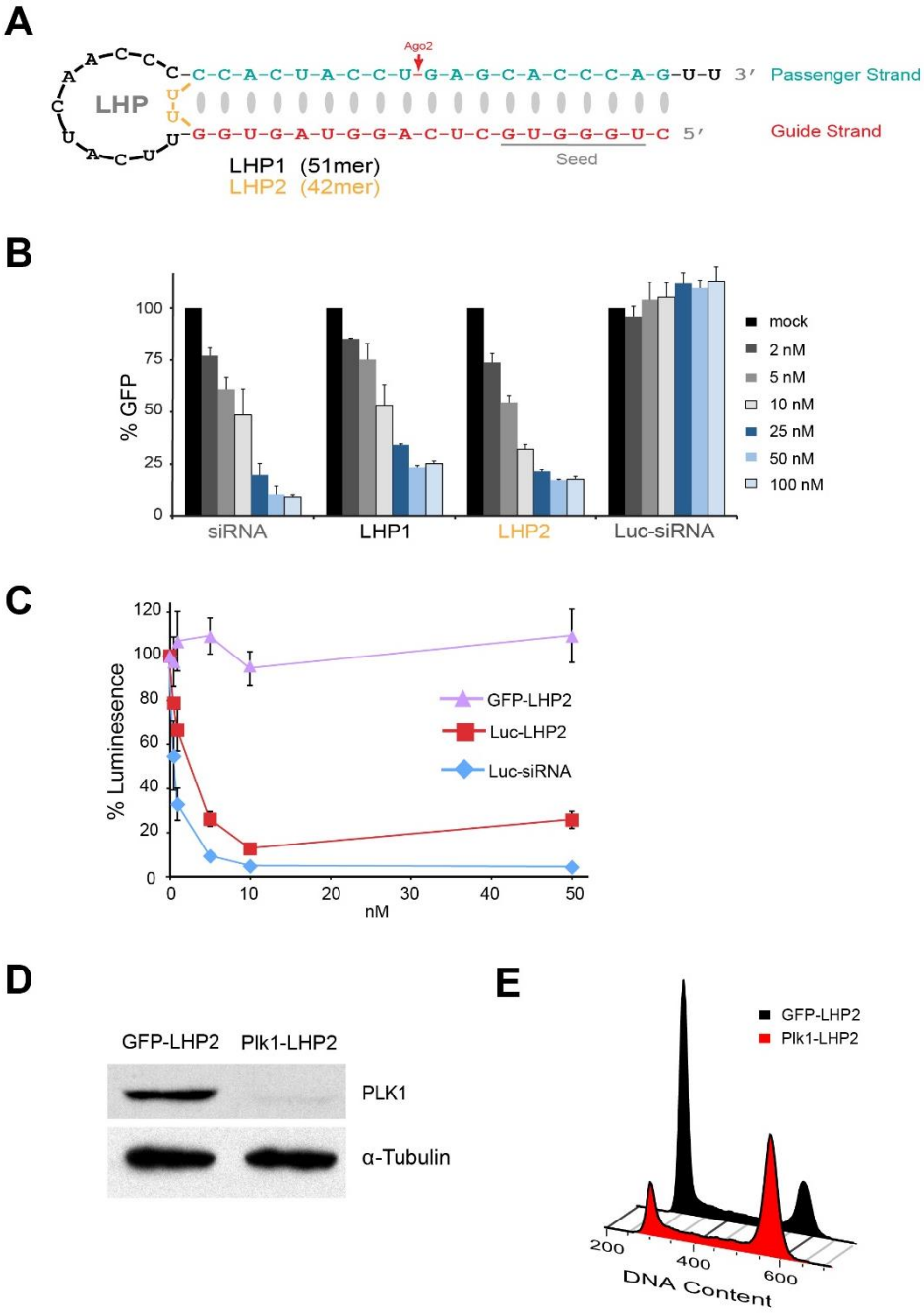

Figure 6.1. Small 2'-F/OMe LHPs are functional for multiple target genes. A) LHP1 (black) and LHP2 (gold) structures of GFP1 targeting sequence. Red arrow indicates expected position of Ago2 passenger sequence cleavage. **B)** Flow cytometry analysis of H1299-dGFP cells transfected with a dose curve of fully 2'-F/OMe modified GFP1 siRNA, GFP1 LHP1, GFP1 LHP2, or control Luc siRNA. Cells were analyzed 48 hr after transfection. **C)** Luciferase activity of H1299-Luc cells 48 hr after transfection with a dose curve of luciferase-targeted LHP2 or siRNA or control GFP LHP2. **D)** Immunoblot analysis of U2OS osteosarcoma cells transfected with Plk1-targeted LHP2 or control GFP LHP2. **E** Flow cytometry analysis of U2OS osteosarcoma cells transfected with Plk1-targeted LHP2 or control GFP LHP2. Cells were stained with propidium iodide to measure DNA content.

Although LHPs advantageously have only one end exposed to exonucleases, to further increase stability and avoid activation of innate immune responses (Behlke, 2008; Davidson and McCray, 2011; Rettig and Behlke, 2012a; Meade et al., 2014) all of the RNAi triggers were synthesized with 2'-F groups on pyrimidines and 2'-OMe groups on purines (**Figure 1.2**). These modifications are highly tolerated by the RNAi machinery and used extensively on therapeutic siRNAs in clinical trials (Rettig and Behlke, 2012a; Sehgal et al., 2015; Juliano, 2016). To analyze for induction of RNAi responses, RNAi triggers were transfected in a dose-dependent fashion into human H1299 lung adenocarcinoma cells constitutively expressing destabilized GFP (Eguchi et al., 2009; Meade et al., 2014) and analyzed by flow cytometry and qRT-PCR (**Figure 6.1B**). GFP LHP1, which contained an 11 nucleotide loop (**Figure 6.1A**), induced a dose-dependent GFP RNAi response that was slightly less efficient than GFP siRNA. However, GFP LHP2, which contained a two nucleotide loop, induced GFP RNAi responses to a similar efficiency as the siRNA. Control luciferase-targeted siRNA, as expected, failed to induce an RNAi response at any of the tested concentrations. Similar results were obtained with two additional independent GFP sequences (GFP2 and GFP6). Together, these observations demonstrate that 42mer LHP2 RNAs are efficient RNAi triggers.

To confirm functionality of 2'-F/OMe LHPs for multiple target genes, we designed and produced 2 nucleotide loop LHP2s targeting the firefly luciferase reporter gene GL3 and the polo-like kinase endogenous proto-oncogene Plk1 following the same design rules used for GFP LHPs. Luc-LHP2 transfected into H1299 cells constitutively expressing GL3 luciferase demonstrated potent RNAi responses (**Figure 6.1C**), similar to those observed for GFP-LHP2 (**Figure 6.1B**). Luc-LHP2 was equally efficacious in human ovarian carcinoma SKOV3-Luc cells (data not shown). These results confirm

that 2'-F/OMe LHP2 molecules are a potent RNAi trigger design that work well in multiple mammalian cell reporter models.

We next targeted Plk1 in U2OS cells where Plk1 depletion induces a phenotypic G2 phase cell cycle arrest (Liu and Erikson, 2003). At 48 hr post transfection, 2'-F/OMe Plk1-LHP2 treated cells displayed a strong reduction in Plk1 protein expression (**Figure 6.1D**). The Plk1 knockdown was paralleled by a distribution of DNA content in the treated population indicative of a G2/M arrest (**Figure 6.1E**). These results demonstrate, for the first time, that 2'-F/OMe minimal loop LHP molecules are efficient RNAi triggers for both reporter and endogenous genes.

Structural determinants of 2'-modified LHP revealed with siRNAs

Small LHPs have been reported to induce RNAi responses in cells independent of Dicer or single-stranded RNase processing (Dallas et al., 2012). Without RNase cleavage of the loop, LHPs loaded into and clipped by Ago2 will generate RISCs primed with a long guide strand targeting oligonucleotides that extend to the Ago2 cleavage site. For example, a 42mer LHP2 (19 nucleotide (nt) guide, 19 nt passenger, 2 nt loop, 3'-UU overhang) will be processed by Ago2 into a 30 nucleotide (nt) guide strand (G-30), and a 38mer LHP3 (19 nt guide, 17 nt passenger, 3'-UU) will generate a 26 nt guide strand (G-26). I explored the tolerance of Ago2 for different length 2'-F/OMe guide strands annealed to a 21mer 2'F/OMe passenger strand (P-21) (**Figure 6.2A**). GFP guide strand sequences were designed based on LHP sequences systematically reduced in size from the 42mer molecule described above. Transfection experiments demonstrated that the RNAi machinery of H1299-dGFP cells tolerated the long guide strands that mimicked Ago2 LHP cleavage products (**Figure 6.2B**). GFP passenger strand oligonucleotides annealed to 24, 26, and 30 nt guide strands all induced RNAi responses similar to those observed with the standard siRNA guide strand of 21 bases

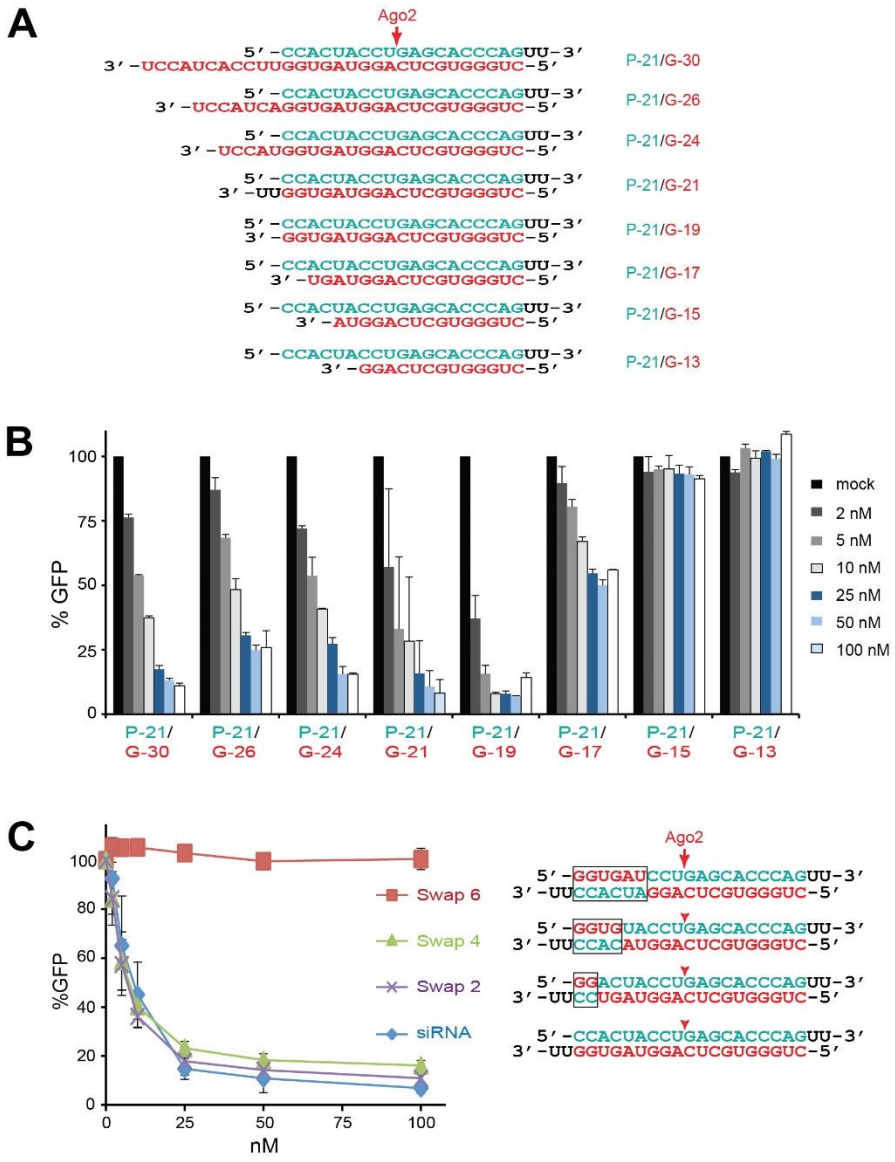

Figure 6.2. Tolerance of RNAi machinery for structure and sequence alteration of RNAi triggers. A) Structures of 2'-F/OMe GFP1 siRNAs studied with variable guide strand lengths annealed to 21 nt passenger strand. Red arrow indicates position of Ago2 passenger strand cleavage. **B)** Flow cytometry analysis of H1299-dGFP cells 48 hr after transfection with dose curves of GFP1 siRNAs containing variable length guide strands. **C)** Right panel: structures of passenger/guide strand sequence exchanged GFP1 siRNAs. Left panel: flow cytometry analysis of H1299-dGFP cells 48 hr after transfection with dose curves of sequence exchanged siRNAs.

(**Figure 6.2B**). This data provides support for the proposed RNase independent mechanism of LHPs. Consistent with previous studies (Chu and Rana, 2008), reduction in guide strand length was only tolerated to 19 bases. The 17 nt guide strand demonstrated a significant decrease in RNAi activity, and the 15 and 13 nt guide strands were completely non-functional (**Figure 6.2B**).

LHPs can induce RNAi responses with minimal-size hairpin structures. However, the size limitations of LHPs have not been thoroughly investigated. Reduction in LHP size can be achieved by shortening the passenger sequence, guide sequence, or loop (Ge et al., 2010b; Dallas et al., 2012). A consequence of LHP shortening via the guide sequence is loss of mRNA complement targeting sequence for RISC. I investigated guide strand complementarity requirements for RNAi induction in 2'-F/OMe 21mer siRNAs by systematic swapping of the complementary 5' guide and 3' passenger strand sequences (**Figure 6.2C**, right panel). As a result, all siRNAs transfected in this experimental set were identical with respect to thermodynamic properties that might influence loading into Ago2 (Preall et al., 2006). The siRNAs with 19, 17, and 15 bases of guide strand to target sequence complementarity gave near identical RNAi responses (**Figure 6.2C**, left panel). However, the siRNA with only 13 bases of mRNA complementary sequence showed no RNAi activity. This result established a theoretical lower limit to 3' guide strand sequence reduction for LHPs.

Minimal size limits of 2'-modified LHPs

We demonstrated that completely 2'-F/OMe modified LHPs with an 11 nt or 2 nt loop induced RNAi responses similar to those induced by siRNA (**Figure 6.1B**). Previous RNAi studies targeting a luciferase plasmid reporter gene with 2'-OH oligonucleotides reported that LHPs maintain function with multiple small hairpin structures: 19 nt guide, 19 nt passenger, UU loop, +/- 3' overhang; 18 nt guide, 18 nt

passenger, UU loop; 19 nt guide, 17 nt passenger (Ge et al., 2010b; Dallas et al., 2012). We synthesized and purified a set of LHPs with 3'-UU overhangs to thoroughly define the lower size limits required for RNAi activity by 2'-F/OMe LHPs in H1299-dGFP cells (**Figure 6.3A**). Consistent with results reported for 2'-OH LHPs (Ge et al., 2010b; Dallas et al., 2012), 2'-F/OMe LHPs with a 19 nt guide strand linked directly to a 17 nt passenger strand (LHP3) efficiently knocked down dGFP expression with low nanomolar EC_{50}s (**Figure 6.3B,C**). Additional truncation of the passenger strand to 15 nt (LHP5) did not adversely affect RNAi responses. Surprisingly, we observed similarly potent RNAi activities using 34mer (LHP8: 17 nt guide, 15 nt passenger) and 32mer (LHP9: 15 nt guide, 15 nt passenger) 2'-F/OMe LHPs. Additional reduction of the passenger strand length (LHP16: 15 nt guide, 13 nt passenger) resulted in diminished RNAi responses. Consistent with our observations using independently synthesized guide strands (**Figure 6.2B**), reduction of guide strand length to 13 nucleotides (LHP17: 13 nt guide, 17 nt passenger; LHP18: 13 nt guide, 13 nt passenger) completely abolished RNAi activity (**Figure 6.3B,C**).

For 2'-OH LHPs, the presence of a 3' dinucleotide overhang is not necessary for RNAi activity (Ge et al., 2010). We generated a second set of oligonucleotides to determine if this observation holds true for 2'-F/OMe LHPs in H1299-dGFP cells (**Figure 6.4A**). Indeed, blunt ended 2'-F/OMe LHPs demonstrated RNAi activities (**Figure 6.4B,C**) similar to their 3'-UU counterparts (**Figure 6.3B,C**). Potent RNAi responses were also observed with 40mer (LHP4: 19 nt guide, 19 nt passenger), 36mer (LHP6: 19 nt guide, 17 nt passenger), 34mer (LHP7: 19 nt guide, 15 nt passenger), and 32mer (LHP10: 15 nt guide, 17 nt passenger) LHP RNAi triggers (**Figure 6.4B,C**). RNAi activity was significantly reduced for LHP13 (28mer: 15 nt guide, 13 nt passenger) and completely lost with LHP14 (26mer: 13 nt guide, 13 nt passenger). These results

established a minimal size of 32 nucleotides (LHP9: 15 nt guide, 15 nt passenger) for functional 2'-F/OMe LHPs.

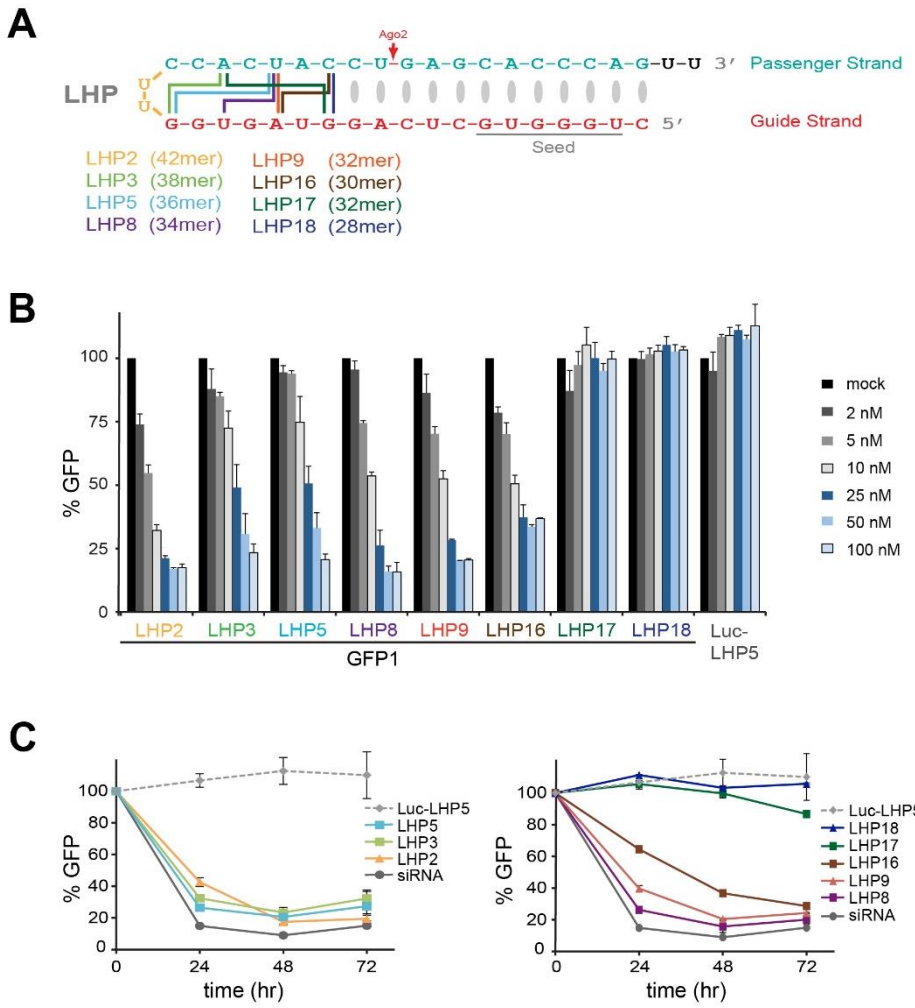

Figure 6.3. Exploration of size reduction in LHPs with 3'-dinucleotide overhangs. A) Structures of size-reduced 2'-F/OMe GFP1 LHPs containing a 3'-UU overhang. Red arrow indicates position of Ago2 passenger sequence cleavage. **B)** Flow cytometry analysis of H1299-dGFP cells 48 hr after transfection with dose curves of size-reduced GFP1 LHPs containing 3'-UU overhangs or control luciferase-targeted LHP5. **C)** Kinetic analysis by flow cytometry of RNAi responses in H1299-dGFP cells transfected with 100 nM LHPs or siRNAs.

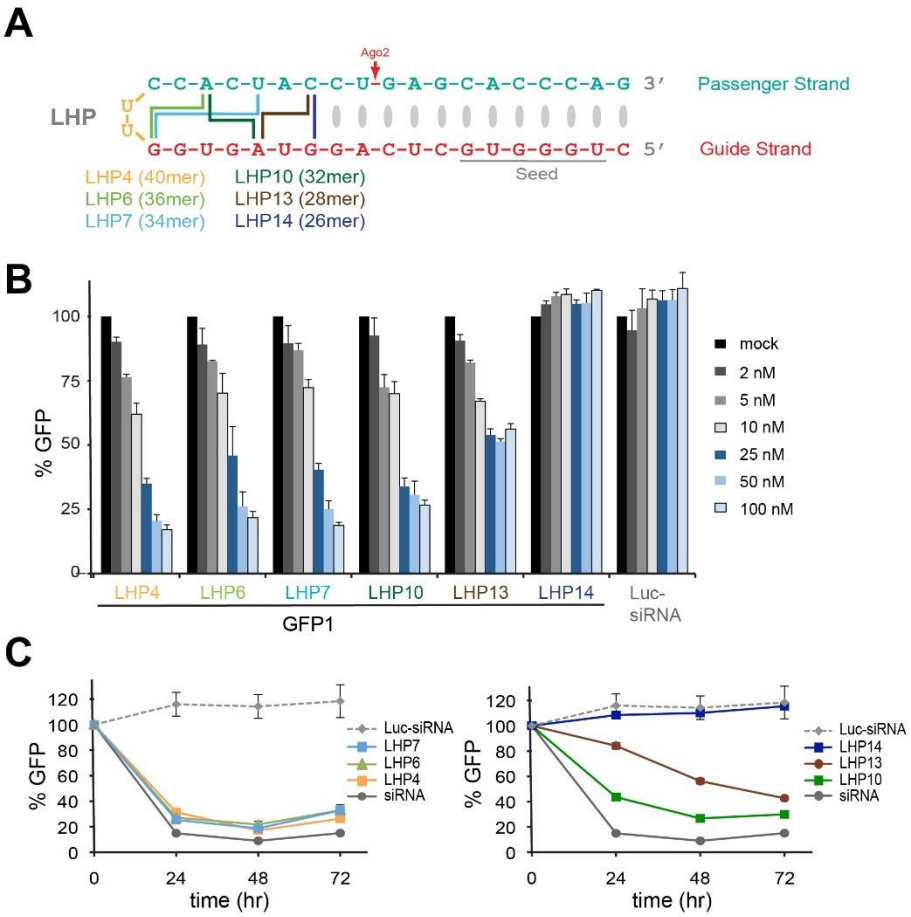

Figure 6.4. Exploration of size reduction in blunt-ended LHPs. A) Structures of size-reduced 2'-F/OMe GFP1 blunt-ended LHPs. Red arrow indicates position of Ago2 passenger sequence cleavage. **B)** Flow cytometry analysis of H1299-dGFP cells 48 hr after transfection with dose curves of size-reduced GFP1 blunt-ended LHPs or control luciferase-targeted siRNA. **C)** Kinetic analysis by flow cytometry of RNAi responses in H1299-dGFP cells transfected with 100 nM LHPs or siRNAs.

Multiple GFP targeting sequences induce RNAi responses as 2'-modified LHPs

Few studies have investigated the RNAi inducing properties of LHPs and none have studied fully 2'-modified LHPs. The limited number of targeting sequences characterized to date warrants further examination of LHP-induced RNAi responses. We studied three different GFP targeting sequences (GFP1, GFP2, GFP6) in H1299-dGFP cells. For each target sequence, we synthesized, purified, and transfected both 2'-OH and 2'-F/OMe molecules with siRNA (21 nt guide, 21 nt passenger), LHP2 (19 nt guide, 19 nt passenger, 2 nt loop, 3'-UU), and LHP7 (19 nt guide, 15 nt passenger) structures (**Figure 6.5**). Potent and sustained RNAi responses were observed for all three siRNA GFP target sequences composed of either 2'-OH or 2'-F/OMe oligonucleotides (**Figure 6.5A**). Interestingly, the 2'-F/OMe siRNAs proved to be more potent than 2'-OH siRNAs for the GFP6 sequence. Strong RNAi activities were maintained for each of the LHP2 molecules. However, the 48 hr dose curves demonstrated modestly diminished potency for most LHP2 sequences relative to their siRNA counterparts (**Figure 6.5B**). LHP size reduction to the LHP7 structure resulted in lowered efficacy for most sequences (**Figure 6.5C**), with only the GFP2 molecule inducing knockdown with efficacy equivalent to its LHP2 counterpart (**Figure 6.5B**). This data indicates that complete 2'-F/OMe modifications of siRNAs and LHPs are generally tolerated by the RNAi machinery. Indeed, the higher melting temperature of 2'-F/OMe duplexes relative to 2'-OH may explain their improved efficacy as small LHP7 structures. The GFP protein knockdown kinetics observed by FACS for all molecules in this set were corroborated at the mRNA level with independent transfections and real-time qPCR analysis (data not shown).

A hallmark of RNAi responses is the specific cleavage of target mRNA opposite nucleotides 10-11 of the guide strand (Meade and Dowdy, 2009). We confirmed RNA

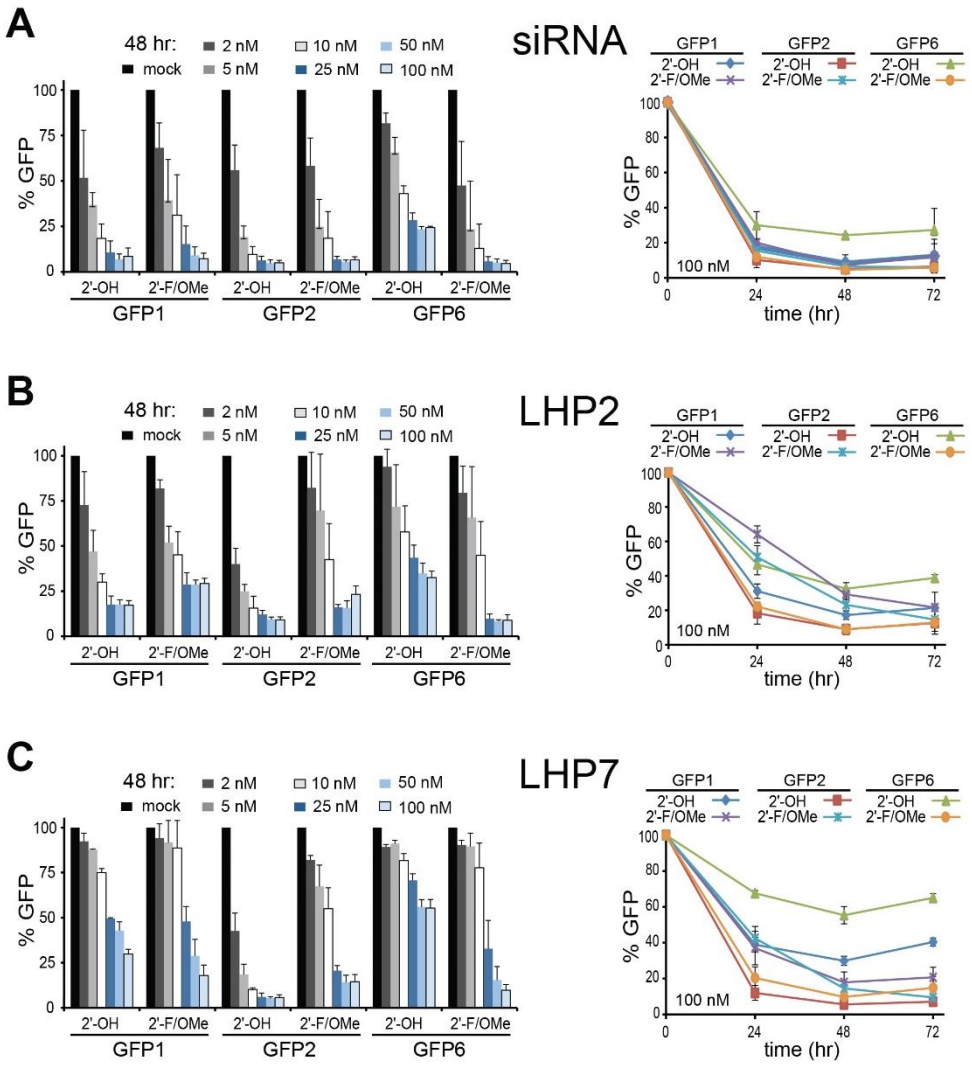

Figure 6.5. Comparison of three distinct GFP targeting sequences using siRNA, LHP2, and LHP7 structures containing 2'-OH or 2'-F/OMe groups. A) Left panel: flow cytometry analysis of H1299-dGFP cells 48 hr after transfection with dose curves of GFP-targeted siRNA containing 2'-OH or 2'-F/OMe groups. GFP1, GFP2, and GFP6 are three discrete siRNA sequences all targeting GFP. Right panel: kinetic analysis by flow cytometry of RNAi responses in H1299-dGFP cells transfected with 100 nM siRNA. **B)** 48 hr dose curve and 3 day kinetic analysis of cells transfected with LHP2 molecules. **C)** 48 hr dose curve and 3 day kinetic analysis of cells transfected with LHP7 molecules.

interference as the mechanism of GFP knockdown for 2'-F/OMe LHPs by performing 5' rapid amplification of cDNA ends (5' RACE) analysis (**Figure 6.6**). We used a common GFP specific primer for PCR amplification from cDNA pools generated by poly-A primed reverse transcription of total RNA isolates from transfected H1299-dGFP cells. The LHP1, LHP2, and LHP7 molecules targeting the GFP1 sequence all generated 5' RACE PCR products the predicted size of 236 bp (**Figure 6.6A**, left panel). LHP7 molecules targeting the GFP2 and GFP6 sequences also yielded expected size PCR products, 543 bp and 344 bp, respectively (**Figure 6.6A**, right panel).

Direct sequencing of gel purified PCR products confirmed the predicted cleavage site for each of the LHPs (**Figure 6.3A**, **Figure 6.4A**, and **Figure 6.6B**). Interestingly, both GFP1-LHP1 and LHP2 appear to induce RISC mediated mRNA cleavage on a fraction of transcripts opposite nucleotides 11-12 of the guide sequence (**Figure 6.6B**). This apparent slight flexibility in the active site of Ago2 could be the consequence of large guide strands that result from Ago2 processing of LHPs (LHP1: 39 nt, LHP2: 30 nt). Indeed, the observed effect correlated positively with predicted guide strand size of the LHPs as RISC loaded with LHP7 molecules (shorter guide strand following Ago2 passenger cleavage) targeting all three GFP sequences demonstrated perfect specificity for the classic mRNA cleavage site (**Figure 6.6B**).

2'-modified LHPs are loaded into Ago2 without Dicer processing

Evidence that LHPs containing 2'-OHs induce RISC mediated gene silencing by an RNase independent mechanism has been reported (Dallas et al., 2012), but processing of fully 2'-modified LHPs has not been studied. We performed Ago2 co-immunoprecipitation (IP) experiments in dGFP-H1299 cells, transfected with 5'-^{32}P-labeled LHPs, to investigate the mechanism of 2'-F/OMe LHP-induced RNAi with respect to Dicer or RNase processing. If the LHPs mediate RNAi responses

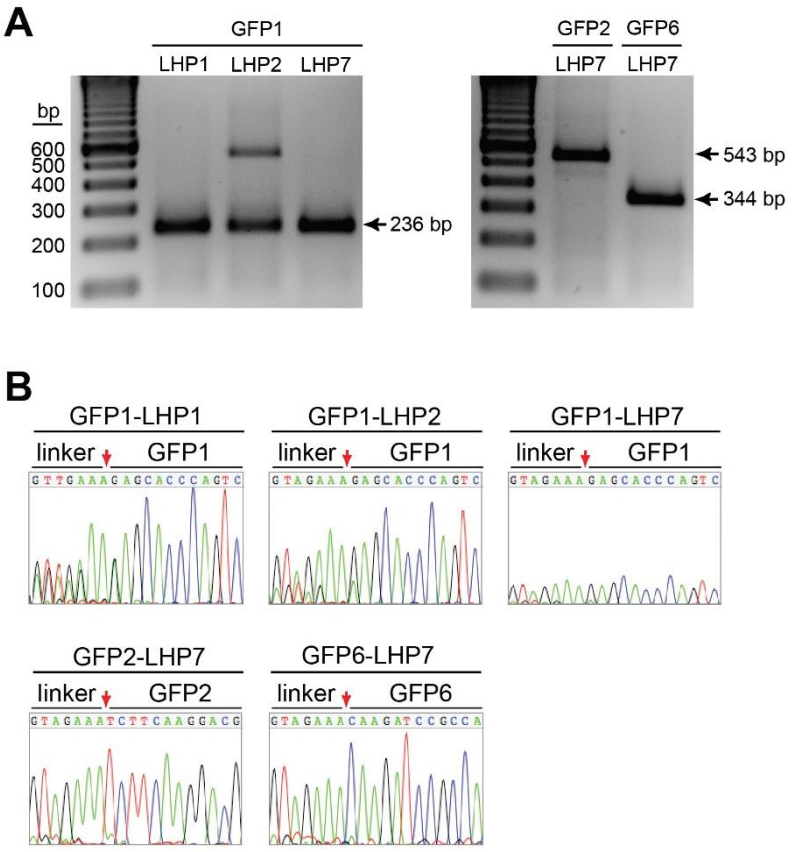

Figure 6.6. 5'-RACE analysis of GFP mRNA from H1299-dGFP cells transfected with 2'-F/OMe LHPs. A) 5' rapid amplification of cDNA ends (RACE) analysis of H1299-dGFP cells transfected with GFP-targeted LHPs. PCR amplification products of anticipated size for GFP1 (236 bp), GFP2 (534 bp), and GFP6 (344 bp) targeted LHPs. **B)** Results of direct sequencing analysis of gel-purified 5' RACE products. Red arrow indicates correct Ago2 cleavage site.

independent of Dicer or single stranded RNase cleavage of the loop, mature RISC will contain long guide strands (LHP2: 30 nt, LHP7: 24) that should co-purify with immunoprecipitated Ago2 and resolve by gel electrophoresis. We synthesized, 5'-^{32}P-labeled, and transfected 2'-F/OMe GFP2-LHP2 and GFP2-LHP7 oligonucleotides. We also synthesized and labeled 30mer, 24mer, and 21mer GFP2 guide strand oligonucleotides for use as molecular weight markers during denaturing gel analysis.

Ago2 IPs of GFP2-LHP2 transfected cells co-purified a ^{32}P oligonucleotide with size equivalent to the 30mer marker (**Figure 6.7A**, left panel). This 30mer is exact length that would be expected from LHP2 passenger cleavage by Ago2 (**Figure 6.3A**). A ^{32}P oligonucleotide pulled down with Ago2 from GFP2-LHP7 migrated similarly to the 24mer marker (**Figure 6.7A**, right panel), as expected from Ago2 cleavage of LHP7 passenger sequence (**Figure 6.4A**). These results indicate that 2'-F/OMe LHPs induce RNAi responses independent of Dicer and RNase processing. LHPs are loaded whole, directly into Ago2/RISC. Recognition appears to be mediated by 5'-phosphate binding to Ago2's MID pocket in a manner analogous to double stranded siRNAs. Ago2 then cleaves the LHP within the passenger sequence, opposite nucleotides 10-11 from the 5'-end. The cleaved fragment is then either ejected or degraded to yield a mature RISC complex containing a relatively long guide strand. This mechanism suggests hydrolysis within the Ago2 active site, at least for passenger sequence cleavage, and occurs independent of 3'-OH contacts with the PAZ domain. Further studies will be necessary to determine whether the cleaved LHP 3'-end associates with the PAZ domain. However, we note that the crystal structure of Ago2-guide strand, shows that nucleotides 15 to 19 are looped out and unstructured (Schirle and MacRae, 2012), suggesting a mechanism to accommodate longer guide strands.

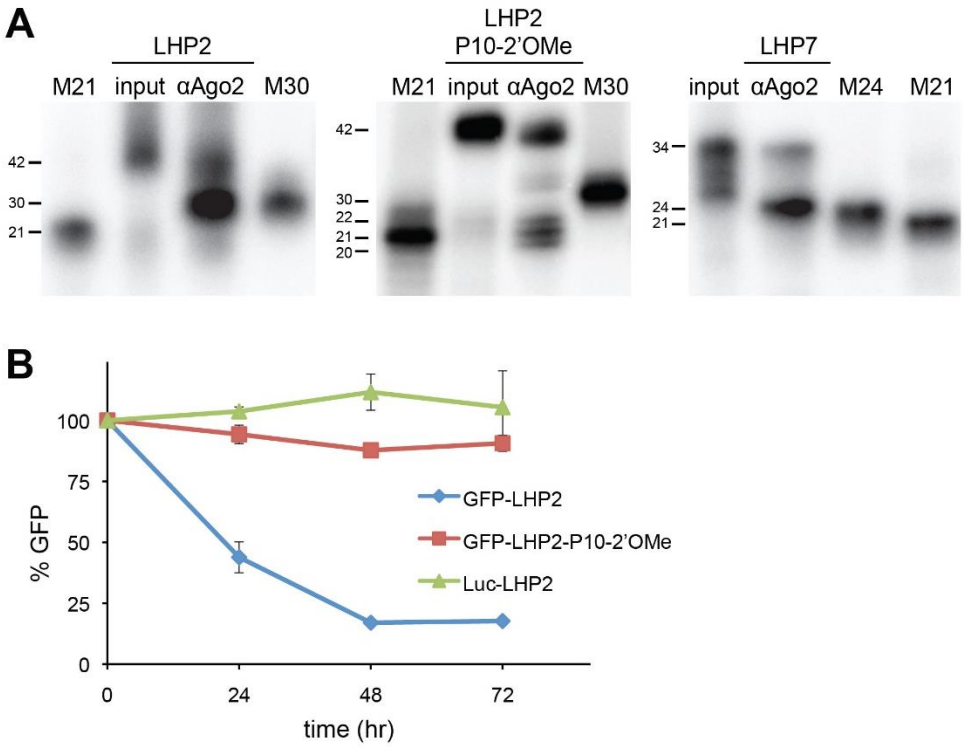

Figure 6.7. Ago2 Co-IP of ^{32}P-labeled 2'-F/OMe LHPs. A) Anti-Ago2 co-immunoprecipitation from cells transfected with ^{32}P-labeled LHPs and analyzed by denaturing gel electrophoresis. LHP2 P10-2'OMe contains a 2'-OMe group in nucleotide 10 at the passenger sequence Ago2 cleavage position. LHP2 and LHP7 both contain a 2'-F at the passenger sequence cleavage position. Input is ^{32}P-labled LHP. M30, M24, and M21 are 30, 24, and 21 nucleotide RNA molecular weight markers, respectively. **B)** Kinetic analysis by flow cytometry of RNAi responses in H1299-dGFP cells transfected with 100 nM LHP2 molecules.

To further study the mechanism of utilized by 2'-modified LHPs, we synthesized a GFP LHP2 with either a 2'-F or 2'-OMe group on nucleotide #10 of the passenger sequence, the expected Ago2 cleavage position. While a 2'-F group is tolerated, a 2'-OMe group inhibits Ago2 slicer activity (Dallas et al., 2012). Consistent with previous work, the 2'-OMe at position 10 on the passenger strand of GFP-LHP2 significantly abated RNAi activity upon transfection into dGFP-H1299 cells (**Figure 6.7B**). Ago2 IPs of cells transfected with this molecule co-purified a ^{32}P oligonucleotide with a mass that paralleled the 42mer LHP oligonucleotide used for transfection (**Figure 6.7A**, center panel). This result indicates that the 2'-OMe of interest does not inhibit Ago2 recognition of the full-length LHP2, but prevents Ago2 catalysis and RISC-mediated targeting of mRNA. The IP also pulled down smaller labeled molecules of 20-22 nt, but these species were present in the input and were likely simply enriched by the IP. Overall, these results suggest that fully 2'-modified LHPs are cleaved in the passenger sequence by Ago2 upon binding of the 5'-end to the Ago2 MID pocket rather than being cleaved prior to RISC loading by Dicer or another endonuclease.

Fully 2'-modified LHPs are functional *in vivo*

To examine the *in vivo* function of fully 2'-modified LHPs, we targeted luciferase as a reporter gene in mice. Intravenous administration of adenovirus expressing Cre recombinase in transgenic Rosa26-LoxP-STOP-LoxP-luciferase (**Figure 4.5A**) mice (Safran et al., 2003) induced stable liver expression of luciferase (**Figure 6.8A**) (Connelly, 1999). 6 mg/kg of 2'-F/OMe modified Luc-LHP2, Luc-LHP7, control GFP-LHP2, or Luc-siRNA were complexed with Invivofectamine 2.0 and systemically delivered to mice by a single intravenous injection. Luciferase expression was measured by non-invasive live animal imaging. All luciferase-targeted RNAi triggers induced knockdown of liver luciferase expression, with siRNA inducing ~80% luciferase

knockdown within 2 days (**Figure 6.8B**). LHPs induced less efficient RNAi responses and, contrary to *in vitro* GFP knockdown (**Figure 6.5**), LHP7 was slightly more potent than LHP2 (**Figure 6.8B**). Importantly, treatment with control GFP-targeted LHP2 did not reduce liver luciferase expression. Luciferase expression returned to normal levels ~3 weeks after treatment. This study provides the first evidence that fully 2'-F/OMe LHPs are functional *in vivo*.

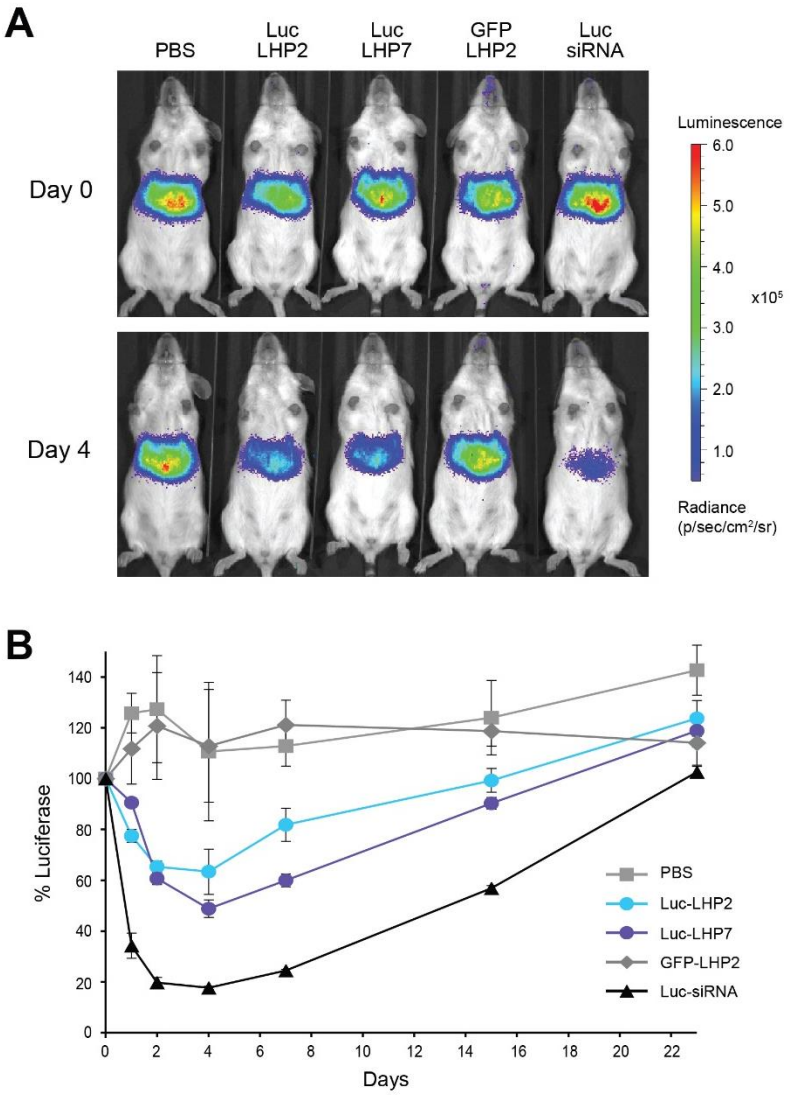

Figure 6.8. In vivo knockdown with 2'-F/OMe LHPs. A) Rosa26-LoxP-STOP-LoxP-Luciferase mice were injected intravenously with adeno-Cre to induce stable expression of luciferase in the liver. 6 mg/kg of 2'-F/OMe Luc-LHP2, Luc-LHP7, Luc-siRNA, and GFP1-LHP2 (control) complexed with Invivofectamine 2.0 were delivered systemically by tail vein injection. **B)** Kinetic analysis of liver luciferase expression in live mice injected intravenously with Invivofectamine-complexed LHPs or siRNA. Luciferase expression was normalized to expression on day 0 prior to treatment.

CONCLUSIONS

Many advantages can be attributed to small synthetic LHPs from a therapeutic development perspective. LHPs are potentially more stable than siRNA as they only have one end accessible to exonucleases. Unlike siRNAs, LHP molecules are composed of only a single oligonucleotide and can therefore be generated from a single column synthesis. Additionally, use of minimal length LHPs (32 nt) instead of siRNAs (42 total nt) can lower production costs. Due to the structure of LHPs, unintended off-target silencing due to unintentional loading of the passenger strand, as can occur with siRNA, cannot occur as LHPs can only be loaded into Ago2 in one orientation due to the positioning of the loop (Dallas et al., 2012). Furthermore, the immunostimulatory properties of dsRNA correlate positively with molecular size. Indeed, smaller is better. Synthetic LHPs can also benefit from improved serum stability (Choung et al., 2006), reduced immune stimulation (Judge and MacLachlan, 2008; Rettig and Behlke, 2012b), and reduced off-target effects (Jackson et al., 2003; Jackson and Linsley, 2010) afforded by chemical modifications at the ribose 2' position (see Chapter 1). Only one study has investigated 2' modifications on LHP sequences targeting a firefly luciferase reporter gene (Ge et al., 2010a). Small LHPs with 2'-OMe modifications on alternating nucleotides of the passenger sequence demonstrated improved stability in human serum and maintained RNAi induction activity consistent with unmodified molecules. The same alternating pattern of 2'-modification on both strands or on the guide strand alone severely diminished the potency of luciferase gene silencing in transfected cells (Ge et al., 2010a). Similar effects were observed with 2'-deoxy substitutions, but 2'-F modifications were not investigated.

This study constitutes the first evidence that small LHPs can function effectively as RNAi triggers when fully 2'-F/OMe modified. We have shown that 2'-modified LHPs

can induce robust RNAi responses against multiple targets with truncation of the loop to a two nucleotide linker (**Figure 6.1**). 2'-F/OMe LHPs do not require 2 nt 3'-overhangs and can be truncated down to a minimal-length 32mer (LHP9; 15 nt passenger, 15 nt guide, 2 nt loop, 2 nt 3'-overhang) while maintaining the ability to induce potent dose-dependent RNAi responses (**Figure 6.3** and **Figure 6.4**). We conducted a thorough analysis of the relationship between ribose 2' group (2'-OH vs 2'-F/OMe), RNAi trigger structure (siRNA vs LHP2 vs LHP7), and target sequence (GFP1 vs GFP2 vs GFP6) that demonstrated that the effectiveness of the RNAi trigger is a function of all three of these properties (**Figure 6.5**). This result suggests that the rules for selecting a potent 2'-OH siRNA sequence cannot be directly applied to 2'-OH or 2'-modified LHPs.

Additionally, our Ago2 co-IP and 2'-OMe passenger cleavage site blockage experiments (**Figure 6.7**) have provided further evidence that LHPs induce an RNAi response through an alternative Dicer-independent mechanism, similar to miR-451 (Cheloufi et al., 2010; Cifuentes et al., 2010; Yang et al., 2010). These experiments indicate that LHPs not pre-processed by Dicer or another endonuclease, but are instead loaded into Ago2 as complete LHP molecules. The 5'-phosphate of the LHP binds to the Ago2 MID pocket, just as is the case for siRNA, but, unlike siRNAs, no 3'-end is available to bind to Ago2's PAZ domain. Ago2 then slices the LHP passenger sequence opposite nucleotides 10-11 of the guide sequence (LHP2) or, to a lesser degree, opposite nucleotides 11-12 if the guide sequence is sufficiently long (LHP7). The sliced passenger sequence fragment is then ejected or degraded and the remaining duplexed passenger sequence is unwound to allow target mRNA binding to the truncated LHP that now functions as a relatively long guide strand in activated RISC. These results suggest that Ago2 slicing of the LHP passenger sequence does not require 3'-OH binding to the Ago2 PAZ domain, but whether or not the 3'-end of the sliced LHP binds to the PAZ

domain after RISC activation remains unknown. This question may be difficult to address as addition of blocking groups to what will become the 3'-end of the LHP following Ago2 slicing of the passenger sequence may prevent Ago2 passenger sequence slicing and, therefore, RISC activation.

We have also demonstrated for the first time that LHPs modified fully with 2'-F and 2'-OMe groups can induce RNAi responses *in vivo* (**Figure 6.8**). The responses induced by LHP2 and the shorter LHP7 were not as strong as those induced by siRNA, but this limited experiment should not be taken as proof that siRNAs are superior to LHPs *in vivo*. As we have shown, the rules for selecting a potent siRNA sequence may not apply directly to LHPs. The luciferase-targeting sequence used in our *in vivo* experiment was selected for a potent siRNA. As such, further experimentation must be conducted with more potent LHP luciferase sequences. Additionally, we utilized Invivofectamine 2.0 to complex our siRNA triggers and deliver them to the liver so that their function could be examine *in vivo*. This delivery reagent may have complexed more poorly with LHPs than siRNAs due to the stem-loop structure characteristic of LHPs.

In summary, we believe that LHPs represent a distinct class of RNAi-inducing triggers and have the potential to be translated into RNAi therapeutics for the treatment of human disease.

ACKNOWLEDGEMENTS

Chapter 6 is currently being prepared for submission for publication of the material. Jonathan Hagopian performed some cellular treatments, 5'-RACE analysis, and *in vivo* experiments. Arjen van den Berg performed Ago2 co-immunoprecipitation experiments. Bryan Meade synthesized oligonucleotides. Akiko Eguchi performed *in vivo* experiments. Caroline Palm-Apergi performed Plk1 knockdown experiments. The dissertation author was the primary investigator and author of this material.

REFERENCES

Behlke, M.A. (2008). Chemical modification of siRNAs for in vivo use. Oligonucleotides *18*, 305–319.

Cheloufi, S., Dos Santos, C.O., Chong, M.M.W., and Hannon, G.J. (2010). A dicer-independent miRNA biogenesis pathway that requires Ago catalysis. Nature *465*, 584–589.

Choung, S., Kim, Y.J., Kim, S., Park, H.-O., and Choi, Y.-C. (2006). Chemical modification of siRNAs to improve serum stability without loss of efficacy. Biochem. Biophys. Res. Commun. *342*, 919–927.

Chu, C.-Y., and Rana, T.M. (2008). Potent RNAi by short RNA triggers. RNA *14*, 1714–1719.

Cifuentes, D., Xue, H., Taylor, D.W., Patnode, H., Mishima, Y., Cheloufi, S., Ma, E., Mane, S., Hannon, G.J., Lawson, N.D., Wolfe, S.A., and Giraldez, A.J. (2010). A novel miRNA processing pathway independent of Dicer requires Argonaute2 catalytic activity. Science *328*, 1694–1698.

Connelly, S. (1999). Adenoviral vectors for liver-directed gene therapy. Curr. Opin. Mol. Ther. *1*, 565–572.

Dallas, A., Ilves, H., Ge, Q., Kumar, P., Shorenstein, J., Kazakov, S.A., Cuellar, T.L., McManus, M.T., Behlke, M.A., and Johnston, B.H. (2012). Right- and left-loop short shRNAs have distinct and unusual mechanisms of gene silencing. Nucleic Acids Res. *40*, 9255–9271.

Davidson, B.L., and McCray, P.B. (2011). Current prospects for RNA interference-based therapies. Nat. Rev. Genet. *12*, 329–340.

Eguchi, A., Meade, B.R., Chang, Y.-C., Fredrickson, C.T., Willert, K., Puri, N., and Dowdy, S.F. (2009). Efficient siRNA delivery into primary cells by a peptide transduction domain-dsRNA binding domain fusion protein. Nat. Biotechnol. *27*, 567–571.

Elbashir, S.M., Harborth, J., Lendeckel, W., Yalcin, A., Weber, K., and Tuschl, T. (2001). Duplexes of 21-nucleotide RNAs mediate RNA interference in cultured mammalian cells. Nature *411*, 494–498.

Ender, C., and Meister, G. (2010). Argonaute proteins at a glance. J. Cell Sci. *123*, 1819–1823.

Fire, A., Xu, S., Montgomery, M.K., Kostas, S.A., Driver, S.E., and Mello, C.C. (1998). Potent and specific genetic interference by double-stranded RNA in Caenorhabditis elegans. Nature *391*, 806–811.

Ge, Q., Dallas, A., Ilves, H., Shorenstein, J., Behlke, M.A., and Johnston, B.H. (2010a). Effects of chemical modification on the potency, serum stability, and

immunostimulatory properties of short shRNAs. RNA *16*, 118–130.

Ge, Q., Ilves, H., Dallas, A., Kumar, P., Shorenstein, J., Kazakov, S.A., and Johnston, B.H. (2010b). Minimal-length short hairpin RNAs: the relationship of structure and RNAi activity. RNA *16*, 106–117.

Hahn, W.C., and Weinberg, R.A. (2002). Modelling the molecular circuitry of cancer. Nat. Rev. Cancer *2*, 331–341.

Harborth, J., Elbashir, S.M., Vandenburgh, K., Manninga, H., Scaringe, S.A., Weber, K., and Tuschl, T. (2003). Sequence, chemical, and structural variation of small interfering RNAs and short hairpin RNAs and the effect on mammalian gene silencing. Antisense Nucleic Acid Drug Dev. *13*, 83–105.

Jackson, A.L., and Linsley, P.S. (2010). Recognizing and avoiding siRNA off-target effects for target identification and therapeutic application. Nat. Rev. Drug Discov. *9*, 57–67.

Jackson, A.L., Bartz, S.R., Schelter, J., Kobayashi, S. V, Burchard, J., Mao, M., Li, B., Cavet, G., and Linsley, P.S. (2003). Expression profiling reveals off-target gene regulation by RNAi. Nat. Biotechnol. *21*, 635–637.

Judge, A., and MacLachlan, I. (2008). Overcoming the innate immune response to small interfering RNA. Hum. Gene Ther. *19*, 111–124.

Juliano, R.L. (2016). The delivery of therapeutic oligonucleotides. Nucleic Acids Res. *347*, 6518–6548.

Kacsinta, A.D., and Dowdy, S.F. (2016). Current views on inducing synthetic lethal RNAi responses in the treatment of cancer. Expert Opin. Biol. Ther. *16*, 161–172.

Kim, D.-H., Behlke, M.A., Rose, S.D., Chang, M.-S., Choi, S., and Rossi, J.J. (2005). Synthetic dsRNA Dicer substrates enhance RNAi potency and efficacy. Nat. Biotechnol. *23*, 222–226.

Li, L., Lin, X., Khvorova, A., Fesik, S.W., and Shen, Y. (2007). Defining the optimal parameters for hairpin-based knockdown constructs. RNA *13*, 1765–1774.

Liu, X., and Erikson, R.L. (2003). Polo-like kinase (Plk)1 depletion induces apoptosis in cancer cells. Proc. Natl. Acad. Sci. U. S. A. *100*, 5789–5794.

Liu, Y.P., Schopman, N.C.T., and Berkhout, B. (2013). Dicer-independent processing of short hairpin RNAs. Nucleic Acids Res. *41*, 3723–3733.

McManus, M.T., Petersen, C.P., Haines, B.B., Chen, J., and Sharp, P.A. (2002). Gene silencing using micro-RNA designed hairpins. RNA *8*, 842–850.

Meade, B.R., and Dowdy, S.F. (2009). The road to therapeutic RNA interference (RNAi): Tackling the 800 pound siRNA delivery gorilla. Discov. Med. *8*, 253–256.

Meade, B.R., Gogoi, K., Hamil, A.S., Palm-Apergi, C., van den Berg, A., Hagopian, J.C., Springer, A.D., Eguchi, A., Kacsinta, A.D., Dowdy, C.F., Presente, A., Lönn, P., Kaulich, M., Yoshioka, N., Gros, E., Cui, X.-S., and Dowdy, S.F. (2014). Efficient delivery of RNAi prodrugs containing reversible charge-neutralizing phosphotriester backbone modifications. Nat. Biotechnol. *32*, 1256–1261.

Michiue, H., Eguchi, A., Scadeng, M., and Dowdy, S.F. (2009). Induction of in vivo synthetic lethal RNAi responses to treat glioblastoma. Cancer Biol. Ther. *8*, 2306–2313.

Preall, J.B., He, Z., Gorra, J.M., and Sontheimer, E.J. (2006). Short interfering RNA strand selection is independent of dsRNA processing polarity during RNAi in Drosophila. Curr. Biol. *16*, 530–535.

Rao, D.D., Vorhies, J.S., Senzer, N., and Nemunaitis, J. (2009). siRNA vs. shRNA: similarities and differences. Adv. Drug Deliv. Rev. *61*, 746–759.

Rettig, G.R., and Behlke, M.A. (2012a). Progress toward in vivo use of siRNAs-II. Mol. Ther. *20*, 483–512.

Rettig, G.R., and Behlke, M.A. (2012b). Progress toward in vivo use of siRNAs-II. Mol. Ther. *20*, 483–512.

Safran, M., Kim, W.Y., Kung, A.L., Horner, J.W., DePinho, R.A., and Kaelin, W.G. (2003). Mouse reporter strain for noninvasive bioluminescent imaging of cells that have undergone Cre-mediated recombination. Mol. Imaging *2*, 297–302.

Schirle, N.T., and MacRae, I.J. (2012). The crystal structure of human Argonaute2. Science *336*, 1037–1040.

Sehgal, A., Barros, S., Ivanciu, L., Cooley, B., Qin, J., Racie, T., Hettinger, J., Carioto, M., Jiang, Y., Brodsky, J., Prabhala, H., Zhang, X., Attarwala, H., Hutabarat, R., Foster, D., Milstein, S., Charisse, K., Kuchimanchi, S., Maier, M. a, Nechev, L., Kandasamy, P., Kel'in, A. V, Nair, J.K., Rajeev, K.G., Manoharan, M., Meyers, R., Sorensen, B., Simon, A.R., Dargaud, Y., Negrier, C., Camire, R.M., and Akinc, A. (2015). An RNAi therapeutic targeting antithrombin to rebalance the coagulation system and promote hemostasis in hemophilia. Nat. Med. *21*, 492–497.

Siolas, D., Lerner, C., Burchard, J., Ge, W., Linsley, P.S., Paddison, P.J., Hannon, G.J., and Cleary, M.A. (2005). Synthetic shRNAs as potent RNAi triggers. Nat. Biotechnol. *23*, 227–231.

Vlassov, A. V, Korba, B., Farrar, K., Mukerjee, S., Seyhan, A.A., Ilves, H., Kaspar, R.L., Leake, D., Kazakov, S.A., and Johnston, B.H. (2007). shRNAs targeting hepatitis C: effects of sequence and structural features, and comparision with siRNA. Oligonucleotides *17*, 223–236.

Wittrup, A., and Lieberman, J. (2015). Knocking down disease: a progress report on siRNA therapeutics. Nat. Rev. Genet. *16*, 543–552.

Woese, C.R., Winker, S., and Gutell, R.R. (1990). Architecture of ribosomal RNA: constraints on the sequence of “tetra-loops”. Proc. Natl. Acad. Sci. U. S. A. *87*, 8467–8471.

Yang, J.-S., Maurin, T., Robine, N., Rasmussen, K.D., Jeffrey, K.L., Chandwani, R., Papapetrou, E.P., Sadelain, M., O’Carroll, D., and Lai, E.C. (2010). Conserved vertebrate mir-451 provides a platform for Dicer-independent, Ago2-mediated microRNA biogenesis. Proc. Natl. Acad. Sci. U. S. A. *107*, 15163–15168.

CHAPTER 7

CONCLUSIONS AND FUTURE DIRECTIONS

CONCLUSIONS AND FUTURE DIRECTIONS

ABSTRACT

Despite its incredible potential for intervention in human disease, RNAi therapeutics have been held back due to the siRNA's size and strong negative charge. To solve this delivery problem, our lab previously developed small interfering ribonucleic neutrals (siRNNs) containing bioreversible phosphotriester groups that neutralize the negative charge of the siRNA backbone. The first generation of siRNNs utilized *t*-butyl-s-acyl-2-thioethyl (*t*Bu-SATE) phosphotriester groups that proved too hydrophobic for biologic use. I utilized molecular modeling and more polar hydroxyl-SATE (O-SATE) phosphotriester groups to generate maximally neutral siRNNs for delivery by conjugated cationic peptide transduction domains (PTDs). Even with an overall cationic charge, these PTD-siRNN conjugates were incapable of self-delivery *in vitro*. To solve this problem, I used conjugatable Aldehyde-SATE (A-SATE) phosphotriesters to make multivalent TAT PTD delivery domain (DD) siRNN conjugates. DD-siRNN conjugates were capable of non-cytotoxic self-delivery and the induction of dose-dependent RNAi responses *in vitro*, a first for siRNNs. However, DD-siRNNs failed to deliver *in vivo* in mouse models. To facilitate *in vivo* delivery of siRNNs, I conjugated siRNNs to *N*-acetylgalactosamine (GalNAc), a hepatocyte-specific targeting domain, through reactive neutralizing phosphotriester groups. I found that single dose systemically administered GalNAc-siRNN conjugates induced extended dose-dependent RNAi responses in mice. This work constituted the first instance of *in vivo* target gene knockdown by siRNNs containing bioreversible neutralizing phosphotriester groups. Finally, I examined induction of RNAi responses by fully 2'-F/OMe modified small, double-stranded, left-handed hairpin (LHP) RNAs containing a 5'-guide-loop-passenger-3' structure. We

confirmed that 2'-modified LHPs induce RNAi responses by an alternative Dicer-independent mechanism and demonstrated that fully 2'-modified minimal-length LHPs are functional *in vitro* and *in vivo*. This establishes minimal-length LHPs as a promising class of efficient RNAi triggers for the application of RNN technology and potential use as an RNAi therapeutic.

INTRODUCTION

The discovery of RNA interference (RNAi) in *C. elegans* (Fire et al., 1998) and subsequent demonstration of RNAi induction in human cells by synthetic short interfering RNAs (siRNAs) introduced a novel mechanism of post-transcriptional regulation of gene expression that spawned a unique new class of therapeutics with the potential to treat human disease (Elbashir et al., 2001). siRNAs utilize a conserved, endogenous RNAi mechanism to achieve exquisite target selectivity for any expressed mRNA with EC_{50} values in the low picomolar range (Wittrup and Lieberman, 2015; Juliano, 2016). Additionally, gene targeting and function of siRNA are entirely dependent on its sequence, thereby allowing rapid target adaptation for truly personalized medicine and to keep pace with the constantly mutating genetic targets in cancer in a way that no other therapeutic can match. However, for all the promise that RNAi holds as a therapeutic, the large size (14,000 Da) and extreme anionic charge of siRNAs results in poor pharmacokinetics and cellular delivery (Behlke, 2008; Meade and Dowdy, 2009; Bramsen and Kjems, 2011; Rettig and Behlke, 2012). Upon systemic administration, siRNAs are rapidly degraded by circulating endonucleases and, due to its high negative charge, is subject to swift renal filtration from the blood (half-life < 5 min) (Gao et al., 2009). Additionally, siRNA molecules are double-stranded RNAs (dsRNAs) that are recognized as viral RNA by the innate immune system leading to the induction of high levels of inflammatory cytokines and interferons following systemic administration (Robbins et al., 2009).

Due to the promise that siRNA holds and the plethora of problems associated with its use as a drug, significant effort has been invested on solving the delivery problem to translate siRNA into the clinic (Rettig and Behlke, 2012; Juliano, 2016). Most delivery approaches have involved encapsulating siRNA molecules in large

nanoparticles or cationic liposomes. Unfortunately, these approaches suffer from a number of problems, including poor cellular delivery, cytotoxicity, and poor pharmacokinetics (Meade and Dowdy, 2009; Schroeder et al., 2010). To avoid the problems inherent in nanoparticle delivery systems, we sought to deliver soluble, monomeric siRNAs by conjugation with small, cationic peptides of a class termed peptide transduction domains (PTDs). PTDs possess a dense cationic charge that is crucial to their ability to translocate across the cell membrane (Gonçalves et al., 2005). Unfortunately, when cationic PTDs and anionic charged siRNAs are covalently linked, the PTD is effectively neutralized by the negative charge of the siRNA phosphodiester backbone and unable to mediate cellular internalization (Jiang et al., 2004).

To enable PTD-mediated delivery of siRNAs, our lab developed short interfering ribonucleic neutrals (siRNNs) featuring bioreversible *t*-butyl-s-acyl-2-thioethyl (*t*Bu-SATE) phosphotriester groups that neutralize the negative charge of the siRNA backbone (Meade et al., 2014). Upon cytosolic entry, SATE phosphotriesters are processed by cytoplasm-restricted thioesterases (**Figure 1.3**) (Zeidman et al., 2009) that convert the neutral phosphotriester into a charged native phosphodiester compatible with the RNAi machinery. The first generation of siRNNs utilizing *t*Bu-SATE phosphotriesters was made possible by the groundbreaking synthesis of RNA oligonucleotides containing *t*Bu-SATE groups (Meade et al., 2014). Although capable of bioreversal and induction of RNAi responses when transfected into cells with cationic lipids, the hydrophobicity of the *t*Bu-SATE group led to extreme insolubility of *t*Bu-SATE siRNNs in physiologic salt conditions.

CONCLUSIONS

Maximizing siRNN neutrality does not facilitate *in vitro* delivery by TAT PTD

To address this issue, we synthesized new O-SATE phosphotriesters that were slightly more polar by way of a terminal hydroxyl group (**Chapter 3**). Unlike *t*Bu-SATE containing siRNNs, O-SATE siRNNs remained soluble in biologically compatible solutions. Additionally, O-SATE siRNNs were bioreversible, stable in human serum, and, importantly, induced RNAi responses upon cellular transfection. With all of our requirements met, the next step was to conjugate O-SATE siRNNs with PTDs. However, we encountered a problem with the degree or percentage of phosphodiester neutralization that we could achieve. Experiments with surrogate irreversible, methyltriester-modified siRNAs conjugated to cationic TAT PTD had suggested that ~70% neutrality was necessary to facilitate PTD-mediated delivery of siRNA (**Chapter 1**). When I started this work, even with O-SATE phosphotriesters, we were limited to 9x insertions on each strand (~45% neutral). Further insertion of phosphotriesters resulted in a marked decrease in the affinity of the RNN oligonucleotides to form a double-stranded species as is required for RNAi induction (**Chapter 3**).

I hypothesized that this limit was due to steric congestion across the major groove and that through selective placement of phosphotriesters we could increase the total number of insertions by minimizing steric congestion. Through analysis of a solution state structure of a fully 2'-F/OMe modified siRNA, I generated the Phosphate Interference Model that predicted potential steric interactions between phosphates across the A-form major groove of siRNA (**Chapter 3**). Using this model, I was able to raise the total number of phosphotriester insertions in a double-stranded siRNN, and consequently degree of neutrality by 20% to 26 phosphotriesters or ~65% neutral that was in the range of neutrality predicted to be necessary to facilitate PTD-mediated siRNN delivery (**Chapter 1**). To conjugate TAT PTD to these highly neutral siRNNs, we utilized Hynic chemistry where the PTD is functionalized with a hydrazine moiety and is

reacted with the siRNN containing a benzaldehyde group attached through a disulfide to the 5' end of the siRNN (**Chapter 3**). This reaction results in the formation of a stable hydrazone bond covalently conjugating the PTD and siRNN. A disulfide was placed between the PTD and siRNN to allow reduction in the cytoplasm and release the PTD from the siRNN. Unfortunately, despite meeting the requirements for stability, bioreversibility, and neutrality, conjugates of these highly neutral siRNNs with 3xTAT PTD were incapable of cellular delivery. Although this attempt at maximizing neutrality failed to generate self-delivering PTD-siRNN conjugates capable of inducing RNAi responses, the Phosphate Interference Model is consulted for each new siRNN we synthesize to ensure that the component single-stranded RNN (ssRNN) oligonucleotides readily hybridize to from a double-stranded species.

TAT PTD delivery domain-siRNN conjugates self-deliver and induce RNAi responses *in vitro*

The failure of highly neutral PTD-siRNN conjugates to self-deliver (**Chapter 3**) may have been due to either the method of PTD attachment or to the PTD itself being neutralized by the remaining negatively charged phosphodiesters on the siRNN. The disulfide bond between the siRNN and PTD was meant to only be reduced in the cytoplasm, but could have been prematurely released in endosomes (Yang et al., 2006; Hastings and Cresswell, 2011). This would prevent the PTD from mediating siRNN endosomal escape to the cytoplasm. Alternatively, despite the PTD-siRNN conjugate possessing an overall cationic charge, residual charged phosphodiesters may have limited the function of the conjugated PTD. To address these issues and create a self-delivering PTD-siRNN, we synthesized an Aldehyde-SATE (A-SATE) phosphotriester that had dual roles of both charge neutralization and acting as a conjugation site by way of a chemically reactive benzaldehyde group (**Chapter 4**). In theory, A-SATEs would

react with hydrazine functionalized peptides to conjugate the peptide directly to the A-SATE phosphotriester. As the A-SATE phosphotriester group contains the requisite thioester bond, it should be subject to intracellular conversion to a charged phosphodiester, resulting in removal of the entire PTD-A-SATE group upon cellular delivery. This approach avoided potential disulfide instability issues and, importantly, could facilitate site-specific conjugation of PTDs in any number and location on a siRNN simply by the selective insertion of A-SATE phosphotriester groups at the time of RNN oligonucleotide synthesis.

We found A-SATE phosphotriester groups to be compatible with RNN oligonucleotide synthesis protocols, stable chemically and biologically, bioreversible even when conjugated to peptides of any length, and able to induce dose-dependent RNAi responses upon transfection of A-SATE containing siRNNs (**Chapter 4**). Although A-SATE groups met our requirements for PTD-mediated delivery of siRNNs, their large size proved to result in greater steric congestion in the siRNA major groove. This limited the number of A-SATEs that could be inserted while maintaining the ability of RNN oligonucleotides to form double-stranded species (siRNN). However, this minor loss in charge neutralization through reduction in the total number of phosphotriester insertions allowed in A-SATE containing siRNNs was more than accounted for by the potential for multiple PTD conjugation provided by A-SATEs.

We utilized A-SATEs to generate siRNNs conjugated to multiple TAT PTD delivery domains (DDs). DD-siRNN conjugates were found to be soluble and importantly, did not form aggregates in biological solutions as do DD-siRNA conjugates (**Chapter 4**). Treatment of cells in culture with DD-siRNN conjugates resulted in induction of non-cytotoxic, dose dependent RNAi responses in the entire cell population. We demonstrated self-delivery of DD-siRNNs and induction of RNAi responses against

GFP and luciferase reporter genes and endogenous genes *in vitro*. We also ascertained the requirements for the number and location of A-SATE phosphotriesters through synthesis of a series of RNN oligonucleotide passenger and guide strands containing A-SATEs. This work constituted the first demonstration of DD-siRNNs capable of self-delivery and subsequent induction of RNAi responses *in vitro*.

With all of our requirements met for PTD-mediated delivery of siRNNs, I tested the ability of DD-siRNNs to induce knockdown expression of a luciferase reporter gene *in vivo* by administration to mice (**Chapter 4**). Unfortunately, TAT PTD DD-siRNN conjugates failed to induce RNAi responses *in vivo* by either subcutaneous or intravenous administration despite repeat dosing and favorable biodistribution. While the reason for this delivery failure remains incompletely understood, it appears that while TAT PTD is capable of delivering macromolecular cargo in animals (Lönn and Dowdy, 2015) and TAT PTD DD-siRNN conjugates efficiently self-deliver and induce siRNA responses *in vitro*, they were not well-suited to siRNN delivery *in vivo* which is the overarching goal of this research. Fortunately, the modular nature of siRNNs and the functionality of A-SATE phosphotriester conjugation allows for the conjugation of alternate delivery domains and the reconfiguration of the siRNN to suit that delivery domain.

GalNAc-siRNN conjugates induce dose-dependent RNAi responses *in vivo*

To test the *in vivo* ability of siRNNs to induce RNAi responses, we sought a targeting domain that would bind to a specific receptor that is highly expressed in a target tissue. For this purpose we selected a hepatocyte-specific *tris*-*N*-acetylgalactosamine (GalNAc) targeting domain (Sliedregt et al., 1999) (**Chapter 5**) that is currently being used in RNAi clinical trials (Wittrup and Lieberman, 2015; Juliano, 2016). The *tris*-GalNAc targeting domain is avidly bound by the hepatic

asialoglycoprotein receptor (ASGPR), also known as the Ashwell-Morell receptor. ASGPR is highly expressed by hepatocytes in the human liver with 10^6 receptors expressed on the surface of each hepatocyte and undergoes recycling by clathrin-mediated endocytosis at a rapid rate of 10-15 min (Spiess, 1990; Cummings and McEver, 2009). To examine GalNAc-targeted siRNN delivery, we synthesized a series of *tris*-GalNAc-Hynic targeting domains with differing GalNAc spacers. I conjugated the *tris*-GalNAc-Hynic domains to ApoB-targeted siRNNs containing a single conjugatable phosphotriester and administered the GalNAc-siRNN conjugates to mice intravenously. Although all GalNAc-siRNN conjugates tested induced RNAi responses, the *tris*-GalNAc targeting domain with amide GalNAc spacers was the most functional and was therefore used for all further GalNAc-siRNN conjugate experiments. These experiments constituted the first demonstration of siRNN-induced RNAi responses *in vivo*.

To optimize GalNAc-siRNN conjugate delivery *in vivo*, I conducted a comparative analysis on the effect of siRNN phosphotriester types and numbers as well as multivalent *tris*-GalNAc-siRNN conjugates (**Chapter 5**). All siRNNs and siRNAs used in these *in vivo* studies were fully 2'-F/OMe modified, but also received further nuclease stabilization in the form of phosphorothioate backbone modifications (**Figure 1.2**) on the 5' and 3' termini of both the passenger and guide strand. siRNNs also contained irreversible dimethylbutyl (DMB) phosphotriesters on the passenger and guide 3' termini. I compared the effect of *tris*-GalNAc-Hynic conjugation to three distinct phosphotriesters, two reversible (A-SATE and A-SATB) and one irreversible (Ax), placed on the 5'-end of the passenger strand (**Chapter 5**). Surprisingly, I found that while GalNAc-siRNN conjugates containing any of the conjugatable phosphotriesters induced strong RNAi responses in mice, the Ax-containing siRNN was the most potent. This result suggested that the *tris*-GalNAc targeting domain did not need to be removed from the 5'-end of the

passenger strand prior to RISC loading as the irreversible Ax phosphotriester is not removed intracellularly. However, the GalNAc-Ax is removed after loading into Ago2 by cleavage of the passenger strand.

I also found that GalNAc-siRNNs containing *t*Bu-SATEs induced stronger siRNA responses than those containing O-SATEs. Contrary to what has been previously reported (Westerlind et al., 2004), I found that conjugation of a single *tris*-GalNAc targeting domain to an siRNN resulted in better delivery and RNAi response induction than conjugation to two *tris*-GalNAc targeting domains, independent of conjugation location on the siRNN. Intravenous treatments of mice of mice also revealed that optimal RNAi responses are induced by siRNNs containing 6 phosphotriesters on each strand, while addition of more *t*Bu-SATE groups decreased RNAi response induction, and treatment with GalNAc-siRNA conjugate induced a poor RNAi response. This trend may have been the result of altered biodistribution of the systemically administered conjugates or less plasma stability of O-SATEs vs. *t*Bu-SATEs.

Charged naked siRNAs do not bind serum albumin and are rapidly cleared by the kidneys (Gao et al., 2009), preventing effective intravenous administration. In contrast, we found that charge neutralized siRNNs avidly bound serum albumin (**Chapter 5**). Support for this was observed when by subcutaneous administration to mice, GalNAc-siRNA and GalNAc-siRNN conjugates both induced similar moderate RNAi responses, with those induced by siRNNs being slightly stronger. However, upon intravenous administration, GalNAc-siRNNs induced strong RNAi responses while GalNAc-siRNA conjugates induced poor RNAi responses.

After determining optimal siRNN configuration, I conducted dose curve and kinetic analyses of ApoB knockdown by intravenously administered ApoB-targeted GalNAc-siRNN conjugates in mice (**Chapter 5**). GalNAc-siRNN conjugates induced

significant dose-dependent ApoB RNAi responses (ED_{50} ~ 10 mg/kg) compared with control GalNAc-siRNN-DMB conjugates ($P < 0.01$ to <0.001) that contained 6x irreversible DMB phosphotriesters on their guide strands, which were unable to induce an RNAi response. Kinetic analysis of single intravenous 25 mg/kg dose of GalNAc-siRNNs showed partial ApoB RNAi responses at 24 and 48 hr that reached a near maximum at 72 hr and were maintained for > 12 days. The GalNAc-siRNN ED_{50} of ~10 mg/kg was higher than desired, but was a function the biophysical attributes of the target ApoB mRNA, including Ago2 accessibility and mRNA synthesis rates combined with the siRNA sequence used. Regardless, under the same experimental conditions, GalNAc-siRNN conjugates induced far stronger RNAi responses than did equivalent charged GalNAc-siRNA conjugates. Cumulatively, this study represents the achievement of the goal of my dissertation research: the synthesis of self-delivering monomeric siRNN conjugates that are converted intracellularly into charged phosphodiester siRNAs that induce robust RNAi responses *in vivo*.

Fully 2'-modified left-handed hairpins induce RNAi responses by an alternative mechanism

We also investigated left-handed hairpin (LHP) molecules, an alternative RNAi trigger that is a promising candidate for RNN phosphotriester technology (**Chapter 6**). Short hairpin RNAs (shRNAs) that have stem lengths of 25-29 base pairs (bp) require Dicer processing to be incorporated into RISC and are commonly expressed in mammalian cells to study gene expression (Rao et al., 2009). However, shRNA triggers with stems ≤ 19 bp are too short for Dicer processing and induce RNAi responses by an alternative processing mechanism. Molecules of this unique class are termed LHPs or right-handed hairpins (RHPs), dependent on whether the loop is situation 3' or 5' to the guide sequence, respectively. Prior reports suggested that LHPs function by an

alternative Dicer-independent, but Ago2-dependent mechanism that was not fully understood (Ge et al., 2010; Dallas et al., 2012).

We conducted the first examination of the function of LHPs that were fully 2'-F/OMe modified, as are most modern siRNA clinical candidates (**Chapter 6**). To better understand the LHP structural requirements for efficient induction of RNAi responses, we synthesized LHPs targeting GFP that contained an 8 nucleotide (nt) loop (LHP1) that was reduced to 2 nucleotides (LHP2). We found that truncation of the loop did not inhibit RNAi induction. We next conducted a systemic LHP shortening through truncation of the passenger and guide sequences. We found that up to 10 nt could be removed from the LHP without negatively impacting induction of RNAi responses. This resulted in a minimal-length 32 nucleotide LHP that contained a 15 nt guide sequence, 15 nt passenger sequence, and a 2 nt 3'-overhang on the end of the passenger strand equivalent. We also examined removal of the 3' dinucleotide overhang in a similar series of systemically shortened LHPs and found that the overhang was dispensable for RNAi induction by fully 2'-modified LHPs.

LHPs have only been analyzed for RNAi induction against a few targets and little work has been done comparing LHPs targeting the same gene with different guide strand sequences. In light of this, we compared three independent sequences of full length GFP LHPs with a 2 nt loop and minimal-length GFP LHPs containing either 2'-OH or 2'-F/OMe groups to GFP siRNAs (**Chapter 6**). We found that the efficiency of RNAi induction is a function of 3 properties: the RNAi trigger structure (LHP vs. siRNA), the ribose 2' group (2'-OH vs 2'-F/OMe), and the targeting sequence. These results illustrated that the rules that have been determined for producing potent siRNAs do not apply directly to LHPs. It is worth noting, however, that the siRNA, full LHP, and

minimal-length LHP structures were all able to induce robust RNAi responses when fully 2'-modified.

As the mechanism that LHPs utilize to become active and capable of inducing an RNAi response is not fully understood, we performed an analysis of LHP-mediated RISC cleavage products and Ago2 co-immunoprecipitations (IPs) on cells transfected with fully 2'-modified LHPs (**Chapter 6**). Specific cleavage of target mRNA opposite nucleotides 10-11 of the guide strand is a hallmark of RNAi responses (Meade and Dowdy, 2009) and can be analyzed by 5' rapid amplification of cDNA ends (5' RACE). We performed 5' RACE analysis on cells transfected with LHPs and found cleavage of the target mRNA in exactly the position expected for Ago2 target cleavage. Ago2 co-IP revealed an LHP species associated with Ago2 with a length that correlated with Ago2 cleavage of the LHP passenger sequence resulting in a long 3' tail on the guide strand. Additionally, Ago2 co-IP of cells transfected with an LHP containing a 2'-OMe group at the predicted passenger sequence Ago2 cleavage site, which prevents Ago2 cleavage, revealed full-length LHP bound to Ago2. Moreover, the LHP with a 2'-OMe passenger strand cleavage block failed to induce an RNAi response. These results suggest that LHPs are not pre-processed by Dicer or another endonuclease prior to Ago2 loading, but are instead loaded as complete LHP molecules into Ago2 wherein Ago2 slices the LHP passenger sequence. This slicing activates RISC for cleavage of target mRNA. This mechanism utilized by LHPs is similar to the mechanism that results in the maturation of miR-451 (Cheloufi et al., 2010; Cifuentes et al., 2010; Yang et al., 2010) and agrees with reports that LHPs are not cleaved by Dicer *in vitro* (Ge et al., 2010) and are fully functional in Dicer$^{-/-}$ cells (Dallas et al., 2012).

Finally, we demonstrated that minimal-length fully 2'-F/OMe modified LHPs are functional *in vivo* through intravenous administration of LHPs complexed with

Invivofectamine 2.0 in mice expressing luciferase in the liver (**Chapter 6**). Although LHPs have been demonstrated to function *in vivo* previously (Dallas et al., 2013; Ma et al., 2014), this study provides the first evidence that fully 2'-modified LHPs, chemical modifications that are essential for RNAi therapeutics to enhance stability and avoid innate immune response induction, are functional *in vivo*.

We believe that minimal-length LHPs represent a promising class of RNAi trigger for the application of RNN technology and use as an RNAi therapeutic. Minimal-length LHPs consist of a single oligonucleotide (32mer) that can be synthesized from a single solid-support and is both smaller and cheaper to manufacture than the two 21mer oligonucleotides that compose a siRNA. Additionally, LHPs also have only one exposed end, thereby limiting exposure to endonuclease activity. For RNN technology, LHPs present an attractive candidate as they can potentially be fully modified with neutralizing phosphotriesters without heed of a reduction in the affinity to form a double-stranded species. Unlike siRNAs that must be a double-stranded upon delivery, LHPs are composed of a single strand and could therefore be delivered as a single strand highly decorated with phosphotriesters. Upon cytoplasmic entry the phosphotriesters will be removed by cytoplasmic thioesterases, allowing the now charged phosphodiester LHP strand to duplex (double-strand) its passenger and guide sequences to form a hairpin species capable of inducing RNAi responses. This approach could allow an RNAi therapeutic to take advantage of the cellular delivery mechanism, termed gymnosis, that single-stranded antisense oligonucleotides slowly cross the lipid bilayer and escape endosomes into the cytoplasm (Stein et al., 2009; Castanotto et al., 2015; Liang et al., 2016). Work is currently underway investigating the function of LHP-RNNs *in vitro* and *in vivo*.

In conclusion, my thesis work has shown: 1) design and synthesis of maximally neutral, double-stranded siRNNs containing bioreversible O-SATE phosphotriesters that are soluble in biologically compatible solutions; 2) the first example of siRNNs capable of self-delivery and RNAi response induction *in vitro* by conjugation to TAT PTD delivery domains through chemically reactive, bioreversible A-SATE phosphotriesters; 3) the first example of delivery and dose-dependent RNAi response induction by siRNNs *in vivo* by utilization of a hepatocyte-specific *tris*-GalNAc targeting domain. Moreover, my establishment of GalNAc-siRNN *in vivo* delivery gives us a tester system to examine the function of new phosphotriesters, conjugation schemes, and endosomal escape domains *in vivo*. Importantly, this work describes the development of readily adaptable, monomeric siRNA prodrugs to overcome the problems associated with current nanoparticle siRNA delivery strategies and introduces a potential RNAi therapeutic candidate for the treatment of human disease.

FUTURE DIRECTIONS

Extra-hepatic delivery

The next great challenge for RNAi therapeutics is extra-hepatic *in vivo* delivery. While GalNAc-siRNA conjugate delivery to the liver works amazingly well, no other cell surface receptor in the human body is known to possess the optimal combination of high expression, rapid turnover, and tissue specificity that characterizes the hepatic ASGPR utilized by GalNAc targeting. Further efforts must center on targeted delivery of RNAi triggers to other tissues and enhancement of cellular delivery. The ability to bind antigens with a high degree of specificity and established therapeutic usage of antibody-drug conjugates make monoclonal antibodies a premier targeting domain for delivery to extra-hepatic tissues (Sievers and Senter, 2013). Early attempts to target siRNAs with

antibodies failed due to formation of heterogeneous aggregates and difficulties with antibody expression (Hamblett et al., 2004; Song et al., 2005; Yao et al., 2012). However, recent impressive work by Genentech demonstrated the generation of homogeneous, defined antibody-siRNA conjugates (ARCs) made by site selective antibody conjugation (Cuellar et al., 2015). Unfortunately, treatment with these ARCs resulted in minimal induction of gene silencing *in vivo*, largely due to endosomal entrapment following ARC internalization and the failure of this group to include an endosomal escape mechanism.

Conjugation to a charged siRNA negatively affects the pharmacokinetics of antibodies, resulting in more rapid clearance of ARCs from the blood than naked antibodies (Cuellar et al., 2015). For this reason, neutral siRNNs may be more adept at targeted *in vivo* delivery by antibodies (**Figure 7.1**). Additionally, siRNN conjugatable bioreversible phosphotriester technology enables site-specific reversible conjugation to make defined ARCs and offers an opportunity for inclusion of endosomal escape domains within the ARC that are essential for efficient delivery.

Endosomal escape enhancement

The dramatic success of GalNAc-siRNA conjugates is made possible due to the high expression (>10^6 per cell) and rapid turnover (every 10-15 min) of the target ASGPR in hepatocytes (Cummings and McEver, 2009). However, the asialoglycoproteins endogenously bound by the hepatic ASGPR are not thought to escape into the cytoplasm. It's possible that GalNAc-siRNNs reach the cytoplasm by inducing extremely rare localized endosomal membrane destabilization events by engagement with ASGPRs. As 5,000 or fewer siRNA molecules can be sufficient to induce a robust RNAi response (Wittrup et al., 2015), an endosomal escape rate of <0.01% would result in more than enough siRNA molecules in the cytoplasm to silence

expression of target genes. Unfortunately, no other ligand-receptor pair in the human body is capable of matching the combination of high expression and rapid turnover of the hepatic ASGPR. In fact, most cell surface receptors are expressed in the range of 10^4-10^5 or fewer with a 90 minute recycling time by way of caveolin or clathrin-mediated endocytosis (Wiley, 1988; Berkers et al., 1991; Schoeberl et al., 2002). Assuming endosomal escape rates of <0.01%, delivery of siRNAs by most cell surface receptors maybe be >100-fold too low for induction of maximal RNAi responses. Indeed, endosomal entrapment has been recognized as a major issue for ARCs (Cuellar et al., 2015) and LNP-mediated siRNA delivery (Gilleron et al., 2013). Escape from endosomes is therefore a key rate-limiting factor for the efficient delivery of siRNA to extra-hepatic tissues.

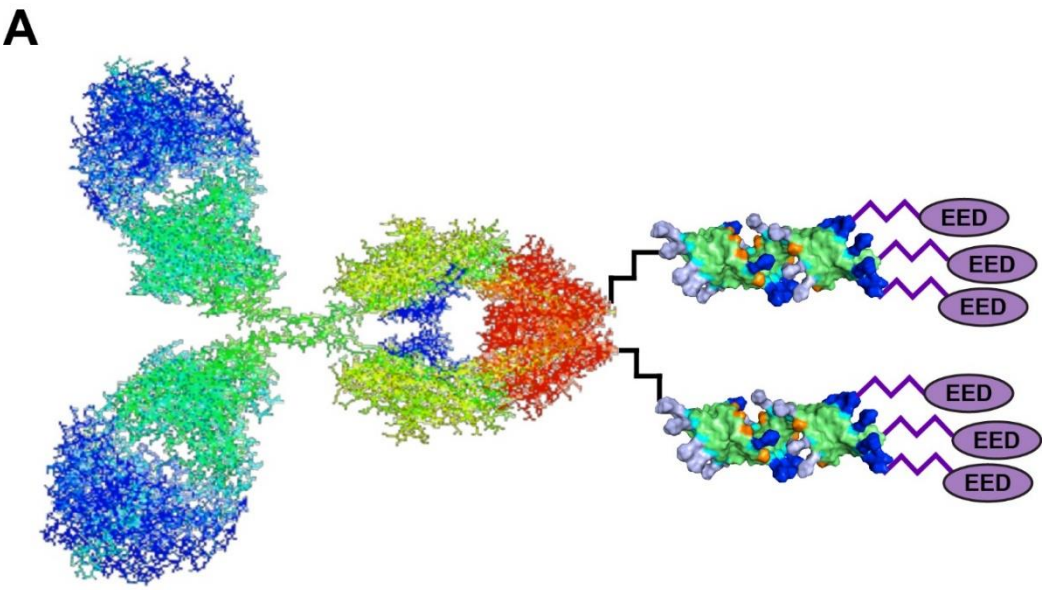

Figure 7.1. Antibody-siRNN-EED ARC for targeted extra-hepatic delivery. A) Extra-hepatic delivery of siRNA will require a combination of highly specific targeting domains and enhancement of endosomal escape. Antibody RNA conjugates (ARCs) containing neutral siRNNs conjugated to clustered endosomal escape domains (EEDs) have the potential to deliver to target tissues and mediate their own endosomal escape to successfully induce RNAi responses.

One approach has been to disrupt or lyse endosomes with small molecule endosomolytic agents such as chloroquine (Maxfield, 1982). Chloroquine functions by passively diffusing across the cell membrane and into endosomes where it becomes protonated as the endosomal pH drops and embeds in the endosomal membrane lipid bilayer by way of a hydrophobic motif. Continued diffusion and endosomal entrapment eventually results in a critically high concentration of chloroquine that lyses the endosome. This functionality can allow co-treatment with endosomolytic agents to enhance delivery of therapeutics suffering from endosomal entrapment. Indeed, I have found that chloroquine treatment enhances delivery of TAT-PTD DD-siRNNs *in vitro* (**FIGURE 7.2**). Other types of small endosomolytic molecules have been developed by the Juliano (Yang et al., 2015) and Khvorova groups (Osborn et al., 2015). While treatment with these molecules has been shown to improve siRNA delivery, they have an inherently slim therapeutic index as lysis of endosomes containing siRNAs is accompanied by lysis of most other endosomes, resulting in severe cytotoxicity and cell death.

An alternative approach to endosomal escape enhancement is to utilize endosomolytic peptides. The most prominent peptide of this class is melittin, a membrane pore-forming peptide originally derived from bee venom (Terwilliger et al., 1982; Lee et al., 2013; Hou et al., 2015). Unlike chloroquine, melittin can lyse cell membranes at physiological pH, as is necessary for its natural hemolytic function (Raghuraman and Chattopadhyay, 2007). Arrowhead Pharmaceuticals has utilized a melittin derivative as part of their two-molecule dynamic polyconjugate (DCP) siRNA delivery technology (Wooddell et al., 2013; Hou et al., 2015). To control melittin for therapeutic use, Arrowhead Pharmaceuticals has reversibly masked its lytic activity with pH-sensitive groups and conjugated it to GalNAc. This approach limits the cytotoxicity of

melittin by causing it to only become active in the low pH environment of hepatocyte endosomes where it is deprotected to lyse the endosome and release co-delivered siRNA molecules into the cytoplasm. This approach is currently under study for anti-HBV RNAi drugs now in phase 2 clinical trials. A next-generation variant of this technology is under development that utilizes protease sensitive protecting groups on melittin (Rozema et al., 2015).

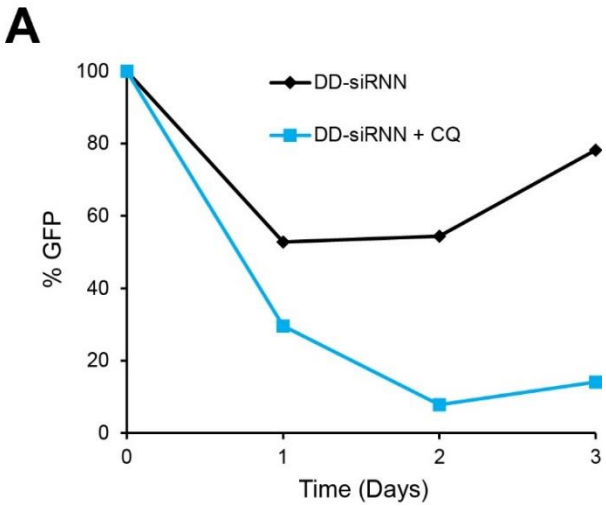

Figure 7.2. Enhancement of endosomal escape. A) Treatment of cultured cells with a sub-effective dose of GFP-targeted TAT PTD delivery domain (DD) siRNN conjugate induces a moderate RNAi response. Additional treatment with chloroquine (CQ) endosomolytic agent releases DD-siRNN conjugates trapped in endosomes, resulting in induction of a strong RNAi response.

Recently our lab employed a real-time, live cell, split GFP phenotypic assay to screen for endosomal escape domains (EEDs) (Lönn et al., 2016). Through use of this assay we developed small, hydrophobic EED peptides capable of enhancing endosomal escape of macromolecular cargo to the cytoplasm by 5 to 8-fold without cytotoxic effects. In contrast, Li and colleagues have discovered a short, charged peptide called aurein 1.2 that enhances escape of endocytosed protein cargo by up to ~5-fold (Li et al., 2015).

While these approaches have shown some success at addressing the issue of endosomal entrapment, a non-cytotoxic 5 to 10-fold enhancement will not be sufficient to

enable efficient extra-hepatic delivery of siRNAs. The physical characteristics of the GalNAc and ASGPR ligand-receptor system suggest that a 100-fold or greater enhancement in endosomal escape will be necessary for successful delivery outside of the liver. While meeting this goal will undoubtedly require further development of endosomal escape enhancers, siRNNs may be well suited to meet this challenge. Using conjugatable phosphotriesters, I have demonstrated that hydrazine functionalized delivery (**Chapter 4**) and targeting domains (**Chapter 5**) can be reversibly conjugated to a siRNN in a site-specific manner. This same technology can be used to make EED-siRNN conjugates that mediate their own endosomal escape (**Figure 7.1**). Additionally, high local concentrations that may improve EED activity could be generated by placement of conjugatable phosphotriesters in tight groups on a siRNN to allow for the conjugation of EEDs in close physical proximity (**Figure 7.1**). An EED-siRNN conjugate approach would also limit cytotoxicity by restricting endosomal membrane disruption to only endosomes that contain siRNNs. This effect can be further limited to target cells by the additional conjugation of targeting domains to EED-siRNNs. Generation of siRNN hybrid conjugates (**Figure 7.1**) requires conjugation chemistries that enable site-specific conjugation of two or more different domains to the same siRNN and is relatively straight-forward.

Alternative siRNN conjugation strategies

Generation of hybrid siRNN conjugates requires the ability to conjugate two or more different molecules to the same siRNN. This can be accomplished by either careful utilization of one conjugation chemistry or usage multiple, compatible conjugation chemistries. For siRNNs, the former approach can addressed using Hynic chemistry and A-SATE phosphotriesters that contain reactive benzaldehyde groups. This approach is further facilitated by the fact that siRNNs are double-stranded molecules

composed of two oligonucleotides strands held together by nucleobase hydrogen bonding. Because of this, each RNN oligonucleotide can be conjugated independently to different molecules by the same chemistry and then duplexed together to make a double-stranded siRNN hybrid conjugate. However, this method is only viable if conjugation to these molecules still allows strand duplexing as is the case for the *tris*-GalNAc targeting domain (**Chapter 5**). Molecules with dense cationic charge, such as TAT PTD, prevent duplexing upon conjugation to an ssRNN oligonucleotide. In this case, conjugation of different molecules is still possible with only A-SATE phosphotriesters by placement of acetal-protected A-SATE (ac-A-SATE) phosphotriesters on one strand and unprotected A-SATEs on the other strand. A double-stranded siRNN composed of these oligonucleotides could be conjugated to two different molecules by the following method: conjugation of molecule 1 to A-SATEs on the passenger strand, purification to remove unreacted molecule 1, deprotection of ac-A-SATEs on the guide strand, conjugation of molecule 2 to deprotected A-SATEs on guide strand, and final purification to remove unreacted molecule 2. However, the multiple purification steps of this process would likely lower the final yield of the hybrid conjugate. Alternatively, insertion of phosphotriesters containing different chemically reactive termini in the same RNN oligonucleotide is possible.

Utilization of phosphotriesters capable of conjugation by chemistries other than Hynic would simplify the synthesis of hybrid siRNN conjugates. Although benzaldehyde containing phosphotriesters (A-SATE, Ax, and A-SATB) are the only reactive phosphotriesters discussed in this dissertation, we have also developed bioreversible phosphotriester groups for other conjugation chemistries: Alkyne-SATE (K-SATE) for copper-catalyzed alkyne-azide cycloaddition (“click” chemistry) (**Figure 7.3A**) (Rostovtsev et al., 2002; Tornøe et al., 2002; Paredes and Das, 2011; Krishna and

Caruthers, 2012), Norbornene-SATE (E-SATE) for inverse electron-demand Diels-Alder reactions (**Figure 7.3B**) (Devaraj and Weissleder, 2011), and Amino-SATE (N-SATE) (Meade, 2010) for reaction with a succinimidyl esters (**Figure 7.3C**). I have demonstrated that K-SATE and E-SATE phosphotriesters react readily with azide and tetrazine functionalized molecules, respectively (data not shown). Both groups are also converted intracellularly by thioesterases into charged phosphodiesters upon transfection into cultured cells. N-SATE phosphotriesters have been well characterized (Meade, 2010) and successfully conjugated to succinimidyl ester functionalized peptides (data not shown). However, unconjugated N-SATE groups containing a primary amine are markedly unstable, undergoing spontaneous decomposition in standard biological media (Meade, 2010). Additionally, strain-promoted azide-alkyne cycloaddition (copper-free click chemistry) (Baskin et al., 2007; Van Delft et al., 2010) has been conducted with a dibenzocyclooctyl (DBCO) functionalized siRNN and an azide-tagged peptide**.** Synthesis of the requisite DBCO-SATE (C-SATE) phosphotriester is currently underway (**Figure 7.3D**). Further characterization of these phosphotriesters and their accompanying conjugation chemistry must be conducted, but use of these groups will enable the synthesis of next-generation siRNN hybrid conjugates.

RNAi therapeutics to treat cancer

Due to continuous tumor DNA mutation rates, at all stages of cancer treatment, failure to respond to anticancer chemotherapeutic or biologic therapeutics is generally a result of DNA mutation-driven drug resistance. Unfortunately, current therapeutic approaches, including targeted small molecule inhibitors and extracellular antibodies, cannot “pharmaco-evolve” to bind the newly mutated cancer target. Moreover, current therapeutic interventions are strictly limited to the “druggable” genome that represents a very restricted number of all genes (~5%). Thus, due to the high rate of DNA mutation,

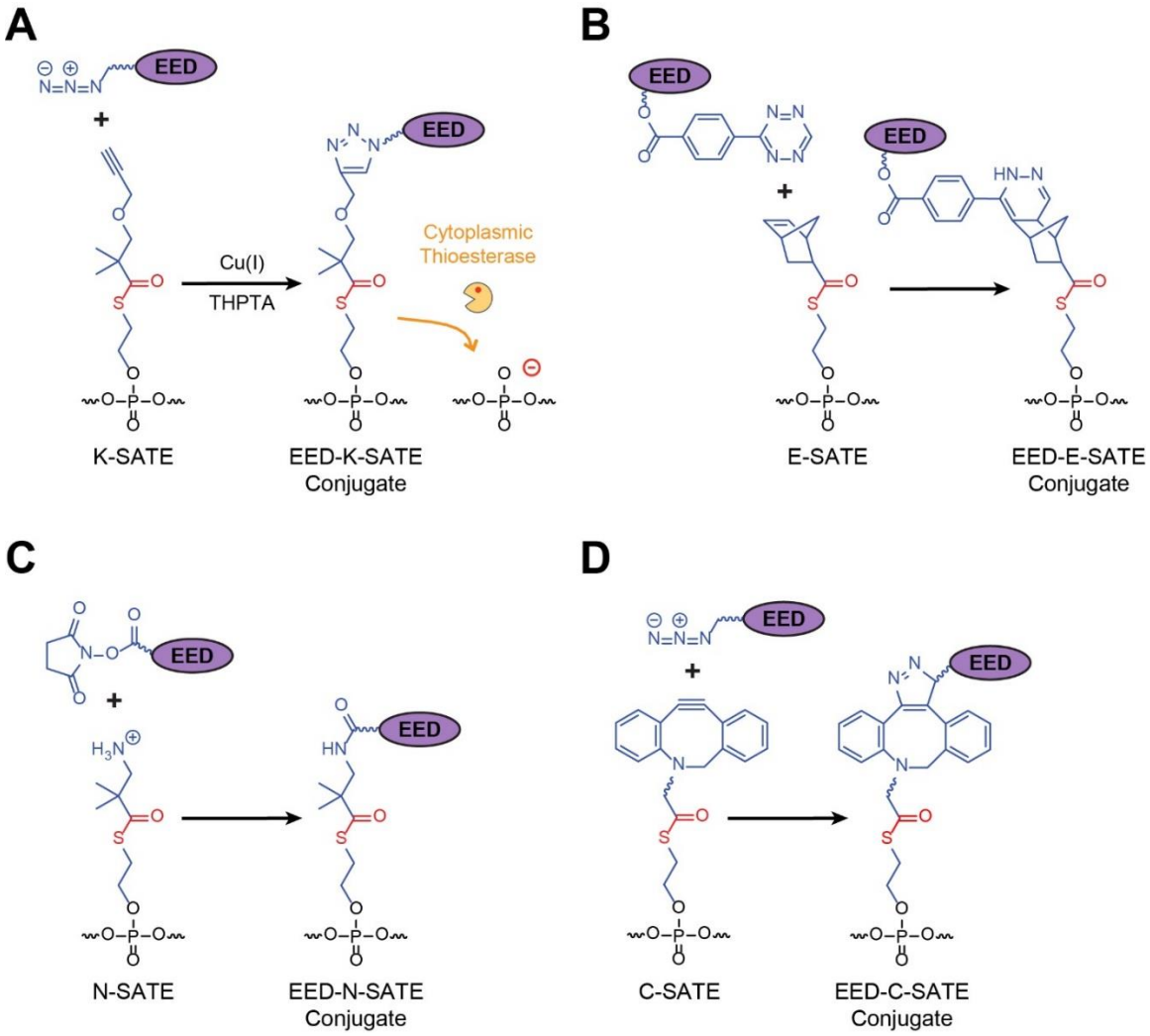

Figure 7.3. Alternative siRNN conjugation strategies. A) Conjugation of azide functionalized endosomal escape domain (EED) to Alkyne-SATE (K-SATE) phosphotriester by copper-catalyzed cycloaddition ("click" chemistry). Cytoplasmic thioesterase processes EED-K-SATE conjugated phosphotriester groups resulting in an RNAi-compatible wildtype charged phosphodiester. Tris-(benzyltriazolylmethyl)amine. (TBTA) is a water soluble Cu(I) stabilizing ligand. **B)** Conjugation of tetrazine functionalized EED to Norbornene-SATE (E-SATE) bioreversible phosphotriester by inverse electron-demand Diels-Alder reaction. **C)** Conjugation of succinimidyl ester functionalized EED to Amino-SATE (N-SATE) bioreversible phosphotriester. **D)** Conjugation of azide functionalized EED to bioreversible dibenzocyclooctyl (DBCO)-SATE (C-SATE) phosphotriester by strain-promoted cycloaddition (copper-free click chemistry).

therapeutic approaches that cannot evolve the therapeutic faster than the rate of cancer's DNA mutation will ultimately not be successful approaches to eradicate cancer deaths. Fortunately, RNAi-inducing siRNA has the potential to perfectly fit the role of an effective and rapidly adaptable cancer therapeutic.

With high potency and the ability to selectively target any expressed mRNA, RNAi therapeutics can act as a therapeutic intervention for any target in the vast "undruggable" genome. Additionally, changing targets is simply a matter of changing the siRNA sequence, allowing more rapid target adaptation than any other existing therapeutic. Unlike conventional chemotherapeutic agents, siRNA can be directed against cancer-specific DNA mutations by sequence, allowing siRNA to affect only mutation-harboring cancer cells and not induce cytotoxic effects on normal tissue. Furthermore, siRNA treatment can induce synthetic lethal responses where the inhibition of two or more separate genes leads to cell death while inhibition of only one gene alone has no lethal effect on the cell. This effect can be leveraged to specifically kill cancer cells by targeting oncogenes, cancer-specific mutations, or pathways necessary for tumor cell survival, but not critical for normal tissue (Michiue et al., 2009; Kacsinta and Dowdy, 2016).

However, for all of the advantages that siRNA has as an anti-cancer therapeutic, it must still reach and be delivered *in vivo* into the cytoplasm of cancer cells in sufficiently high enough numbers to induce RNAi responses. The work that I have done during my dissertation and the future directions that I have outlined here all build to the purpose of extrahepatic siRNA delivery for the treatment of human disease, particularly cancer. Reaching this goal will require development of hybrid siRNN conjugates containing targeting domains to deliver siRNNs specifically to tumors and endosomal escape

enhancers to facilitate sufficient cytoplasmic delivery of siRNNs to induce cancer-specific lethal RNAi responses.

REFERENCES

Baskin, J.M., Prescher, J.A., Laughlin, S.T., Agard, N.J., Chang, P. V, Miller, I.A., Lo, A., Codelli, J.A., and Bertozzi, C.R. (2007). Copper-free click chemistry for dynamic in vivo imaging. Proc. Natl. Acad. Sci. U. S. A. *104*, 16793–16797.

Behlke, M.A. (2008). Chemical modification of siRNAs for in vivo use. Oligonucleotides *18*, 305–319.

Berkers, J.A., van Bergen en Henegouwen, P.M., and Boonstra, J. (1991). Three classes of epidermal growth factor receptors on HeLa cells. J. Biol. Chem. *266*, 922–927.

Bramsen, J.B., and Kjems, J. (2011). Chemical modification of small interfering RNA. Methods Mol. Biol. *721*, 77–103.

Castanotto, D., Lin, M., Kowolik, C., Wang, L.A., Ren, X.Q., Soifer, H.S., Koch, T., Hansen, B.R., Oerum, H., Armstrong, B., Wang, Z., Bauer, P., Rossi, J., and Stein, C.A. (2015). A cytoplasmic pathway for gapmer antisense oligonucleotide-mediated gene silencing in mammalian cells. Nucleic Acids Res. *43*, 9350–9361.

Cheloufi, S., Dos Santos, C.O., Chong, M.M.W., and Hannon, G.J. (2010). A dicer-independent miRNA biogenesis pathway that requires Ago catalysis. Nature *465*, 584–589.

Cifuentes, D., Xue, H., Taylor, D.W., Patnode, H., Mishima, Y., Cheloufi, S., Ma, E., Mane, S., Hannon, G.J., Lawson, N.D., Wolfe, S.A., and Giraldez, A.J. (2010). A novel miRNA processing pathway independent of Dicer requires Argonaute2 catalytic activity. Science *328*, 1694–1698.

Cuellar, T.L., Barnes, D., Nelson, C., Tanguay, J., Yu, S.F., Wen, X., Scales, S.J., Gesch, J., Davis, D., Van Brabant Smith, A., Leake, D., Vandlen, R., and Siebel, C.W. (2015). Systematic evaluation of antibody-mediated siRNA delivery using an industrial platform of THIOMAB-siRNA conjugates. Nucleic Acids Res. *43*, 1189–1203.

Cummings, R.D., and McEver, R.P. (2009). C-type Lectins. In Essentials of Glycobiology, A. Varki, R.D. Cummings, J.D. Esko, H.H. Freeze, P. Stanley, C.R. Bertozzi, G.W. Hart, and M.E. Etzler, eds. (New York: Cold Spring Harbor Laboratory Press), p.

Dallas, A., Ilves, H., Ge, Q., Kumar, P., Shorenstein, J., Kazakov, S.A., Cuellar, T.L., McManus, M.T., Behlke, M.A., and Johnston, B.H. (2012). Right- and left-loop short shRNAs have distinct and unusual mechanisms of gene silencing. Nucleic Acids Res. *40*, 9255–9271.

Dallas, A., Ilves, H., Shorenstein, J., Judge, A., Spitler, R., Contag, C., Wong, S.P., Harbottle, R.P., Maclachlan, I., and Johnston, B.H. (2013). Minimal-length Synthetic shRNAs Formulated with Lipid Nanoparticles are Potent Inhibitors of Hepatitis C Virus IRES-linked Gene Expression in Mice. Mol. Ther. Nucleic Acids

2, e123.

Van Delft, P., Meeuwenoord, N.J., Hoogendoorn, S., Dinkelaar, J., Overkleeft, H.S., Van Der Marel, G.A., and Filippov, D. V (2010). Synthesis of oligoribonucleic acid conjugates using a cyclooctyne phosphoramidite. Org. Lett. *12*, 5486–5489.

Devaraj, N.K., and Weissleder, R. (2011). Biomedical applications of tetrazine cycloadditions. Acc. Chem. Res. *44*, 816–827.

Elbashir, S.M., Harborth, J., Lendeckel, W., Yalcin, A., Weber, K., and Tuschl, T. (2001). Duplexes of 21-nucleotide RNAs mediate RNA interference in cultured mammalian cells. Nature *411*, 494–498.

Fire, A., Xu, S., Montgomery, M.K., Kostas, S.A., Driver, S.E., and Mello, C.C. (1998). Potent and specific genetic interference by double-stranded RNA in Caenorhabditis elegans. Nature *391*, 806–811.

Gao, S., Dagnaes-Hansen, F., Nielsen, E.J.B., Wengel, J., Besenbacher, F., Howard, K.A., and Kjems, J. (2009). The effect of chemical modification and nanoparticle formulation on stability and biodistribution of siRNA in mice. Mol. Ther. *17*, 1225–1233.

Ge, Q., Ilves, H., Dallas, A., Kumar, P., Shorenstein, J., Kazakov, S.A., and Johnston, B.H. (2010). Minimal-length short hairpin RNAs: the relationship of structure and RNAi activity. RNA *16*, 106–117.

Gilleron, J., Querbes, W., Zeigerer, A., Borodovsky, A., Marsico, G., Schubert, U., Manygoats, K., Seifert, S., Andree, C., Stöter, M., Epstein-Barash, H., Zhang, L., Koteliansky, V., Fitzgerald, K., Fava, E., Bickle, M., Kalaidzidis, Y., Akinc, A., Maier, M., and Zerial, M. (2013). Image-based analysis of lipid nanoparticle-mediated siRNA delivery, intracellular trafficking and endosomal escape. Nat. Biotechnol. *31*, 638–646.

Gonçalves, E., Kitas, E., and Seelig, J. (2005). Binding of oligoarginine to membrane lipids and heparan sulfate: structural and thermodynamic characterization of a cell-penetrating peptide. Biochemistry *44*, 2692–2702.

Hamblett, K.J., Senter, P.D., Chace, D.F., Sun, M.M.C., Lenox, J., Cerveny, C.G., Kissler, K.M., Bernhardt, S.X., Kopcha, A.K., Zabinski, R.F., Meyer, D.L., and Francisco, J.A. (2004). Effects of drug loading on the antitumor activity of a monoclonal antibody drug conjugate. Clin. Cancer Res. *10*, 7063–7070.

Hastings, K.T., and Cresswell, P. (2011). Disulfide reduction in the endocytic pathway: immunological functions of gamma-interferon-inducible lysosomal thiol reductase. Antioxid. Redox Signal. *15*, 657–668.

Hou, K.K., Pan, H., Schlesinger, P.H., and Wickline, S.A. (2015). A role for peptides in overcoming endosomal entrapment in siRNA delivery - A focus on melittin. Biotechnol. Adv.

Jiang, T., Olson, E.S., Nguyen, Q.T., Roy, M., Jennings, P.A., and Tsien, R.Y. (2004). Tumor imaging by means of proteolytic activation of cell-penetrating peptides. Proc. Natl. Acad. Sci. U. S. A. *101*, 17867–17872.

Juliano, R.L. (2016). The delivery of therapeutic oligonucleotides. Nucleic Acids Res. *347*, 6518–6548.

Kacsinta, A.D., and Dowdy, S.F. (2016). Current views on inducing synthetic lethal RNAi responses in the treatment of cancer. Expert Opin. Biol. Ther. *16*, 161–172.

Krishna, H., and Caruthers, M.H. (2012). Alkynyl phosphonate DNA: a versatile “click”able backbone for DNA-based biological applications. J. Am. Chem. Soc. *134*, 11618–11631.

Lee, M.-T., Sun, T.-L., Hung, W.-C., and Huang, H.W. (2013). Process of inducing pores in membranes by melittin. Proc. Natl. Acad. Sci. U. S. A. *110*, 14243–14248.

Li, M., Tao, Y., Shu, Y., LaRochelle, J.R., Steinauer, A., Thompson, D., Schepartz, A., Chen, Z.-Y., and Liu, D.R. (2015). Discovery and characterization of a peptide that enhances endosomal escape of delivered proteins in vitro and in vivo. J. Am. Chem. Soc. *137*, 14084–14093.

Liang, X.H., Shen, W., Sun, H., Kinberger, G.A., Prakash, T.P., Nichols, J.G., and Crooke, S.T. (2016). Hsp90 protein interacts with phosphorothioate oligonucleotides containing hydrophobic 2’-modifications and enhances antisense activity. Nucleic Acids Res. *44*, 3892–3907.

Lönn, P., and Dowdy, S.F. (2015). Cationic PTD/CPP-mediated macromolecular delivery: charging into the cell. Expert Opin. Drug Deliv. *12*, 1627–1636.

Lönn, P., Kacsinta, A.D., Cui, X.-S., Hamil, A.S., Kaulich, M., Gogoi, K., and Dowdy, S.F. (2016). Enhancing Endosomal Escape for Intracellular Delivery of Macromolecular Biologic Therapeutics. Sci. Rep. *6*, 32301.

Ma, H., Dallas, A., Ilves, H., Shorenstein, J., MacLachlan, I., Klumpp, K., and Johnston, B.H. (2014). Formulated minimal-length synthetic small hairpin RNAs are potent inhibitors of hepatitis C virus in mice with humanized livers. Gastroenterology *146*, 63–6.e5.

Maxfield, F.R. (1982). Weak bases and ionophores rapidly and reversibly raise the pH of endocytic vesicles in cultured mouse fibroblasts. J. Cell Biol. *95*, 676–681.

Meade, B.R. (2010). Synthesis of bioreversible, phosphotriester-modified siRNA oligonucleotides. University of California, San Diego.

Meade, B.R., and Dowdy, S.F. (2009). The road to therapeutic RNA interference (RNAi): Tackling the 800 pound siRNA delivery gorilla. Discov. Med. *8*, 253–256.

Meade, B.R., Gogoi, K., Hamil, A.S., Palm-Apergi, C., van den Berg, A., Hagopian, J.C., Springer, A.D., Eguchi, A., Kacsinta, A.D., Dowdy, C.F., Presente, A., Lönn, P.,

Kaulich, M., Yoshioka, N., Gros, E., Cui, X.-S., and Dowdy, S.F. (2014). Efficient delivery of RNAi prodrugs containing reversible charge-neutralizing phosphotriester backbone modifications. Nat. Biotechnol. *32*, 1256–1261.

Michiue, H., Eguchi, A., Scadeng, M., and Dowdy, S.F. (2009). Induction of in vivo synthetic lethal RNAi responses to treat glioblastoma. Cancer Biol. Ther. *8*, 2306–2313.

Osborn, M.F., Alterman, J.F., Nikan, M., Cao, H., Didiot, M.C., Hassler, M.R., Coles, A.H., and Khvorova, A. (2015). Guanabenz (Wytensin™) selectively enhances uptake and efficacy of hydrophobically modified siRNAs. Nucleic Acids Res. *43*, 8664–8672.

Paredes, E., and Das, S.R. (2011). Click chemistry for rapid labeling and ligation of RNA. Chembiochem *12*, 125–131.

Raghuraman, H., and Chattopadhyay, A. (2007). Melittin: a membrane-active peptide with diverse functions. Biosci. Rep. *27*, 189–223.

Rao, D.D., Vorhies, J.S., Senzer, N., and Nemunaitis, J. (2009). siRNA vs. shRNA: similarities and differences. Adv. Drug Deliv. Rev. *61*, 746–759.

Rettig, G.R., and Behlke, M.A. (2012). Progress toward in vivo use of siRNAs-II. Mol. Ther. *20*, 483–512.

Robbins, M., Judge, A., and MacLachlan, I. (2009). siRNA and innate immunity. Oligonucleotides *19*, 89–102.

Rostovtsev, V. V, Green, L.G., Fokin, V. V, and Sharpless, K.B. (2002). A stepwise huisgen cycloaddition process: Copper(I)-catalyzed regioselective “ligation” of azides and terminal alkynes. Angew. Chemie - Int. Ed. *41*, 2596–2599.

Rozema, D.B., Blokhin, A., Wakefield, D.H., Benson, J., Carlson, J., Klein, J.J., Almeida, L., Perillo-Nicholas, A., Hamilton, H.L., Chu, Q., Hegge, J.O., Wong, S.C., Trubetskoy, V., Hagen, C., Kitas, E., Wolff, J.A., and Lewis, D.L. (2015). Protease-triggered siRNA delivery vehicles. J. Control. Release.

Schoeberl, B., Eichler-Jonsson, C., Gilles, E.D., and Muller, G. (2002). Computational modeling of the dynamics of the MAP kinase cascade activated by surface and internalized EGF receptors. Nat. Biotechnol. *20*, 370–375.

Schroeder, A., Levins, C.G., Cortez, C., Langer, R., and Anderson, D.G. (2010). Lipid-based nanotherapeutics for siRNA delivery. J. Intern. Med. *267*, 9–21.

Sievers, E.L., and Senter, P.D. (2013). Antibody-drug conjugates in cancer therapy. Annu. Rev. Med. *64*, 15–29.

Sliedregt, L.A., Rensen, P.C., Rump, E.T., van Santbrink, P.J., Bijsterbosch, M.K., Valentijn, A.R., van der Marel, G.A., van Boom, J.H., van Berkel, T.J., and Biessen, E.A. (1999). Design and synthesis of novel amphiphilic dendritic

galactosides for selective targeting of liposomes to the hepatic asialoglycoprotein receptor. J. Med. Chem. *42*, 609–618.

Song, E., Zhu, P., Lee, S.-K., Chowdhury, D., Kussman, S., Dykxhoorn, D.M., Feng, Y., Palliser, D., Weiner, D.B., Shankar, P., Marasco, W.A., and Lieberman, J. (2005). Antibody mediated in vivo delivery of small interfering RNAs via cell-surface receptors. Nat. Biotechnol. *23*, 709–717.

Spiess, M. (1990). The asialoglycoprotein receptor: a model for endocytic transport receptors. Biochemistry *29*, 10009–10018.

Stein, C.A., Hansen, J.B., Lai, J., Wu, S.J., Voskresenskiy, A., Høg, A., Worm, J., Hedtjärn, M., Souleimanian, N., Miller, P., Soifer, H.S., Castanotto, D., Benimetskaya, L., Ørum, H., and Koch, T. (2009). Efficient gene silencing by delivery of locked nucleic acid antisense oligonucleotides, unassisted by transfection reagents. Nucleic Acids Res. *38*, e3.

Terwilliger, T.C., Weissman, L., and Eisenberg, D. (1982). The structure of melittin in the form I crystals and its implication for melittin's lytic and surface activities. Biophys. J. *37*, 353–361.

Tornøe, C.W., Christensen, C., and Meldal, M. (2002). Peptidotriazoles on solid phase: [1,2,3]-Triazoles by regiospecific copper(I)-catalyzed 1,3-dipolar cycloadditions of terminal alkynes to azides. J. Org. Chem. *67*, 3057–3064.

Westerlind, U., Westman, J., Törnquist, E., Smith, C.I.E., Oscarson, S., Lahmann, M., and Norberg, T. (2004). Ligands of the asialoglycoprotein receptor for targeted gene delivery, part 1: Synthesis of and binding studies with biotinylated cluster glycosides containing N-acetylgalactosamine. Glycoconj. J. *21*, 227–241.

Wiley, H.S. (1988). Anomalous binding of epidermal growth factor to A431 cells is due to the effect of high receptor densities and a saturable endocytic system. J. Cell Biol. *107*, 801–810.

Wittrup, A., and Lieberman, J. (2015). Knocking down disease: a progress report on siRNA therapeutics. Nat. Rev. Genet. *16*, 543–552.

Wittrup, A., Ai, A., Liu, X., Hamar, P., Trifonova, R., Charisse, K., Manoharan, M., Kirchhausen, T., and Lieberman, J. (2015). Visualizing lipid-formulated siRNA release from endosomes and target gene knockdown. Nat. Biotechnol. *33*, 870–876.

Wooddell, C.I., Rozema, D.B., Hossbach, M., John, M., Hamilton, H.L., Chu, Q., Hegge, J.O., Klein, J.J., Wakefield, D.H., Oropeza, C.E., Deckert, J., Roehl, I., Jahn-Hofmann, K., Hadwiger, P., Vornlocher, H.-P., McLachlan, A., and Lewis, D.L. (2013). Hepatocyte-targeted RNAi therapeutics for the treatment of chronic hepatitis B virus infection. Mol. Ther. *21*, 973–985.

Yang, B., Ming, X., Cao, C., Laing, B., Yuan, A., Porter, M.A., Hull-Ryde, E.A., Maddry, J., Suto, M., Janzen, W.P., and Juliano, R.L. (2015). High-throughput screening

identifies small molecules that enhance the pharmacological effects of oligonucleotides. Nucleic Acids Res. *43*, 1987–1996.

Yang, J., Chen, H., Vlahov, I.R., Cheng, J.-X., and Low, P.S. (2006). Evaluation of disulfide reduction during receptor-mediated endocytosis by using FRET imaging. Proc. Natl. Acad. Sci. U. S. A. *103*, 13872–13877.

Yang, J.-S., Maurin, T., Robine, N., Rasmussen, K.D., Jeffrey, K.L., Chandwani, R., Papapetrou, E.P., Sadelain, M., O'Carroll, D., and Lai, E.C. (2010). Conserved vertebrate mir-451 provides a platform for Dicer-independent, Ago2-mediated microRNA biogenesis. Proc. Natl. Acad. Sci. U. S. A. *107*, 15163–15168.

Yao, Y., Sun, T., Huang, S., Dou, S., Lin, L., Chen, J., Ruan, J., Mao, C., Yu, F., Zeng, M., Zang, J., Liu, Q., Su, F., Zhang, P., Lieberman, J., Wang, J., and Song, E. (2012). Targeted delivery of PLK1-siRNA by ScFv suppresses Her2+ breast cancer growth and metastasis. Sci. Transl. Med. *4*, 130ra48.

Zeidman, R., Jackson, C.S., and Magee, A.I. (2009). Protein acyl thioesterases (Review). Mol. Membr. Biol. *26*, 32–41.